

An-Najah National University

Faculty of Graduate Studies

Enhancing Earthquake Resistance of Local Structures by Reducing Superimposed Dead Load

By

Hasan J. Alnajajra

Supervisor

Dr. Abdul Razzaq A. Touqan

Co-Supervisor

Dr. Monther B. Dwaikat

**This Thesis is Submitted in Partial Fulfillment of the Requirements for
the Degree of Master of Structural Engineering, Faculty of Graduate
Studies, at An-Najah National University, Nablus, Palestine.**

2018

**Enhancing Earthquake Resistance of Local Structures by
Reducing Superimposed Dead Load**

By

Hasan J. Alnajajra

This thesis was defended successfully on 8/2/2018 and approved by:

Defense Committee Members

Signature

- Dr. Abdul Razzaq A. Touqan / Supervisor**
- Dr. Monther B. Dwaikat / Co-Supervisor**
- Dr. Maher A. Amro / External Examiner**
- Dr. Riyad A. Awad / Internal Examiner**

III

DEDICATION

To our first and only perfect teacher who had laid out the groundwork for the spiritual education of mankind our prophet Mohammed Peace be upon him.

To the one who didn't just give me birth, he gave me a good life. He didn't just provide me education, he gave me good life experience. It is men like him, who become loving and glorious fathers.

To the one who always being there for me to love me and care for me when I felt like no one else did. No one can ever take your place ever.

To my second mother who stood strong beside me when my whole world was darker and made it full of brightness. The one who granted me the true love and happiness. You did not allow me to give up but inspired me to insist on success. My darling wife.

To the gift of Allah and the sight of our eyes who represent the continuity of our life. My lovely kids "Tameem, Sham, and Waseem".

To those who were the gift of my father and mother, my brothers and sisters, particularly my brother "Abedelkareem".

To my father and mother in law and all other relatives who wish me all success in life.

I present this thesis.

ACKNOWLEDGMENT

While my first gratitude appreciation must be directed to my creator
Allah (SWT).

I will never forget to express my great appreciation to my teachers for their generous support which they offered to me along through the whole period of my study.

My special gratitude appreciation is directed towards my supervisors:

Dr. Abdul Razzaq A. Touqan.

Dr. Monther B. Dwaikat.

To all the teaching staff teachers and supervisors.

To the great center of science; An-Najah National University.

My special appreciation to Dr. Haitham Ayyad, Dr. Mohammad Manasrah, and Mr. Mohammad Abuhamdieh.

Besides, everyone who contributed in completing this research.

الإقرار

أنا الموقع أدناه مقدم الرسالة التي تحمل عنوان

Enhancing Earthquake Resistance of Local Structures by Reducing Superimposed Dead Load

أقر بأن ما اشتملت عليه هذه الرسالة إنما هو نتاج جهدي الخاص، باستثناء ما تمت الإشارة إليه حيثما ورد، وأن هذه الرسالة ككل، أو أي جزء منها لم يقدم من قبل لنيل أية درجة علمية أو بحث علمي أو بحثي لدى أية مؤسسة تعليمية أو بحثية أخرى.

DECLARATION

The work provided in this thesis, unless otherwise referenced, is the researcher's own work, and has not been submitted elsewhere for any other degree or qualification.

Student's Name

اسم الطالب:

Signature

التوقيع:

Date

التاريخ:

TABLE OF CONTENTS

DEDICATION	III
ACKNOWLEDGMENT	IV
DECLARATION	V
TABLE OF CONTENTS	VI
LIST OF FIGURES	XII
LIST OF TABLES	XV
LIST OF ABBREVIATIONS	XVIII
LIST OF SYMBOLS	XX
ABSTRACT	XXVIII
CHAPTER 1	1
INTRODUCTION	1
1.1 General	2
1.2 Problem Statement	3
1.3 Research Questions	7
1.4 Research Objectives	8
1.4.1 Research Overall Objective	8
1.4.2 Research Sub-objectives	8
1.5 Research Scope and Limitations	8
1.6 Structure of the Thesis	9
CHAPTER 2	12
LITERATURE REVIEW	12
2.1 Introduction	13
2.2 Earthquakes Phenomena	14
2.2.1 Causes of Earthquakes	14
2.2.2 Theory of Plate Tectonics	14
2.3 Seismicity of Palestine	16
2.3.1 Earthquake Sources in Palestine	16

2.3.2 Historical Overview for the Dead Sea Earthquakes	18
2.4 Earthquake Resistant Buildings	20
2.5 Lateral-Force Resisting Systems.....	20
2.5.1 Structural Diaphragms	21
2.5.2 RC Moment Resisting Frames	21
2.5.3 RC Shear Walls.....	22
2.6 Basics of Seismic Analysis	22
2.7 Types of RC Slabs.....	24
2.8 Literature Review.....	25
2.9 Summary	28
CHAPTER 3.....	31
STRUCTURAL ANALYSIS.....	31
3.1 Introduction.....	32
3.2 Description of the Studied Buildings.....	33
3.3 Materials Properties	37
3.4 Loads on the Building.....	38
3.5 Validation of Members Sizes.....	39
3.5.1 Minimum Slab Thickness	39
3.5.2 Estimating of Beams Depths.....	44
3.5.3 Estimating of Trial Sections of Columns.....	45
3.6 Structural Modeling	48
3.7 Modeling Criteria.....	48
3.7.1 Members Stiffness	48
3.7.2 Base Fixity	49
3.7.3 Modeling Phase.....	50
3.7.4 Finite Element Mesh Sensitivity Analysis.....	50
3.8 Models Checking Process	52
3.9 Verification of Results for Gravity Loads Analysis	53

VIII

3.9.1 Check of Compatibility.....	54
3.9.2 Check of Equilibrium.....	55
3.9.3 Check of stress-strain relationship.....	56
3.10 Earthquake Consequences on Structures	65
3.10.1 The Fundamental Natural Period.....	65
3.10.2 Damping.....	67
3.11 Ground Motion Input Parameters	67
3.12 Seismic Analysis Approach	70
3.12.1 Seismic Design Category.....	70
3.12.2 Structural Irregularities	73
3.12.3 Diaphragm Rigidity	74
3.12.4 The Most legitimated Procedure of Analysis	74
3.13 Modal Response Spectrum Method.....	76
3.13.1 Basic Principles of Modal and Spectral Analysis.....	76
3.13.2 Response Spectrum Concept	77
3.13.3 Minimum Number of Modes	80
3.13.4 Modal Combination Technique	81
3.14 Verification of Modal Properties	82
3.14.1 Verification of the Fundamental Periods.....	83
3.14.2 Verification of the Effective Modal Mass Ratios.....	85
3.14.3 Verification of the Total Displacement of Stories.....	89
3.14.4 Check of the Story Shears.....	91
3.14.5 Verification of the Base Overturning Moment.....	93
3.15 Commentaries	94
3.16 Design Approach.....	96
3.17 Inelastic Seismic Response of Buildings	97
3.17.1 Fundamental Parameters of Inelastic Behavior	98
3.17.2 Other Parameters of Inelastic Behavior	99

3.18 Design Response Spectrum.....	99
3.19 Scaling of Forces.....	100
3.19.1 Seismic Base Shear of ELF Analysis	100
3.19.2 The Base Shear Coefficient	100
3.19.3 Discussion of the Results	103
3.20 Drifts and P-Delta Effect	104
3.20.1 Load Combinations.....	104
3.20.2 Redundancy Factor	106
3.20.3 Orthogonal Loading.....	107
3.20.4 The Second Order Effect	108
3.20.5 The Allowable Story Drift.....	110
CHAPTER 4.....	113
DESIGN OF SPECIAL MOMENT RESISTING FRAMES	113
4.1 Introduction.....	114
4.2 Design Rules of SMRFs.....	115
3.4 Design and Detailing of SMRFs.....	116
4.4 Modeling of RC Members	116
4.4.1 Modeling of RC Members Stiffness	116
4.4.2 Reviewing of Diaphragm Rigidity.....	117
4.5 SMRFs Layout and Proportioning	118
4.5.1 General Requirements of Special Frame Beam.....	118
4.5.2 General Requirements of Special Frame Column	119
4.6 Factored Load Patterns	120
4.7 Preliminary Design Check	123
4.7.1 Introduction and Overview	123
4.7.2 Overview of the most Important Points.....	124
4.8 Scope of the Detailed Design Examples.....	127
4.8.1 Design of the Selected Beam Span.....	129

4.8.2 Detailing of the Selected Beam	136
4.8.3 Design of the Selected Column	143
4.8.4 Detailing of the Selected Column.....	156
4.8.5 Checks on the Beam-Column Joint	160
4.8.6 Detailing of the Beam-Column Joint.....	162
CHAPTER 5.....	163
QUANTITY SURVEYING AND COST ESTIMATION	163
5.1 Introduction.....	164
5.2 Design Results from Different Evaluation Perspectives	165
5.2.1 Comparison of Concrete and Steel Quantities.....	165
5.2.2 Comparison of Materials Cost	169
CHAPTER 6.....	171
CONCLUSIONS, RECOMMANEDATIONS, AND FUTURE WORK	171
6.1 Conclusions	172
6.1.1 General Conclusions	172
6.1.2 Specific Conclusions.....	172
6.2 Recommendations	174
6.3 Future Work	176
REFERENCES	177
APPENDICES.....	196
APPENDIX A	197
SUPPORTING DOCUMENTS	197
APPENDIX B	200
CHECKS FOR SIZES OF STRUCTURAL MEMBERS	200
APPENDIX C	207
CHECKS FOR GRAVITY LOADS ANALYSIS.....	207
APPENDIX D	229
ELASTIC RESPONSE SPECTRUMS OF PROPOSED SITES	229

APPENDIX E.....	232
ACCUMULATED MODAL MASS PARTICIPATION RATIOS AS GIVEN BY SAP2000	232
APPENDIX F.....	236
SUBSTANTIATION OF FUNDAMENTAL PERIODS AND EFFECTIVE MODAL MASS RATIOS.....	236
APPENDIX G	249
VERIFICATION OF THE TOTAL DISPLACEMENT OF STORIES, STORY SHEARS, AND BASE OVERTURNING MOMENTS	249
APPENDIX H	274
P – Δ ANALYSIS	274
APPENDIX I.....	279
CHECKS OF DRIFTS LIMITS.....	279
APPENDIX J.....	289
CHECKS ON THE GEOMETRIES OF RC MEMBERS IN SMRFs	289
APPENDIX K	292
COLUMN DESIGN AIDS	292
APPENDIX L.....	297
COLUMNS BUCKLING LOADS	297
المخلص	ب

LIST OF FIGURES

Figure 1.1: 20cm thick filling material overlying 25cm ribbed slab with hidden beams	6
Figure 2.1: World's tectonic plates	15
Figure 2.2: Basic structure of Earth's surface.....	16
Figure 2.3: Seismicity map and earthquakes of the DSTF	17
Figure 2.4: Tectonic location and borders of the DSTF	18
Figure 2.5: The 11 February 2004 earthquake	19
Figure 2.6: The general components of lateral force-resisting systems	21
Figure 2.7: The effect of inertia forces	23
Figure 2.8: The resultant of seismic forces	24
Figure 3.1: Typical floor plan of the twelve buildings	35
Figure 3.2: Schematic part of the typical section of Model 3N-SR.....	37
Figure 3.3: Typical floor plan of Model 3N-SR	40
Figure 3.4: Distinguished panels which govern slab thickness of Model 3N-SR.....	41
Figure 3.5: Part of slab to be considered with internal and edge beams	42
Figure 3.6: Cross-sections of internal and edge beams in Model 3N-SR...	42
Figure 3.7: Tributary area of an interior column in Model 3N-SR.....	45
Figure 3.8: Points where moments were read for sensitivity analysis.....	51
Figure 3.9: 3D portal-frame of Model 3N-SR	55
Figure 3.10: CS and MS definition	59
Figure 3.11: Width of CS and MS along frame X2 in Model 3N-SR	59
Figure 3.12: Seismic zonation map of Palestine.....	69
Figure 3.13: Standardized elastic response spectrum referenced by the ASCE/SEI 7-10.....	78
Figure 3.14: Elastic response spectrum of Model 3N-SR	80

XIII

Figure 3.15: Maximum foreseeable side deflection of models on rock (Nablus).....	95
Figure 3.16: Maximum foreseeable side deflection of models on soft rock (Nablus).....	95
Figure 3.17: Maximum foreseeable side deflection of models on stiff soil (Nablus).....	96
Figure 3.18: Maximum foreseeable side deflection of models on soft clay (Jericho)	96
Figure 4.1: Dimensional guidelines of special frame members.....	119
Figure 4.2: RC modules contained in the calculation sheet.....	128
Figure 4.3: Definition of bending moments and beam hinges.....	130
Figure 4.4: Maximum horizontal spacing of restrained bars	132
Figure 4.5: Overhanging flange widths for torsional design	135
Figure 4.6: Reinforcement details (in centimeters) of the special beam ..	136
Figure 4.7: Anchorage details for bar size less than $\varnothing 25$	139
Figure 4.8: End hook of hoops less than 16mm in diameter	141
Figure 4.9: Spacing details of long. bars in beams	141
Figure 4.10: Local axes of the column under design	143
Figure 4.11: Cross-sectional dimensions of the restraint T-beam	145
Figure 4.12: Concepts required for strong column-weak beam theory	149
Figure 4.13: Explanatory figure illustrates the meaning of hx	150
Figure 4.14: Probable moments of beams at column top and bottom joints	153
Figure 4.15: Reinforcement details (in centimeters) of the special column	156
Figure 4.16: End hook details of $\varnothing 10$ hoops	158
Figure 4.17: Probable moments of beams generating shears on the studied joint	160

Figure 4.18: Free body diagram of the joint under investigation 160

Figure 4.19: Reinforcement details (in centimeters) of the beam-column joint
..... 162

Figure 5.1: Comparison in beams concrete volume..... 165

Figure 5.2: Comparison in columns concrete volume 166

Figure 5.3: Comparison in beams steel reinforcement 167

Figure 5.4: Comparison in columns steel reinforcement 168

Figure 5.5: Material cost for models in different locations 169

LIST OF TABLES

Table 3.1: Models information and labels	34
Table 3.2: Geometry of models.....	36
Table 3.3: Relative flexural stiffness of internal and edge beams	43
Table 3.4: The average value of the relative flexural stiffness of beams ...	43
Table 3.5: Ultimate self-weights of structural elements included within the tributary area	45
Table 3.6: Ultimate weights of distributed loads over the tributary area ...	46
Table 3.7: Procedures to elect the appropriate mesh size	52
Table 3.8: Check of equilibrium due to self-weights of structural elements in Model 3N-SR.....	56
Table 3.9: Check of equilibrium due to the distributed loads over slabs of Model 3N-SR.....	56
Table 3.10: DDM limitations and checks	58
Table 3.11: Required date before the analysis through the DDM	60
Table 3.12: Total Mu value of the slab in the CS calculated by DDM, SAP2000, and errors	61
Table 3.13: Total Mu value of the beam calculated by DDM, SAP2000, and errors	62
Table 3.14: Total Mu value of the slab in the MS calculated by DDM, SAP2000, and errors	62
Table 3.15: Mu values and corresponding errors	63
Table 3.16: Maximum expected compressive force acts on the column ...	64
Table 3.17: Tn values and their counterpart values of $CuTa$	66
Table 3.18: Declaration of prerequisites of SDC	73
Table 3.19: A proof of separation of modes	82
Table 3.20: Seismic DL of stories of Model 3N-SR.....	84
Table 3.21: Seismic SDL of stories of Model 3N-SR	84

Table 3.22: Verification of the fundamental period of Model 3N-SR	85
Table 3.23: Verification of effective modal mass ratios of the efficient modes of Model 3N-SR.....	88
Table 3.24: Maximum displacements of the generalized SDF systems of Model 3N-SR.....	90
Table 3.25: Modal and the maximum expected displacements of floors of Model 3N-SR.....	91
Table 3.26: The generalized shear forces, and the total story shears of Model 3N-SR	92
Table 3.27: The modal overturning moments, and the resultant overturning moment of Model 3N-SR	93
Table 3.28: Scaling up factors of MRS base shears.....	102
Table 3.29: Verification of MRS base shears	103
Table 3.30: Load cases defined inside SAP2000, and required to obtain δx_e values	107
Table 3.31: Generation of <i>EQ</i> load cases.....	108
Table 3.32: Stability analysis of Model 3N-SR	110
Table 3.33: Check of drift limits of Model 3N-SR.....	111
Table 4.1: Checks on limiting dimensions for RC framing members of model 3N-SR	120
Table 4.2: Ultimate loads defined inside SAP2000, and required for strength design.....	122
Table 4.3: Newest geometry of models	124
Table 4.4: <i>Tn</i> versus <i>CuTa</i> values of the new models	125
Table 4.5: Scaling up factors of MRS base shears of the new models	126
Table 4.6: Verification of MRS base shears of the new models.....	127
Table 4.7: Factored axial forces and biaxial moments obtained by computer	144

XVII

Table 4.8: Design forces and moments affecting column upper section ..	147
Table 4.9: Determination of the design capacity of the biaxial loaded column	148
Table 4.10: Column nominal moments matching axial loads	149
Table 4.11: Column maximum probable moments.....	152

LIST OF ABBREVIATIONS

<i>ACI</i>	: American Concrete Institute
<i>ASCE/SEI</i>	: American Society of Civil Engineers - Structural Engineering Institute
<i>CS</i>	: Column strip
<i>DDM</i>	: Direct design method
<i>DL</i>	: Dead load
<i>DSTF</i>	: Aqaba-Dead Sea Transform Fault
<i>EL</i>	: Earthquake load
<i>ELF</i>	: Equivalent lateral force
<i>FEM</i>	: Finite element method
<i>IBC</i>	: International Building Code
<i>JBC</i>	: Jordanian National Building Code for Loads and Forces
<i>LFRS</i>	: Lateral force-resisting system
<i>LL</i>	: Live load
<i>MRF</i>	: Moment resisting frame
<i>MRS</i>	: Modal response spectrum
<i>MS</i>	: Middle strip
<i>PGA</i>	: Peak ground acceleration
<i>PH</i>	: Plastic hinge
<i>RC</i>	: Reinforced concrete
<i>RH</i>	: Response history
<i>SDC</i>	: Seismic Design Category
<i>SDL</i>	: Superimposed dead load
<i>SMRF</i>	: Special moment resisting frame
<i>SRSS</i>	: Square root of the sum of squares
<i>SW</i>	: Shear wall
<i>UBC</i>	: Uniform Building Code
<i>2D</i>	: Two-dimensional
<i>3D</i>	: Three-dimensional
<i>1J – SC</i>	: Model sustains a $SDL = 1kN/m^2$, and built in Jericho over a soft clay layer

XIX

- 1N – R : Model sustains a $SDL = 1kN/m^2$, and built in Nablus over a rock layer
- 1N – SR : Model sustains a $SDL = 1kN/m^2$, and built in Nablus over a soft rock layer
- 1N – SS : Model sustains a $SDL = 1kN/m^2$, and built in Nablus over a stiff soil layer
- 3J – SC : Model sustains a $SDL = 3kN/m^2$, and built in Jericho over a soft clay layer
- 3N – R : Model sustains a $SDL = 3kN/m^2$, and built in Nablus over a rock layer
- 3N – SR : Model sustains a $SDL = 3kN/m^2$, and built in Nablus over a soft rock layer
- 3N – SS : Model sustains a $SDL = 3kN/m^2$, and built in Nablus over a stiff soil layer
- 5J – SC : Model sustains a $SDL = 5kN/m^2$, and built in Jericho over a soft clay layer
- 5N – R : Model sustains a $SDL = 5kN/m^2$, and built in Nablus over a rock layer
- 5N – SR : Model sustains a $SDL = 5kN/m^2$, and built in Nablus over a soft rock layer
- 5N – SS : Model sustains a $SDL = 5kN/m^2$, and built in Nablus over a stiff soil layer

LIST OF SYMBOLS

A_{ch}	: Cross-sectional area of the column core measured to the centers of the outside laterally supported longitudinal bars around the perimeter of the column
A_{cp}	: Area of the gross concrete cross-section to resist torsion
A_g	: Gross cross-sectional area of column
A_j	: Effective cross-sectional area of beam-column joint
$A_{l,min}$: Minimum area of longitudinal steel to resist torsion
A_s	: Area of beam flexural steel
$A_{s,max}$: Maximum permitted area of beam flexural steel
$A_{s,min}$: Minimum required area of beam flexural steel
$A_{sh,min}$: Minimum required area of the legs of hoops and crossties in each direction per unit length along the column confinement zones
A_{st}	: Area of column longitudinal reinforcing bars
$A_{st,max}$: Maximum permitted area of column longitudinal reinforcing bars
$A_{st,min}$: Minimum required area of column longitudinal reinforcing bars
$A_{t,min}$: Minimum area of transverse steel to resist torsion
A_v	: Area of shear reinforcement
A_v/s	: Total area of shear reinforcement per unit length along a specified length of beam
$A_{v,min}/s$: Minimum required area of web vertical bars per unit length along a specified length of the member
A_x	: Torsion amplification factor
B	: Dimension of the structure perpendicular to the direction of the earthquake loads
C	: Horizontal spacing between the center of longitudinal bar adjacent to a hoop and the nearest face of the hoop
C_1	: Resultant compressive force of a rectangular compression zone (Whitney Stress Block) as described in Section 4.8.5
C_d	: Deflection amplification factor
C_s	: Seismic response coefficient

C_u	: Factor for upper limit on the calculated period
D	: Clear spacing between longitudinal bars
DF^{bot}	: Moment distribution factor at the bottom of the column
DF^{top}	: Moment distribution factor at the top of the column
D_n	: Maximum prospective displacement of the n th-mode SDF system
E_h	: Horizontal seismic load effect
E_c	: Modulus of elasticity of concrete
E_{cb}	: Modulus of elasticity of beam concrete
E_{cs}	: Modulus of elasticity of slab concrete
E_v	: Vertical seismic load effect
F_a	: Short period site coefficient
F_v	: Long period site coefficient
I_b	: Moment of inertia of gross section of beam about neutral axis
I_{cr}	: Moment of inertia of cracked section transformed to concrete
I_e	: Earthquake importance factor
I_g	: Moment of inertia of gross (uncracked) concrete section about the neutral axis, with negligence of reinforcing bars
I_s	: Moment of inertia of gross section of slab about neutral axis
L_n^h	: Modal participation factor of an n th-mode
M_1	: Smaller factored end moment of column
M_2	: Larger factored end moment of column
M_b	: Anticipated base overturning moment of structure
M_{bo}	: Modal overturning moment
M_n	: Modal mass of the n th-mode
M_n^*	: Effective modal mass or modal participation mass of an n th-mode
M_{nb}	: Nominal flexural strength of beam
M_{nc}	: Nominal flexural strength of column
M_{no}	: Overturning moments in the n th-mode
M_o	: Total factored static moment

M_{pr}	: Probable flexural strength of the member at joint faces
M_{prc}^{bot}	: Probable flexural capacity at the bottom of the column
M_{prc}^{top}	: Probable flexural capacity at the top of the column
M_u	: Factored moment at section
M_{u2}	: Total design moments of column affecting about local axis 3
M_{u3}	: Total design moments of column affecting about local axis 3
$M_{u2,ns}$: Factored moment about local axis 2 of column cross-section under the design seismic load plus concurrent gravity
$M_{u2,s}$: Factored moment about local axis 2 of column cross-section under the design seismic load
$M_{u3,ns}$: Factored moment about local axis 3 of column cross-section under the design seismic load plus concurrent gravity
$M_{u3,s}$: Factored moment about local axis 3 of column cross-section under the design seismic load
$M_{u,hogging}$: Factored hogging moment
$M_{u,sagging}$: Factored sagging moment
M_{11}	: Plate bending moment in local direction 1
N_u	: Factored axial force normal to cross-section occurring simultaneously with V_u or T_u
P_c	: Critical buckling load of column
P_{cp}	: Perimeter of the gross concrete cross-section to resist torsion
P_i	: Resultant of the static distributed forces over each floor level
$P_{u,avg}^{bot}$: Average of the design axial loads affecting at the bottom of the column for sway in both directions within a plane
$P_{u,avg}^{top}$: Average of the design axial loads affecting at the top of the column for sway in both directions within a plane
P_u	: Factored axial force normal to member cross-section
P_{u2}	: Design uniaxial load of column section at an eccentricity e_2

XXIII

P_{u3}	: Design uniaxial load of column section at an eccentricity e_3
P_{u0}	: Maximum design uniaxial load of column section at zero eccentricities
P_x	: Accumulated unfactored vertical loads act over the level x
Q_E	: Seismic effect of orthogonal loading
R	: Response modification factor
S_1	: 5% damped, dimensionless coefficient of one second period horizontal spectral acceleration for rock
S_{D1}	: 5% damped, design spectral response acceleration coefficient at long period for deterministic site
S_{DS}	: 5% damped, design spectral response acceleration coefficient at short period for deterministic site
S_{M1}	: 5% damped, spectral response acceleration coefficient at long period for deterministic site
S_{MS}	: 5% damped, spectral response acceleration coefficient at short period for deterministic site
S_S	: 5% damped, dimensionless coefficient of short time period horizontal spectral acceleration for rock
$S_a(g)$: Maximum spectral response acceleration
T_0	: Period in the boundary between the first and the second ranges of periods
T_1	: Fundamental time period of vibration as described in Section 3.10.1
T_1	: Resultant tension force developed in the tension zone at the level of steel bars as described in Section 4.8.5
T_a	: Approximate fundamental period
T_L	: Long-transition period or the period in the boundary between the third range and the fourth range of periods
T_n	: Natural period of vibration
T_S	: Period in the boundary between the second range and the third range of periods
T_{th}	: Threshold torsional moment
T_u	: Design torsional moment at section

U	: Strength of a member or cross-section required to resist factored internal loads
$U1$: Peak value of the displacements of floors in X-Direction as given by SAP2000
V	: Total seismic force at the base of a given structure
V_c	: Nominal shear strength of concrete section
V_e	: Maximum probable shear force at joint faces
V_j	: Shear force at the center of the beam-column joint
V_n	: Nominal shear strength
V_s	: Nominal shear strength provided by shear reinforcement
V_{sway}	: Shear force at section under a design seismic action
V_u	: Factored shear force at section
V_x	: Seismic shear forces between levels x and $x - 1$
W	: Total seismic weight of structure
Z	: Seismic zone factor
a	: Depth of the equivalent rectangular compressive block
a_{pr}	: Depth of the equivalent rectangular compressive block due to the effect of M_{pr}
b_c	: Cross-sectional dimension of the column core measured to the centers of the outside laterally supported longitudinal bars around the perimeter of the column
b_s	: Slab panel width along edge axes in two-way slabs
b_w	: Width of beam web
c	: Depth of the neutral axis measured from the top surface of the member
c_1	: Width of column cross-section measured in a direction parallel to the longitudinal axis of the beam
c_2	: Width of the column cross-section measured in a plan perpendicular to the longitudinal axis of the beam
c_c	: Concrete cover
d	: Effective depth of member
$d_{agg.}$: Maximum aggregate size
d_b	: Diameter of reinforcing bar
$d_{b,min}$: Diameter of the smallest flexural reinforcing bar

$d_{b,max}$: Diameter of the largest flexural reinforcing bar
d_h	: Diameter of one leg of hoop
e_2	: Eccentricity of the factored applied load with respect to the local axis 2 of column cross-section
e_3	: Eccentricity of the factored applied load with respect to the local axis 3 of column cross-section
f'_c	: Compressive strength of concrete
f_y	: Yield strength of steel
g	: Standard acceleration due to gravity ($9.81m/s^2$)
h	: Thickness or depth of member
h_{min}	: Minimum thickness or depth of member
h_n	: Building height above the base level
h_s	: Thickness of flange/slab
h_{sx}	: Height of level x over the level $x - 1$
h_w	: Depth of beam excluding the flange
h_x	: Maximum center-to-center spacing of secured longitudinal bars around the perimeter of the column
k	: Effective length factor of column
l	: Center-to-center span length
l_1	: Span of beam measured center-to-center of the joints
l_2	: Center-to-center span length in direction perpendicular to l_1
l_d	: Development length in tension for straight bars
l_{dh}	: Development length in tension for hooked bars
l_{ext}	: Straight extension at the end of standard hook
l_n	: Clear span length
l_{n1}	: Clear span length in direction that moments are being determined
l_o	: Confinement zone length of a member
l_{st}	: Lab splice lengths of reinforcement in tension
l_u	: Unsupported length of column
m	: No. of shear reinforcing legs at section
n	: Number of stories above the base as described in Section 3.14.1

n	: No. of longitudinal bars set in one layer as described in Section 4.8.2
q_u	: Total factored load per unit area of the slab
r	: Radius of gyration of cross-section as described in Section 3.5.2
r	: Minimum inside bent radius of standard hook as described in Section 4.8.2
r_{max}	: Estimated peak value of a response component
r_n	: Force or displacement response component
s	: Center-to-center spacing of shear reinforcement
s_o	: Center-to-center spacing of hoops within the confinement zone length of column
w_i	: Seismic weight of story i
w_n	: Uniform service (unfactored) weight of the beam web
w_u	: Uniform factored weight of the beam web
α_f	: Beam relative flexural stiffness
α_{f1}	: Beam relative flexural stiffness in the studied direction
α_{f2}	: Beam relative flexural stiffness in perpendicular to l_1
α_{fm}	: Average value of α_f of all beams surrounding a panel
β	: Ratio of long to short clear span lengths as described in Section 3.5.1
β	: Ratio of the shear demand to the shear capacity of the story as described in Section 3.20.4
β_1	: Factor relates the depth of the equivalent rectangular compressive block to the depth of the neutral axis
γ_c	: Unit weight of reinforced concrete
δ_i	: Static lateral deflection at level i
δ_s	: Moment magnifier for unbraced frames
δ_x	: Amplified displacement at the floor above, measured at center of mass
δ_{x-1}	: Amplified displacement at the floor below, measured at center of mass
δ_{xe}	: Elastic displacement at each level
ε_t	: Extreme-tensile strain of flexural steel
ζ	: Damping ratio

XXVII

θ	: Stability coefficient for P-delta effects
θ_{max}	: Maximum allowable value of θ
λ	: Factor of concrete mechanical properties
ρ	: Redundancy or reliability factor
ρ_g	: Ratio of longitudinal steel area to the gross column area
$\rho_{g,min}$: Minimum reinforcement ratio in columns
\emptyset	: Diameter of reinforcing bar
ϕ_n	: Natural mode of vibration
ϕ	: Strength reduction factor
ψ_c	: Bar concrete cover factor
ψ_e	: Bar coating factor
ψ_r	: Bar confining reinforcement factor
ψ_t	: Bar location factor
ω_n	: Natural frequency of vibration
Γ_n	: Modal participation factor of an n th-mode
Δ	: Inter-story drift
$\Delta_{allowable}$: Allowable inter-story drift
Ψ	: End restraint factor of a member
Ω_o	: System overstrength factor
$(EI)_{eff}$: Effective flexural stiffness of the column cross-section
$[U_x]$: Peak value of the displacements of a structure in X-Direction
$[V_n]$: Internal story shears of the n th-mode
$[V_x]$: Maximum shear forces in stories
$[f_n]$: Equivalent static modal elastic forces applied at every story level in the n th-mode
$[m]$: Mass matrix
$[u_n]$: Column vector denotes the displacement envelop of the MDF system in the n th-mode
$[\Phi]$: Modal matrix
$[l]$: Influence vector
$[\phi_n]$: Column vector of the n th mode shape
$[\phi_n^T]$: Matrix transpose of column vector of the n th mode shape

**Enhancing Earthquake Resistance of Local Structures by Reducing
Superimposed Dead Load**

By

Hasan J. Alnajajra

Supervisor

Dr. Abdul Razzaq A. Touqan

Co-Supervisor

Dr. Monther B. Dwaikat

ABSTRACT

The geographical location of Palestine along the Aqaba-Dead Sea Transform Fault, the highest seismic active boundary in the Middle East, had put the country in a major hazard over the past history. Although seismic hazards across the area with relatively low probability, the less attention given towards seismic guidelines in both design and construction in the local practice is expected to play a significant role on the intensities of the coming ground shakings.

Ribbed slab systems supported on embedded beams and overloaded by superimposed dead loads (SDLs) are a common flooring system in the local construction industry. Literatures focus on the seismic response behavior of ribbed slabs, hidden beams, or heavy constructions indicate an earthquake-prone buildings. Hence, the existing of such undesirable factors combined exceedingly exacerbates the strength of earthquake shaking.

In this respect, the factor of SDL which is one reason of heavy construction is studied. Solid slab with drop beams construction is utilized as a flooring system in a set of reinforced concrete framed structures. The framed

structures are supposed to be built on three different soil profile types in Nablus, and one more sensitive soil profile type in Jericho. At every particular site, there are three structures sustaining a SDLs of 1kN/m^2 , 3kN/m^2 , and 5kN/m^2 . This, however, is to investigate the impact of the reduction in the SDL at different site effects on the materials cost (Concrete, and steel) of frame beams and columns.

The representative computational models are constructed, analyzed and designed using the finite element program SAP2000, Version 19.1.1. The analysis is done by means of modal response spectrum method described in the Minimum Design Loads for Buildings and Other Structure (ASCE/SEI 7-10), whereas the design is accomplished on the basis of the Building Code Requirements for Structural Concrete and Commentary (ACI 318-14).

In final conclusion, the developed approach of reducing SDL from 5kN/m^2 to 1kN/m^2 can reduce the materials cost in the skeletal elements of about 25%.

CHAPTER 1
INTRODUCTION

1.1 General

As a natural disaster, earthquakes are an inevitable geophysical phenomenon that are neither expected nor prevented. They occur all over the world and cause catastrophic havoc to the environment due to the damage of man-made structures, injuries, and death toll.

Annually, people die in natural disasters. 95% of the deaths are due to collapse of buildings in earthquakes (Jia and Yan, 2015), mostly in developing countries (Kenny, 2009). All around the globe, however, in 2015, the Emergency Events Database shows that “earthquakes killed more people than all other types of disaster put together, claiming nearly 750,000 lives between 1994 and 2013” (CRED, 2015). For the 21st century, Holzer and Savage (2013) expectations push towards shocking, about “ 2.57 ± 0.64 ” millions of fatalities worldwide due to earthquakes. Thus, earthquakes are still the supreme expensive disaster in terms of lives lost.

Without any doubt, the majority of earthquake deaths are attributable to the collapse or the damage of building structures rather than the earthquake itself. Hence, the high percentage of economic and human losses can be controlled or extremely mitigated by immersing an integrated earthquake resistance system to the building with an adequate attention to the design, detailing and construction methods.

In general, components of buildings are divided into two main groups. The first group encompasses structural components such as beams, columns, walls, footings, etc. These skeletal members are used to carry and transfer

loads on the structure safely to the approved soil stratum. The second group is the non-structural components, which are enclosed by the architectural components, the mechanical, and the electrical installations. They are essential to operate the building and to facilitate the occupant life.

Experiences from the past revealed that non-structural components are vulnerable to earthquakes (Filiatrault et al., 2001, Gillengerten, 2001).

They contribute to economic losses, threaten the human life and undermine the rescue process. For instance, the total loss of 1994 Northridge earthquake was \$18.5 billion with about 50% participation ratio accounted to non-structural damage (Qu et al., 2014). Clearly, non-structural elements have received a great attention with the advance of performance based design. The performance of a building during an earthquake is defined by the performance of both structural and non-structural components altogether (Taghavi et al., 2003). As a consequence, non-structures protection is well insured alongside the structure itself. However, seismic behavior of non-structural components still requires a proper concern (Ghogare et al., 2016).

1.2 Problem Statement

Unlike the developed countries that mainly use steel in multi-story construction (Öztürk and Öztürk, 2008), concrete construction is still preferable in the Arab world (Rizk, 2010) and in many other countries in the region. For instance, nearly 75% of Turkish construction buildings are built of reinforced concrete (RC) frames (Vona, 2014). At a local level, Palestinians are not familiar with steel construction as much as concrete.

Concrete buildings are spread in West Bank and Gaza Strip on a very large scale (Ministry of local government, 2002).

Palestine is highly vulnerable to earthquake. In addition, the vast majority of inhabited areas are prone to earthquakes (Al-Dabbeek, 2010). Seismological studies point to damaging earthquakes that are likely to strike the region (Al-Dabbeek, 2010). Past earthquakes in different countries of the world demonstrated that guidelines and provisions for earthquake resistance have been forgotten and easily neglected (Bilham, 2010). Indeed, on contrary to what has been anticipated and warned about, most of RC buildings in Palestine are designed and constructed regarding gravity loads only. Engineers rarely look into the effect of seismic and wind forces through their designs (Al-Dabbeek, 2007).

Nowadays, Engineering Bureaus Board in Palestinian Engineers Association is affirming the mandatory of seismic design. An official document on 26/11/2015 stipulated it for public buildings composed of more than seven floors (Appendix A). Henceforth, it is expected that earthquake design in Palestine will acquire a great momentum in the near future.

In West Bank and Gaza Strip, two main systems of buildings floors are commonplace, they are RC ribbed slabs, and solid slabs (Deliverable, 2014, Ministry of local government, 2002). In the past decades, solid slabs with drop beams constituted the floors of overwhelming majority of buildings (Kurraz, 2015). For the time being, waffle and ribbed slabs with shallow RC

beams are prevailing style of roofs in Palestine (Kurraz, 2015), Jordan and many other countries (Musmar et al., 2014).

Hawajri (2016), declared that “bad construction practices” along with many other factors make structures in the Palestinian Territories vulnerable to earthquakes. Ribbed slabs supported by hidden beams and overloaded by high superimposed dead loads (SDLs) are a typical feature in the multi-story buildings in Palestine. The above mentioned construction version, in author’s opinion, is one of the most principal manifestations of badness in the local construction practice. As the thesis topic focuses on the effect of SDL, it becomes necessary to note the followings:

- The SDL adjusted for wearing materials of slab and partitions is “3 to 4kN/m²” (Deliverable, 2014). This additional weight looks great compared to “0.479 to 0.718kN/m²” in the United States (Leet and Uang, 2005), for example. Additional weights tend to overweight the whole structure without any contribution to develop its stiffness. Statically, load carrying members derive their strength from size and reinforcement. Dynamically, overweight and enlargement of structural members magnify the aggressive dynamic force against the building. However, a real example for a ribbed slab with hidden beams system and overloaded by filling material is shown in Figure 1.1.



Figure 1.1: 20cm thick filling material overlying 25cm ribbed slab with hidden beams

It should be noted that in the 2010 earthquake of Haiti, and despite the millions of affected peoples and buildings, low-rise residences with lightweight roofs have had a positive impact in reducing the damage and losses (Deek, 2015). On the other hand, during 1995-Kobe earthquake of Japan, the most damage of wooden houses are because of “overweight upper floors and heavy roof-tiles of conventional Japanese style” (Iwai and Matsumori 2004).

- Water and plumbing systems are installed inside the infill material between the slab and the floor tiles. In this case, liquids leakage will be unnoticeable. In the meantime, they deteriorate both concrete and reinforcement at an increasing rate. To sum up, concrete deteriorates, steel corrodes and slab starts failure. In the latest place, piping systems are sway prohibited. In multi-story wood frame buildings, stud walls

shrinkage caused plumbing breaks (Thornburg et al., 2015). Certainly, small ground settlement or ground shaking have the capability to damage such vulnerable systems. It is worth mentioning that during Northridge earthquake, “the single most disruptive type of non-structural damage was breakage of water lines inside buildings” (Filiatrault et al., 2001).

The final analysis gives the impression that it will not be enough to know the behavior of seismic designed structures in Palestine but, it comes to be so urgent to reconsider the present construction scenario in Palestine without omitting materials cost. Materials cost, is a critical topic that cannot be condoned in developing countries due to the absence of national industry. Recently, reviewed by Kurraz (2015), building materials share with about 40% from the total construction cost of residential buildings in the Middle East developing countries.

1.3 Research Questions

Seismological studies put Palestinian cities in the seismic risk. Therefore, reviewing or altering the construction systems in Palestine seems a must.

This research project concentrates on two ultimate questions:

- How does the local construction flooring systems place structures in the seismic risk?
- To what extent does the reduced SDL enhance the seismic behavior of the structures?

1.4 Research Objectives

1.4.1 Research Overall Objective

The main idea of this research is to strengthen the earthquake resistance of buildings by decreasing the seismic generated forces acting upon their skeletons rather than increasing their lateral capacity. This proposed system is supposed to be safer, and economical than the today's system, and it does not conflict with the prevailing style of construction in Palestine. For instance, building materials available in local markets will be used. Upon the research outcomes, this new typology of buildings will be recommended as a reasonable system that may be followed in seismic areas.

1.4.2 Research Sub-objectives

- To investigate the impact of lessening the SDL on the seismic response of the structure. The SDL will be gradually lowered from 5kN/m^2 to 3kN/m^2 then, down to 1kN/m^2 .
- To display the advantages of the introduced construction system over the traditional system not only through a structural point, but also through an economic analysis of the results.

1.5 Research Scope and Limitations

Four groups of three different models of RC regular buildings of commercial and medical use will be traded herein. They are basically distinguished by the SDL they support. This difference, of course, will register many

disparities as the sizes of structural elements in each model and their fundamental periods.

This study is intended primarily for the local community in Palestine, but its benefit also extends further to other communities in neighboring countries – such as Jordan - that may use the same prototype of construction.

The Jordanian National Building Code for Loads and Forces (JBC) (MPWH, 2006) will be utilized for live load intensity. Seismic loads will be calculated as per the International Building Code Provisions (IBC 2015) (International Code Council, 2014), and the Minimum Design Loads for Buildings and Other Structures (ASCE/SEI 7-10) (ASCE, 2010). Finally, design and detailing of the structure will be carried out according to the Building Code Requirements for Structural Concrete and Commentary (ACI 318-14) (ACI 318, 2014).

The impact of earthquakes is not limited to ground shaking, other effects such as tsunami for example, are not taken in consideration throughout the design procedures of buildings and similar constructions. These are advanced topics. Usually, it is preferable to avert constructing works at locations where such hazard is potential (NIBS, 2012). It remains to mention that non-mandatory considerations like thermal and sound insulations are excluded from the comparison in all cases.

1.6 Structure of the Thesis

This research thesis consists of six chapters and twelve appendices. The followings are a summary of the contents of the chapters:

Chapter 1 (Introduction). Chapter 1 sets the problem statement, research questions, research objectives as well as research scope and limitations.

Chapter 2 (Literature review). This chapter includes a description of an earthquakes mechanism, the seismicity of the region with relevant data, the concept and requirements of earthquake resistance, and principles of seismic analysis. This chapter also contains a detailed literature review on heavy constructions and flooring systems in the context of vulnerability to earthquakes. Finally, the overall image of the suggested models is emerged.

Chapter 3 (Structural analysis). In this chapter, structural models and construction sites are carefully selected, loads and modelling criteria are outlined. Analysis results obtained from the computer aided analysis software (SAP2000) are verified thorough a series of hand calculation procedures.

Chapter 4 (Design of special moment resisting frames). This chapter highlights the concept of sway special frames, predesign requirements according to the ACI 318-14 Code. A detailed design calculation sheets for beam, column, and a beam-column joint in a special moment resisting frame are also involved.

Chapter 5 (Quantity surveying and cost estimation). In this chapter, the quantities of structural materials (concrete, and steel) consumed by skeletal members in the designed models are computed. Material costs are estimated as well. Final results are graphically presented, then discussed as a comparison among different models.

Chapter 6 (Conclusions, recommendations and future work). Chapter 6 provides conclusions drawn from the research with a focus on what has been observed from results presented in Chapter 5. Recommendations and suggestions for future works are also presented.

CHAPTER 2
LITERATURE REVIEW

2.1 Introduction

Earthquakes have disastrous consequences for most societies. A few seconds of land instability are enough to bring annihilation to the buildings and cause significant number of dead, wounded, and missing people. “In recent earthquakes, buildings have acted as weapons of mass destruction. It is time to formulate plans for a new United Nations mission — teams of inspectors to ensure that people do not construct buildings designed to kill their occupants” Bilham (2010) said.

Predominantly, the concept of RC structures sounds familiar to humankind's. Yet, over the preceding earthquakes, a lot of extensive damaged RC structures have been observed across the world (B.S and Tajoddeen, 2014). The issue can be summed up, but not limited to, negligence of the minimum requirements of code and provisions (mass irregularities, soft story, etc.), negligence of seismic design, ill-conceived construction practice, use of poor material, and unskilled labor (Isler, 2008).

Whatsoever, the behavior of multi-story RC structures that are designed and implemented in accordance with the seismic requirements could not be denied (Pampanin, 2012). Despite the recurrence of earthquakes in their home country, Japanese succeeded in mitigating the collapse of buildings through the seismic design of almost all buildings and the good Japanese code and provisions (Haseeb et al., 2011). Elsewhere, well designed RC structures in Nepal demonstrated an ability to afford earthquakes of

magnitudes up to 7.8. They suffered only slight non-structural damage (Adhikari et al., 2015).

However, the choice of thesis topic is carefully selected and argued throughout this text, detailing of the seismicity of the region, and description of real-life structures. In the meantime, scholarly materials are also analyzed comprehensively in order to derive a better feedback, and to obtain a real understanding into the sensitive issues.

2.2 Earthquakes Phenomena

2.2.1 Causes of Earthquakes

An earthquake is a broad-banded natural vibration motion of the ground caused by either natural endogenous phenomena like volcanic activities and tectonic processes, or by artificial events as explosions and collapse of cavities. Though, seismologists believe that 90 percent of all earthquakes phenomena are attributable to the tectonic movements (Armouti, 2015). Thus, earthquakes can most reliably be explained through tectonic actions.

2.2.2 Theory of Plate Tectonics

Since it was launched in the 1960s (Day, 2012), it still represents the global perspective to the worldwide seismicity model. According to the theory, as illustrated in Figure 2.1, Earth's crust is broken into at least 15 (Dowrick, 2003) large, rigid slabs of lithosphere called tectonic plates that sometimes comprise many continents.

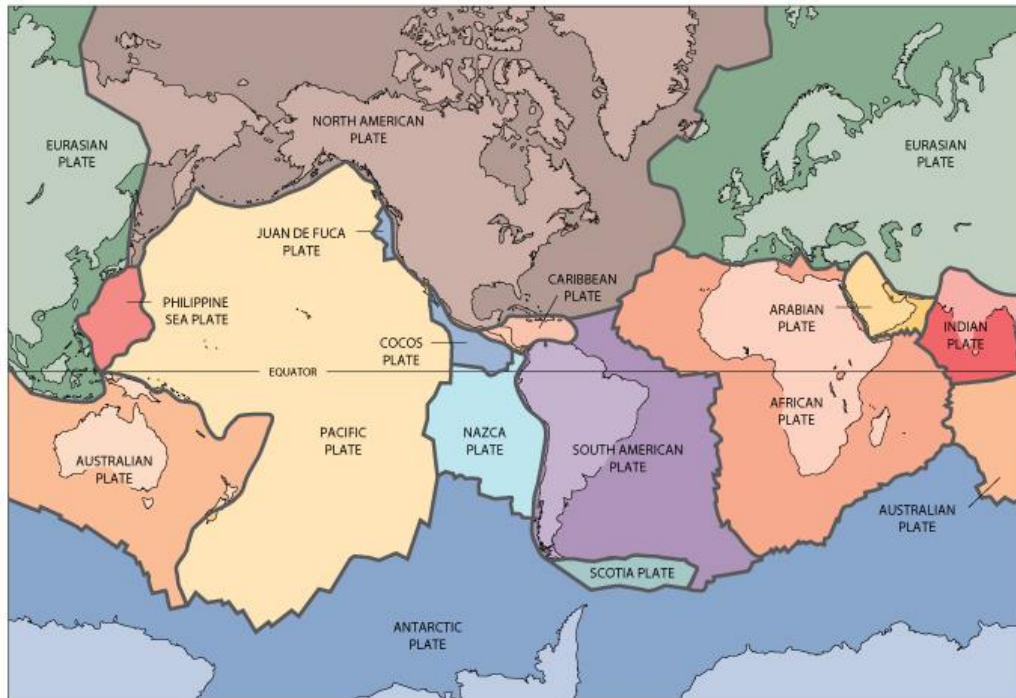


Figure 2.1: World's tectonic plates (U.S. Geological Survey, 2016)

As shown in Figure 2.2, tectonic plates are underlined by the asthenosphere layer. Asthenosphere is a soft viscoelastic shell that lets plates to move against each other. The adjacent plates are prevented from differential displacements due to the friction at their adjoining boundaries. Friction forces induce shear stresses in a form of strain energy that is stored at plate boundaries. The surface lies between two adjacent boundaries along which movement is prevented is physically termed faults and considered the source of most earthquakes (Udías et al., 2014). The moment that stored energy increases beyond the level that material strength can hold the adjacent boundaries, fracture and slippage occur along the fault interface causing a phenomenon called the elastic rebound. The elastic rebound releases the stored energy randomly in all directions surrounding the fault in the form of shock strain waves which points to the onset of an earthquake incident.

Seismic strain waves of two types are propagated. They are body waves and surface waves. These two types are further subdivided into two types: P waves, and S waves then, Love waves, and Rayleigh waves.

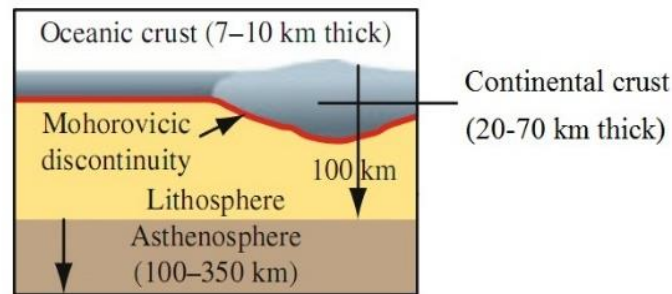


Figure 2.2: Basic structure of Earth's surface (Bangash, 2011)

2.3 Seismicity of Palestine

2.3.1 Earthquake Sources in Palestine

The State of Palestine is historically proven to be prone to earthquakes. These earthquakes were a gloom events to Palestinians due to their horrible damage and the large number of deaths, estimated in hundreds and probably in thousands (United Nations, 2014). The geographical location of Palestine puts the country along the Aqaba-Dead Sea Transform Fault (DSTF) (Levi et al., 2010) which is the most seismically active plate boundary in the Middle East (Ben-Avraham et al., 2005), chiefly eastern Mediterranean territories (Moustafa, 2015, Levi et al., 2010). Figure 2.3 demonstrates a lot of earthquakes that hit Palestine during the past centuries. Rightly, they struck along the DSTF (Al-Dabbeek et al., 2008).

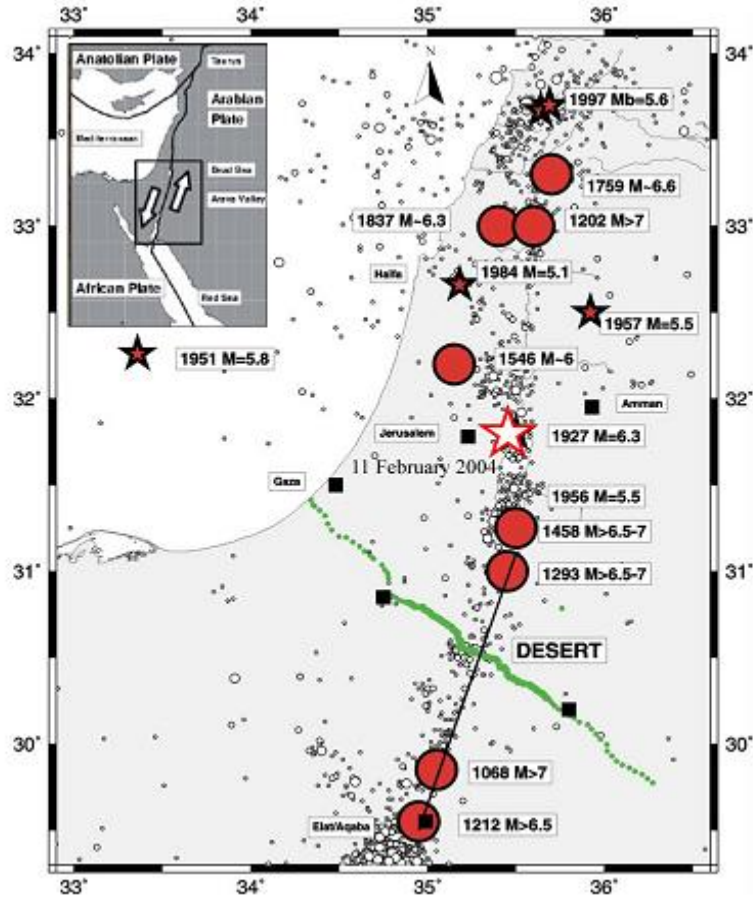


Figure 2.3: Seismicity map and earthquakes of the DSTF (Al-Dabbeek et al., 2008)

The DSTF controls the relative movement between Arabian plate to the east and Sinai sub-plate to the west. It is an approximately 1000km fault long (Klinger et al., 2015, Sadeh et al., 2012), oriented from the Red Sea at south to Taurus mountains zone in Turkey to the north (Arango and Lubkowsky, 2012, Klinger et al., 2000b). Figure 2.4 is a topographic map for the tectonic location and borders of the DSTF. Naturally, it can be inferred from the figure that DSTF sets the whole Levant at a significant hazard of earthquakes (UNDP, 2014).

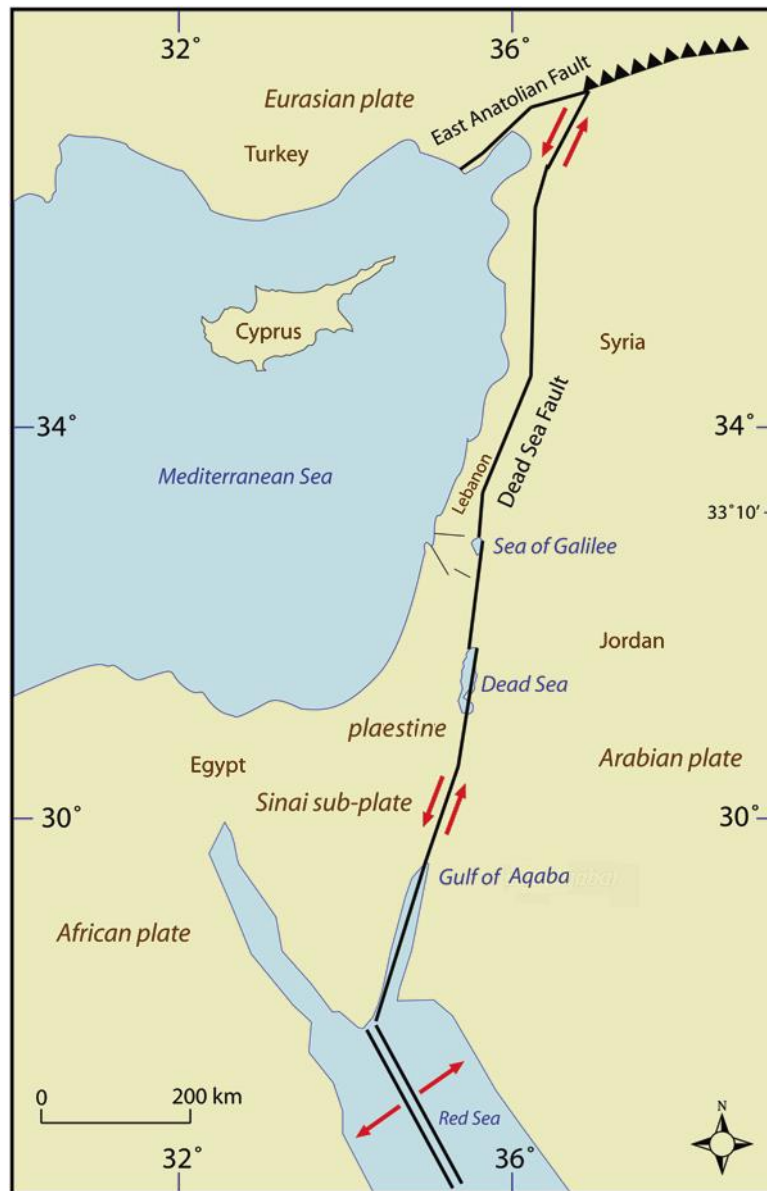


Figure 2.4: Tectonic location and borders of the DSTF (Garfunkel et al., 2014)

2.3.2 Historical Overview for the Dead Sea Earthquakes

Going back to the past, historical archives states that the DSTF has a notable historical record of damaging earthquakes with a magnitude of nearly seven (Klinger et al., 2000a). The eleventh of July 1927 registered the largest devastating earthquake. Its epicenter was at the north to Jericho with a magnitude of 6.3 (Al-Dabbeek and El-Kelani, 2005). Locally, this event is

called Nablus earthquake. Earthquakes are not discontinued, for instance, the eleventh of February 2004 earthquake which displayed in Figure 2.5, was epicentered in the Dead Sea and scored a magnitude of 4.9 (Hawajri, 2016).

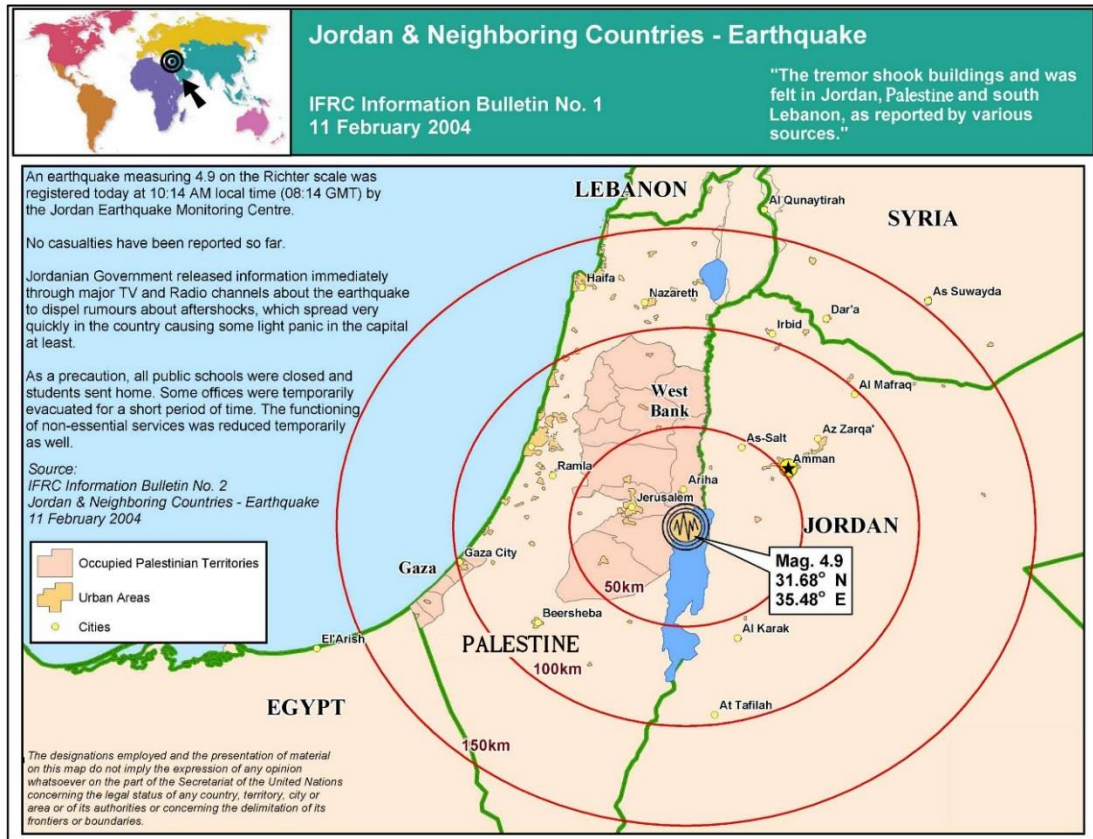


Figure 2.5: The 11 February 2004 earthquake (Hawajri, 2016)

The aforementioned earthquake was felt in Jordan, Gaza Strip and many cities in the West Bank. Fortunately, its damage was trivial with no casualties (Al-Dabbeek and El-Kelani, 2005). Then, it was followed by many other earthquakes that sometimes left a moderate structural and a non-structural damages for many local RC buildings (Hawajri, 2016).

More or less, the seismotectonic setting of the region indicates that the Dead Sea area still an active source for many damaging earthquakes beyond a magnitude of 6. They are expected to take place any time in the near future

and to leave formidable destruction and losses due to the high vulnerability of existing buildings in Palestine (Hawajri, 2016).

2.4 Earthquake Resistant Buildings

The foremost function of different kinds of buildings and structures is to support and transfer gravity loads safely (Kevadkar and Kodag, 2013). Gravity loads are vertical actions and common in nature, in a form of dead loads (DLs), live loads (LLs), and snow loads. Out of these vertical loads, a structure may experience a temporarily horizontal forces resulted from earthquakes or winds. Sometimes, they have considerable intensities and cannot be ignored. However, buildings and structures designed for gravity loads might not accommodate lateral loads (Rai et al., 2011). Therefore, providing structures with structural systems that have a sufficient strength for gravity loads coupled with a suitable stiffness for occasional horizontal loads, is really worthwhile.

2.5 Lateral-Force Resisting Systems

RC building structures resist gravity loads through the integration of slabs, columns, bearing walls, and footings. Meanwhile, they resist seismic loads through the integration of diaphragms, framing columns, shear walls, and footings. Figure 2.6, displays the common components of gravity load-carrying system, and lateral force-resisting system (LFRS).

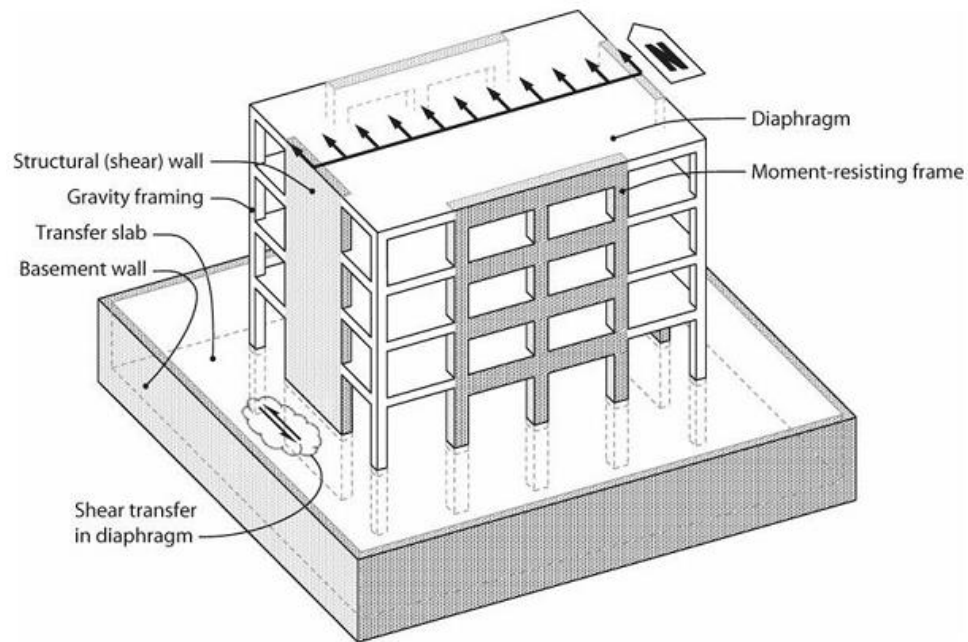


Figure 2.6: The general components of lateral force-resisting systems (Moehle, 2015)

It is worth mentioning that an earthquake resistant building does not only require a well-defined LFRS. Commitment to buildings code, seismic reinforcement, proper detailing, engineering supervision, and using of materials with a good quality are also needed (Moehle, 2015).

2.5.1 Structural Diaphragms

In RC buildings, whereas slabs carry and transmit gravity loads to the bearing system of the structure, they act as diaphragms to transmit and distribute horizontal loads to the LFRS, and to tie the structure together such that it operates as one unit in the case of an earthquake threat.

2.5.2 RC Moment Resisting Frames

Moment Resisting Frames (MRFs) are a network of RC horizontal members (beams) and vertical members (columns) connected together at rigid joints.

They are designed for both gravity and earthquake loads. Most often, they generate an adequate lateral resistance through bending resistance of girders and columns (Yakut, 2004). MRFs offer a good level of ductility such that they undergo large lateral deflections to dissipate a great energy under violent earthquakes (Elnashai and Di Sarno, 2008). MRFs are economical up to 20 – 25 stories (Arum and Akinkunmi, 2011).

2.5.3 RC Shear Walls

Shear walls (SWs) are RC vertical plates with constant cross sections ranging in width from 200 mm to 400 mm (Kevadkar and Kodag, 2013) along the entire height of construction. SWs frequently extend from the foundations to the building upstairs. They are mainly designed for earthquake loads; their influence by gravity loads is usually of minor importance (Priestley and Paulay, 1992). Contrariwise to MRFs, SWs are used to control lateral displacements (Agrawal and Charkha, 2012). However, their behavior is not as ductile as that of MRF (Chen and Lui, 2006). As a final point, SWs are economically effective for buildings up to 25 - 30 stories (Elnashai and Di Sarno, 2008).

2.6 Basics of Seismic Analysis

Perhaps what distinguishes earthquakes from most other dynamic excitations, is that earthquakes apply in a form of support motions rather than by external forces applying on the above-ground portion of buildings (Clough and Penzien, 2003). For further interpretation, in the event of

earthquakes, the internally developed inertia forces due to the vibration (acceleration) of structure mass (diaphragm and all the elements that is rigidly attached to it) are the main causative of deformations and structural deteriorations, in lieu of external imposed pressures (Booth, 2014, Taranath, 2004).

If the ground and the base of the building shown in Figure 2.7 go a sudden incipient motion to the left, the ground floor and its contents will oppose to move with the base because of the inertia of their mass that resists the motion (Taranath, 2004).

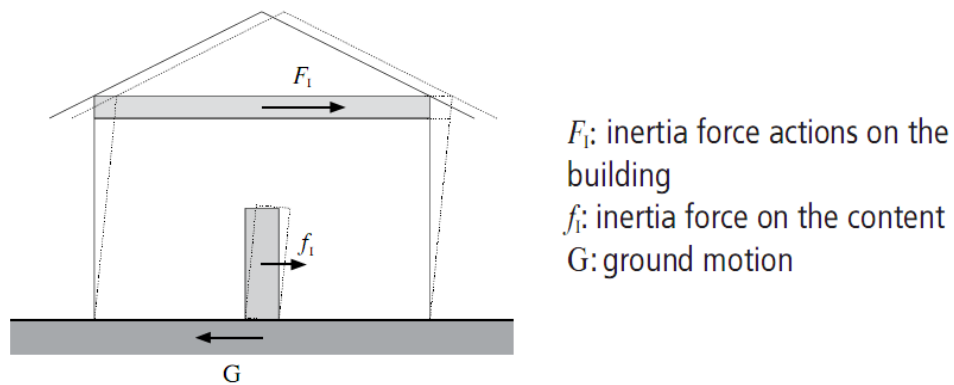


Figure 2.7: The effect of inertia forces (Arya et al., 2014)

As a result, the story with its contents will shift in an opposite direction just like if the structure is withdrawn to the right by a fictitious force, i.e. inertia force (Arya et al., 2014). These imaginary unseen forces are known as seismic loads (Ishiyama et al., 2004). Seismic loads are reversible in nature, and equal a portion of the weight of the building in their intensities (Elnashai and Di Sarno, 2008).

Most of the mass of buildings is concentrated at their ceilings (Ishiyama et al., 2004), subsequently, seismic loads are more influential at the roofs of buildings as shown in Figure 2.8.

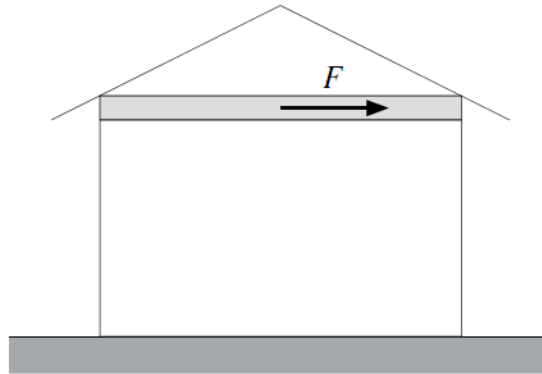


Figure 2.8: The resultant of seismic forces (Arya et al., 2014)

In fact, the deformation process is more complicated than what has been explained earlier. They may be described in three dimensions because of the simultaneous three dimensional ground motion. However, seismic loads caused by the horizontal accelerations are only regarded for earthquake design; vertical component is less than the horizontal ones (Elnashai and Di Sarno, 2008, Chen and Lui, 2006), and is also counteracted by the inherent strength of members provided for gravity design (Priestley and Paulay, 1992).

2.7 Types of RC Slabs

Civil engineers, labors, and contractors have practiced different traditional typologies of concrete slabs. Slabs could be classified with reference to different criteria such as the shape of plan, and the method of construction. Too, slabs may be assorted to one-way slabs and two-way slabs (McCormac

and Brown, 2015, Aghayere and Limbrunner, 2014, Subramanian, 2014, Nilson et al., 2010).

If the ratio of one slab panel length to its width is greater than 2, the slab is recommended to be designed as one-way slab, otherwise, it is a two-way slab. When the one-way slab is made with voids, it is called one-way ribbed slab (one-way joist system). If not, it is assigned to be one-way solid slab. A specific types of two-way slabs are waffle slabs (two-way joist systems), flat plates (two-way solid slabs) that are directly supported by columns, and flat slabs which are flat plates with column capitals and/or drop panels. However, the selection of slab type depends on economy, aesthetic features, loading, and lengths of the spans (Hassoun and Al-Manaseer, 2015).

At present, hollow slab systems have been developed by means of modern technologies. The created slab saves up to 35% of the dead weight of solid slab (Gavgani and Alinejad, 2015). Despite the almost equalized bending capacity of the two systems (Johnson et al., 2015), there still a main difference in shear resistance (Churakov, 2014) which is highly dropped in the voided slab systems.

2.8 Literature Review

Several researches on the seismic behavior of RC structures have recently been conducted worldwide and aimed to provide basic data on the safety and cost-effective versions of construction.

Mohamed (2014), investigated the lateral stability of buildings roofed by ribbed slabs. He highlighted that ribbed slabs of six stories, bare frames, RC

commercial building failed to satisfy the requirements of Egyptian Code response spectra. It has been well documented that deficient side resistance and the resulting building damage have been due to the weak frame actions resulted by the lack of deep beams. Therefore, he pointed that there is a need to retrofit these non-seismic designed buildings to improve their seismic capacity. In a closely related theme, Novelli et al. (2014) studied the seismic vulnerability of Wadi Musa city in Jordan on the basis of fragility curves. Fragility curves are utilized to estimate the value of the ground acceleration at which the failure capacity of buildings is exceeded (Kostov and Vasseva, 2000). Novelli and partners were surprised when fragility curves of modern buildings that have one way ribbed slabs of 250mm depth go over those for foregoing buildings roofed by flat slabs with a thickness of 120mm. They explained the situation on the basis that modern structures were composed of heavy slabs settled on one way frames. This led to sizeable increment in mass of the roofs, which was not met by parallel enlargement in lateral capacity of frames. Thereupon, they appear most vulnerable to the seismic risk. In another approach, Barbat et al. (2009), claimed that there is no indication inside the Eurocode 8 (CEN, 2005), International Building Code (International Code Council, 2004), and Uniform Building Code (UBC 97) (International Conference of Building, 1997) to consider systems of waffled slabs as component of an earthquake resisting system. Then, they showed that their probabilistic analysis provides a collapse probability of nearly 1% for moment resisting frame systems and 30% for waffled slab floors systems.

Finally, they recommended the depth beams as an only possible solution to develop the lateral stiffness of waffled slab floors buildings.

Another comparison was carried out by Kyakula et al. (2006). They pointed out that at shorter spans, and because of standard sizes of the manufactured blocks and minimum required thickness of topping, the total depth of the ribbed slab exceeds the required thickness of the solid slab. At medium spans, ribbed slabs need shear reinforcement, while solid ones do not need. For longer spans, topping increases the cost unreasonably. Kyakula et al. (2006), restated that keys and groves provided in hollow clay blocks enhanced the friction resistance to grip the blocks firmly in concrete. Even so, the current shape of manufactured blocks weakens shear strength of the slab.

Paultre et al. (2013) provided information on the state of construction in Haiti, and the main causes of damage of too many engineered buildings during the 12 January 2010 Haiti earthquake. They indicated that two way ribbed slabs are inadequate in zones of high seismic activity. Instead, lighter solid slabs shall be used. During earthquake events, concrete blocks in joist slabs may detach or crash and endanger people's lives.

Pardakhe and Nalamwar (2015), examined the effect of using light weight block masonry on the overall cost of construction for earthquakes. They explained that the using of light weight concrete blocks in walls has reduced the total construction cost of structures by approximately 29% of that required for constructions loaded with red brick blocks. Hence, lightweight construction is more cost-effective.

Taqieddin (2014), discussed the serviceability of wide-hidden beams under vertical loadings. He went to that hidden beams demonstrate large deflection values due to their shallow depths. The amount of compression steel reinforcement needed to recover long term deflection values at midspan overstepped the amount of reinforcement needed for flexure. He also asserts on that regardless the aesthetic appearance, other options are better on all other aspects.

Arakere and Doshi (2015), checked the performance of multi-story building made of drop beams and hidden beams during an earthquake ground excitation. They set the precedence to drop beams in the seismic design. Hidden beams result in 10% increment in both drift of model and base shear due to the decreased stiffness of the structure and its high fundamental period.

2.9 Summary

Seismic design theory defines the seismic forces in a form of horizontal actions equal a portion of the weight of the building (Elnashai and Di Sarno, 2008). As most of the building weight is concentrated at roofs and floors (Ishiyama et al., 2004); Kamali et al. (2014) introduced a perception that “one of the most important and remarkable solutions for improving the general stability of the structure is roof lightweight”.

In the midst of all the above, the outline of thesis project is:

- To use two way solid slabs with drop beams and false ceiling instead of present-day system which is two way ribbed slab with hidden beams.
- Beyond that, SDL over that slab will be decreased to the lowest permitted level.
- Then, pipes installed beneath slabs and hid through false ceiling.

Undoubtedly, the event of earthquake shakes building structure, its contents, and occupants. Therefore, designers must pay an attention towards seismic analysis and design of building structure. The suggested system, however, is expected to be an effective key to get rid of many problems:

- This category of construction is desirable in seismic zones due to the higher lateral stiffness provided by drop beams. For tall buildings established in regions of seismic activity; “ribbed-slab-column frames” is convenient as a gravity load structural system (El-Shaer, 2014).
- Solid slabs do not contain any blocks. Accordingly, neither blocks anchorage is needed, nor blocks downfall is expected.
- Covering materials do not take part in structural stiffness. Thereby, less infill material over slab will underweight the slab without prejudice to stiffness. This contributes not only to a less construction amounts of concrete and steel, but also enhances the dynamic resistance of the building against winds and earthquakes to the extent that it may allow to nullify the P-Delta effect. The notion of P-Delta

effect automatically means to induce an extra internal forces inside structural members.

- The using of flexible fittings and the placement of pipes underneath floors let them move freely and stop damage. Therein, this system is compatible with the performance based design principle and turn to save money, time, and effort exerted in maintenance. As conventional rough calculations, non-structural systems account for 40% of the total estimated cost of buildings.

CHAPTER 3
STRUCTURAL ANALYSIS

3.1 Introduction

At all the earthquakes, the stability of building structures is disturbed through a direct action (ground motion) or indirect actions (soil liquefaction, landslide hazard, etc.) (Haseeb et al., 2011). Admittedly, buildings collapse during earthquakes is ultimately attributable to the ground movement (Moehle, 2015). Hence, ground motion hazard is still capturing the attention of engineers who are interested in the seismic design of buildings.

Pursuing this further, the method, in which a structure responds when it is exposed to a sudden ground shaking, is governed by two factors (Panas 2014). The first factor is with high inaccuracy since it depends on an imperfect field data; this is the intensity of earthquake excitation. The second factor is the goodness of the structure, and estimated by its seismic design, detailing and the construction process.

The philosophy of earthquake design is that the design must fulfil the following objectives (Bertero, 1996):

- Avoid non-structural damage due to minor earthquakes which often occur.
- Avoid structural damage and to limit non-structural damage due to moderate earthquakes that occur betweenwhiles.
- Prevent downfall or the significant structural damage due to strong earthquakes which scarcely occur.

The foregoing precepts will not be really accomplished unless the building structure has an adequate strength, stiffness, and ductility alongside with a

reasonable extra implementation cost, maintenance throughout its service, and to abandon some architectural styles even if they were familiar in gravity loads design (Bertero, 1996).

3.2 Description of the Studied Buildings

Improving the resistance of structures by increasing members strength to withstand seismic forces is not always preferable (Barmo et al., 2014). Irrespective of the proven performance of light construction over the massive class as discussed previously, specifically, the study targets to quantify the positives of reducing SDLs in terms of engineering and economy indexes.

What makes the value of the study is that it encompasses nine commercial buildings built on three different host sites (rock, soft rock, and stiff soil) in Nablus. Moreover, it is broadened to include Jericho, the nearest Palestinian city to the DSTF, with three hospitals built on a soft clay soil. The study, however, utilizes a group of three RC models supposed to be contiguous at the abovementioned four different locations. To make it easier for the reader, each model adjusted a different designation as shown in Table 3.1.

Table 3.1: Models information and labels

No.	SDL (kN/m ²)	Occupancy	City	Soil Profile	Model Designation
1	1	Commercial	Nablus	Rock	1N-R
2	3	Commercial	Nablus	Rock	3N-R
3	5	Commercial	Nablus	Rock	5N-R
4	1	Commercial	Nablus	Soft rock	1N-SR
5	3	Commercial	Nablus	Soft rock	3N-SR
6	5	Commercial	Nablus	Soft rock	5N-SR
7	1	Commercial	Nablus	Stiff soil	1N-SS
8	3	Commercial	Nablus	Stiff soil	3N-SS
9	5	Commercial	Nablus	Stiff soil	5N-SS
10	1	Hospital	Jericho	Soft clay	1J-SC
11	3	Hospital	Jericho	Soft clay	3J-SC
12	5	Hospital	Jericho	Soft clay	5J-SC

Hereinafter, the name of every model consists of two parts. The first number, in the prefix, is the SDL sustained by the structure (kN/m²), and the second letter refers to the name of the city where the model is built, whereas the suffix points to the soil profile beneath the structure. For example, the designation 3N-SR means, a model sustains a $SDL = 3 \text{ kN/m}^2$, and built in Nablus over a soft rock layer.

Every model characterizes a building of ten stories above the grade. The twelve models, are alike in the framing plan, three bays by three bays, as shown in Figure 3.1. In all models, the external perimeter walls for any model are of glass. The LFRS for each model is RC special-moment resisting frames in each direction, and of 6m center-to-center apart forming 18.0m × 18.0m floor plan building.

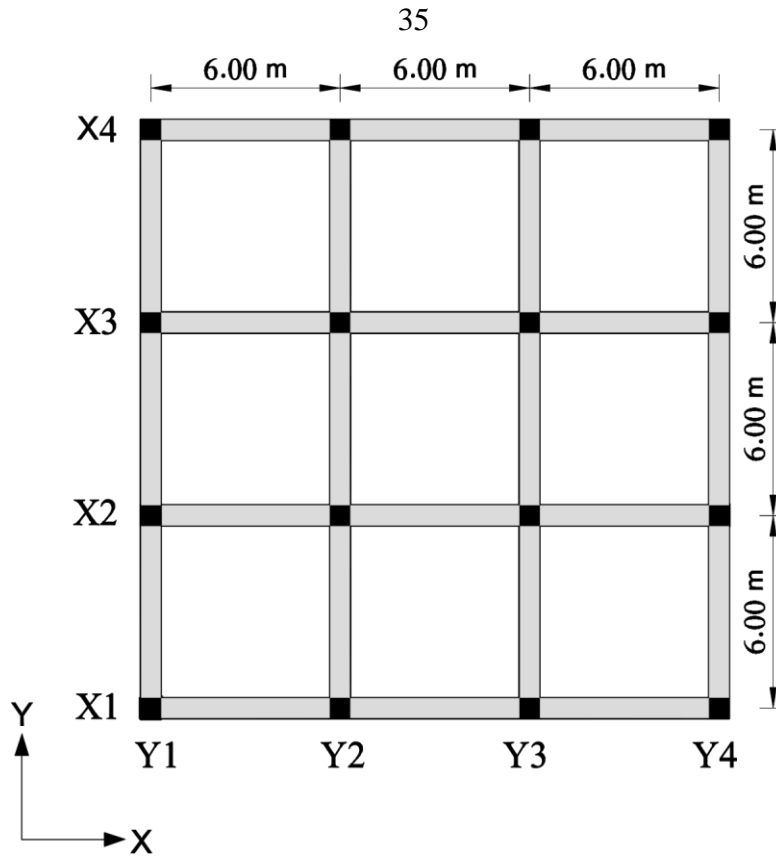


Figure 3.1: Typical floor plan of the twelve buildings

In all models, gravity loads are distributed and sustained by 13cm thick, two-way solid slabs supported by rectangular drop continuous beams run in both directions, and set centrally on columns. In every model, beams and columns are kept in the same size. The clearance of all stories is identical in all models, it is 2.95m per single story. Table 3.2, however, shows the other consequent differences between models. It should be noted that the dimensions shown in Table 3.2 have been gotten after a number of iterations so that, they are expected to realize the forthcoming requirements and checks.

For research purposes, all of the calculations regarding Model 3N-SR will be covered herein in detail. However, important parts of figures and

calculations of the other models may be briefly addressed here, while the rest will be inserted into the appendices. However, Figure 3.2 shows a typical section through Model 3N-SR.

Table 3.2: Geometry of models

Model	No. of Stories	Vertical Height (m)		Thickness of Slabs (mm)	Beams Sections (mm)		Columns Sections (mm)	
		Single story	Structure		Width	Depth	Length	Width
1N-R	10	3.4	34	130	650	400	650	650
1N-SR	10	3.4	34	130	650	400	650	650
1N-SS	10	3.4	34	130	650	400	650	650
1J-SC	10	3.4	34	130	650	400	650	650
3N-R	10	3.55	35.5	130	700	450	700	700
3N-SR	10	3.55	35.5	130	700	450	700	700
3N-SS	10	3.55	35.5	130	700	450	700	700
3J-SC	10	3.55	35.5	130	700	450	700	700
5N-R	10	3.7	37	130	750	500	750	750
5N-SR	10	3.7	37	130	750	500	750	750
5N-SS	10	3.7	37	130	750	500	750	750
5J-SC	10	3.7	37	130	750	500	750	750

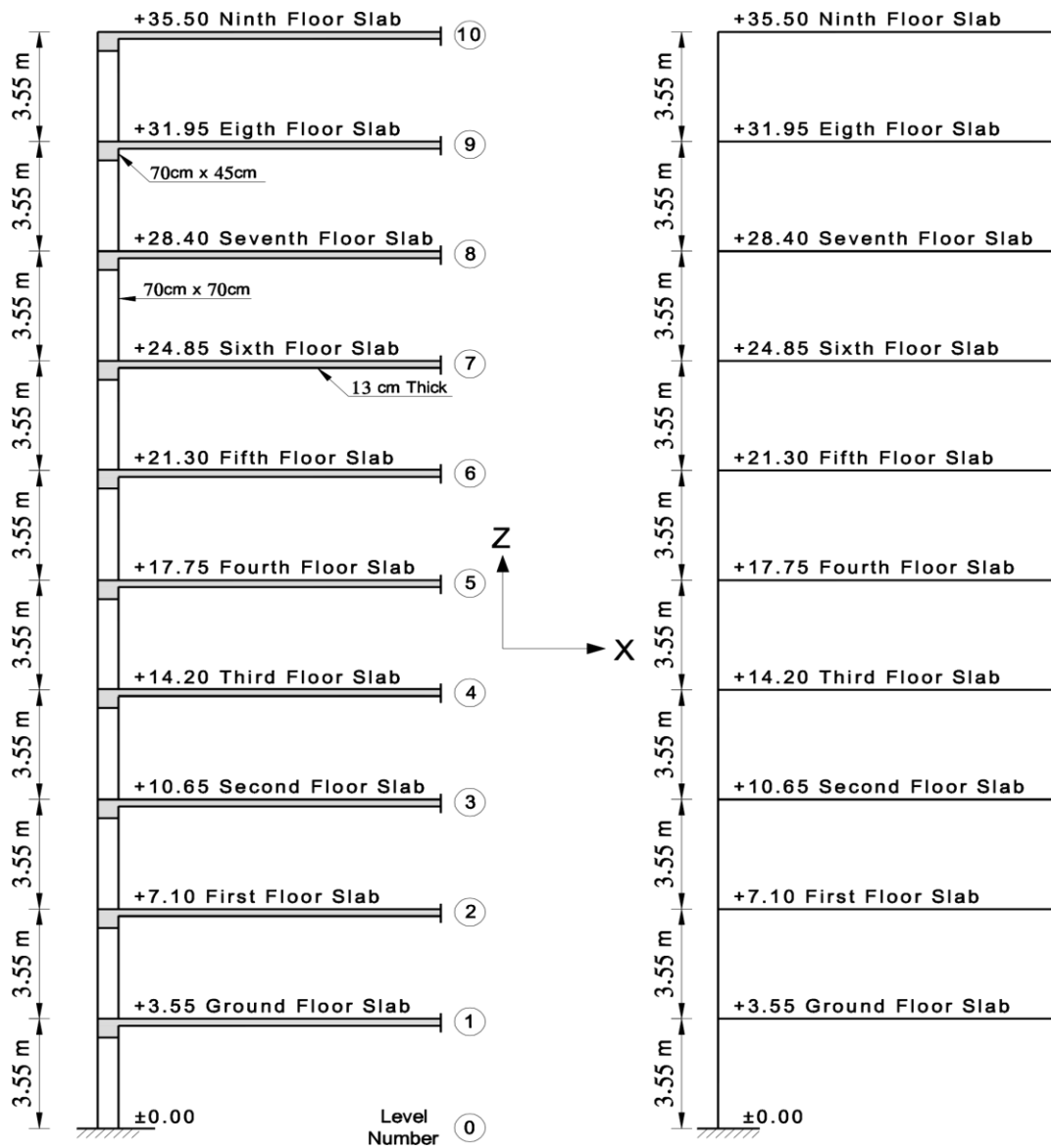


Figure 3.2: Schematic part of the typical section of Model 3N-SR

3.3 Materials Properties

RC is a construction material that is commonly used in every type of construction. If “economically designed and executed”, it became competitive structural material (Hassoun and Al-Manaseer, 2015). Plain concrete has a relatively high compressive strength, and low strength in tension. Therefore, it is primarily reinforced with steel in a form of rounded

bars to compensate its weakness in tension. This final product called RC and has a unit weight (γ_c) of $25kN/m^3$ according to the JBC (2006). The strength of plain concrete and steel bars are, typically, expressed in terms of compressive strength of concrete (f'_c), and yielding stress of steel (f_y).

For all structural elements composing the assessed models, concrete strength of $f'_c = 23.5MPa$, and steel strength of $f_y = 420MPa$ are used.

3.4 Loads on the Building

Dead and live loads in addition to seismic loads acting in the horizontal direction will only be considered during the analysis and design of models.

DL is taken as the weight of the structure itself, plus the SDL. The weight of the structure is determined by the foreknowledge of the dimensions of structural members and unit weights. The structural components of models are inherently RC. SDL is the part of DL that is assigned for partition walls, tiles and accessories, and building utilities (water pipes, air conditioning ducts, etc.) (Leet and Uang, 2005). SDLs ($1kN/m^2$, $3kN/m^2$, and $5kN/m^2$) are excerpted from the local experience of the author. Saudi Building Code (SBCNC, 2007) points $0.4kN/m^2$ as an equivalent distributed DL for the glass frame walls. Really, this value is marginal, it composes only 8 percent ($SDL = 5 kN/m^2$) to 40 percent ($SDL = 1 kN/m^2$) of the SDLs. Thus, perimeter glass walls and their loading effect are not worthwhile.

LLs are those produced by the occupancy of the building. The JBC adjusts $4kN/m^2$ as a LL for both commercial and hospital buildings.

Seismic loads cause a multidirectional vibration to buildings resting on the earth. Since the targeted structures are originally symmetrical and uniform, seismic loads along either one of the two horizontal – orthogonal - directions yield the same results, however, the attention is paid on the global X-Direction.

3.5 Validation of Members Sizes

Initial sizes of members composing a structure are required even in the case of computer analysis. They are ordinarily prerequisite to perform an elementary frame analysis, and to obtain a rough overview of the quantities of construction materials for cost estimation.

3.5.1 Minimum Slab Thickness

Fundamentally, the preliminary depths of slabs and beams are estimated to satisfy serviceability requirements. Figure 3.3 is the typical floor plan of Model 3N-SR. With reference to Table 3.2, note that:

- Slab thickness = 130mm.
- Beams sections are of 700mm width by 450mm total depth.
- Columns sections are of 700mm length by 700mm width.

As slab panels are rectangular in shape, and the ratio of long side (6000mm) to short side (6000mm) is 1.0; two way action is expected.

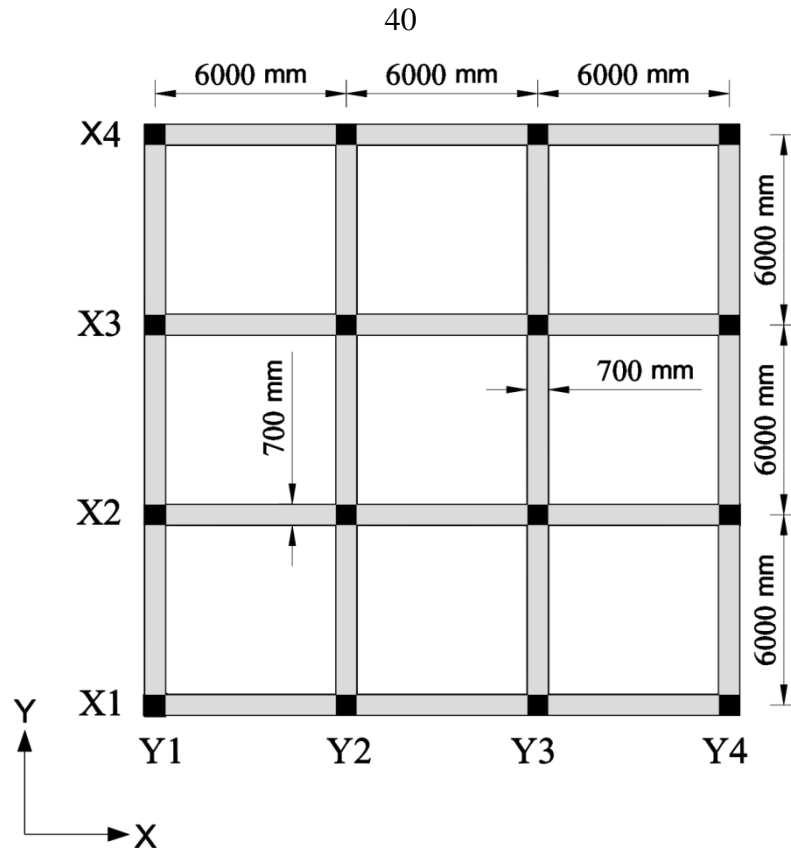


Figure 3.3: Typical floor plan of Model 3N-SR

Section 8.3.1.2 of the ACI 318-14 Code sets the minimum thickness of two way slabs resting on beams on all sides to control deflection. Slab thickness depends mainly on the average value of relative flexural stiffness of all beams (α_{fm}) on the perimeter of the panel. Beam relative flexural stiffness (α_f) is given by the ACI 318-14 Code in Section 8.10.2.7 as:

$$\alpha_f = \frac{E_{cb}I_b}{E_{cs}I_s} \quad [3.1a]$$

Where:

E_{cb} and E_{cs} are the modulus of elasticity of beam and slab concrete.

I_b is the moment of inertia of gross section of beam about neutral axis.

I_s is the moment of inertia of gross section of slab has a width defined laterally by the centerlines of panels at each side of the beam?

$$\alpha_f = \frac{I_b}{I_s} \quad [3.1b] \dots \text{for the same concrete.}$$

Figure 3.4 shows three different panels to be checked during the determination of minimum slab thickness. They are:

- Corner panel, with two edge beams, and two internal beams.
- One edge panel, with one edge beam, and three internal beams.
- Internal panel, with four internal beams.

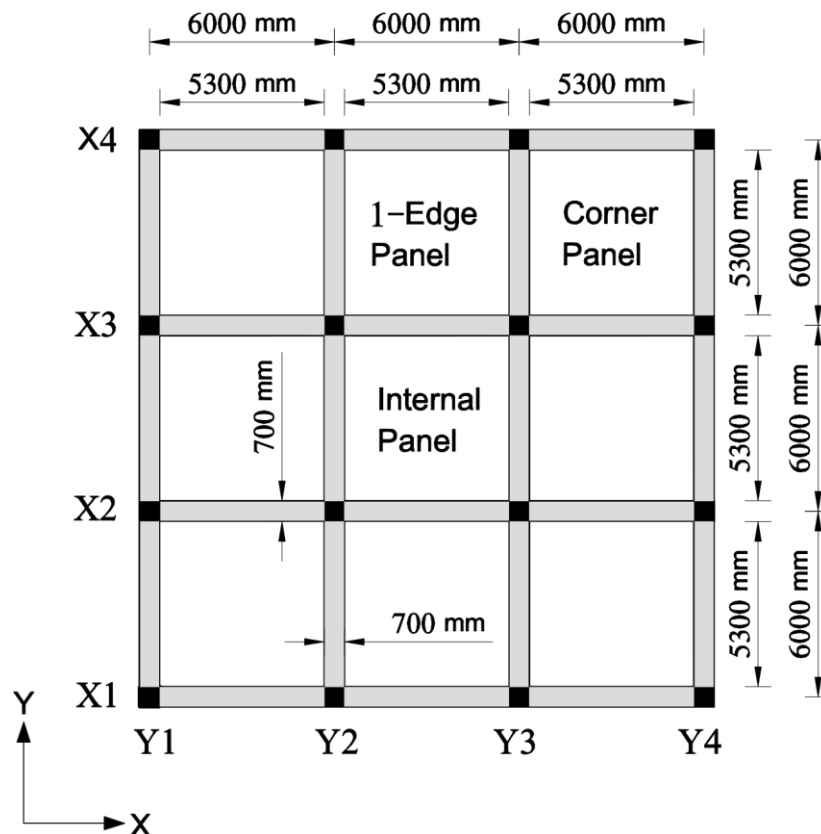


Figure 3.4: Distinguished panels which govern slab thickness of Model 3N-SR

Effective Sections of Beams

According to Section 8.4.1.8 of the ACI 318-14 Code, the flange width of beam section equals to the web width adds to an offset of slab equals to the minimum of $(h_w, 4h_s)$ on each side of the beam as shown in Figure 3.5.

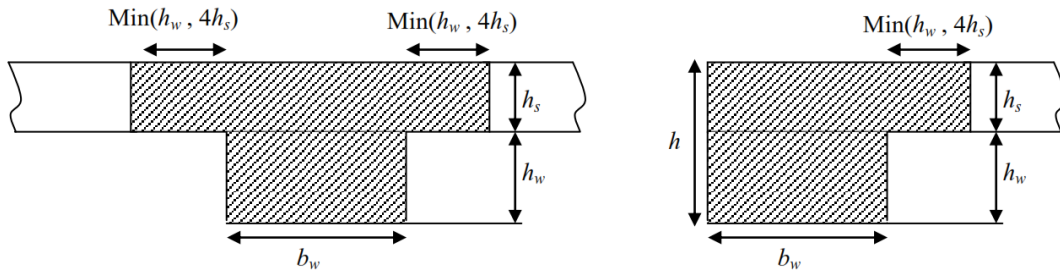


Figure 3.5: Part of slab to be considered with internal and edge beams

Thus, the added extension to the width of the principal rectangular beam is the minimum of $(h_w = 320\text{mm}, 4h_s = 520\text{mm}) = 320\text{mm}$. The cross-sections of internal and edge beams are shown in Figure 3.6.

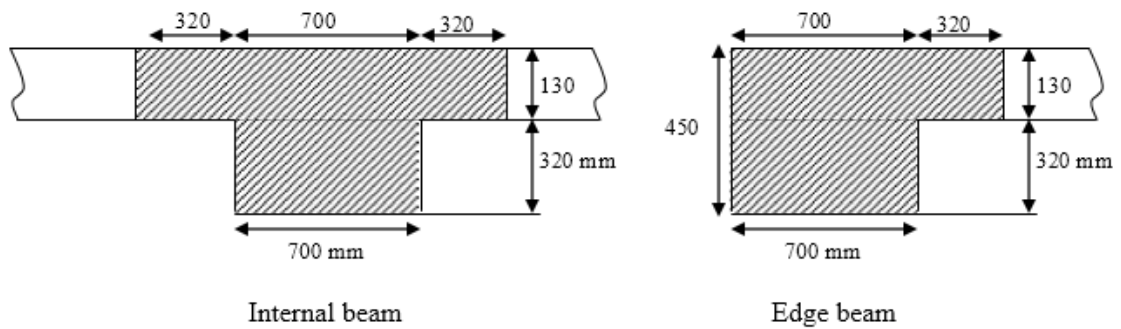


Figure 3.6: Cross-sections of internal and edge beams in Model 3N-SR

Effective Sections of Slabs

The width of the effective section of slabs (b_s) is calculated as:

$$b_s = 6000/2 + 6000/2 = 6000\text{mm} \dots \text{along the internal axes.}$$

$$b_s = 6000/2 + 700/2 = 3350\text{mm} \dots \text{along the edge axes.}$$

Flexural Stiffness of Beams and Adjacent Slabs

Table 3.3 indicates the values of the relative flexural stiffness of internal and edge beams.

Table 3.3: Relative flexural stiffness of internal and edge beams

<i>Internal Beam I_b (mm⁴)</i>	7.12E+09
<i>Internal Slab Panel I_s (mm⁴)</i>	1.10E+09
<i>Internal Beam α_f</i>	6.47
<i>Edge Beam I_b (mm⁴)</i>	6.32E+09
<i>Edge Slab Panel I_s (mm⁴)</i>	6.13E+08
<i>Edge Beam α_f</i>	10.3

Slab Thickness

Table 3.4 shows the calculation steps needed to determine the thickness of the slab.

Table 3.4: The average value of the relative flexural stiffness of beams

Panel*	Corner	Edge	Internal
l_{n1} (mm)	5300	5300	5300
l_{n2} (mm)	5300	5300	5300
l_n (mm)	5300	5300	5300
β	1	1	1
α_{fm}	8.39	7.43	6.47

* l_{n1} : Clear span length in direction that moments are being determined

l_{n2} : Clear span length in direction perpendicular to l_{n1}

l_n : Maximum clear span length

β : Ratio of long to short clear span lengths

According to Section 8.3.1.2 of the ACI 318-14 Code, for $\alpha_{fm} > 2$ then, the minimum slab thickness (h_{min}) is the greater of:

$$\frac{l_n \left(0.8 + \frac{f_y}{1400} \right)}{36 + 9\beta} \quad [3.2a]$$

$$90mm \quad [3.2b]$$

$$\Rightarrow Eq. [3.2a] = \frac{5300(0.8 + 420/1400)}{36 + 9 \times 1} = 130mm.$$

$$\Rightarrow Eq. [3.2b] = 90mm.$$

Select the most critical case, $h_{min} = 130mm$.

\therefore The actual slab thickness of $130mm \geq h_{min} = 130mm$ is thus OK.

Surprisingly, minimum slab thickness is 130mm in all of the twelve models. Calculation steps of the minimum slab thickness for the remaining models are found in Appendix B.

3.5.2 Estimating of Beams Depths

Section 9.3.1.1 in the ACI 318-14 Code specifies the minimum beams depth to govern deflection. With reference to Figure 3.3, center-to-center span length (l) is 6000mm for all spans in every story in Model 3N-SR.

$$\text{Select the most critical case, } h_{min} = \frac{l}{18.5} = \frac{6000}{18.5} = 324mm.$$

\therefore The provided 450mm depths of beams $\geq 324mm$ are thus OK.

The actual beams depths in the remaining models are also found to be conservative as shown in Appendix B.

3.5.3 Estimating of Trial Sections of Columns

Columns cross-sections have to be determined as for the load effects in the lowest story of the building. The tributary area of the most heavily loaded column is shown in Figure 3.7. Tables 3.5 and 3.6 give a brief statement of the main points required to assess the capacity of column section.

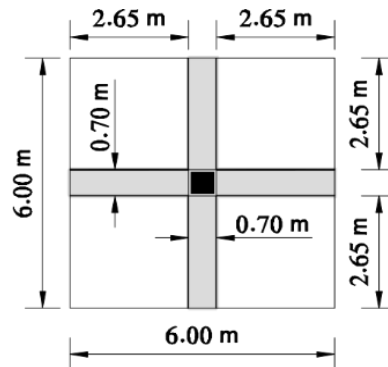


Figure 3.7: Tributary area of an interior column in Model 3N-SR

Table 3.5: Ultimate self-weights of structural elements included within the tributary area

Types of Elements in the Tributary Area	Load Factor	γ_c (kN/m ³)	Dimensions (m)			Mass and Weight Modifier*	Factored Weights of Elements (kN) in the Tributary Area
			Length	Width	Depth		
Slab	1.2	25	6	6	0.13	1	140
Beams	1.2	25	11.3	0.7	0.45	0.711	75.9
Column	1.2	25	3.55	0.7	0.7	0.873	45.6
Σ							262
Total ultimate weight of elements (kN) included within the tributary area in 10-stories							2620

* A self-weight multiplier less than 1.0 is applied for beams and columns to ensure that weight is accounted for only once at shared joints and lines

$$\text{Mass or weight modifier of beam} = \frac{\text{beam depth} - \text{slab depth}}{\text{beam depth}}$$

$$\text{Mass or weight modifier of column} = \frac{\text{column length (story height } c/c) - \text{beam depth}}{\text{column length (story height } c/c)}$$

Table 3.6: Ultimate weights of distributed loads over the tributary area

Load Pattern	Load Factor	Intensity (kN/m ²)	Tributary Area		Total Factored Loads (kN) on the Tributary Area
			Length (m)	Width (m)	
SDL	1.2	3	6	6	130
LL	1.6	4	6	6	230
Σ					360
Total ultimate weight (kN) over the tributary area in 10-stories					3600

Thus, the total factored axial force (P_u) = 2620 + 3600 = 6220kN.

The framing columns could be considered sidesway inhibited under the applied gravity loads. According to Section 6.2.5 of the ACI 318-14 Code, a braced column is being short if its slenderness ratio is:

$$\frac{kl_u}{r} \leq 34 + 12 \left(\frac{M_1}{M_2} \right) \quad [3.3a]$$

$$\frac{kl_u}{r} \leq 40 \quad [3.3b]$$

Where:

k is the effective length factor of the column.

l_u is the unsupported length of the column.

r is the radius of gyration of column cross-section.

M_1 is the smaller factored end moment of the column.

M_2 is the larger factored end moment of the column.

According to Section R6.2.5 of the ACI 318-14 Code, k could be taken equal to 1.0. To be more conservative, (M_1/M_2) is assumed to be zero.

According to Clause b of Section 6.2.5.1 of the ACI 318-14 Code, r could be taken as 0.30 times the dimension in the direction stability is being studied for rectangular columns. Hence,

$$\Rightarrow Eq. [3.3a] = \frac{1 \times (3.55 \times 0.873)}{0.3 \times 0.70} = 14 \leq (34 + 12 \times 0 = 34).$$

$$\Rightarrow Eq. [3.3b] = \frac{1 \times (3.55 \times 0.873)}{0.3 \times 0.70} = 14 \leq 40.$$

Column slenderness ratio is 14 which is less than 34; short column case.

Hassoun and Al-Manaseer (2015) stated that the maximum strength of a rectangular tied-uniaxial loaded short columns informed in Section 22.4.2.2 of the ACI 318-14 Code may be taken as:

$$P_u = 0.65 \times 0.80 \times A_g \times [0.85f'_c + \rho_g(f_y - 0.85f'_c)] \quad [3.4]$$

Where:

A_g is the gross cross-sectional area of the column.

ρ_g is ratio of longitudinal steel area to the gross column area.

$f'_c = 23.5MPa$, and $f_y = 420MPa$. Using minimum reinforcement ratio in columns ($\rho_{g,min}$) = 1.0% then,

$$6220 \times 10^3 = 0.65 \times 0.80 \times A_g [0.85(23.5) + 0.01(420 - 0.85 \times 23.5)]$$

$$\Rightarrow A_g = 499 \times 10^3 mm^2.$$

As a square section, length = width = $\sqrt{499 \times 10^3} = 706mm$.

\therefore The actual section dimensions of 700mm \approx 706mm are thus OK.

The cross-sections of columns in the other models are also OK. For more information, refer to Appendix B.

3.6 Structural Modeling

The objective of mathematical modeling is to determine the developed loads, stresses and displacements of members corresponding to any external load pattern. McKenzie (2013) declared that buildings are materialistic in nature, look like three dimensional (3D) masses, subsequently, idealizing of any structure shall be done through a model that performs its geometry, construction materials properties, supports, and the loading pattern.

Analytical and design mechanisms of spatial models are very complex, therefore, a finite element approach is inevitable. In this place, the commercially available finite element program SAP2000, Version 19.1.1 (CSI, 2017b) is adopted here to construct, analyze, and design the structural models.

3.7 Modeling Criteria

3.7.1 Members Stiffness

Modeling member stiffness upon uncracked section properties deems convenient when analyzing RC framed structures contra gravity loads; cracks propagation under service-vertical loads is somewhat trivial, member forces are inconsiderably affected (Priestley and Paulay, 1992). In the case of seismic analysis, the conventional design situation is to minimize the moment of inertia of members by a reduction factors inside codes (NIBS, 2012).

Section 12.7.3(a) of the ASCE/SEI 7-10 Standards, calls to incorporate the effect of cracking in modeling, even so, neither standards (NIBS, 2012), nor the modern world seismic codes (Bosco et al., 2008) recommend explicit parameters to express the effective stiffness of the members. Recently reviewed by Pique and Burgos (2008), Priestley (2003) confirmed that the reduction factors inside codes are still inappropriate to visualize the realistic stiffness of members as they do not consider the effect of axial and bending reinforcement. Bosco et al. (2008) indicated that the role of the coded reduction factors is still doubtful; they lead to a non-conservative results. Reduction factors result in decreasing of seismic loads, and, as a result, internal forces in members will be decreased further (Bosco et al., 2008). On top of this, Bosco et al. (2008) claimed that Paulay (1997) called to sweep these factors since they do not stand on reliable basis.

In final consideration, the typical practice procedure accept to utilize members stiffness based on the gross uncracked section properties (Pique and Burgos, 2008).

3.7.2 Base Fixity

In seismic analysis problems, ground motion is presupposed to be recognized and not depending on the response of the structure. This is analogues to say that “foundation soil is rigid, implying no soil-structure interaction”, except where the structure is constructed on “very flexible soil” where the vibration of structure affects the base motion (Chopra, 2012). In the final analysis, the

targeted soil profile types in the research are compatible with the assumption of fixed-base models.

3.7.3 Modeling Phase

- All of models are generated using centerline dimensions.
- Only structural components are involved in modeling, so that floor plates are refined as 4-nodes shell elements. All beams and columns are modeled using line elements.
- Axial, shear, flexural, and torsional deformations are involved.
- All columns are fully fixed with foundations.
- Self-weights of slabs, beams, and columns are not added, the software considers them automatically.
- Property modifiers as for mass and weight of beams and columns have to be dealt with as shown previously in Table 3.5.
- SDL, and LL contributions are represented by entering a uniformly distributed area weights identical to their intensities.
- Any other issues such as, but not limited to, diaphragm rigidity, P-delta effect will be taken up in place where needed.

3.7.4 Finite Element Mesh Sensitivity Analysis

Operating the finite element method (FEM) for analysis, displays inaccuracies between the supposed answers and the upcoming results. The accuracy of results depends mainly on the mesh density or elements size. Nevertheless, high mesh densities complicate the model, and time-

consuming. However, it is advisable to balance between the accuracy related to meshing and the time it takes to run, and to analyze the model (Coronado et al., 2011).

For this reason, mesh sensitivity study is performed to detect the appropriate level of meshing able to produce static and dynamic parameters within a reasonable domain of error.

To do that, slab panels of the fourth floor slab in Model 3N-SR (Level 5) will be subdivided into square sub-panels. When the calculated error (difference), for example, in moments between two comparable points in Figure 3.8 is less than 5%, the finer refined model will be accompanied for analysis and design, and so on.

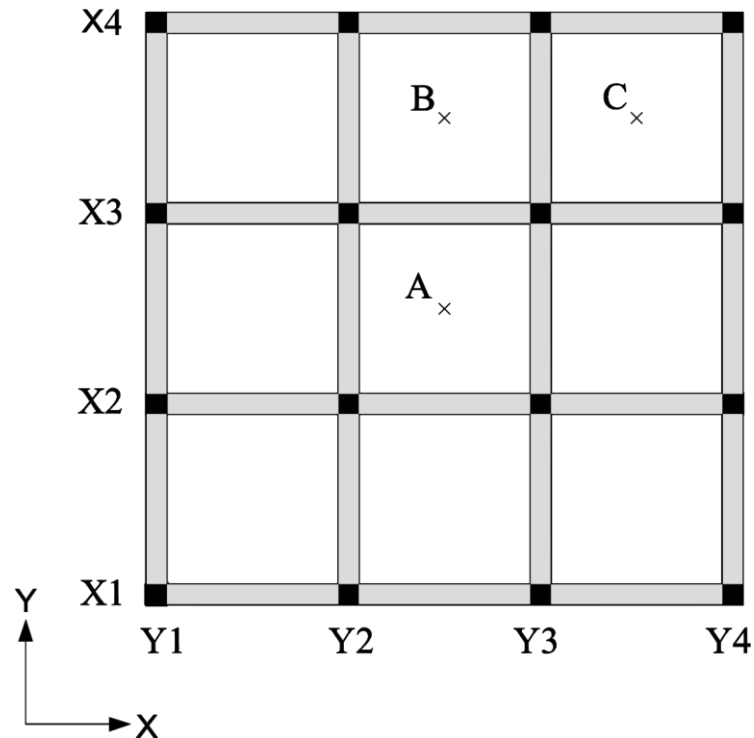


Figure 3.8: Points where moments were read for sensitivity analysis

Hereinafter, the error or difference is:

$$Error = \frac{\text{max. value} - \text{min. value}}{\text{min. value}} \times 100\% \quad [3.5]$$

At this level, note that error is calculated in a more conservative manner, that difference is divided by the smaller value. Calculations required to select the proper mesh size (0.75m × 0.75m) are shown in Table 3.7.

Table 3.7: Procedures to elect the appropriate mesh size

Case No.	Mesh Size	Moment Values (M11)* at			Error %		
		A	B	C	A	B	C
1	1.2m × 1.2m	11.3	11.3	11.6	8.85	8.85	8.62
2	1.0m × 1.0m	12.3	12.3	12.6			
3	0.75m × 0.75m	11.9	11.9	12.2	3.36	3.36	3.28

* M11 is the plate bending moment in local direction 1 as given by SAP2000
Moments are inferred from the load combination 1.2DL + 1.6LL

Error between moment values at point A in cases 2 & 3, for example, is:

$$\frac{(12.3 - 11.9)}{11.9} \times 100\% = 3.36\%$$

Since all error values between the read moments at cases 2 & 3 ≤ 5%, the third case (0.75m × 0.75m mesh size) is best fit.

3.8 Models Checking Process

By the universality of analysis and design of building structures, increased demand is placed on the computer software. “Whichever analysis method is adopted during design, it must always be controlled by the designer, i.e. not a computer!” McKenzie (2013) said. Thus, computerized results obtained

with reliance on non-checked models have to be rejected, even if they look as pretty answers.

Honestly, the producers of SAP2000 specified an acceptance criteria (CSI, 2017a) for any independent value compared to that obtained by the program as follows:

- External forces and moments. The difference shall not exceed 5% between an exact and approximate solution.
- Internal forces and moments. The difference shall not exceed 10% between two approximate solutions having similar hypothesis.
- For experimental values. The difference shall not exceed 25% between two approximate solutions having dissimilar hypothesis.

These percentages, however, should not be exceeded during the verification of the computerized answers. Otherwise, one should look for reasons!

3.9 Verification of Results for Gravity Loads Analysis

In solid mechanics, the physical impacts of any external applying loads could be described by three basic principles (Chen and Duan, 2000):

- The condition of geometrical compatibility. Meaning that elements joined at shared nodes, lines, and edges before loading, deform after loading without splitting or overlapping at the common lines (Logan, 2012).

- The equation of equilibrium. Meaning that the summation of all forces in either horizontal or vertical direction must equal zero. In addition, moments must be zero about any point.
- The generalized stress-strain relationship or constitutive law. These equations are intended to verify the meshing of the structure to capture accurately internal details of forces and displacements.

In final analysis, these three techniques are being applied to prove the results of static analysis obtained by SAP2000.

3.9.1 Check of Compatibility

Inter-elements compatibility of Model 3N-SR, shown in Figure 3.9, are tested as for the effects of the load combination $1.2DL + 1.6LL$. It is clear that the adjacent nodes endure an equal displacements without opening at shared lines. Meaning that, model compatibility has been successfully applied.

Compatibility condition is also applied in all other models as shown in Appendix C.

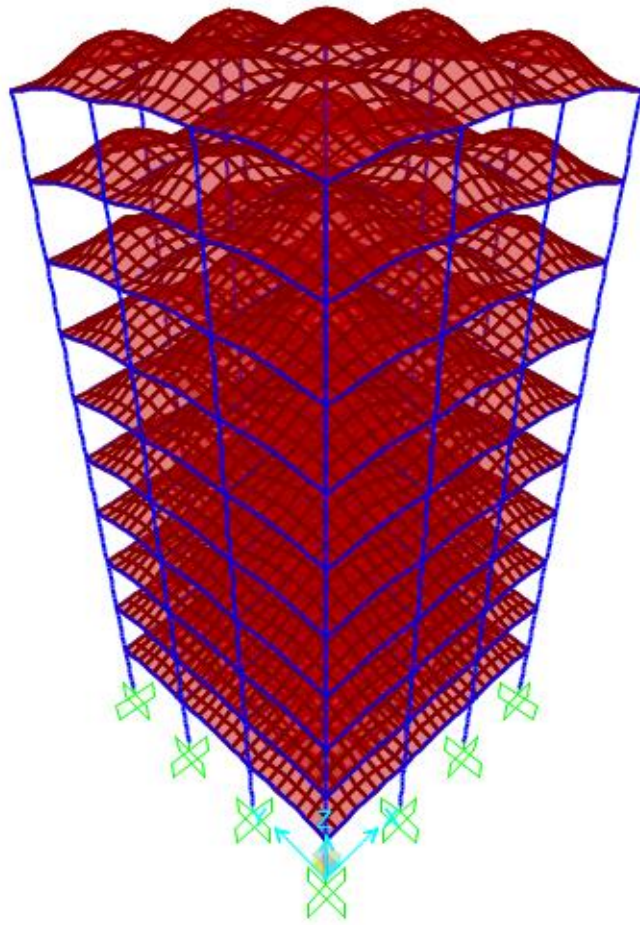


Figure 3.9: 3D portal-frame of Model 3N-SR

3.9.2 Check of Equilibrium

Gravity loads are, naturally, vertical loads. Therefore, horizontal reactions, and moments are nonexistent. Implying that only vertical reactions, i.e. global Z-Direction are arose. Tables 3.8 and 3.9 show the main components required to review the equilibrium state in Model 3N-SR resulted from service loads.

Equilibrium condition also succeeds in all other models as shown in Appendix C.

Table 3.8: Check of equilibrium due to self-weights of structural elements in Model 3N-SR

Types of Elements in Single Story	γ_c (kN/m ³)	Dimensions (m)			Mass and Weight Modifier	No. of Elements in Single Story	Weights of Elements (kN) in Single Story
		Length	Width	Depth			
Slab Panels	25	6	6	0.13	1	9	1053
Beams	25	6	0.7	0.45	0.711	24	806
Columns	25	3.55	0.7	0.7	0.873	16	608
Σ							2467
Total service weights (kN) of elements for the building (10–Stories)							24670
Global FZ (kN)– SAP2000							24670
Error %							0.00
Evaluation of error (max. 5%)							OK

Table 3.9: Check of equilibrium due to the distributed loads over slabs of Model 3N-SR

Load Pattern	Intensity (kN/m ²)	Slab Dimensions (m)		Total Load (kN) on a Single Slab
		Length	Width	
SDL	3	18	18	972
LL	4	18	18	1296
Total service SDLs (kN) for the building (10–Stories)				9720
Global FZ (kN)– SAP2000				9720
Error %				0.00
Evaluation of error (max. 5%)				OK
Total service LLs (kN) for the building (10–Stories)				12960
Global FZ (kN)– SAP2000				12960
Error %				0.00
Evaluation of error (max. 5%)				OK

3.9.3 Check of stress-strain relationship

Model 3N-SR is targeted, here, to make sure that stress-strain relationship is achieved. The check is done through two different approaches:

- Verification of moment values generated in an interior span of slab and beam.
- Verification of the value of a compressive force applies on a column.

Direct Design method

The direct design method (DDM) is an approximate method for the analysis of two way slabs (Hassoun and Al-Manaseer, 2015). It employs a set of moment coefficients to determine moment values at critical sections, and gives reliable solutions for slabs with symmetrical dimensions and loading systems (McCormac and Brown, 2015).

The check targets the total factored moments (M_u) affect the beam and both middle and column strip slabs emerged from the interior span (Y2-Y3) of frame X2 in the fourth floor slab (Level 5) of Model 3N-SR.

Checking of Model Adequacy for DDM

DDM is applicable when all of the preconditions stated by the ACI 318-14 Code, Section 8.10.2 are met. Table 3.10 shows what have been required to apply the DDM and the corresponding proofs. It is worth mentioning, that those requirements were found to be satisfied for any other model as shown in Appendix C.

Table 3.10: DDM limitations and checks

Item	<i>For every direction, there must be at least three continuous spans</i>
Check	<i>There are, exactly, three spans in every direction</i>
Item	<i>For every direction, adjacent spans measured center to center of supports, must not differ by more than one – third the longer span ($l_{short} \geq (2/3) l_{long}$)</i>
Check	<i>All spans are of 6 m long, i.e. $l_{short}/l_{long} = 1 \geq (2/3)$</i>
Item	<i>Panels must be rectangular. The longer span of the panel, measured center to center of supports, must not exceed two times the shorter span ($l_{long}/l_{short} \leq 2$)</i>
Check	<i>All spans are of 6 m long, i.e. $l_{long}/l_{short} = 1 \leq 2$</i>
Item	<i>The largest permitted offset of a column, from the general centerline, is 10% of the span in the direction of offset</i>
Check	<i>Column offsets do not exist</i>
Item	<i>All loads must be only due to gravity, and uniformly distributed over the entire panel. In addition, service live load shall not exceed two times the service dead load</i>
Check	$LL = 4 \text{ kN/m}^2$, $DL = DL_{slab} + SDL = 25 \times 0.13 + 3 = 3.25 + 3 = 6.25 \text{ kN/m}^2$, $LL < DL \Rightarrow LL < 2DL$
Item	<i>For a panel supported by beams in both directions, the relative stiffness of beam in two orthogonal directions must conform to:</i>
	$0.2 \leq \frac{\alpha_{f1} l_1^2}{\alpha_{f2} l_2^2} \leq 5.0 \quad [ACI 318-14 \text{ Code, Eq. 8.10.2.7a}]^*$
Check	$l_1 = l_2 = 6.0\text{m}$ α_f for internal beam = 6.47, α_f for edge beam = 10.3 <i>Whatever the numerator and the denominator, the above equation is satisfied</i>

* α_{f1} is the beam relative flexural stiffness in the studied direction

α_{f2} is the beam relative flexural stiffness in the perpendicular direction

Column Strip (CS) Versus Middle Strip (MS)

CS and MS have been defined in accordance with Sections 8.4.1.5, and 8.4.1.6 of the ACI 318-14 Code. CS is identified by a slab width on each side of the column centerline, as shown in Figure 3.10, and equals to 0.25 times the smaller of the panel dimensions, including beams if they are existent. The remaining portion of the panel bounded by two column strips is the MS.

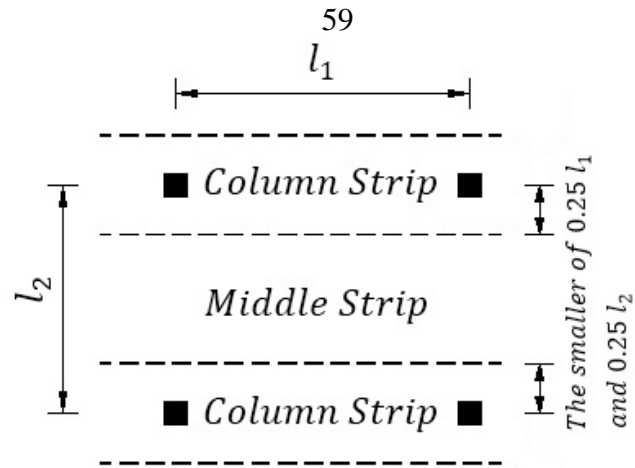


Figure 3.10: CS and MS definition

Analysis of Internal Span (Y2-Y3)

The internal span (Y2-Y3) of frame X2 is shown in Figure 3.11 and has been considered to calculate static moment values due to the effect of the load combination $1.2DL + 1.6LL$.

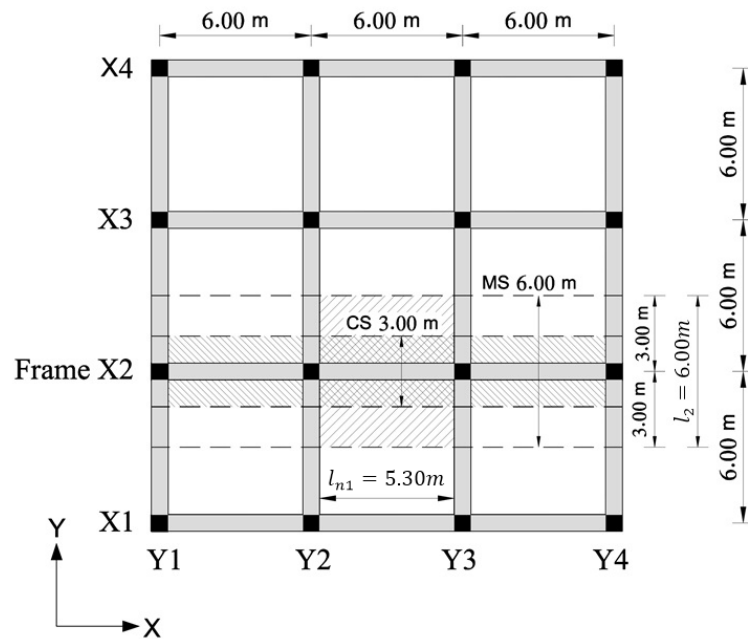


Figure 3.11: Width of CS and MS along frame X2 in Model 3N-SR

Table 3.11 contains the input data required for analysis by the DDM. Tables 3.12 through 3.14 display the calculation steps to obtain M_u values and the associated percentage of errors.

Table 3.11: Required data before the analysis through the DDM

$$l_1 = 6.0m$$

$$l_2 = 6.0m$$

$$l_{n1} = 5.30m$$

$$MS\ Width = 6.0m$$

$$CS\ Width = 3.0m$$

$$Effective\ Width\ of\ Beam = 1.34m$$

$$DL\ of\ Slab = 25 \times 0.13 = 3.25\ kN/m^2$$

$$SDL\ on\ Slab = 3\ kN/m^2$$

$$LL\ on\ Slab = 4\ kN/m^2$$

$$q_u = 1.2 \times (DL + SDL) + 1.6LL = 13.9\ kN/m^2$$

$$W_{n(Self-weight\ of\ the\ Web\ of\ the\ Beam)} = \gamma_c \times 0.7 \times 0.32 = 5.60\ kN/m$$

$$W_{u(Self-weight\ of\ the\ Web\ of\ the\ Beam)} = 1.2 \times w_n = 6.72\ kN/m$$

$$\alpha_{f1} = 6.47$$

$$l_2/l_1 = 1.0$$

$$\alpha_{f1} l_2/l_1 = 6.47$$

Table 3.12: Total M_u value of the slab in the CS calculated by DDM, SAP2000, and errors

<i>According to Section 8.10.3.2 of the ACI 318 – 14 Code; the Total Factored Static Moment</i>		
<i>of the Span is $M_o = \frac{q_u \times l_2 \times (l_{n1})^2}{8} = \frac{13.9 \times 6 \times (5.3)^2}{8} = 293 \text{ kN.m}$</i>		
<i>Moment Coefficients of the Interior Span According to Section 8.10.4.2 of the ACI 318 – 14 Code</i>		
-0.65	0.35	-0.65
<i>Total M_u at the Ends and the Middle of the Span (kN.m)</i>		
$-0.65 \times 293 = -190$	$0.35 \times 293 = 103$	$-0.65 \times 293 = -190$
<i>According to Sections 8.10.5.1, and 8.10.5.5 of the ACI 318 – 14 Code; % Moments in CS = 0.75</i>		
<i>According to Sections 8.10.5.7.1 of the ACI 318 – 14 Code; % Moments of Slab in CS = $1 - 0.85 = 0.15$</i>		
<i>M_u at the Ends and the Middle of the Slab in the CS (kN.m/m); DDM</i>		
$\frac{0.75 \times 0.15 \times -190}{(3 - 1.34)} = -12.9$	$\frac{0.75 \times 0.15 \times 103}{(3 - 1.34)} = 6.98$	$\frac{0.75 \times 0.15 \times -190}{(3 - 1.34)} = -12.9$
<i>M_u at the Ends and the Middle of the Slab in the CS (kN.m/m); M11 – SAP2000</i>		
-8.64	5.42	-8.64
<i>Total M_u of Slab in the CS; DDM = $\frac{2 \times -12.9 }{2} + 6.98 = 19.9 \text{ kN.m/m}$</i>		
<i>Total M_u of Slab in the CS; SAP2000 = $\frac{2 \times -8.64 }{2} + 5.42 = 14.1 \text{ kN.m/m}$</i>		
<i>Error = $\frac{19.9 - 14.1}{14.1} \times 100\% = 41.1\% > 25\%$</i>		<i>(Not OK)</i>

Table 3.13: Total M_u value of the beam calculated by DDM, SAP2000, and errors

<i>From the Previous Table; Total M_u at the Ends and the Middle of Span (kN.m)</i>		
-190	103	-190
<i>According to Sections 8.10.5.1, and 8.10.5.5 of the ACI 318 – 14 Code; % Moments in the CS = 0.75</i>		
<i>According to Sections 8.10.5.7.1 of the ACI 318 – 14 Code; % Moments of the beam in CS = 0.85</i>		
<i>The Total Factored Static Moment due to the Self – Weight of Web of the Beam is</i>		
$M_o = \frac{w_u \times (l_{n1})^2}{8} = \frac{6.72 \times (5.3)^2}{8} = 23.6 \text{ kN.m}$		
<i>Moment Coefficients of the Interior Span According to Section 8.10.4.2 of the ACI 318 – 14 Code</i>		
0.65	0.35	0.65
<i>M_u at the Ends and the Middle of the Beam (kN.m); DDM</i>		
$(0.75 \times 0.85 \times -190) + (-0.65 \times 23.6) = -136$	$(0.75 \times 0.85 \times 103) + (0.35 \times 23.6) = 73.9$	$(0.75 \times 0.85 \times -190) + (-0.65 \times 23.6) = -136$
<i>M_u at the Ends and the Middle of the Beam (kN.m); M3 – SAP2000</i>		
-122	99.7	-122
<i>Total M_u of the Beam ; DDM = $\frac{2 \times -136 }{2} + 73.9 = 210 \text{ kN.m}$</i>		
<i>Total M_u of the Beam ; SAP2000 = $\frac{2 \times -122 }{2} + 99.7 = 222 \text{ kN.m}$</i>		
<i>Error = $\frac{222 - 210}{210} \times 100\% = 5.71\% \leq 25\%$ (OK)</i>		

Table 3.14: Total M_u value of the slab in the MS calculated by DDM, SAP2000, and errors

<i>From the Previous Table; Total M_u at the Ends and the Middle of Span (kN.m)</i>		
-190	103	-190
<i>% Moments in MS = 1 – % Moments in MS = 1 – 0.75 = 0.25</i>		
<i>M_u at the Ends and the Middle of the MS (kN.m/m); DDM</i>		
$\frac{0.25 \times -190}{(6-3)} = -15.8$	$\frac{0.25 \times 103}{(6-3)} = 8.58$	$\frac{0.25 \times -190}{(6-3)} = -15.8$
<i>M_u at the and the Middle Ends of the MS (kN.m/m); M11 – SAP2000</i>		
-12.0	10.0	-12.0
<i>Total M_u of the MS; DDM = $\frac{2 \times -15.8 }{2} + 8.58 = 24.4 \text{ kN.m/m}$</i>		
<i>Total M_u of the MS; SAP2000 = $\frac{2 \times -12.0 }{2} + 10.0 = 22.0 \text{ kN.m/m}$</i>		
<i>Error = $\frac{24.4 - 22.0}{22.0} \times 100\% = 10.9\% \leq 25\%$ (OK)</i>		

Commentaries

Table 3.15 compares the values of the total factored moments M_u affecting the beam and both middle and column strip slabs emerged from the interior span (Y2-Y3) of frame X2 in the fourth floor slab (Level 5) of all the investigated buildings. Models are represented by the means of the SDL they support.

Table 3.15: M_u values and corresponding errors

Item	SDL=1kN/m ²	SDL=3kN/m ²	SDL=5kN/m ²
M_u of the Slab in the CS (kN.m/m) – DDM	15.4	19.9	25.1
M_u of the Slab in the CS (kN.m/m) – SAP2000	13.5	14.1	15.2
Error in M_u of the Slab in the CS (%)	14.1	41.1	65.1
Evaluation of Percentage of Error	OK	Not OK	Not OK
M_u of the Beam (kN.m) – DDM	177	210	243
M_u of the Beam (kN.m) – SAP2000	178	222	264
Error in M_u of the Beam (%)	0.565	5.71	8.64
Evaluation of Percentage of Error	OK	OK	OK
M_u of the MS (kN.m/m) – DDM	20.6	24.4	28.1
M_u of the MS (kN.m/m) – SAP2000	18.7	22.0	25.1
Error in M_u of the MS (%)	10.2	10.9	12.0
Evaluation of the Percentage of Error	OK	OK	OK

It is clear that for models sustaining $SDLs = 3 \text{ kN/m}^2$, and 5 kN/m^2 , the error in M_u value for the slab defined between the outer edges of beam flange and the outside boundary of the CS has exceeded the permitted value (Not OK).

It is feasible, if not likely, that the defect is because that the ACI 318-14 Code does not consider the increased capability of deep girders to absorb portions

of CS slab moments as the value $\alpha_{f_1}l_2/l_1$ increases. For beams with $\alpha_{f_1}l_2/l_1 \geq 1.0$, Section 8.10.5.7.1 of the ACI 318-14 Code always limits the beam portion of moments in CS by 0.85 which may not be true. This, however, could be highlighted on the basis that SAP2000 considers the development in $\alpha_{f_1}l_2/l_1$ value. As the beam section grows, moments obtained by SAP2000 go over those calculated as per the DDM.

Check of Column Compressive Force

The axial compressive force exerted on an interior column in the ground floor level has to be calculated and compared to that assigned by SAP2000 as in Table 3.16.

Table 3.16: Maximum expected compressive force acts on the column

Load Pattern	Reference	Ultimate Load Value (kN) in 10–stories
Weight of slabs, beams, columns	Table 3.5	2620
Distributed SDL & LL	Table 3.6	3600
	Σ	6220
	Global FZ (kN)–SAP2000	5981
	Error %	4.00
	Evaluation of error (max. 10%)	OK

Commentaries

The same approach is followed for all models as will be seen in Appendix C. The axial compressive force obtained by SAP2000 was less than that calculated by the tributary area method. This could be illustrated on the basis that SAP2000 considers the axial deformation of columns. Since the interior columns experience more axial deformations than the external columns, light

loaded (outer) columns interfere to maintain the structural stability by carrying part of loads sustained by the heavy loaded columns. Thus, this step is responsible for lowering the compressive force acts on the interior columns.

3.10 Earthquake Consequences on Structures

The response of a structure to a ground motion activity depends on its natural period (T_n) and damping ratio (ζ) (Booth, 2014, Chopra, 2012). Therefore, the determination of these two parameters is the first step towards any earthquake analysis and design process.

3.10.1 The Fundamental Natural Period

Natural period T_n is the time taken by undamped system to complete one cycle during free vibration. The fundamental time period (T_1) of building skeletons refers to the first mode period which is always the longest modal time of vibration in the horizontal direction of interest. Time periods for the first mode and the subsequent modes of 3D models are gained from most structural analysis computer software. The referenced fundamental periods in Table 3.17 of models under research are reported by SAP2000 analysis. Periods calculated by a rigorous mathematical modeling of RC structures are, obviously, highly sensitive to stiffness assumptions (Ghosh and Fanella, 2003). To make sure that significant low design base shear is not due to a doubtful long time period caused by either unrealistic stiffness reduction factors (Ghosh and Fanella, 2003), or unduly modeling simplifications

(NIBS, 2012), or undetected modeling errors (NIBS, 2009), building codes impose a limit on the fundamental periods produced by rational structural analysis.

Table 3.17: T_n values and their counterpart values of $C_u T_a$

Model	S_{D1}^a	T_1 (sec) ^b	C_t	x	h_n (m)	T_a (sec)	C_u	$C_u T_a$ (sec)	Check ^c
1N-R	0.250	1.49	0.0466	0.900	34	1.11	1.45	1.61	OK
3N-R	0.250	1.54	0.0466	0.900	35.5	1.16	1.45	1.68	OK
5N-R	0.250	1.55	0.0466	0.900	37	1.20	1.45	1.74	OK
1N-SR	0.388	1.49	0.0466	0.900	34	1.11	1.40	1.56	OK
3N-SR	0.388	1.54	0.0466	0.900	35.5	1.16	1.40	1.62	OK
5N-SR	0.388	1.55	0.0466	0.900	37	1.20	1.40	1.68	OK
1N-SS	0.475	1.49	0.0466	0.900	34	1.11	1.40	1.56	OK
3N-SS	0.475	1.54	0.0466	0.900	35.5	1.16	1.40	1.62	OK
5N-SS	0.475	1.55	0.0466	0.900	37	1.20	1.40	1.68	OK
1J-SC	0.938	1.49	0.0466	0.900	34	1.11	1.40	1.56	OK
3J-SC	0.938	1.54	0.0466	0.900	35.5	1.16	1.40	1.62	OK
5J-SC	0.938	1.55	0.0466	0.900	37	1.20	1.40	1.68	OK

^a S_{D1} values are quoted from Table 3.18

^b T_1 values are reported by SAP2000 as in Appendix E

^c Check is OK if $T_1 \leq C_u T_a$

In the same way, Section 12.8.2 of the ASCE/SEI 7-10 Provisions defines an upper bound value that shall not be exceeded by the rationally computed period T_1 as:

$$\text{Upper limit on } T_1 = C_u T_a \quad [3.6]$$

Where:

C_u is the factor for upper limit on the calculated period determined from Table 12.8-1 of the ASCE/SEI 7-10.

T_a is the approximate fundamental period.

Section 12.8.2.1 of the ASCE/SEI 7-10 provides an empirical formula to calculate the approximate period of Vibration T_a as follows:

$$T_a = C_t h_n^x \quad [3.7]$$

Where:

C_t and x values are determined from Table 12.8-2 of the ASCE/SEI 7-10.

h_n is the building height (above the base) in meters.

Note that fundamental periods of intended models are found to be under their upper limit as in Table 3.17.

3.10.2 Damping

Once the seismic activity on a building decays, the amplitude of vibration dies away steadily with time. This form of energy dissipation is called damping. For civil engineering structures, ζ is a unitless measure of damping (Chopra, 2012) with a value less than 10% (Chopra, 2012, Elnashai and Di Sarno, 2008). A near-universal assumption, yet, is that $\zeta = 5\%$ (Williams, 2016, Booth, 2014). This percent is also explicitly applied for each mode inside SAP2000. Considering that when $\zeta \leq 20\%$, damping effect on periods or frequencies of vibrated systems are almost biliary (Sucuoglu, 2015, Chopra, 2012).

3.11 Ground Motion Input Parameters

The time variation of ground acceleration is the most common way of identifying the seismic intensity of earthquakes (Chopra, 2012). In

earthquake engineering, ground motion parameters are often defined by the most predicted destructive potential of an earthquake ground motion, i.e. the peak values. Hence, the horizontal peak ground acceleration (PGA) seems a reasonable metric of the ground shaking. PGA is usually given in forms of the seismic zone factor (Z). Z is a dimensionless coefficient of the expected horizontal PGA as (SII, 2009):

$$Z = \frac{PGA}{g} \quad [3.8]$$

Where:

PGA is what experienced by a particular station on rock during an earthquake.

g is the standard acceleration due to gravity ($9.81m/s^2$).

According to the NIBS (2012), the ASCE/SEI 7-10 defines the hazard of seismic action based on three parameters. The first two values are dimensionless coefficients (S_S, S_1) of spectral accelerations quantified in terms of 2% of being exceeded in 50 years; 2475-years return period (Charney, 2015). The third value is the spectral time period (T_L) that expresses the commencement of long period behavior.

Nevertheless, the basic ground motion parameters (S_S, S_1) corresponding to 10% probability occurs of being exceeded in 50 years (475-years return period) is closer to the low to high seismicity of Palestine. This trend is also prevalent in a number of building codes as in Israel (Amit et al., 2015), Jordan (Jimenez et al., 2008), Saudi Arabia (SBCNC, 2007), and Eurocode 8 (Fardis et al., 2015). Figure 3.12, however, marks a definite value of Z on

the rock for various communities of Palestine, with a reference exceedance probability of 10% in 50 years.

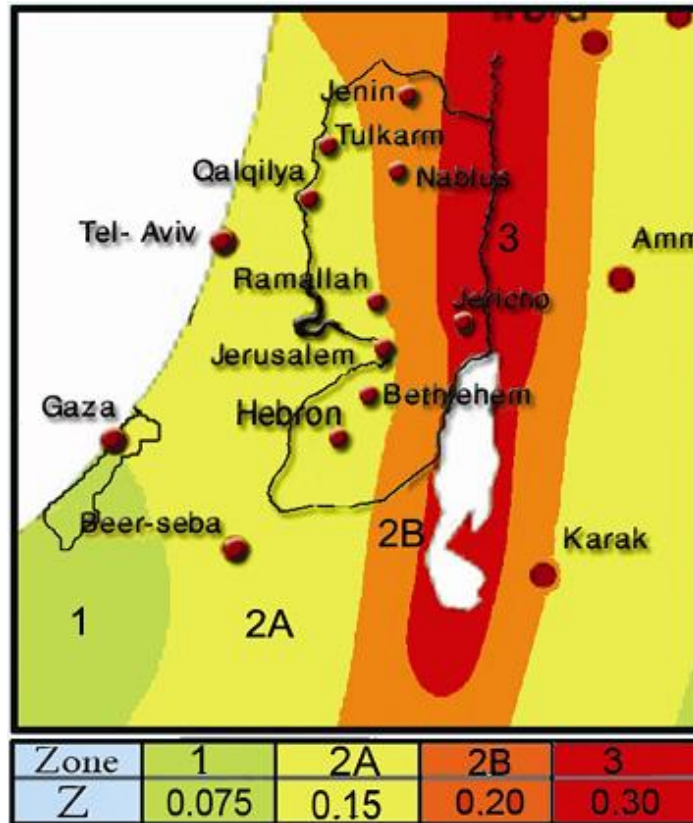


Figure 3.12: Seismic zonation map of Palestine (ESSEC, 2017)

- S_5 is the 5% damped, dimensionless coefficient of short time period ($T = 0.2\text{sec}$) horizontal spectral acceleration for rock or site class B (ASCE, 2010).
- S_1 is the 5% damped, dimensionless coefficient of one second period horizontal spectral acceleration for rock or site class B (ASCE, 2010).
- T_L is a long-transition period in seconds resembles the onset of the constant-displacement spectral plateau (Sucuoglu, 2015). For Palestinian Territories, T_L could be taken as 4.0sec. (SII, 2009).

The 50-years horizontal spectral acceleration coefficients could be assumed as (SII, 2009):

$$S_5 = 2.50Z \quad [3.9]$$

$$S_1 = 1.25Z \quad [3.10]$$

3.12 Seismic Analysis Approach

3.12.1 Seismic Design Category

Seismic codes use the Seismic Design Category (SDC) concept to “regulate the resistance of the structure to earthquake-induced failure through various design and detailing measures” (Hamburger, 2009).

Step 1: Select the most appropriate Risk Category.

Risk Category is a ranking given to buildings based on the risk accompanying inadmissible performance in the event of earthquakes (ASCE, 2010), and is determined from Table 1.5-1 of the ASCE/SEI 7-10.

Step 2: Set the earthquake importance factor I_e .

I_e is a factor to provide further strength for risk-critical entities (Charney, 2015), and is determined from Table 1.5-2 of the ASCE/SEI 7-10.

Step 3: Based on the location of the building, determine S_5 and S_1 values.

Step 4: Upon the Soil profile name, assign the site classification.

Different soils with an engineering properties are characterized in Table 20.3-1 of the ASCE/SEI 7-10.

Step 5: Based on the site class and the values of S_S and S_1 , define site coefficients; F_a and F_v .

The influence of the non-rock site is expressed by both short and long period site coefficients F_a , and F_v respectively. They are determined from Tables 11.4-1, and 11.4-2 of the ASCE/SEI 7-10.

Step 6: Adjust spectral acceleration coefficients from probabilistic to pragmatic ground motion parameters. The two site-amplified spectral accelerations are then (ASCE, 2010):

$$S_{MS} = F_a S_S \quad [3.11]$$

$$S_{M1} = F_v S_1 \quad [3.12]$$

- S_{MS} is the 5% damped, spectral response acceleration coefficient at short period for deterministic site (ASCE, 2010).
- S_{M1} is the 5% damped, spectral response acceleration coefficient at long period for deterministic site (ASCE, 2010).

Step 7: Define the design spectral acceleration parameters; S_{DS} and S_{D1} .

- S_{DS} is the 5% damped, design spectral response acceleration coefficient at short period for deterministic site (ASCE, 2010).
- S_{D1} is the 5% damped, design spectral response acceleration coefficient at long period for deterministic site (ASCE, 2010).

Seismic design are based on the design earthquake. In conformance with the ASCE/SEI 7-10, the design-level ground motion is less severity than that considered to happen only once every 2475 year. Hence, design spectral

acceleration parameters are nearly 67% of spectral response acceleration parameters S_{MS} and S_{M1} as (ASCE, 2010):

$$S_{DS} = (2/3)S_{MS} = (2/3)S_s F_a \quad [3.13a]$$

$$S_{D1} = (2/3)S_{M1} = (2/3)S_1 F_v \quad [3.14a]$$

S_s and S_1 are essentially corresponding to 2% chance of exceedance in 50 years. In other words, they are much larger than the maximum anticipated earthquake adopted at this place, i.e. 10% chance of exceedance in 50 years. Thus, S_s and S_1 values do not need to be reduced so that, the preceding equations could be rewritten as (Touqan and Salawdeh, 2015):

$$S_{DS} = S_s F_a \quad [3.13b]$$

$$S_{D1} = S_1 F_v \quad [3.14b]$$

Where:

$$S_{S_{10\% Prob.}} = (2/3)S_{S_{2\% Prob.}} \quad [3.15]$$

$$S_{1_{10\% Prob.}} = (2/3)S_{1_{2\% Prob.}} \quad [3.16]$$

Step 8: Pick out the most appropriate SDC.

SDC is a classification imputed to the structure based on its Risk Category and the hazardousness of the design earthquake ground motion, i.e. S_{DS} and S_{D1} . SDCs are determined from Tables 11.6-1, 11.6-2 of the ASCE/SEI 7-10. In final analysis, the outcomes of earlier steps are shown in Table 3.18.

Table 3.18: Declaration of prerequisites of SDC

General		Step 1	Step 2	Step 3		Step 4	Step 5		Step 6		Step 7		Step 8
Model	Z	Risk Cat.	I_e	S_S	S_1	Site Class	F_a	F_v	S_{MS}	S_{M1}	S_{DS}	S_{D1}	SDC
1N-R	0.2	III	1.25	0.500	0.250	B	1	1	0.500	0.250	0.500	0.250	D
3N-R	0.2	III	1.25	0.500	0.250	B	1	1	0.500	0.250	0.500	0.250	D
5N-R	0.2	III	1.25	0.500	0.250	B	1	1	0.500	0.250	0.500	0.250	D
1N-SR	0.2	III	1.25	0.500	0.250	C	1.2	1.55	0.600	0.388	0.600	0.388	D
3N-SR	0.2	III	1.25	0.500	0.250	C	1.2	1.55	0.600	0.388	0.600	0.388	D
5N-SR	0.2	III	1.25	0.500	0.250	C	1.2	1.55	0.600	0.388	0.600	0.388	D
1N-SS	0.2	III	1.25	0.500	0.250	D	1.4	1.9	0.700	0.475	0.700	0.475	D
3N-SS	0.2	III	1.25	0.500	0.250	D	1.4	1.9	0.700	0.475	0.700	0.475	D
5N-SS	0.2	III	1.25	0.500	0.250	D	1.4	1.9	0.700	0.475	0.700	0.475	D
1J-SC	0.3	IV	1.5	0.750	0.375	E	1.2	2.5	0.900	0.938	0.900	0.938	D
3J-SC	0.3	IV	1.5	0.750	0.375	E	1.2	2.5	0.900	0.938	0.900	0.938	D
5J-SC	0.3	IV	1.5	0.750	0.375	E	1.2	2.5	0.900	0.938	0.900	0.938	D

Commentaries

The rise of S_{D1} value above that of S_{DS} in the last group in Table 3.18 is really striking! Because of this concern, calculation was carefully revised, and no errors were found. Any similar case was not, additionally, found in literatures. Researcher's own vision, therefore, ends to that the ASCE/SEI 7-10 Standards has to be revised.

3.12.2 Structural Irregularities

Buildings with irregular configurations have a dramatic vulnerability to earthquakes. A visual inspection of the layouts and potential elevations of models confirms that they are free from structural irregularities themes in Tables 12.3-1, and 12.3-2 of the ASCE/SEI 7-10.

3.12.3 Diaphragm Rigidity

Seismic loads act at any floor level are distributed to the LFRS components depending on the rigidity of the diaphragms (Duggal, 2013). The length to width ratio of the diaphragms in every one of the models is less than 3. None of the models has horizontal irregularities. Wherefore, according to Section 12.3.1.2 of the ASCE/SEI 7-10, the concrete slabs in the surveyed models are assumed rigid diaphragms.

3.12.4 The Most legitimated Procedure of Analysis

The ASCE/SEI 7-10, Table 12.6-1 emphasizes three analytical methods to determine the design-level forces developed by seismic loads in a particular structure. The classification is:

- The equivalent lateral force method (ELF).
- The modal response spectrum method (MRS).
- The response history method (RH).

Those three methods were valid to use, despite that, MRS method is only aligned with the current scenario.

The vibrational response behavior of a building to seismic activities leads to deformations within the building. The deformations, i.e. the overall seismic response of the building depends on the distribution of forces upon the structure which in turn depend on the dynamic characteristics of the building system like vibratory periods, stiffness, amplitudes, etc. (Khan, 2013). The ability of MRS method to combine the dynamic characteristics of the

structure with the spectral accelerations to evaluate the applying seismic loads, generates a well-designed structure that is able to resist earthquake loads better than those designed by ELF analysis (Finley and Cribbs, 2004). The followings are also some of ELF analysis disadvantages, but not limited to:

- ELF method is constrained to use in some irregularities, height, and period cases. “It assumes a gradually varying distribution of mass and stiffness along the height and negligible torsional response” (NIBS, 2009). However, it is acceptable to say that ELF method is constrained to use for regular structures not taller than 48.8m, and periods less than $3.5T_S$ (Tremblay et al., 2016), where $T_S = S_{D1}/S_{DS}$. The $3.5T_S$ limit is to perceive the effect of higher modes in high rise buildings (NIBS, 2009).
- MRS analysis enables to determine the maximum displacement behavior of structures (Doğangün and Livaoğlu, 2006) needed to make an adequate separation between adjacent entities to avoid hammering and pounding effect.
- MRS methods takes into consideration the randomness of earthquake loads i.e. the vertical component of forces (Khan, 2013).

Next, some of RH analysis disadvantages are debated through, but not limited to:

- Seismic analysis and design of buildings in a specific area are exact and most reliable if a deterministic time history data is available (Nair

and Akshara, 2017). Perhaps such site specific envelopes do not exist at every location until the analysis and design are complete.

- RH method is more demanding in terms of computational efforts, and skills. As a consequence, method of RH analysis is usually used for complex or very important structures (Charney, 2015, Armouti, 2015). For instance, RH method is performed in Japan, where structures are more than 60 m in height (Nakai et al., 2012).

In conclusion, the selection of MRS tool in this research comes at the expense of insufficiency of ELF method, and the difficulty of RH method.

3.13 Modal Response Spectrum Method

In long-term period structures, modes other than the fundamental one significantly influence the structural response. Consequently, it is markedly wrong to ignore these higher modes when assessing the response of structures (Chen and Lui, 2006).

3.13.1 Basic Principles of Modal and Spectral Analysis

In conformance with Trifunac and Todorovska (2008), the roots of MRS method are referred to 1930s as follow:

- The oscillation of a linear elastic undamped system is permanently a superposition of a simple harmonics.
- As any linear elastic system, buildings skeletons possess a particular number of what's called natural modes of vibration (ϕ_n), and each mode has its own frequency (ω_n).

- When these normal modes become known, the motion of the building could be calculated. Peak amplitudes are targeted since they are most influential rather than the motion itself of the building.
- The largest possible amplitude of the total motion (mixed modes) is a combination of the amplitudes values of each independent free vibration.

Hence, the way to divide a multi degree of freedom (MDF) system into a group of single degree of freedom systems (SDF) in order to extract their own mode shapes and natural frequencies is referred to as modal analysis (Elnashai and Di Sarno, 2008).

When the analysis is centralized about the maximum seismic response quantities, maxima of a series of modes are calculated with reference to a predefined response spectrum. Later, maxima are combined to estimate the overall response of the structure. This so-called MRS method of analysis (Elnashai and Di Sarno, 2008).

3.13.2 Response Spectrum Concept

The central core of response spectrum, is that it introduces the maximum response values of buildings (displacement, velocity, acceleration) that may happen during potential earthquakes, as these are the ones that control the design (Williams, 2016). The graph of the absolute peak response of all possible linear elastic SDF systems, having a certain damping level, as a function of T_n when subjected to a transient component of a ground motion, is recognized as the elastic response spectrum for that measure (Chopra, 2012).

The force-based seismic design approach, adopted here, claims that the ground acceleration results in forces that damage buildings during earthquakes, therefore, the dominant ground motion parameter, accordingly, is the pseudo acceleration response spectrum (Bommer and Martinez-Pereira, 2000). In the light of that, the formal response spectrum introduced by the ASCE/SEI 7-10 Provisions as in Figure 3.13 will be accompanied.

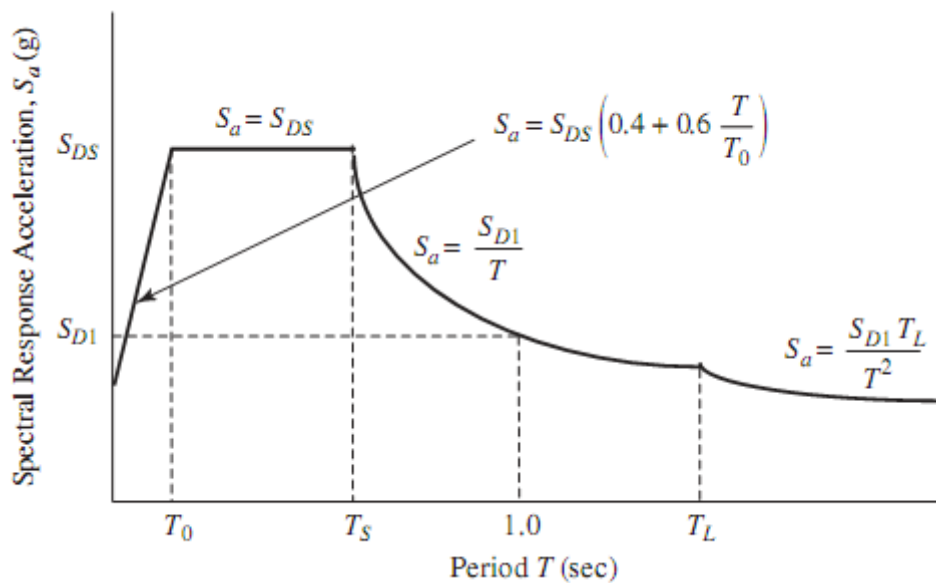


Figure 3.13: Standardized elastic response spectrum referenced by the ASCE/SEI 7-10

The pseudo spectral acceleration (S_a) or, for brevity, spectral acceleration is nearly what is observed by a building, when modeled as a particle on a massless upright bar having T_n similar to that of the building (U.S. Geological Survey, 2017). The maximum story shears are the most affective (Ishiyama et al., 2004) during the design. Thus, S_a takes out the maximum base shear when multiplied by mass (Armouti, 2015).

The 5% damped spectral response acceleration, i.e. S_a is taken relative to T in 4 different ranges defined by:

- The period in the boundary between the first and the second range of periods (T_0), such that:

$$T_0 = 0.2 \frac{S_{D1}}{S_{DS}} \quad [3.17]$$

- The period in the boundary between the second range and the third range of periods (T_S), such that:

$$T_S = \frac{S_{D1}}{S_{DS}} \quad [3.18]$$

- The period in the boundary between the third range and the fourth range of periods, i.e. T_L .

Figure 3.14, however, shows the elastic response spectrum of Model 3N-SR (soft rock site).

Recall that:

$$T_0 = 0.2 \frac{0.388}{0.6} = 0.129sec.$$

$$T_S = \frac{0.388}{0.6} = 0.647sec.$$

$$T_L = 4.0sec.$$

Standardized response spectrum for the studied locations are provided in Appendix D.

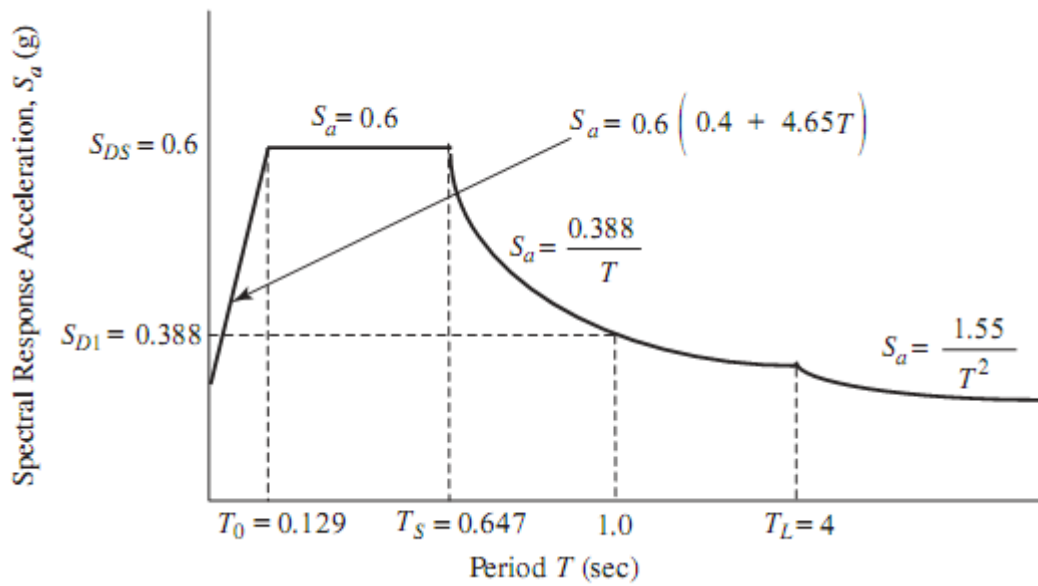


Figure 3.14: Elastic response spectrum of Model 3N-SR

Commentaries

For the soft clay site of Jericho, we have found that $S_{D1} = 0.9375 > S_{DS} = 0.90$. Thus, the elastic response spectrum regarding the soft clay ground is idealized on the basis that the difference between S_{DS} and S_{D1} values is small enough to consider $S_{DS} = S_{D1} \approx 0.90$.

3.13.3 Minimum Number of Modes

In general, it is not necessary to carry all the higher modes for the superposition process. According to Section 12.9.1 of the ASCE/SEI 7-10 Standards, the minimum number of modes required to analyze the MDF system is such that their accumulated effective modal mass account for up to 90 percent of the of the actual mass, separately in X and Y directions.

The revision of SAP2000 analysis indicates that, for all models, the first mode is mainly translational in X-Direction, the second mode is mainly

translational in Y-Direction, and third modes is prevalently rotational about Z-Axis. This is conceptually OK, with an emphasis on that, the first, fourth, and the seventh modes were efficient to assemble at least 90% of the entire mass in all of the studied models.

Spreadsheets are downloaded from SAP2000, and have been shortened regarding only the X-Direction, and placed inside Appendix E.

3.13.4 Modal Combination Technique

Maximum modal response quantities of different modes do not occur simultaneously. The upper-bound response of the structure, therefore, cannot be obtained by the merely sum of the modal maxima (Williams, 2016, Booth, 2014, Clough and Penzien, 2003). Alternatively, a probabilistic approach sounds more sensible in order to estimate the topmost actual response of the building (Sucuoglu, 2015). Among the different statistical combination rules, the square root of the sum of squares rule (SRSS) will be employed, in this place, for the calculation purposes. Let r_n is any force or displacement parameter, then the peak value of the response component (r_{max}) is (Sucuoglu, 2015):

$$r_{max} \approx \sqrt{\sum_{n=1}^N r_{n,max}^2} \quad [3.19]$$

However, SRSS approximate method is conservative when modes of vibration are not close together, i.e. in compliance with Fardis et al. (2015), Sucuoglu (2015), Nuclear Regulatory Commission (2012), and Grey (2006),

for natural modes i and j such that $T_i > T_j$, $T_j/T_i \leq 0.80$ must be guaranteed. Separation of modes in all models has been guaranteed down in Table 3.19 as the ratio T_j/T_i is always less than 0.80.

Table 3.19: A proof of separation of modes

Model	$T_n(sec)$			Check 1	Check 2
	T_1	T_4	T_7	T_4/T_1	T_7/T_4
1N-R	1.49	0.469	0.256	0.315	0.546
3N-R	1.54	0.487	0.267	0.316	0.548
5N-R	1.55	0.492	0.272	0.317	0.553
1N-SR	1.49	0.469	0.256	0.315	0.546
3N-SR	1.54	0.487	0.267	0.316	0.548
5N-SR	1.55	0.492	0.272	0.317	0.553
1N-SS	1.49	0.469	0.256	0.315	0.546
3N-SS	1.54	0.487	0.267	0.316	0.548
5N-SS	1.55	0.492	0.272	0.317	0.553
1J-SC	1.49	0.469	0.256	0.315	0.546
3J-SC	1.54	0.487	0.267	0.316	0.548
5J-SC	1.55	0.492	0.272	0.317	0.553

3.14 Verification of Modal Properties

Physical modeling, advanced mathematics and interpretation of results are some demands of the dynamic analysis compared to those of static analysis which in most often are hand-based techniques. Therefore, the dependency on software developed solutions to structural dynamics is inevitable and unavoidable. Nevertheless, the above reasoning does not exempt from an evidencing of results.

3.14.1 Verification of the Fundamental Periods

According to NIBS (2012), static lateral deflections could be accurately serve to estimate the value of T_1 by a procedure known as Rayleigh's method. With respect to Anderson and Naeim (2012), the relationship of this approximate (Sucuoglu, 2015) procedure is shown below and is employed, herein, to check up T_1 values computed by SAP2000.

$$T_1 = 2\pi \sqrt{\frac{\sum_{i=1}^n w_i \delta_i^2}{g \sum_{i=1}^n P_i \delta_i}} \quad [3.20]$$

Where:

n is the number of stories above the base.

w_i is the seismic weight of story i (kN).

δ_i is the static lateral deflection at level i (m).

P_i is the resultant of the static distributed forces over each level in the intended direction (kN).

Determination of Seismic Weight

Effective seismic weights are those which firmly attached to the building such that they experience the same lateral accelerations as the building (Charney, 2015). That is to say, for every story in the meant models, the seismic weight is its full DL added to the SDL. As a principle, DL of each story consists of slab own weight plus two halves of weights for columns above and below the intended level. SDL contributions were shown before in Table 3.1.

Tables 3.20 and 3.21 include calculations of the components contained in the effective seismic weight of every story in Model 3N-SR.

Table 3.20: Seismic DL of stories of Model 3N-SR

Types of Elements in Single Story	γ_c (kN/m ³)	Dimensions (m)			Mass and Weight Modifier	No. of Elements in Single Story	Weights of Elements (kN) in Single Story
		Length	Width	Depth			
Slab Panels	25	6	6	0.13	1	9	1053
Beams	25	6	0.7	0.45	0.711	24	806
Columns	25	3.55	0.7	0.7	0.873	16	608
Seismic DL (kN) of 10 th -Story							2163
Seismic DL (kN) of any other story							2467

Table 3.21: Seismic SDL of stories of Model 3N-SR

Load Pattern	Intensity (kN/m ²)	Slab Dimensions (m)		Total Load (kN) on a Single Slab
		Length	Width	
SDL	3	18	18	972
Seismic SDL (kN) of any story				972

Thus, the seismic weight of any story = seismic DL + seismic SDL of that story.

Table 3.22 displays the terms required by Rayleigh's method, and the testing process of the same model. Participations of DLs and SDLs to the seismic weight of each model are tabulated in Appendix F.

Fundamental periods of vibration for all models were successfully checked and provided within Appendix F.

Table 3.22: Verification of the fundamental period of Model 3N-SR

<i>Level</i>	<i>w_i (kN)</i>	<i>p_i (kN/m²)^a</i>	<i>floor Area (m²)</i>	<i>P_i (kN)</i>	<i>δ_i (m)^b</i>	<i>w_i δ_i² (kN.m²)</i>	<i>P_i δ_i (kN.m)</i>
10	3135	10	324	3240	0.707	1566	2290
9	3439	10	324	3240	0.685	1613	2219
8	3439	10	324	3240	0.651	1456	2108
7	3439	10	324	3240	0.603	1250	1954
6	3439	10	324	3240	0.541	1008	1754
5	3439	10	324	3240	0.466	745	1508
4	3439	10	324	3240	0.376	486	1219
3	3439	10	324	3240	0.274	259	889
2	3439	10	324	3240	0.164	92.7	532
1	3439	10	324	3240	0.0587	11.8	190
<i>Σ</i>						8488	14662
<i>T₁ (sec) – Rayleigh</i>							1.53
<i>T₁ (sec) – SAP2000</i>							1.54
<i>Error %</i>							0.608
<i>Evaluation of error %^c</i>							OK

^a These values of static distributed loads were randomly chosen by the author, and were assigned in the +X-Direction

^b These are equivalent to U1 given by SAP2000 at the center of mass of each diaphragm

^c Acceptance level of error is 10%

3.14.2 Verification of the Effective Modal Mass Ratios

In modal analysis, the contribution of modes to the whole dynamic response of a structure is weighted through two idioms; the effective modal mass, and the modal participation factor (Semblat et al., 2000).

The effective modal mass or modal participation mass (M_n^*) of an n th-mode is the part of the total mass of MDF system subjected to a seismic excitation in that mode (Paultre, 2013). The effective modal mass ratio or the modal participation mass ratio of an n th-mode is the ratio of its effective modal mass M_n^* to the total seismic mass of the structure.

The modal participation factor (Γ_n) of an n th-mode could be thought of as the extent to which the n th-mode takes part in the whole response of the system (Chopra, 2012).

The numerical formula of the M_n^* is (Chopra, 2012):

$$M_n^* = \Gamma_n L_n^h \quad [3.21]$$

The determination of M_n^* depends on further analysis as follows-down (Chopra, 2012):

$$\Gamma_n = \frac{L_n^h}{M_n} \quad [3.22]$$

The modal excitation factor (L_n^h) of an n th-mode measures the degree to which an earthquake tends to activate the response in the deflection shape of the same mode (Anderson and Naeim, 2012). It is (Chopra, 2012):

$$L_n^h = \phi_n^T m \iota \quad [3.23]$$

In the meantime, the scalar divisor (M_n) is the modal mass of the n th-mode. It depends on the mode shape, and the mass distributed up the structure (Clough and Penzien, 2003). It is defined as (Chopra, 2012):

$$M_n = \phi_n^T m \phi_n \quad [3.24]$$

Where:

$[\phi_n]$ is the column vector of the n th-mode shape. The subscript T on $[\phi_n]$ denotes to a matrix transpose.

$[m]$ is the mass matrix.

$[\iota]$ is the influence vector.

It should be noted that the above formulas are derived on the basis of discretizing 3D systems into two dimensional (2D) systems subjected to earthquake ground motion acts only in one horizontal direction. Metaphorically, let it be the X-Direction. Implying that, neither translation in the Y-direction nor rotation about Z-axis is likely to occur.

However, due to the augmentation of computational steps which are mostly in a form of matrices, only main calculations are discussed here, others are transferred to Appendix F.

The Natural Mode Shapes

The horizontal displacement of the center of mass, in X-Direction, at each floor level in a single mode is read, from SAP2000, and arranged as a displacement column vector. Modes are normalized so that the maximum ordinate is unity. The made up vector of dimensionless quantities is designated as the n th-mode shape $[\phi_n]$. Meanwhile, the independent natural mode shapes or eigenvectors constituting the structural response could be assembled in a matrix called the modal matrix $[\Phi]$ (Chopra, 2012) which is available in Appendix F.

Mass Matrix

The mass matrix $[m]$ contains only the translational seismic masses of each floor in the preselected X-Direction. For all models, $[m]$ is 10×10 square-diagonal matrix characterized in Appendix F. It should be noted that off-diagonal entries are zeros, since there is no translational-rotational coincidence between the mass coefficients.

Seismic mass of each story level – in kilograms – equals to the product of the constant $(1000/g) = 102$ and the corresponding seismic weight in kN.

The Influence Vector

The objective of utilizing the influence vector $[\iota]$, is to specify which degrees of freedom are triggered by the earthquake (Williams, 2016). As the current research deals with the X component of the earthquake that affects intentional models, $[\iota]$ is a column vector given an influence coefficients of 1.0 as shown in Appendix F.

In the final analysis, the effective modal mass ratios of modes instituting the structural response of Model 3N-SR have been calculated and approved in Table 3.23.

Table 3.23: Verification of effective modal mass ratios of the efficient modes of Model 3N-SR

	$L_n^h (kg)$	$M_n (kg)$	Γ_n	$M_n^* (kg)$	M_n^* Ratio		Error				
					Calculated	SAP2000	Error %	Level ^a			
L_1^h	2.12E+06	M_1	1.63E+06	Γ_1	1.30	M_1^*	2.75E+06	0.792	0.791	0.0930	OK
L_4^h	-7.57E+05	M_4	1.62E+06	Γ_4	-0.469	M_4^*	3.55E+05	0.102	0.102	0.147	OK
L_7^h	4.94E+05	M_7	1.71E+06	Γ_7	0.288	M_7^*	1.42E+05	0.0409	0.0366	11.6	Not OK

^a Acceptance level of error is 10%

It should be noticed that the first mode has the largest modal participation factor. Consequently, it is greatly expected to be excited by the ground shaking. On the other hand, the lower contributions of the 4th, and the 7th modes to the structural behavior is because of the negative and positive

values of mode shapes that wipe each other out (Paultre, 2013). The effective modal masses are also augmenting the past argument.

Commentaries

With references to Table E.2 in Appendix E, the 3D analysis of SAP2000 indicated that among the three modes of interest, the structure is moving remarkably in the Y-direction during the 7th mode. Wherefore, its effective modal mass in X-Direction was somewhat less than what has been resulted by the manual solution, and caused a very slight increase in the error over the allowable percent. This is only the case of Models 3N-R, 3N-SR, 3N-SS, and 3J-SC. Checks concerning other models were alright as shown in Tables F.4, and F.12.

3.14.3 Verification of the Total Displacement of Stories

The peak value of the displacements of a structure $[U_x]$ responds to an impulsive ground motion in X-Direction, is a superposition of the displacement contributions of an N modes $[u_n]$ constituting the total response of the structure. Where $[u_n]$ is a column vector denotes the displacement envelop of the MDF system in the n th-mode as (Chopra, 2012):

$$u_n = \Gamma_n \phi_n D_n \quad [3.25]$$

Where D_n is the maximum prospective displacement of the n th-mode SDF system as (Chopra, 2012):

$$D_n = \frac{S_a}{\omega_n^2} \quad [3.26]$$

Where:

S_a is the pseudo spectral acceleration.

ω_n is natural circular frequency of vibration, given as (Chopra, 2012):

$$\omega_n = \frac{2\pi}{T_n} \quad [3.27]$$

Table 3.24 displays the deformation response D_n of the 1st, 4th, and 7th basic modes of Model 3N-SR.

Table 3.24: Maximum displacements of the generalized SDF systems of Model 3N-SR

Mode No.	$T_n(sec)^a$	$\omega_n (rad/sec)$	$S_a (g)^b$	$D_n (mm)$
1	1.54	4.09	0.252	148
4	0.487	12.9	0.600	35.3
7	0.267	23.5	0.600	10.6

^a Natural periods are obtained by SAP2000 analysis. Refer to Table E.2

^b Spectral accelerations are gained from the acceleration response spectrum shown in Figure D.2

Table 3.25 brings the displacement contribution vectors of the 1st, 4th, and 7th basic modes of Model 3N-SR. Total displacement of floors are also calculated and evidenced as those of SAP2000. The deformation response of the decomposed SDF systems characterizing the attempted models, the generalized displacements in the dominant modes, and final displacement envelopes of all models are inserted into Appendix G. Values are also checked and were within the accepted range.

Table 3.25: Modal and the maximum expected displacements of floors of Model 3N-SR

Story	u_n (mm)			U_x (mm)	$U1$ (mm) ^a	Error	
	u_1	u_4	u_7	SRSS	SAP2000	Error %	Level ^b
10	192	-16.5	3.06	193	193	0.368	Accepted
9	185	-12.0	0.989	185	186	0.349	Accepted
8	174	-5.45	-1.35	174	175	0.374	Accepted
7	159	2.10	-2.82	159	160	0.371	Accepted
6	140	9.10	-2.61	141	141	0.369	Accepted
5	118	14.0	-0.863	119	119	0.369	Accepted
4	92.7	15.8	1.40	94.0	94.3	0.359	Accepted
3	65.5	14.1	2.86	67.0	67.3	0.337	Accepted
2	37.9	9.48	2.71	39.1	39.3	0.328	Accepted
1	13.1	3.58	1.21	13.6	13.6	0.351	Accepted

^a These horizontal displacements are read at the center of mass of each diaphragm, and were due to the effect of an earthquake ground acceleration (Acceleration Response Spectrum) in the X-Direction

^b Acceptance level of error is 10%

Commentaries

It should be noted that the displacement profile along the building height is substantially equals that of the 1st mode. This could be illustrated on the basis that the 1st mode has a superior modal excitation factor; $L_n^h = 2.12 \times 10^6 kg$ which composes 2.80, and 4.29 times the modal excitation factors owing to the 4th, and 7th modes, respectively, as given in Table 3.23.

3.14.4 Check of the Story Shears

The equivalent static modal elastic forces [f_n] applied at every story level (j) in the n th-mode, are those which produce the same deformation history

$[u_n]$ extracted by the dynamic analysis (Sucuoglu, 2015). For every intended mode, $[f_n]$ is recovered by (Sucuoglu, 2015):

$$f_n = \Gamma_n m \phi_n S_a \quad [3.28]$$

The internal story shears of the n th-mode $[V_n]$, could be then obtained by the static analysis of the building. Afterwards, the maximum shear force $[V_x]$ in the j th-story is a combination of internal story shears of the N modes by means of SRSS combination rule. Table 3.26 however, compares the total story shears of Model 3N-SR with those of SAP2000.

Table 3.26: The generalized shear forces, and the total story shears of Model 3N-SR

Story	f_n (kN)			V_n (kN)			V_x (kN)		Error	
	f_1	f_4	f_7	V_1	V_4	V_7	SRSS	SAP2000 ^a	Error %	Level ^b
10	1027	-882	542	1027	-882	542	1459	1486	1.90	OK
9	1086	-702	192	2114	-1585	734	2742	2740	0.0505	OK
8	1023	-319	-263	3136	-1904	471	3699	3699	0.00922	OK
7	935	123	-548	4072	-1781	-76.7	4445	4469	0.549	OK
6	824	533	-507	4896	-1248	-584	5086	5097	0.227	OK
5	692	822	-168	5588	-427	-751	5654	5659	0.0785	OK
4	544	926	272	6132	500	-480	6171	6196	0.405	OK
3	385	826	555	6517	1326	75.3	6651	6668	0.268	OK
2	222	555	526	6739	1881	601	7022	7039	0.233	OK
1	76.7	209	236	6816	2090	837	7178	7202	0.332	OK

^a These are elastic story shears generated within the columns of each story due to the effect of an earthquake ground acceleration (Acceleration Response Spectrum) in the X-Direction

^b Acceptance level of error is 10%

The effective modal shear forces, and the overall story shears of models are detailed in Appendix G. Maxima are also checked and were within the accepted interval.

3.14.5 Verification of the Base Overturning Moment

The lateral seismic forces $[f_n]$ tend to overturn the building about Y-Axis locates on the base of the building. The anticipated base overturning moment (M_b) of 3D structure, is a combination of the modal overturning moments (M_{bo}) that resulted by an algebraic summation of the overturning moments (M_{no}) caused by each individual force applied at every story level j in the n th-mode. The aforementioned explanation is illustrated as (Chopra, 2012):

$$M_{no} = f_n h_x \quad [3.29]$$

Where h_x is the height of the j th-floor above the base. Then:

$$M_{bo} = \sum_{j=1}^{10} M_{noj} \quad [3.30]$$

For all the cases we have:

$$M_{bo} = SRSS(M_{1o}, M_{4o}, M_{7o}) \quad [3.31]$$

Table 3.27 highlights the effective modal overturning moments, and their resultant in Model 3N-SR. Finally, the maximum value of the base overturning moment is approved as that of SAP2000. The generalized overturning moments of modes, and the entire base overturning moments of all cases are detailed in Appendix G. Final results are also checked and were within the accepted interval.

Table 3.27: The modal overturning moments, and the resultant overturning moment of Model 3N-SR

Story	$h_x(m)$	$f_n (kN)$			$M_{no} (kN.m)$		
		f_1	f_4	f_7	M_{1o}	M_{4o}	M_{7o}
10	35.5	1027	-882	542	36472	-31327	19237
9	31.95	1086	-702	192	34705	-22439	6136
8	28.4	1023	-319	-263	29049	-9058	-7468
7	24.85	935	123	-548	23237	3049	-13609
6	21.3	824	533	-507	17551	11345	-10802
5	17.75	692	822	-168	12290	14583	-2976
4	14.2	544	926	272	7726	13154	3857
3	10.65	385	826	555	4095	8802	5913
2	7.1	222	555	526	1579	3939	3732
1	3.55	76.7	209	236	272	743	836
$M_{bo} (kN.m)$					166977	-7207	4856
$M_b (kN.m) - SRSS$					167203		
$M_b (kN.m) - SAP2000$					167911		
Error %					0.424		
Check of Error*					OK		

* Acceptance level of error is 10%

3.15 Commentaries

The similarity of the lateral deflections of any three constructions at the same site conditions as in Figure 3.15 through 3.18, despite the disparities in the dimensions of their structural systems, vertical height, and sustained SDL is extremely surprising!

According to Alnajajra et al. (2017), this could be analyzed in a view of two hypotheses as:

- Buildings damage during earthquakes does not necessarily mean that they were not subjected to a convenient seismic design, but rather because they were not originally designed properly against static loads.

- The proportioning of structural members of a structure to commensurate with the static design requirements and in a way that ensures that its fundamental periods below the upper limit ($T_1 \leq C_u T_a$), is an integral part of the good seismic design.

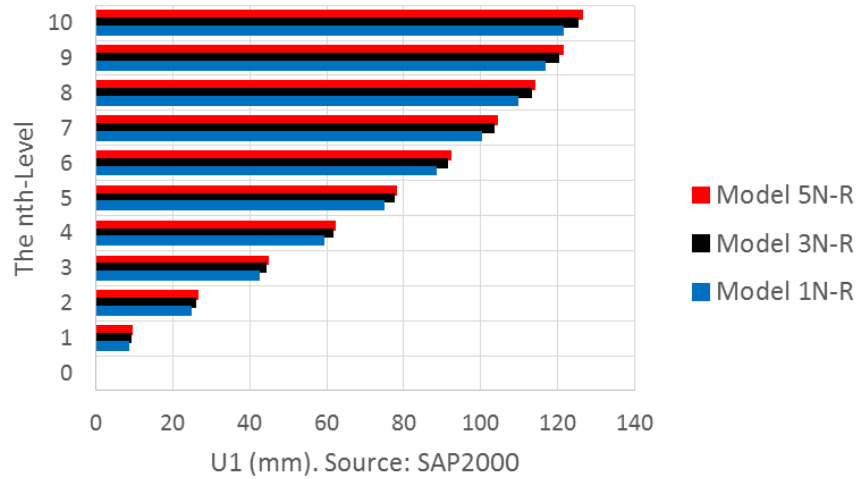


Figure 3.15: Maximum foreseeable side deflection of models on rock (Nablus)

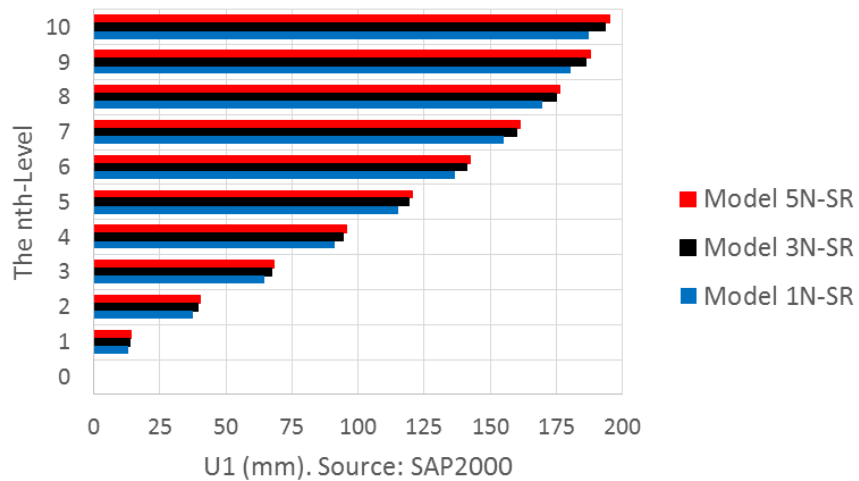


Figure 3.16: Maximum foreseeable side deflection of models on soft rock (Nablus)

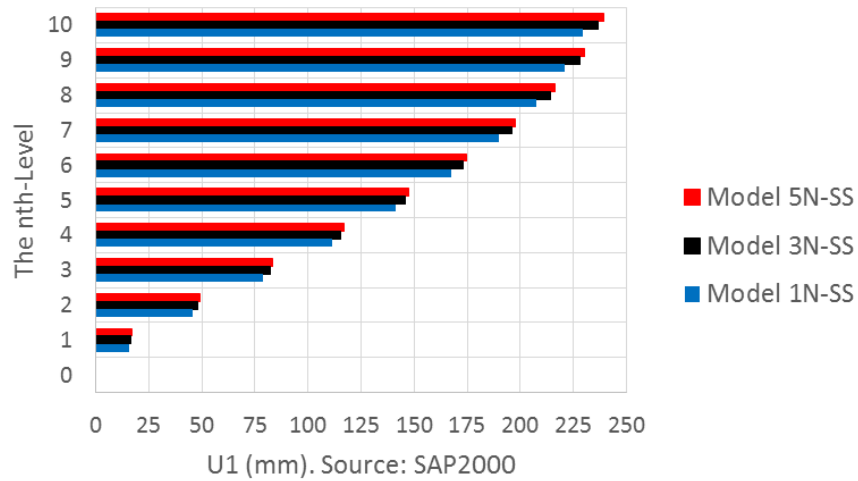


Figure 3.17: Maximum foreseeable side deflection of models on stiff soil (Nablus)

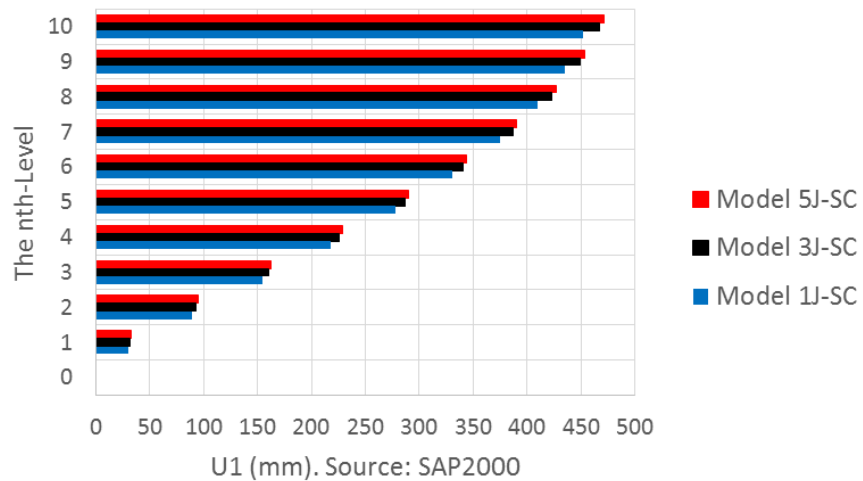


Figure 3.18: Maximum foreseeable side deflection of models on soft clay (Jericho)

The exact values of the lateral displacement at every floor level in the intentional models are referenced in Appendix G.

3.16 Design Approach

All of the calculations regarding the seismic discipline were and will remain according to the strength or force-based design provisions. That is to

underline the required strength, with checks that lateral drifts are less than the prescribed limits provided in codes (Moehle, 2015).

3.17 Inelastic Seismic Response of Buildings

The dimensioning of LFRSs to elastically survive serious earthquakes, clashes with a statement of challenges as:

- It entails an oversized members that would attract a great hostile forces, in addition to being neither practical nor economically feasible option.
- Well-designed structures have demonstrated a quite resistance towards strong earthquakes, even if they were designed to bear a fraction of forces that would generate if the structure completely behaves as a linearly elastic (Fardis et al., 2015).

Safety, performance, and economy are, of course, design objectives that must not be overlooked during any design process. Though safety is not debatable, it is always better to trade-off between the performance and economy (Bertero, 1996). Hence, the purpose of even the recent seismic design codes is to prevent buildings collapse rather than the prevention of damage (Fardis et al., 2015, NIBS, 2012). Stable resistance to reversed cycles of stronger shaking with a tolerated level of damage is possible thanks to the ductility. That is to afford large lateral deformability beyond the elastic limit, with a capacity to waste the imparted energy with least degradation in strength (Sucuoglu, 2015).

3.17.1 Fundamental Parameters of Inelastic Behavior

Design parameters may be used concurrently with linear analysis, to adjust the elastic response values to approximate values that describe the potential inelastic behavior of the buildings (Chen and Lui, 2006). For each system, the design parameters are:

- The response modification factor (R). For every linear elastic system, the lateral strength is transformed to that accounts for inelastic deformation capacity by the means of R (Chen and Lui, 2006).
- The system overstrength factor (Ω_o). This factor considers the exceeding of the actual strength of structure to that prescribed by the design codes due to factors of safety, confinement of concrete, strain hardening of steel, etc. (Duggal, 2013).
- The deflection amplification factor (C_d). Maximum lateral deflections likely to be delivered by a system having a lateral strength reduced by R equal its lateral deflections, as it entirely behaves as a linearly elastic system, times the factor C_d (Chen and Lui, 2006).

For special sway RC frames, the values of the foregoing design coefficients are investigated with reference to Table 15.4-1 of the ASCE/SEI 7-10 as:

$$R = 8, \Omega_o = 3, \text{ and } C_d = 5.5 .$$

It should be also emphasized on that the structural framing system employed for the intended models in SDC D, i.e. special RC moment resisting frames are validated by Table 15.4-1 of the ASCE/SEI 7-10 Provisions with unlimited construction height.

3.17.2 Other Parameters of Inelastic Behavior

The Minimum Eccentricity

Inherent torsion results from the mismatch between the center of rigidity (center of reactions) and the center of mass (center of actions) at each diaphragm. This is not the case here, because of the symmetry of plans. In terms of pure practicality, the ASCE/SEI 7-10 supposes that the center of mass may be shifted each way from its presumed location by a distance equals 0.05 of the diaphragm dimension normal to the direction of applied load (B). The researcher emphasized onto the accidental torsion by inserting an eccentricity ratio of 5% into SAP2000.

The Torsion Amplification Factor

The intentional models are free from structural irregularities themes in Tables 12.3-1, and 12.3-2 of the ASCE/SEI 7-10. Wherefore, there is no need to amplify the accidental torsion, i.e. torsion amplification factor (A_x) is taken as unity.

3.18 Design Response Spectrum

The design (ductile) response spectrum for inelastic systems is merely derived by scaling the spectral acceleration ordinates of the elastic response spectrum down by the factor (R/I_e) (Moehle, 2015, Chen and Lui, 2006), simultaneous with a minimum eccentricity ratio 5% multiplied with $A_x = 1.0$.

3.19 Scaling of Forces

Section of 12.9.4.1 of the ASCE/SEI 7-10 provides that design modal base shear shall not be less than 85% of that determined by ELF procedure. The scaling up condition is to ensure that modeling assumptions do not cause a high flexible structure and thus, an underestimation of the base shear force (Chen and Lui, 2006). From an economic point of view, MRS analysis seems, as a result, more cost-effective than ELF method (Moehle, 2015).

Since $T_1 \leq C_u T_a$ is applicable for all the targeted buildings, inelastic base shear values obtained by MRS analysis will be checked to see if they are less than those calculated by the ELF analysis performed using $T = T_1$.

3.19.1 Seismic Base Shear of ELF Analysis

The total seismic force acts at the base of a given structure (V) is determined in accordance with Section 12.8.1 of the ASCE/SEI 7-10 as:

$$V = C_s W \quad [3.32]$$

Where:

C_s is the seismic response coefficient.

W is the total seismic weight of the structure.

3.19.2 The Base Shear Coefficient

The ratio of the maximum base shear force, may strike a building, to the seismic weight of the building is so-called the seismic response coefficient

(C_s). C_s value could be determined with reference to Section 12.8.1.1 of the ASCE/SEI 7-10 as:

$$C_s = \frac{S_{DS}}{\left(\frac{R}{I_e}\right)} \quad [3.33]$$

But not less than:

$$C_s = 0.01 \quad [3.34a]$$

$$C_s = 0.044 S_{DS} I_e \quad [3.34b]$$

$$C_s = \frac{0.75 S_1}{\left(\frac{R}{I_e}\right)} \dots \text{for } S_1 \geq 0.4 \quad [3.34c]$$

and not more than:

$$C_s = \frac{S_{D1}}{T \left(\frac{R}{I_e}\right)} \dots \text{for } T \leq T_L \quad [3.35a]$$

$$C_s = \frac{S_{D1} T_L}{T \left(\frac{R}{I_e}\right)} \dots \text{for } T \geq T_L \quad [3.35b]$$

- Equation [3.34c] is not applicable since the previously submitted values of S_1 in Table 3.18 were always less than 0.40.
- Equation [3.35a] has been chosen to determine the upper limit value of C_s since T_1 values in Table 3.17 were always less than $T_L = 4.0sec$.

The products of the preceding equations, and the consequent scaling factors are contained in the Table 3.28.

Table 3.28: Scaling up factors of MRS base shears

Model	Important Constants						C_s	$Min C_s$			$Max C_s$		W	$V (kN)$			SF^c
	T_1	S_1	I_e	S_{DS}	S_{D1}	R		Eq.[3.33]	Eq.[3.34a]	Eq.[3.34b]	Eq.[3.35a]	C_s		ELF^a	$0.85 \times V_{ELF}$	MRS^b	
1N-R	1.49	0.250	1.25	0.500	0.250	8	0.0781	0.0100	0.0275	0.0262	0.0262	24905	653	555	563	1.00	
3N-R	1.54	0.250	1.25	0.500	0.250	8	0.0781	0.0100	0.0275	0.0254	0.0254	34086	865	735	750	1.00	
5N-R	1.55	0.250	1.25	0.500	0.250	8	0.0781	0.0100	0.0275	0.0252	0.0252	43560	1098	933	953	1.00	
1N-SR	1.49	0.250	1.25	0.600	0.388	8	0.0938	0.0100	0.0330	0.0407	0.0407	24905	1013	861	846	1.02	
3N-SR	1.54	0.250	1.25	0.600	0.388	8	0.0938	0.0100	0.0330	0.0394	0.0394	34086	1342	1141	1125	1.02	
5N-SR	1.55	0.250	1.25	0.600	0.388	8	0.0938	0.0100	0.0330	0.0391	0.0391	43560	1704	1448	1429	1.02	
1N-SS	1.49	0.250	1.25	0.700	0.475	8	0.109	0.0100	0.0385	0.0498	0.0498	24905	1241	1054	1033	1.03	
3N-SS	1.54	0.250	1.25	0.700	0.475	8	0.109	0.0100	0.0385	0.0482	0.0482	34086	1643	1396	1373	1.02	
5N-SS	1.55	0.250	1.25	0.700	0.475	8	0.109	0.0100	0.0385	0.0479	0.0479	43560	2086	1773	1743	1.02	
1J-SC	1.49	0.375	1.50	0.900	0.938	8	0.169	0.0100	0.0594	0.118	0.118	24905	2940	2499	2384	1.05	
3J-SC	1.54	0.375	1.50	0.900	0.938	8	0.169	0.0100	0.0594	0.114	0.114	34086	3893	3309	3164	1.05	
5J-SC	1.55	0.375	1.50	0.900	0.938	8	0.169	0.0100	0.0594	0.113	0.113	43560	4943	4201	4014	1.05	

$$^a V = C_s \times W$$

^b This columns represents Global FX values gained from SAP2000 analysis due to the effect of inelastic (design) acceleration response spectrum described in Section 3.18, and predefined in the X-Direction

$$^c \text{Scaling factor} \geq \frac{0.85 \times V_{ELF}}{V_{MRS}}$$

3.19.3 Discussion of the Results

A continuation to what was mentioned in Section 3.19, it is certain that design response spectrum of the last three construction sites in Table 3.28 are noncompliant with the code requirements, unless they are multiplied by the amplification factors received from the table. Accordingly, the meant response spectrums have been enlarged as required then, the new base shears are verified again as in Table 3.29.

Table 3.29: Verification of MRS base shears

Model	C_S	W	V (kN)			Check*
			ELF	$0.85 \times V_{ELF}$	MRS	
1N-R	0.02622	24905	653	555	563	OK
3N-R	0.02537	34086	865	735	750	OK
5N-R	0.0252	43560	1098	933	953	OK
1N-SR	0.041	24905	1013	861	863	OK
3N-SR	0.039	34086	1342	1141	1148	OK
5N-SR	0.039	43560	1704	1448	1457	OK
1N-SS	0.050	24905	1241	1054	1064	OK
3N-SS	0.048	34086	1643	1396	1400	OK
5N-SS	0.048	43560	2086	1773	1778	OK
1J-SC	0.118	24905	2940	2499	2503	OK
3J-SC	0.114	34086	3893	3309	3323	OK
5J-SC	0.113	43560	4943	4201	4214	OK

* The check is OK for $V_{MRS} \geq 0.85 \times V_{ELF}$

3.20 Drifts and P-Delta Effect

The side deflection of LFRSs is expressed by means of horizontal drift. The ASCE/SEI 7-10 defines the design inter-story story drift (Δ) of a story under consideration as the lateral displacement of that floor relative to the floor below. Mathematically, it is:

$$\Delta = \delta_x - \delta_{x-1} \quad [3.36]$$

Where:

δ_x is the amplified displacement at the floor above measured at its center of mass.

δ_{x-1} is the amplified displacement at the floor below measured at its center of mass.

Considering that:

$$\delta_x = \frac{C_d \delta_{xe}}{I_e} \quad [3.37]$$

The elastic displacement δ_{xe} at each level is obtained through the application of the envelope of the load combinations referenced in Table 3.30. $C_d = 5.5$, and $I_e = 1.25$ conform to commercial structures built in Nablus, and $I_e = 1.5$ conforms to hospitals constructed in Jericho.

3.20.1 Load Combinations

Section 2.4.1 of the ASCE/SEI 7-10 articulates the load combinations required for the allowable stress-based design approach. In order to obtain

the maximum prospected inter-story drifts, only load combinations related to seismic action will be dealt with. These combinations are:

$$DL + 0.7EL \quad [3.38]$$

$$DL + 0.75LL + 0.75(0.7EL) \quad [3.39]$$

$$0.6DL + 0.7EL \quad [3.40]$$

Where DL , LL , and EL are the dead, live, and earthquake load respectively.

In accordance with clause 1 of Section 12.4.2 in the ASCE/SEI 7-10, EL in Equation [3.38], and Equation [3.39] shall be taken as:

$$EL = E_h + E_v \quad [3.41]$$

Where E_h , and E_v are the horizontal and vertical seismic load effects.

$$\Rightarrow Eq. [3.38] = DL + 0.7E_h + 0.7E_v.$$

$$\Rightarrow Eq. [3.39] = DL + 0.75LL + 0.525E_h + 0.525E_v.$$

In accordance with clause 2 of Section 12.4.2 in the ASCE/SEI 7-10, EL in Equation [3.40] shall be taken as:

$$EL = E_h - E_v \quad [3.42]$$

$$\Rightarrow Eq. [3.40] = 0.6DL + 0.7E_h - 0.7E_v.$$

As per Section 12.4.2.1 of the ASCE/SEI 7-10, E_h is equivalent to:

$$E_h = \rho Q_E \quad [3.43]$$

On the other hand, Section 12.4.2.2 of the ASCE/SEI 7-10 states that E_v is equivalent to:

$$E_v = 0.2S_{DS}DL \quad [3.44]$$

Where:

ρ is the redundancy or reliability factor.

Q_E is the seismic effect of orthogonal loading.

S_{DS} is the 5% damped, design spectral acceleration coefficient at short period for deterministic site.

$$\Rightarrow Eq. [3.38] = DL + 0.7\rho Q_E + 0.7(0.2S_{DS}DL).$$

$$\Rightarrow Eq. [3.39] = DL + 0.75LL + 0.525\rho Q_E + 0.525(0.2S_{DS}DL).$$

$$\Rightarrow Eq. [3.40] = 0.6DL + 0.7\rho Q_E - 0.7(0.2S_{DS}DL).$$

3.20.2 Redundancy Factor

The extent to which the lateral stability is negatively affected by the failure of structural elements is measured through the reliability factor (ρ) (Booth, 2014). For SDC D, ρ could be taken, conservatively, as 1.3 (Hassoun and Al-Manaseer, 2015). To this point, the recent equations could be rearranged into the following formulas:

$$\Rightarrow Eq. [3.38] = (1 + 0.14S_{DS})DL + 0.91Q_E.$$

$$\Rightarrow Eq. [3.39] = (1 + 0.105S_{DS})DL + 0.75LL + 0.683Q_E.$$

$$\Rightarrow Eq. [3.40] = (0.6 - 0.14S_{DS})DL + 0.91Q_E.$$

However, Table 3.30 shows the load cases that have added by researcher to SAP2000 program to obtain δ_{xe} values.

Table 3.30: Load cases defined inside SAP2000, and required to obtain **δ_{xe} values**

Model	S_{DS}	Eq. [3.38]	Eq. [3.39]	Eq. [3.40]
1N-R	0.5	$1.07DL + 0.91Q_E$	$1.05DL + 0.75LL + 0.683Q_E$	$0.530DL + 0.91Q_E$
3N-R	0.5	$1.07DL + 0.91Q_E$	$1.05DL + 0.75LL + 0.683Q_E$	$0.530DL + 0.91Q_E$
5N-R	0.5	$1.07DL + 0.91Q_E$	$1.05DL + 0.75LL + 0.683Q_E$	$0.530DL + 0.91Q_E$
1N-SR	0.6	$1.08DL + 0.91Q_E$	$1.06DL + 0.75LL + 0.683Q_E$	$0.516DL + 0.91Q_E$
3N-SR	0.6	$1.08DL + 0.91Q_E$	$1.06DL + 0.75LL + 0.683Q_E$	$0.516DL + 0.91Q_E$
5N-SR	0.6	$1.08DL + 0.91Q_E$	$1.06DL + 0.75LL + 0.683Q_E$	$0.516DL + 0.91Q_E$
1N-SS	0.7	$1.10DL + 0.91Q_E$	$1.07DL + 0.75LL + 0.683Q_E$	$0.502DL + 0.91Q_E$
3N-SS	0.7	$1.10DL + 0.91Q_E$	$1.07DL + 0.75LL + 0.683Q_E$	$0.502DL + 0.91Q_E$
5N-SS	0.7	$1.10DL + 0.91Q_E$	$1.07DL + 0.75LL + 0.683Q_E$	$0.502DL + 0.91Q_E$
1J-SC	0.9	$1.13DL + 0.91Q_E$	$1.09DL + 0.75LL + 0.683Q_E$	$0.474DL + 0.91Q_E$
3J-SC	0.9	$1.13DL + 0.91Q_E$	$1.09DL + 0.75LL + 0.683Q_E$	$0.474DL + 0.91Q_E$
5J-SC	0.9	$1.13DL + 0.91Q_E$	$1.09DL + 0.75LL + 0.683Q_E$	$0.474DL + 0.91Q_E$

3.20.3 Orthogonal Loading

Section 12.5 of the ASCE/SEI 7-10 needs that a structure be outfitted for seismic forces that may act in any direction causes in unfavorable load effects. The critical direction of loading is not easy to be defined because of the erratic nature of ground shaking. In conformance with the NIBS (2012), for SDCs D through F, Section 12.5 of the ASCE/SEI 7-10 emphasize the analyst on the principle of loading the structure with 100% of the spectrum in the main horizontal direction, i.e. X-Direction instantaneous with 30% of the same spectrum invades the second horizontal direction, i.e. Y-Direction. In a related manner, Section 12.8.4.2 of the ASCE/SEI 7-10 declares that the

orthogonal spectrum is applied at zero eccentricity (Charney, 2015). Thus, the term EQ in every one of the load situations in Table 3.30 results in eight load cases. They, however, are demonstrated in Table 3.31 in a compacted manner.

Table 3.31: Generation of EQ load cases

Major Load Direction	Major Spectrum Applied at Eccentricity*	Orthogonal Spectrum Applied at Zero Eccentricity
X-Direction (+X, -X)	+0.05 $A_x B$	+0.3 Y
	-0.05 $A_x B$	-0.3 Y
		+0.3 Y
		-0.3 Y

* $A_x = 1.0$

3.20.4 The Second Order Effect

In unbraced frames, when floors move laterally by the inertial forces, and interaction of the translated gravity loads with the lateral deflections may generate an additional (secondary) moments inside structural members as well as magnifying of the drift of story. This destabilizing effect is referred to as $P - \Delta$ effect. Section 12.8.7 of the ASCE/SEI 7-10 requires that $P - \Delta$ effect has to be taken into account whenever the stability coefficient (θ) determined by Equation [3.45] is greater than 0.10.

$$\theta = \frac{P_x \Delta I_e}{V_x h_{sx} C_d} \quad [3.45]$$

Where:

P_x is the accumulated unfactored vertical loads act over the level x .

Δ is the inter-story drift defined in *Eq. [3.36]* of this research.

I_e is the seismic importance factor.

V_x is the generated seismic shear forces between levels x and $x - 1$.

h_{sx} is the height of level x over the level $x - 1$.

C_d is the deflection amplification factor.

Section 12.8.7 of the ASCE/SEI 7-10 sets an upper limit value for θ as the smallest of:

$$\frac{0.5}{\beta C_d} \quad [3.46a]$$

$$2.5 \quad [3.46b]$$

Where β is the ratio of the shear demand to the shear capacity of the story.

Conservatively, β is taken as 1.0 (ASCE, 2010).

$$\Rightarrow Eq. [3.46a] = \frac{0.5}{1 \times 5.5} = 0.0909.$$

A meticulous analysis to the $P - \Delta$ effect on every model has been accomplished and supplemented in Appendix H. The analyst indicates that for all stories, no model is vulnerable to that effect. As an example, Table 3.32 is a sample calculation to check the potential impact of $P - \Delta$ phenomenon in Model 3N-SR.

Table 3.32: Stability analysis of Model 3N-SR

Level	P_{DL} (kN)	P_{LL} (kN)	P_x (kN)	δ_{xe} (mm)*	δ_x (mm)	Δ (mm)	V_x (kN)	h_{sx} (mm)	θ	$P - \Delta$
10	3135	1296	4431	28.4	125	4.70	226	3550	0.00590	NONE
9	3439	1296	9166	27.3	120	7.21	412	3550	0.0103	NONE
8	3439	1296	13901	25.7	113	9.71	547	3550	0.0158	NONE
7	3439	1296	18636	23.5	103	12.1	656	3550	0.0220	NONE
6	3439	1296	23371	20.7	91	14.2	753	3550	0.0282	NONE
5	3439	1296	28106	17.5	77	16.0	838	3550	0.0344	NONE
4	3439	1296	32841	13.8	60.9	17.4	913	3550	0.0402	NONE
3	3439	1296	37576	9.88	43.5	18.1	978	3550	0.0444	NONE
2	3439	1296	42311	5.78	25.4	16.6	1037	3550	0.0433	NONE
1	3439	1296	47046	2.01	8.85	8.85	1064	3550	0.0250	NONE

* This column adjusts for lateral deflections at the center of mass for each level as obtained by SAP2000

Commentaries

According to the ASCE/SEI 7-10 Standards, $P - \Delta$ effect is effective whenever $0.10 < \theta \leq \theta_{max} = 0.0909$.

Where θ_{max} is the limit that wherever exceeded, a structure would have to be redesigned.

The analysis of the above inequality goes deeper than the fact that the upper limit is less than the lower limit. For models having $0.0909 < \theta < 0.10$, the result is really shocking!

Models shall be redesigned due to $P - \Delta$ instability which never applies! This, however, appears odd, and need to be reconsidered by the ASCE/SEI 7-10 committee.

3.20.5 The Allowable Story Drift

The considerable deviation of building skeletons under earthquake lateral loading may contribute greatly to the damage of fragile non-structural components of the buildings (Sucuoglu, 2015). For the status here, Section 12.12.1 of the ASCE/SEI 7-10 limits these lateral deflections or drifts as:

$$\Delta_{allowable} = 0.015h_{sx} \quad [3.47a] \dots \text{for Risk Cat. III.}$$

$$\Delta_{allowable} = 0.010h_{sx} \quad [3.48a] \dots \text{for Risk Cat. IV.}$$

Where h_{sx} is the height of level x over the level $x - 1$.

Section 12.12.1.1 of the ASCE/SEI 7-10 Standards necessitates that for buildings belong to SDC D through F, the above limits have to be minimized by the factor ρ . The application of $\rho = 1.3$ for structural models in SDC D, turns the two previous equations into:

$$\Delta_{allowable} = 0.0115h_{sx} \quad [3.47b] \dots \text{for Risk Cat. III.}$$

$$\Delta_{allowable} = 0.00769h_{sx} \quad [3.48b] \dots \text{for Risk Cat. IV.}$$

Table 3.33 implicates checks on story drifts regarding Model 3N-SR. For each model, drift limits have been checked and tabulated in Appendix I

Table 3.33: Check of drift limits of Model 3N-SR

Level	h_{sx} (mm)	Δ (mm)	$\Delta_{allowable}$ (mm) ^a	Check ^b
10	3550	4.70	40.8	OK
9	3550	7.21	40.8	OK
8	3550	9.71	40.8	OK
7	3550	12.1	40.8	OK
6	3550	14.2	40.8	OK
5	3550	16.0	40.8	OK
4	3550	17.4	40.8	OK
3	3550	18.1	40.8	OK
2	3550	16.6	40.8	OK
1	3550	8.85	40.8	OK

^a $\Delta_{allowable} = 0.0115h_{sx}$

^b The check is OK for $\Delta \leq \Delta_{allowable}$

Commentaries

It is worth mentioning, that actual drifts of stories in models built over soft clay soil were a little bit larger than the allowable values. Needless to say, here comes the spirit of the code. From the start point, the ASCE/SEI 7-10 Code requires that a fundamental period shall not exceed a specific value. This is to avoid structure flexibility that may attract $P - \Delta$ effect, and leads to magnify drifts beyond the allowable limits. In our example, the periods of the meant structures are at the margin of that accepted by the code and hence, the anticipated drifts of the structures we have become marginal.

It should be also asserted on that at a particular site, floors of any superimposed load almost drift within the same limits. This, however, is consistent with what have already said in Section 3.15 of this research.

CHAPTER 4
DESIGN OF SPECIAL MOMENT RESISTING
FRAMES

4.1 Introduction

Most of civil structural framings are liable to seismic hazards during their service life. As mentioned previously in Chapter I, data of live losses in the last few decades, and the prospects for future victims due to earthquakes, strongly affirm the need towards an earthquake resistant constructions. Earthquake resistant construction is the process of putting seismic design and construction techniques into effect to produce a well-designed and constructed structures exposed to major earthquakes (Haseeb et al., 2011).

Seismic design of RC members depends primarily on the ductile response behavior to survive major earthquakes in a stable manner (Sucuoglu, 2015). This intended seismic response is essentially based on the design, and the structural detailing of the structural components (Nilson et al., 2010). Structural systems having an approved design concept and a good amount of detailing often response in a good fashion despite major drawbacks in the analysis (Dowrick, 2003).

The assemblies of RC frame beams, frame columns, and interconnecting joints that are duly designed and detailed as per the ACI 318-14 Code; Sections 18.6 through 18.8, are expected to have the highest level of ductility and strength to sustain the most severe likely ground excitations. These assemblies are addressed to the special moment resisting frames (SMRFs), and were found to best fit the studied models assigned to high Seismic Design Categories, i.e. D.

SMRFs models are able to dissipate a generous amount of seismic energy through the multiple post-yielding deformation cycles caused by the inelastic rotation reversals of girder plastic hinges as the system sways to right and left (Moehle, 2015). This larger dissipative supply of SMRF leads to design a structure for one-eighth of the elastic force to promote more reliable ductile response behavior beyond the elastic limit (Sucuoglu, 2015).

This chapter, however, focuses on the rules of the ACI 318-14 Code for the detailed design of the SMRFs employed in the surveyed RC buildings with emphasis on skeletal members. At the end of this chapter, an example is given, with the material and geometrical properties as well as the main assumptions for the structural analysis and design calculations.

4.2 Design Rules of SMRFs

The seismic response of the well-designed SMRFs has been quite satisfactory (Moehle, 2015). The good performance of SMRF models is greatly guaranteed if the following stringent design provisos are applied (Duggal, 2013):

- Failure should be ductile; avoid failure embrittlement modes such as shear, and lap splices failures.
- Flexural failure must come before shear failure.
- Beams damage should precede that of columns.
- Connections shall be stronger than members spanning to them.

These observations, however, will be encountered in the design process.

3.4 Design and Detailing of SMRFs

The design and detailing of the RC elements embedded in LFRSs of the concerned twelve models, shall comply with cast-in-place special beam-column frames provisions provided by the ACI 318-14 Code, and given for:

- Horizontal members exposed essentially to moment and shear actions with or without axial load. These are beams (ACI 318, 2014). “All requirements of beams are contained in 18.6 regardless of the magnitude of axial compressive force”, the ACI 318-14 Code dictates.
- Vertical members exposed essentially to axial compressive force and could resist flexure and shear. These are columns (ACI 318, 2014). “This section (Section 18.7) applies to columns of special moment frames regardless of the magnitude of axial force”, the ACI 318-14 Code dictates.
- Joints of the intersecting members. These are listed under section 18.8 of the ACI 318-14 Code.

4.4 Modeling of RC Members

Neither modeling criteria nor analysis assumptions that have been discussed in Chapter 3 of this research will be altered except the stiffnesses of members that are reduced to account for cracking.

4.4.1 Modeling of RC Members Stiffness

The rationales behind the declination in stiffness of concrete structural members under serious seismic threats are (Booth, 2014):

- The outset of plasticity. This is considered in the non-linear analysis in which modeling of the plastic hinges relies on the premise of the ductile response spectrum.
- The cracking process that is not limited to plastic hinge zones. Cracks flow along the member span during the multiple sway cycles of the building.

Consequently, member forces should be on stiffness values matching the inelastic deformation response, i.e. cracked concrete section.

Stiffness reduction associated with concrete cracking (I_{cr}) is approximated by the ACI 318-14 Code; Section 6.6.3.1.1 calls to apply a partial stiffness modifiers to the gross-section moment of inertia for RC members loaded close to or after the yield level as $0.7I_g$ for columns, $0.35I_g$ for beams, and $0.25I_g$ for solid slabs. Where I_g is the moment of inertia of gross (uncracked) concrete section about the neutral axis, with negligence of reinforcing bars. SAP2000 program is set by the author to consider the above approach of the ACI 318-14 Code.

4.4.2 Reviewing of Diaphragm Rigidity

Concrete slabs with span-to-depth ratio of 3 or less and free from horizontal irregularities (ASCE, 2010), and having at least 50mm thick (ACI 318, 2014) could be qualified as rigid diaphragms. The assumption means that the diaphragm is flexible in bending in the vertical direction with infinite in-plane stiffness, i.e. allows axial in-plane deformations in floors and beams to be negligibly small (Moehle, 2015, Chen and Lui, 2006).

This assumption, however, seem acceptable to characterize the actual performance of reinforced concrete slabs (Chopra, 2012, Clough and Penzien, 2003), and showed a quite satisfactory behavior along the history (ACI 318, 2014, Arya et al., 2014). As for beam-slab concrete construction system, reinforcement provided in gravity design usually ensures that slabs perform well both as flexural elements and horizontal diaphragms transferring seismic loads (Duggal, 2013, Duggal, 2007).

In the final analysis, as diaphragms of the models under research match both requirements of the ASCE/SEI 7-10, and the ACI 318-14, they are truly rigids.

4.5 SMRFs Layout and Proportioning

The followings are limits placed by the ACI 318-14 on the range of geometries allowed in SMRFs.

4.5.1 General Requirements of Special Frame Beam

- Beam clear span (l_n) shall not be less than four times its effective depth (d).
- Width of beam web (b_w) shall be larger than or equal the minimum of three tenths of its depth (h), or 250mm.
- b_w shall not exceed the width of the column measured in a plan perpendicular to the longitudinal axis of the beam (c_2) plus the lesser of $2c_2$ and three halves the width of the column measured in a direction parallel to the longitudinal axis of the beam (c_1)

4.5.2 General Requirements of Special Frame Column

- The shortest cross-sectional dimension of the column shall be 300mm at minimum.
- The shortest cross-sectional dimension of the column, shall be at least four tenths the other perpendicular dimension within the section.

The ACI 318-14 Code dimensional rules of frame members of SMRFs are illustrated in Figure 4.1. Table 4.1 also validates the geometries of frame beams and frame columns inherent in the Model 3N-SR. Tests on other models can be found in Appendix J.

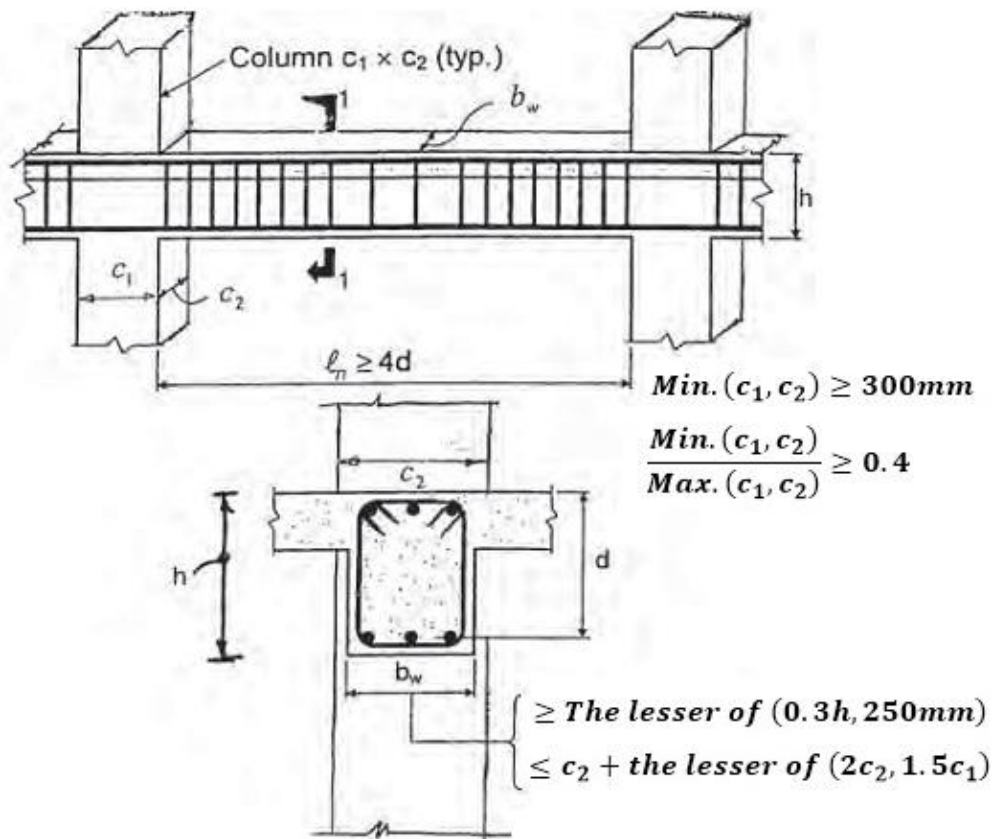


Figure 4.1: Dimensional guidelines of special frame members (Taranath, 2004)

Table 4.1: Checks on limiting dimensions for RC framing members of model 3N-SR

Required Items for Beams				Required Items for Columns	
$l_n(mm)$	$h(mm)$	$d(mm)^*$	$b_w(mm)$	$c_1(mm)$	$c_2(mm)$
5300	450	390	700	700	700

Check of the ACI 318-14 Dimensional Restrictions on Beams

$$l_n/d = (5300/390) = 13.6 \geq 4$$

$$b_w = 700mm \geq \{min. (0.3h = 135mm, 250mm)\}$$

$$b_w(mm) = 700mm \leq \{c_2 = 700mm\} + \{min. (2c_2 = 1400mm, 1.5c_1 = 1050mm)\}$$

Check of the ACI 318-14 Dimensional Restrictions on Columns

$$c_1 = c_2 = 700mm \geq 300mm$$

$$c_1/c_2 = (700mm/700mm) = 1.00 \geq 0.4$$

* $d(mm) = h(mm) - 60mm$

4.6 Factored Load Patterns

Strength design under Section 5.3.1 of the ACI 318-14 Code, and Section 2.3.2 of the ASCE/SEI 7-10 Standards demands the analysis of the structural system according to the load patterns considering both gravity and seismic loads. The relevant load combinations are:

$$1.4DL \quad [4.1]$$

$$1.2DL + 1.6LL \quad [4.2]$$

$$1.2DL + 1.0LL + 1.0EL \quad [4.3]$$

$$0.9DL + 1.0EL \quad [4.4]$$

Where DL , LL , and EL are the dead, live, and earthquake load respectively.

In accordance with clause 1 of Section 12.4.2 in the ASCE/SEI 7-10, EL in Equation [4.3] shall be taken as:

$$EL = E_h + E_v \quad [4.5]$$

Where E_h , and E_v are the horizontal and vertical seismic load effects.

$$\Rightarrow Eq. [4.3] = 1.2DL + 1.0LL + 1.0E_h + 1.0E_v.$$

In accordance with clause 2 of Section 12.4.2 in the ASCE/SEI 7-10, EL in Equation [4.4] shall be taken as:

$$EL = E_h - E_v \quad [4.6]$$

$$\Rightarrow Eq. [4.4] = 0.9DL + 1.0E_h - 1.0E_v.$$

As per Section 12.4.2.1 of the ASCE/SEI 7-10, E_h is equivalent to:

$$E_h = \rho Q_E \quad [4.7]$$

On the other hand, ASCE/SEI 7-10, Section 12.4.2.2 states that E_v is equivalent to:

$$E_v = 0.2S_{DS}DL \quad [4.8]$$

Where:

ρ is the redundancy or reliability factor and taken as 1.3.

Q_E is the seismic effect of orthogonal loading.

S_{DS} is the 5% damped, design spectral acceleration coefficient at short period for deterministic site.

$$\Rightarrow Eq. [4.3] = 1.2DL + 1.0LL + 1.3Q_E + 0.2S_{DS}DL.$$

$$\Rightarrow Eq. [4.4] = 0.9DL + 1.3Q_E - 0.2S_{DS}DL.$$

To sum up, the required load combinations are:

$$Eq. [4.1] = 1.4DL.$$

$$Eq. [4.2] = 1.2DL + 1.6LL.$$

$$Eq. [4.3] = (1.2 + 0.2S_{DS})DL + 1.0LL + 1.3Q_E.$$

$$Eq. [4.4] = (0.9 - 0.2S_{DS})DL + 1.3Q_E.$$

However, these four load combinations are added by the author into SAP2000 program as in Table 4.2.

Table 4.2: Ultimate loads defined inside SAP2000, and required for strength design

Model	S_{DS}	Eq. [4.1]	Eq. [4.2]	Eq. [4.3]	Eq. [4.4]
1N-R	0.5	1.4DL	1.2DL + 1.6LL	1.30DL + 1.0LL + 1.3Q _E	0.800DL + 1.3Q _E
3N-R	0.5	1.4DL	1.2DL + 1.6LL	1.30DL + 1.0LL + 1.3Q _E	0.800DL + 1.3Q _E
5N-R	0.5	1.4DL	1.2DL + 1.6LL	1.30DL + 1.0LL + 1.3Q _E	0.800DL + 1.3Q _E
1N-SR	0.6	1.4DL	1.2DL + 1.6LL	1.32DL + 1.0LL + 1.3Q _E	0.780DL + 1.3Q _E
3N-SR	0.6	1.4DL	1.2DL + 1.6LL	1.32DL + 1.0LL + 1.3Q _E	0.780DL + 1.3Q _E
5N-SR	0.6	1.4DL	1.2DL + 1.6LL	1.32DL + 1.0LL + 1.3Q _E	0.780DL + 1.3Q _E
1N-SS	0.7	1.4DL	1.2DL + 1.6LL	1.34DL + 1.0LL + 1.3Q _E	0.760DL + 1.3Q _E
3N-SS	0.7	1.4DL	1.2DL + 1.6LL	1.34DL + 1.0LL + 1.3Q _E	0.760DL + 1.3Q _E
5N-SS	0.7	1.4DL	1.2DL + 1.6LL	1.34DL + 1.0LL + 1.3Q _E	0.760DL + 1.3Q _E
1J-SC	0.9	1.4DL	1.2DL + 1.6LL	1.38DL + 1.0LL + 1.3Q _E	0.720DL + 1.3Q _E
3J-SC	0.9	1.4DL	1.2DL + 1.6LL	1.38DL + 1.0LL + 1.3Q _E	0.720DL + 1.3Q _E
5J-SC	0.9	1.4DL	1.2DL + 1.6LL	1.38DL + 1.0LL + 1.3Q _E	0.720DL + 1.3Q _E

4.7 Preliminary Design Check

4.7.1 Introduction and Overview

Models under investigation have been modeled and designed using the standard SAP2000 software. The study and thus the design, though, just take care of the major earthquake resisting members, i.e. the beam-column frames.

The visual inspection of the design data reveals an overly high longitudinal reinforcement for columns. However, the researcher is of the view that the relaxation in the columns vertical reinforcement is conservative. Since the greatest number of bars happens at the splices, no more than 3% reinforcement is spliced at any section (Wight, 2016). This practice alleviates constructability problems, and results in better design. To account for this concern, sections of building modules (beams, columns) are thoroughly enlarged as in Table 4.3, and no more than 6% reinforcement throughout the lap splice length are found.

Table 4.3: Newest geometry of models

Model	No. of Stories	Vertical Height (m)*		Depths of Slabs (mm)	Beams Sections (mm)		Columns Sections (mm)	
		Single story	Structure		Width	Depth	Length	Width
1N-R	10	3.4	34	130	650	400	650	650
					750	500	750	750
3N-R	10	3.55	35.5	130	700	450	700	700
					800	550	800	800
5N-R	10	3.7	37	130	750	500	750	750
					850	600	850	850
1N-SR	10	3.4	34	130	650	400	650	650
					750	500	750	750
3N-SR	10	3.55	35.5	130	700	450	700	700
					800	550	800	800
5N-SR	10	3.7	37	130	750	500	750	750
					850	600	850	850
1N-SS	10	3.4	34	130	650	400	650	650
					750	500	750	750
3N-SS	10	3.55	35.5	130	700	450	700	700
					800	550	800	800
5N-SS	10	3.7	37	130	750	500	750	750
					850	600	850	850
1J-SC	10	3.4	34	130	650	400	650	650
					750	500	750	750
3J-SC	10	3.55	35.5	130	700	450	700	700
					800	550	800	800
5J-SC	10	3.7	37	130	750	500	750	750
					850	600	850	850

* The clearance of all stories in all models is 2.95m per single story in the old edition versus 2.85m in the last edition.

4.7.2 Overview of the most Important Points

Upon the new dimensioning of the beam-column frames, the author re-made sure that fundamental periods (T_1) and the design modal base shears of models fall within the range prescribed in the ASCE/SEI 7-10 Code. These checks are described in Tables 4.4 through 4.6.

Table 4.4: T_n versus $C_u T_a$ values of the new models

Model	S_{D1}	T_1 (sec) ^a	C_t	x	h_n (m)	T_a (sec)	C_u	$C_u T_a$ (sec)	Check ^b
1N-R	0.250	1.08	0.0466	0.900	34	1.11	1.45	1.61	OK
3N-R	0.250	1.12	0.0466	0.900	35.5	1.16	1.45	1.68	OK
5N-R	0.250	1.14	0.0466	0.900	37	1.20	1.45	1.74	OK
1N-SR	0.388	1.08	0.0466	0.900	34	1.11	1.40	1.56	OK
3N-SR	0.388	1.12	0.0466	0.900	35.5	1.16	1.40	1.62	OK
5N-SR	0.388	1.14	0.0466	0.900	37	1.20	1.40	1.68	OK
1N-SS	0.475	1.08	0.0466	0.900	34	1.11	1.40	1.56	OK
3N-SS	0.475	1.12	0.0466	0.900	35.5	1.16	1.40	1.62	OK
5N-SS	0.475	1.14	0.0466	0.900	37	1.20	1.40	1.68	OK
1J-SC	0.938	1.08	0.0466	0.900	34	1.11	1.40	1.56	OK
3J-SC	0.938	1.12	0.0466	0.900	35.5	1.16	1.40	1.62	OK
5J-SC	0.938	1.14	0.0466	0.900	37	1.20	1.40	1.68	OK

^a T_1 values are collected from SAP2000

^b Check is OK if $T_1 \leq C_u T_a$

Table 4.5: Scaling up factors of MRS base shears of the new models

Model	Important Constants					C_s Eq.[3.33]	Min C_s		Max C_s		C_s	W	V (kN)			SF^c
	T_1	I_e	S_{DS}	S_{D1}	R		Eq.[3.34a]	Eq.[3.34b]	Eq.[3.35a]	ELF^a			$0.85 \times V_{ELF}$	MRS^b		
1N-R	1.08	1.25	0.500	0.250	8	0.0781	0.0100	0.0275	0.0362	0.0362	29959	1084	921	907	1.02	
3N-R	1.12	1.25	0.500	0.250	8	0.0781	0.0100	0.0275	0.0349	0.0349	39642	1383	1175	1161	1.02	
5N-R	1.14	1.25	0.500	0.250	8	0.0781	0.0100	0.0275	0.0343	0.0343	49623	1700	1445	1436	1.01	
1N-SR	1.08	1.25	0.600	0.388	8	0.0938	0.0100	0.0330	0.0561	0.0561	29959	1682	1429	1384	1.04	
3N-SR	1.12	1.25	0.600	0.388	8	0.0938	0.0100	0.0330	0.0541	0.0541	39642	2146	1824	1768	1.04	
5N-SR	1.14	1.25	0.600	0.388	8	0.0938	0.0100	0.0330	0.0532	0.0532	49623	2639	2243	2183	1.03	
1N-SS	1.08	1.25	0.700	0.475	8	0.109	0.0100	0.0385	0.0687	0.0687	29959	2059	1750	1692	1.04	
3N-SS	1.12	1.25	0.700	0.475	8	0.109	0.0100	0.0385	0.0663	0.0663	39642	2627	2233	2162	1.04	
5N-SS	1.14	1.25	0.700	0.475	8	0.109	0.0100	0.0385	0.0651	0.0651	49623	3231	2746	2669	1.03	
1J-SC	1.08	1.50	0.900	0.938	8	0.169	0.0100	0.0594	0.163	0.163	29959	4879	4147	3938	1.06	
3J-SC	1.12	1.50	0.900	0.938	8	0.169	0.0100	0.0594	0.157	0.157	39642	6225	5291	5032	1.06	
5J-SC	1.14	1.50	0.900	0.938	8	0.169	0.0100	0.0594	0.154	0.154	49623	7656	6507	6207	1.05	

^a $V = C_s \times W$

^b This columns represents Global FX values gained from SAP2000 analysis due to the effect of inelastic (design) acceleration response spectrum described in Section 3.18, and predefined in the X-Direction

^c $Scaling\ factor \geq \frac{0.85 \times V_{ELF}}{V_{MRS}}$

Table 4.6: Verification of MRS base shears of the new models

Model	C_s	W	V (kN)			Check*
			ELF	$0.85 \times V_{ELF}$	MRS	
1N-R	0.03617	29959	1084	921	925	OK
3N-R	0.03488	39642	1383	1175	1184	OK
5N-R	0.03427	49623	1700	1445	1450	OK
1N-SR	0.05613	29959	1682	1429	1439	OK
3N-SR	0.05413	39642	2146	1824	1839	OK
5N-SR	0.05318	49623	2639	2243	2249	OK
1N-SS	0.06872	29959	2059	1750	1760	OK
3N-SS	0.06627	39642	2627	2233	2248	OK
5N-SS	0.0651	49623	3231	2746	2749	OK
1J-SC	0.163	29959	4879	4147	4174	OK
3J-SC	0.157	39642	6225	5291	5334	OK
5J-SC	0.154	49623	7656	6507	6517	OK

* The check is OK for $V_{MRS} \geq 0.85 \times V_{ELF}$

4.8 Scope of the Detailed Design Examples

The design of all elements would generally achieved automatically over the computational models of the investigated buildings. In order to verify design results obtained from the computer output, a complete example element (interior span of a beam, column, and beam-column joint) shown in Figure 4.2, and belong to Model 3N-SR are fully designed and compared with that produced by SAP2000 solver.

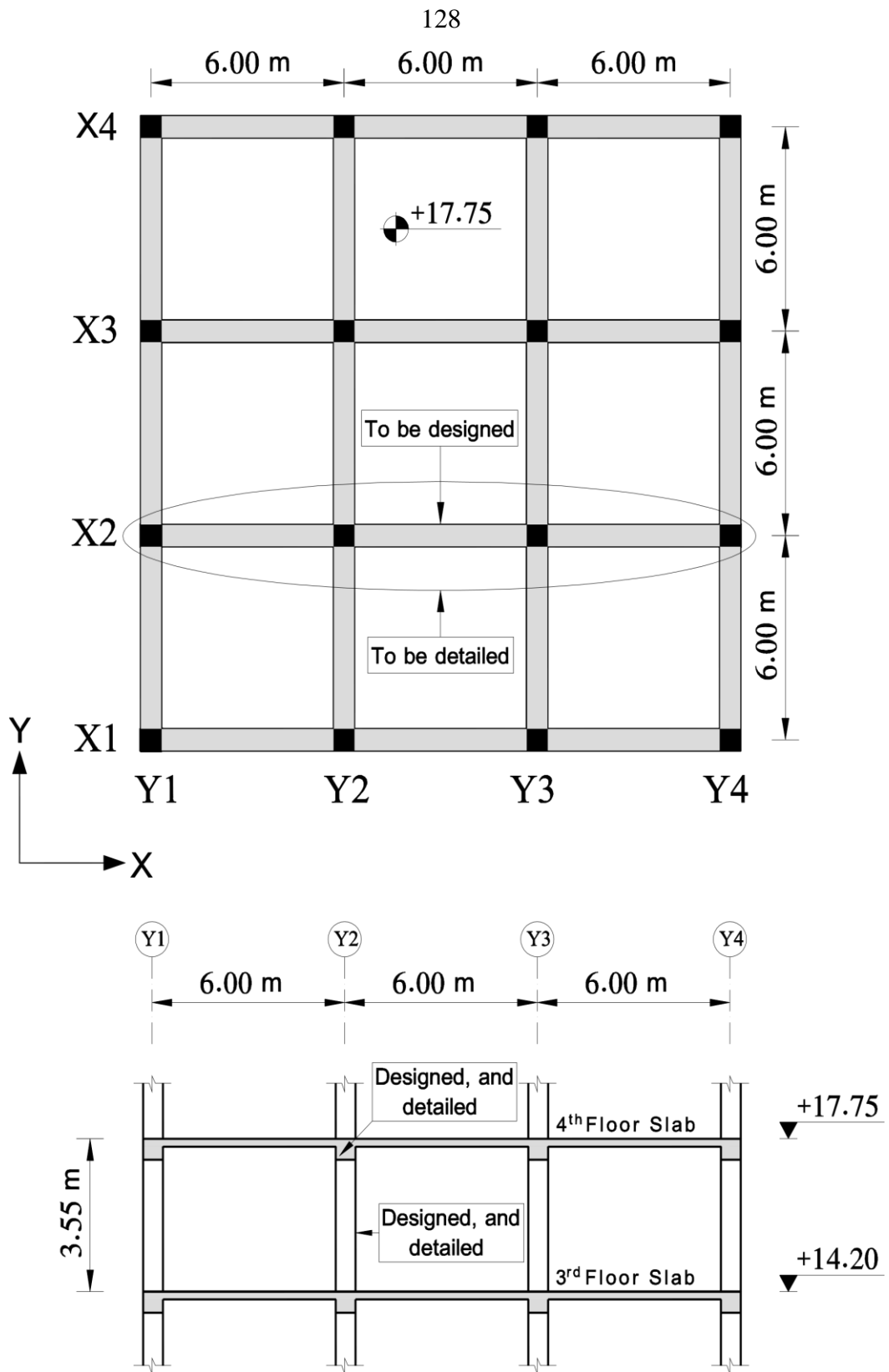


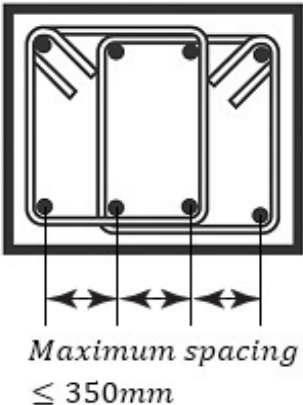
Figure 4.2: RC modules contained in the calculation sheet

4.8.1 Design of the Selected Beam Span

ACI 318-14	Discussion	Calculations
Materials Properties and Requirements		
19.2.1.1	The specified concrete compressive strength f'_c , shall be at least $21MPa$.	$f'_c = 23.5MPa$ is employed for the concrete structures.
20.2.2.4	Steel grades higher than $420MPa$ are not permitted.	$f_y = 420MPa$ is employed for the reinforcing steel bars.
Beam Geometry		
9.3.1.1	Beam Clear Span	$l_n = 5200mm$.
	Beam Depth If the beam depth satisfies the Code requirements, and is neither attached to nor supporting constructions exposed to damage by large deflections, the code allows to design the beam without deflection check.	The beam depth ($h = 550mm$) satisfies the code requirements. It is previously confirmed and is not modified here.
	Beam Flange Width For design purposes, the width of the beam is assumed to be b_w as generally considered in the common practice.	An approximate practice permits the beam to be designed as a rectangular section with $b_w = 800mm$.
Load Combinations for the Required Strength (U)		
5.3.1	The beam have to sustain the effects of the gravity loads and earthquake loads combined in different load patterns.	SAP2000 will try all these load patterns for the design: <ul style="list-style-type: none"> • $U_1 = 1.4DL$ • $U_2 = 1.2DL + 1.6LL$ • $U_3 = 1.32DL + 1.0LL + 1.3Q_E$ • $U_4 = 0.780DL + 1.3Q_E$

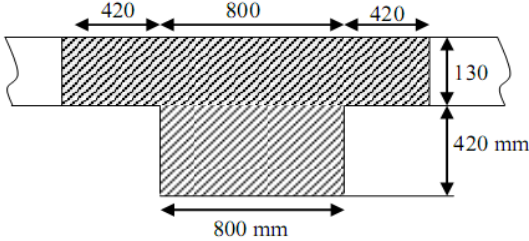
Analysis		
<p>Through the inspection of the analysis results, the critical load combination is $U_3 = 1.32DL + 1.0LL + 1.3Q_E$. Figure 4.3 shows the reversible bending moments obtained from SAP2000 analysis in the U_3 loading case.</p>		
<p>Figure 4.3: Definition of bending moments and beam hinges (Booth, 2014)</p>		
<p>The design end moments are obtained just at the column face, i.e. 400mm from the center of the support. Span end moments developed in the plastic hinges (PHs) are $M_u^- = -273kN.m$, and $M_u^+ = +20.8kN.m$.</p>		
<p>18.6.3.2</p>	<p>For the beam section lies on the column face, $M_u^+ \geq 50\%$ of M_u^- shall be warranted.</p> <p>The section also requires that at any one section along the beam span, M_u^+ and M_u^- shall not be less than 25% of $M_{u,max}$ applying on the face of either joints.</p>	<p>Positive end moment: $M_u^+ = 0.5 \times 273 = +137kN.m$. Rely $M_u^+ = 137kN.m \geq 20.8kN.m$.</p> <p>Moments through span: $M_u^+ \geq 0.25 \times 273 = +68.3kN.m$. $M_u^- \geq 0.25 \times 273 = -68.3kN.m$.</p>
<p>Note: The design procedures of negative moment propagated at the column face, ($M_u^- = -273kN.m$) will only be discussed in details.</p>		
Design of the Negative Moments in the Beam PHs		
<p>9.5.2.1, 22.3.1.1</p>	<p>The factored axial compressive force is considered in the beam design if $P_u < 0.10f_c' A_g$.</p>	<p>As the beam axial deformation approaches zero, the beam is not subjected to any internal axial compression. Thus, the member is designed without the effect of axial load.</p>
<p>9.5.1.2, 21.2.1</p>	<p>Assume tension controlled section with moment reduction factor $\phi = 0.9$.</p>	<p>This assumption will be checked later.</p>
<p>9.7.1.1, 20.6.1.3.1</p>	<p>Consider one row of reinforcement.</p>	<p>The concrete cover $c_c = 40mm$.</p>
	<p>Let d_h be the diameter of the hoop, and d_b the diameter of the rebar then, $d = h - c_c - d_h - 0.5d_b$</p>	<p>$d_h \approx 10mm$. $0.5d_b \approx 10mm$. $= 550 - 40 - 10 - 10 = 490mm$.</p>

9.6.1.2	<p>The required area of flexural steel (A_s) is (Hassoun and Al-Manaseer, 2015):</p> $A_s = \frac{0.85f'_c b_w d}{f_y} \left[1 - \sqrt{1 - \frac{2.61M_u}{f'_c b_w d^2}} \right]$ <p>A_s provided shall not be less than the greater of:</p> <p>(a) $A_{s,min} = \frac{0.25\sqrt{f'_c}}{f_y} b_w d$</p> <p>(b) $A_{s,min} = \frac{1.4}{f_y} b_w d$</p>	$A_s = 1535mm^2$. $A_{s,min} = 1131mm^2$. $A_{s,min} = 1307mm^2$.
18.6.3.1	<p>The quantity of longitudinal steel bars is limited to $A_{s,max} = 0.025b_w d$</p>	$A_{s,max} = 9800mm^2$. Use $A_s = 1535mm^2$.
R22.2.1	<p>The depth of the equivalent rectangular compressive block (a) is:</p> $a = \frac{A_s f_y}{0.85 f'_c b_w}$	$a = \frac{1535(420)}{0.85(23.5)(800)} = 40.3mm$
22.2.2.4.3	<p>a is related to the depth of the neutral axis (c) by the factor $\beta_1 = 0.85$</p>	
22.2.2.4.1	<p>$c = a/\beta_1$</p>	$c = 40.3/0.85 = 47.5mm$.
22.2.1	<p>The extreme-tensile strain (ϵ_t) is:</p> $\epsilon_t = 0.003 (d - c)/c$	$\epsilon_t = 0.003 \left(\frac{490 - 47.5}{47.5} \right) = 0.0280$
9.3.3.1	<p>For $P_u < 0.1f'_c A_g$, $\epsilon_t \geq 0.004$ should be registered.</p>	<p>The beam section is not subjected to axial force; assume $P_u < 0.1f'_c A_g$. $\epsilon_t = 0.0280 \geq 0.004$ OK.</p>
21.2.2	<p>Check: $\phi = 0.9$ occurs at $\epsilon_t \geq 0.005$</p>	$\epsilon_t = 0.0280 \geq 0.005$ OK.
	<p>Verification of result! The maximum permitted margin of error is 5%.</p>	$A_{s,SAP2000} = 1537mm^2$. $A_{s,hand cal.} = 1535mm^2$. $Error = \frac{1537 - 1535}{1535} = 0.130\%$ which is acceptable .

Design of Confinement in the Beam PHs		
	The controlling load case still $U_3 = 1.32DL + 1.0LL + 1.3Q_E$.	
18.6.4.1(a)	There must be a confinement zone of length $2h$ at either ends (PHs) of the beam.	This is the length of the beam PHs. $2h = 2 \times 55\text{cm} = 110\text{cm}$.
18.6.4.2	As shown in Figure 4.4, for instance, the maximum horizontal spacing of a secured bars in the flexural yielding region not to exceed 350mm centers.	
		
	Figure 4.4: Maximum horizontal spacing of restrained bars (ACI 318, 2014)	
	<p>The number of required legs could be calculated approximately by the formula:</p> $\frac{b_w - 2c_c - 2d_h - d_b}{350} + 1; \text{ if } d_h = 8\text{mm}, \text{ and } d_b \approx 20\text{mm} \text{ then,}$ $\# \text{ of legs} = \frac{800 - 80 - 16 - 20}{350} + 1 = 3 \text{ legs.}$ <ul style="list-style-type: none"> Use $\emptyset 8$ bar (two-legged hoop + one-crosstie), with an area of shear reinforcement of beam web; $A_v = 3\pi \times 8^2/4 = 151\text{mm}^2$. 	
18.6.4.4	Spacing of hoops (s) in the beam PHs shall not exceed the least of: (a) $d/4$ (b) $6 \times d_{b,min}$ (c) 150mm	<p>Assume: $\text{min. } d_{bar} = 14\text{mm}$.</p> $= 490/4 = 123\text{mm.}$ $= 6(14) = 84\text{mm} \quad \textbf{Governs.}$ $= 150\text{mm.}$ <p>Select $s = 75\text{mm} \leq 84\text{mm}$.</p>
	Let A_v/s = the area of web vertical bars per unit length of the beam due to shear at the specified location.	$A_v/s = 151/75 = 2.01\text{mm}^2/\text{mm}$.

Design of Shear in the Beam PHs		
R18.6.5	<p>Probable Moment</p> <p>The probable flexural strength of the member at joint faces (M_{pr}), assumes a tensile stress in tension steel = $1.25f_y$ with a moment reduction factor $\phi = 1.0$.</p> <p>According to Hassoun and Al-Manaseer (2015), beam probable moment could be calculated by:</p> $M_{pr} = A_s(1.25f_y) \left(d - \frac{a_{pr}}{2} \right)$	<p>Hinging moments:</p> $M_{u,hogging} = -273kN.m.$ $M_{u,sagging} = +137kN.m.$ $a_{pr} = \frac{1537(525)}{0.85(23.5)(800)} = 50.5mm.$ $M_{pr,hogg.} = 1537(525) \left(490 - \frac{50.5}{2} \right) = 375kN.m.$ <p>Similarly, $M_{pr,sagg.} = 249kN.m.$</p>
18.6.5.1	<p>The maximum probable shear force (V_e) developed due to the formation of beam plastic hinges, i.e M_{pr} is:</p> $V_e = \frac{\sum M_{pr}}{l_n} + V_{u(gravity)}$	<p>$V_{u(gravity)} = 140kN$ is obtained from computer analysis in the load case $U = 1.32DL + 1.0LL$.</p> $V_e = \frac{375 + 249}{5.20} + 140 = 260kN.$
19.2.4.2	<p>The factor of concrete mechanical properties is $\lambda = 1.0$.</p>	
22.5.5.1	<p>For members without axial force, the concrete nominal shear strength is</p> $V_c = 0.17\lambda\sqrt{f'_c}b_wd$	$V_c = 0.17(1)\sqrt{23.5}(800)(490)/1000 = 323kN.$
9.5.1.2, 21.2.1	<p>The shear reduction factor $\phi = 0.75$.</p>	
22.5.1.2	<p>The cross-sectional dimensions shall fulfil $V_e \leq 5\phi V_c$</p>	$5\phi V_c = 5(0.75)(323) = 1211kN.$ $V_e = 260kN \leq 5\phi V_c = 1211kN \text{ OK.}$
18.6.5.2	<p>V_c must be neglected when the following two conditions occur simultaneously.</p> <p>(a) $V_{sway} \geq V_e/2$</p> <p>(b) $P_u < f'_c A_g/20$</p>	
	<p>V_{sway} from SAP2000 analysis in the load case $U = 1.3Q_E$.</p> <p>(a) $V_{sway} = 60.2kN \not\geq 260/2 = 130kN$</p> <p>(b) $P_u = 0.00kN < 0.05f'_c A_g$</p> <p><i>Because only one condition occurs, V_c exists and equals 323kN.</i></p>	

22.5.10.1	At every section where $V_e > \phi V_c$, transverse reinforcement shall be provided such that $V_s > V_e/\phi - V_c$. Where V_s = the contribution of the web transverse steel in the nominal shear strength.	$V_e = 260kN > 0.75(323) = 242kN$. $V_s > 260/0.75 - 323 = 23.7kN$.
22.5.10.5.3	$A_v/s = V_s/f_y d$	$A_v/s = 23.7 \times 10^3 / (420 \times 490)$ $= 0.115mm^2/mm$.
9.6.3.1	At every section where $V_e > 0.5\phi V_c$, $A_{v,min}/s$ shall be provided.	$V_e = 260kN > 0.5\phi V_c = 121kN$.
9.6.3.3	$A_{v,min}/s$ shall be the greater of: (a) $\frac{0.062\sqrt{f'_c}b_w}{f_y}$ (b) $\frac{0.35b_w}{f_y}$	$\frac{0.062\sqrt{23.5}(800)}{420} = 0.572mm^2/mm$. $\frac{0.35(800)}{420} = 0.667mm^2/mm$. Rely $A_v/s = 2.01mm^2/mm$, as yet controls.
9.7.6.2.2	For $V_s \leq 2V_c$, specified spacing of hoops (s) shall be the lesser of: (a) $d/2$ (b) $600mm$	$V_s = 23.7kN \leq 2V_c = 646kN$. $= 490/2 = 245mm$ Governs. $= 600mm$. $s_{provd} = 75mm \ll 245mm$ OK.
	Verification of result! The maximum permitted margin of error is 5%.	$A_v/s_{SAP2000} = 1.87mm^2/mm$. $A_v/s_{hand cal.} = 2.01mm^2/mm$. $Error = \frac{2.01 - 1.87}{1.87} = 7.49\%$, which is slightly over the permitted value.
Design for Torsion		
	Continue with the load case $U_3 = 1.32DL + 1.0LL + 1.3Q_E$.	The design torsional moment (T_u) at the face of beam-column connection is given from SAP2000 analysis as $T_u = 4.30kN.m$.

<p>9.2.4.4(a)</p>	<p>Let A_{cp} and P_{cp} denoting the area and the perimeter of the gross concrete cross-section then, the overhanging flange width used for A_{cp} and P_{cp} calculations shall equal to the web width adds to an offset of slab equals to the minimum of (beam web width, 4 times the slab depth) on each side of the beam.</p> <p>The T-beam section required for torsional design calculations is shown in Figure 4.5.</p>  <p style="text-align: center;">Figure 4.5: Overhanging flange widths for torsional design</p>
<p>9.2.4.4(b)</p>	<p>The beam flanges shall be ignored in the cases where the parameter A_{cp}^2/P_{cp} calculated for a T-beam is less than that calculated for the same beam without flanges.</p> <p>$(A_{cp}^2/P_{cp})_{T-beam, Figure 4.5} = 68.9 \times 10^6 mm^3$.</p> <p>$(A_{cp}^2/P_{cp})_{Rec.beam, 800mm \times 550mm} = 71.7 \times 10^6 mm^3$.</p> <ul style="list-style-type: none"> As a result, consider rectangular section effect.
<p>9.5.4.1, 22.7.4.1</p> <p>9.5.1.2, 21.2.1</p> <p>9.5.4.1</p>	<p>The threshold torsion (T_{th}) for solid cross-section shall be calculated as:</p> $T_{th} = 0.083\lambda\sqrt{f'_c}(A_{cp}^2/P_{cp})$ <p style="text-align: right;">$= 0.083(1)\sqrt{23.5} \times (71.7 \times 10^6)/10^6$ $= 28.8 kN.m$.</p> <p>Torsional strength reduction factor $\phi = 0.75$.</p> <p>If $T_u < \phi T_{th}$ then, the torsional effect shall be neglected so that, minimum torsional reinforcement ($A_{l,min}, A_{t,min}$) is not needed.</p> <p>Where $A_{l,min}$ = the minimum area of longitudinal steel to resist torsion, and $A_{t,min}$ = the minimum area of transverse steel to resist torsion.</p> <p style="text-align: right;">$\phi T_{th} = 0.75 \times 28.8 = 21.6 kN.m$. $T_u = 4.30 kN.m < 21.6 kN.m$, accordingly ignore the effect of torsion.</p>
	<p>Verification of results!</p> <p>The maximum permitted margin of error is 5%.</p> <p style="text-align: right;">$A_{l,min_{SAP2000}} = 0.0$. $A_{l,min_{hand cal.}} = 0.0$. Error = 0.0%, which is at best.</p> <p style="text-align: right;">$A_{t,min_{SAP2000}} = 0.0$. $A_{t,min_{hand cal.}} = 0.0$. Error = 0.0%, which is at best.</p>

4.8.2 Detailing of the Selected Beam

Figure 4.6 shows the longitudinal and transverse reinforcement of the beam example.

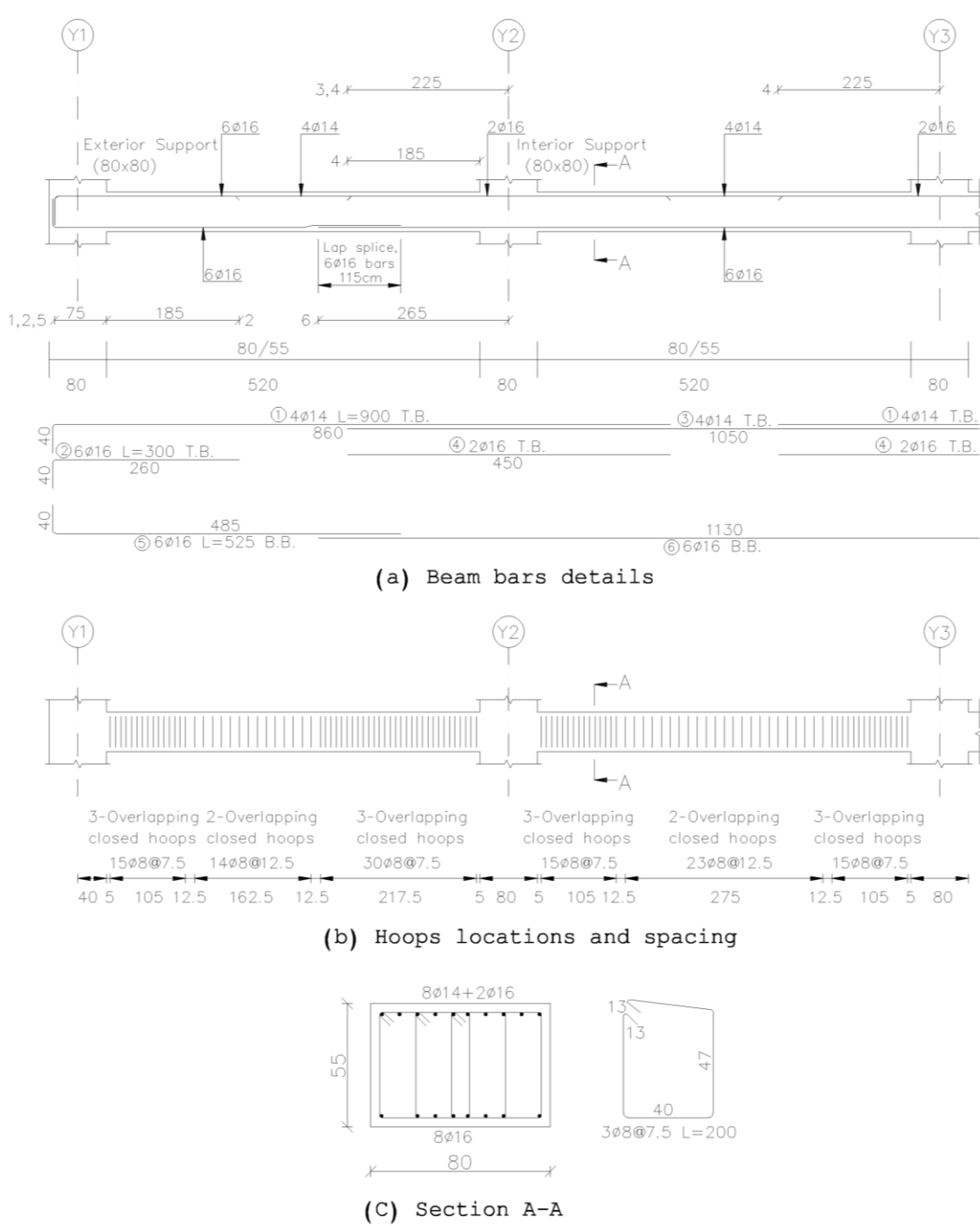
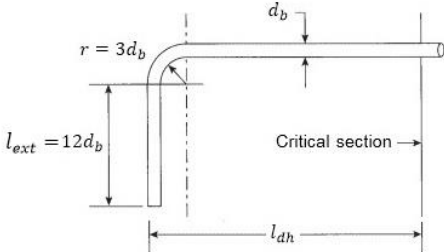


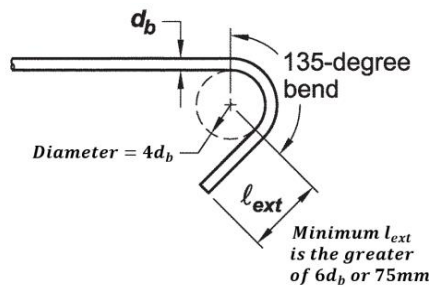
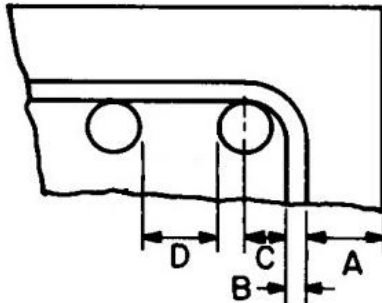
Figure 4.6: Reinforcement details (in centimeters) of the special beam

ACI 318-14	Discussion	Calculations
	The detailing operations of reinforcement including bars lengths will generally take place within the common construction practice following the local design offices.	In no case should this sequence violate the ACI 318-14 Code minimum requirements for detailing and constructability issues.
The Development Lengths		
	<p>Case 1: Interior supports; negative moments. Use 8Ø14 plus 2Ø16 top bars.</p> <p>Bars shall extend beyond the columns center-lines Y2, and Y3 to at least $(c_1/2 + l_n/3)$</p>	<ul style="list-style-type: none"> The focus is on the shorter reinforcing bars (2Ø16). The longer bars (8Ø14) having smaller diameters thus, they are by default OK. <p>$= (80/2 + 520/3) = 213cm.$ $l_{2Ø16} = 450cm \geq 2(213) = 426cm.$</p>
<p>9.7.1.2, 25.4.2.1, 25.4.2.2, 25.4.2.4</p> <p>18.8.5.1, 18.8.5.3b</p>	<p>Let ψ_t be the bar location factor, and ψ_e refers to the bar coating factor then, the development length in tension for straight bars (l_d) is the maximum of:</p> <p>(a) $\left(\frac{f_y \psi_t \psi_e}{2.1 \lambda \sqrt{f'_c}} \right) d_b$ (b) 300mm</p> <p>The development length in tension for straight bars (l_d) having $d_b \leq 36mm$ is the maximum of:</p> <p>(a) $3.25 \left(\frac{f_y d_b}{5.4 \lambda \sqrt{f'_c}} \right)$ (b) $3.25(8d_b)$ (c) $3.25(150mm)$</p>	<ul style="list-style-type: none"> For top bars; $\psi_t = 1.3.$ For uncoated bars; $\psi_e = 1.0.$ <p>$= \frac{420 \times 1.3 \times 1}{2.1 \times 1 \times \sqrt{23.5}} \times 1.6 = 85.8cm.$ $= 30cm.$</p> <p>$= 3.25 \left(\frac{420 \times 1.6}{5.4(1)\sqrt{23.5}} \right) = 83.4cm.$ $= 3.25(8 \times 1.6) = 41.6cm.$ $= 3.25 \times 15 = 48.8cm.$</p> <p>The available 2Ø16 bars length of 185cm is larger than $l_d = 85.8cm$, consequently sufficient.</p>

	Case 2: Interior span and interior supports; positive moments.	Use 6Ø16 bottom bars.
9.7.1.3, 25.5.2.1	The lap splice lengths of reinforcement in tension (l_{st}) the greatest of: (a) $1.3l_d$ (b) 300mm	$= 1.3 \times 85.8cm = 112cm.$ $= 30cm.$ Provide $115cm \geq 112cm.$
18.6.3.3	Lap splices are neither permitted inside joints nor within plastic hinging zones.	
R25.4.1.1	Bars shall extend beyond the face of the support; the point of peak stresses.	This condition is automatically achieved where $l_{st} + 2h \geq l_d.$ In the final consideration: $l_{6\phi 16} = 520 + 2(80) + 2(2h) + 2l_{st}$ $= 520 + 160 + 220 + 2(115)$ $= 1130cm.$
	Case 3: Exterior supports; negative moments.	Use 6Ø16 plus 4Ø14 top bars. Assume $c_c = 5cm$ on bar extension beyond the hook. <ul style="list-style-type: none"> The focus is on the shorter reinforcing bars (6Ø16). The longer bars (4Ø14) having smaller diameters thus, they are by default OK.
R25.4.1.1	Bars shall extend inside the beam span beyond the point of peak stress in the steel. Bars shall extend inside the joint beyond the point of peak stress in the steel.	Place bars with length more than $l_n/3 = 173cm.$ The available length of bars is satisfactory. $(185cm \geq 173cm \geq l_d = 85.8cm)$ The Available anchorage length 75cm is less than $l_d = 85.8cm$ hence, a standard hook is required at column side.

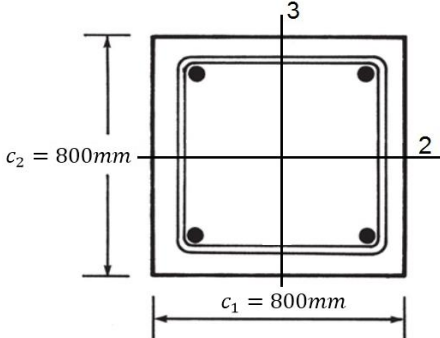
<p>9.7.1.2, 25.4.3.1, 25.4.3.2</p> <p>18.8.5.1</p>	<p>Let ψ_c be the bar concrete cover factor, and ψ_r refers to the confining reinforcement factor then, the development length in tension for hooked bars (l_{dh}) is the peak of:</p> <p>(a) $\frac{0.24f_y\psi_e\psi_c\psi_r}{\lambda\sqrt{f'_c}}d_b$</p> <p>(b) $8d_b$</p> <p>(c) $150mm$</p> <p>The development length in tension for hooked bars (l_{dh}) having $d_b \leq 36mm$ is the maximum of:</p> <p>(a) $\frac{f_y}{5.4\lambda\sqrt{f'_c}}d_b$</p> <p>(b) $8d_b$</p> <p>(c) $150mm$</p>	<ul style="list-style-type: none"> • $\psi_e = 1.0$. • $\psi_c = 1.0$. • $\psi_r = 1.0$. $= \frac{0.24(420)(1)^3}{1 \times \sqrt{23.5}} \times 1.6 = 33.3cm.$ $= 8 \times 1.6 = 12.8cm.$ $= 15cm.$ $= \frac{420}{5.4 \times 1 \times \sqrt{23.5}} \times 1.6 = 25.7cm.$ $= 12.8cm.$ $= 15cm.$ <p>The provided length $75cm \geq 33.3cm$ thus, the available anchorage length of $75cm$ is satisfactory for achieving anchorage using 90-degree bent hook.</p>
<p>25.3.1</p>	<p>The standard hook geometry for bars developed in tension is shown in Figure 4.7.</p>  <p>Figure 4.7: Anchorage details for bar size less than $\varnothing 25$ (ACI 318, 2014)</p>	<ul style="list-style-type: none"> • $l_{ext} = 12 \times 1.6 = 19.2cm.$ • $r = 3 \times 1.6 = 4.80cm.$ <p>Provide $40cm \geq l_{ext} + r + d_b = 19.2 + 4.8 + 1.6 = 25.6cm.$ Thus, the total length of $6\varnothing 16$ top bars at exterior supports becomes $40 + 75 + 185 = 300cm.$</p>
<p>Case 4: Exterior supports; positive moments.</p>	<p>The provided $6\varnothing 16$ bottom bars conform to the requirements of the ACI Code.</p>	

Transverse Steel Requirements		
18.6.4.1(a)	Hoops shall be provided over the beam PHs, with limited spacing.	In this respect, $s = 7.5cm$.
18.6.4.4	The first hoop is placed at a distance not exceeding 5cm from the column face.	
18.6.3.3	The entire lap splice length shall be enclosed by hoops at spacing not exceeding the lesser of: (a) $d/4$ (b) 100mm	$= 49/4 = 12.3cm$. $= 10cm$ Governs. Select $s = 7.5cm \leq 10cm$ similar to the spacing of hoops in the beam PHs.
18.6.4.2, 25.7.2.3(b)	Where hoops are obligatory required by the code (PHs, and lap splices), no unrestrained bar shall be further than 150mm clear on both sides from a laterally supported bar. The number of required legs could be nearly evaluated as: $\frac{b_w - 2c_c - 2d_h - 2d_b}{300 + d_b} + 1$; if $d_h = 8mm$, and $d_b = 16mm$ then, $\# \text{ of legs} = \frac{800 - 80 - 16 - 32}{300 + 16} + 1 = 4 \text{ legs.}$	
9.7.6.1.2, 18.6.4.2, 25.7.2.3(a)	In the beam PHs and lap splices, every corner and alternate longitudinal bar shall be restrained by ties having hooks with an extension bend not more than 135-degree. This condition is obviously satisfied in Figure 4.6(c), so that the total legs of hoops along PHs and lap splices is six. <ul style="list-style-type: none">• 3Ø8 hoops@7.5cm are required over the total length of PHs.• 3Ø8 hoops@7.5cm are required over the total length of splices.	
18.6.4.6	Where hoops are not obligatory required by the code, stirrups having seismic hooks spaced by not more than $d/2$ are eligible. The author is of the opinion to use closes hoops instead of open stirrups. Over the reaming length of the interior and exterior beam spans, and in order to account for A_v/s produced by SAP2000; <ul style="list-style-type: none">• Use 2Ø8 hoops@12.5cm with $A_v/s = 1.61 \text{ mm}^2/\text{mm}$. Note: The selected hoop spacing of 12.5cm also satisfies Section 9.7.6.2.2 of the ACI 318-14 Code.	
9.7.6.1.2, 18.6.4.2, 25.7.2.3(a)	Every corner and alternate longitudinal bar shall be restrained by ties having hooks with an extension bend not more than 135-degree.	<ul style="list-style-type: none">• This condition is obviously satisfied in Figure 4.6(c).

<p>25.3.2</p>	<p>The standard hook geometry for hoops is shown in Figure 4.8.</p>  <p>Figure 4.8: End hook of hoops less than 16mm in diameter (ACI 318, 2014)</p> <ul style="list-style-type: none"> • $l_{ext} \geq \max. (6 \times 0.8 = 4.8cm, 7.5cm) = 7.5cm.$ • $Diameter = 4 \times 0.8 = 3.2cm.$ 	
<p>Minimum and Maximum Bar Spacing for 8Ø14 Plus 2Ø16 Longitudinal Bars</p>		
	<p>For two or more bars placed in one layer as shown in Figure 4.9, the actual clear spacing between bars (D) may be calculated as (Taylor et al., 2016):</p> $D = \frac{b_w - 2A - m(B + C) - (n - m/2)d_b}{n - 1}, \text{ where:}$ <p>Where: $C =$ the greater of $\begin{cases} 2d_h \text{ for hoops less than } \text{Ø}16 \text{ bar diameter.} \\ 0.5d_b. \end{cases}$</p> <p>$m =$ No. of legs. $n =$ No. of longitudinal bars.</p>  <p>Figure 4.9: Spacing details of long. bars in beams (Taylor et al., 2016)</p> <ul style="list-style-type: none"> • Assume the worst case, i.e. all bars are of Ø16 diameter. $A = 40mm, B = 8mm, c = \max. (16mm, 8mm) = 16mm, m = 6, n = 10,$ and $d_b = 16mm.$ $D = \frac{800 - (2 \times 40) - 6(8 + 16) - (10 - 6/2) \times 16}{10 - 1} = 51.6mm.$	
<p>9.7.2.1, 25.2.1</p>	<p>Minimum clear spacing between longitudinal bars in the same layer shall be not less than the greatest of:</p> <ol style="list-style-type: none"> 25mm d_b $(4/3)d_{agg}.$ 	<p>$d_{agg} =$ the maximum aggregate size in the concrete mixture, may be taken as 20mm (Taylor et al., 2016).</p> <p>$= 25mm.$ $= 14mm.$ $\approx (4/3) \times 20 = 26.7mm$ Governs.</p> <p>51.6mm clear spacing, therefore enough.</p>

9.7.2.2, 24.3.1, 24.3.2, 24.3.2.1	<p>The maximum bar spacing at the tension face shall be at most the smaller of:</p> <p>(a) $380 \left(\frac{280}{2f_y/3} \right) - 2.5c_c$</p> <p>(b) $300 \left(\frac{280}{2f_y/3} \right)$</p>	<p>The concrete cover to the primary steel is: $c_c = 40 + 10 = 50mm$.</p> <p>$= 380 \left(\frac{280}{2 \times 420/3} \right) - 2.5 \times 50$</p> <p>$= 230mm$ Governs.</p> <p>$= 300 \left(\frac{280}{2 \times 420/3} \right) = 300mm$.</p> <p>The available $51.6mm$ clear spacing subsequently enough.</p>
Integrity Requirements		
9.7.7.2	<ul style="list-style-type: none"> • At least 25% of the beam max. positive moment steel, but not less than 2-bars, shall be continuous. • Beam longitudinal bars shall be enclosed by closed stirrups over the clear span of the beam. 	These conditions are fully met.
9.7.7.3	<ul style="list-style-type: none"> • Longitudinal bars of the beam shall be bounded by the vertical bars of the column. 	
9.7.7.5	<ul style="list-style-type: none"> • Positive moment bars shall be spliced near or at the supports. • Negative moment steel shall be spliced near or at midspan. 	
18.6.3.1	<ul style="list-style-type: none"> • There must be at least 2 continuous bars at both top and bottom faces of the beam. 	

4.8.3 Design of the Selected Column

ACI 318-14	Discussion	Calculations
Materials Properties and Requirements		
19.2.1.1	The specified concrete compressive strength f'_c , shall be at least $21MPa$.	$f'_c = 23.5MPa$ is employed for the concrete structures.
20.2.2.4	Steel grades higher than $420MPa$ are not permitted.	$f_y = 420MPa$ is employed for the reinforcing steel bars.
Load Combinations for the Required Strength (U)		
5.3.1	The column have to resist the effects of the gravity loads, and lateral loads combinations simultaneously.	The computer program uses the following load combinations for design: <ul style="list-style-type: none"> • $U_1 = 1.4DL$ • $U_2 = 1.2DL + 1.6LL$ • $U_3 = 1.32DL + 1.0LL + 1.3Q_E$ • $U_4 = 0.780DL + 1.3Q_E$
Preliminary Remark		
	The internal forces are variable along the column length. Hence, the controlling internal forces are considered for designing the whole column.	
Analysis		
	<p>Notes:</p> <ul style="list-style-type: none"> • The column was analyzed and designed at its two end sections. The design results were quite identical. • The analysis and the subsequent design steps of longitudinal bars needed for the column top section ($275mm$ below the column upper joint) are only discussed by the researcher. <p>Through the inspection of the analysis results, the critical load combination is $U_3 = 1.32DL + 1.0LL + 1.3Q_E$. Column cross-section is shown in Figure 4.10.</p> <div style="text-align: center;">  </div> <p>Figure 4.10: Local axes of the column under design</p> <p>As the study is on purpose “global axis X of the structure”, it should be noted that the column local axis 2 is oriented so that it coincides with the global axis X.</p>	

(Continued)

To avoid potential errors associated with the complicated combinations of loading effects having \pm signs, eight combinations of signs of the column axial forces and biaxial moments are examined through the design process. Internal moments acting on column upper section are given in Table 4.7.

Table 4.7: Factored axial forces and biaxial moments obtained by computer

Case	P_u (kN)	$M_{u3,ns}$ (kN.m)	$M_{u2,ns}$ (kN.m)	$M_{u3,s}$ (kN.m)	$M_{u2,s}$ (kN.m)
1	-3623	13.6	-13.6	189	68.5
2	-3623	13.6	-13.6	189	-68.5
3	-3623	13.6	-13.6	-189	68.5
4	-3623	13.6	-13.6	-189	-68.5
5	-3597	13.6	-13.6	189	68.5
6	-3597	13.6	-13.6	189	-68.5
7	-3597	13.6	-13.6	-189	68.5
8	-3597	13.6	-13.6	-189	-68.5

Where:

P_u = the factored axial compressive force from the analysis in the loading case
 $U_3 = 1.32DL + 1.0LL + 1.3Q_E$.

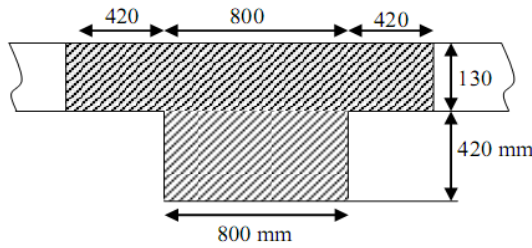
$M_{u3,ns}$ = the factored end moment about local axis 3 from the analysis in the loading case $U = 1.32DL + 1.0LL$.

$M_{u2,ns}$ = the factored end moment about local axis 2 from the analysis in the loading case $U = 1.32DL + 1.0LL$.

$M_{u3,s}$ = the factored end moment about local axis 3 from the analysis in the loading case $U = 1.3Q_E$.

$M_{u2,s}$ = the factored end moment about local axis 2 from the analysis in the loading case $U = 1.3Q_E$.

9.5.2.1, 22.4.1.1	The factored axial compressive force is effective if $P_u > 0.1f'_cA_g$.	<ul style="list-style-type: none"> • P_u is either 3597kN or 3623kN. • $0.1f'_cA_g = 1540kN$. <p>Since $P_u > 0.1f'_cA_g$, the axial load could not be ignored; beam-column action in either vibrating options.</p>
----------------------	---	---

	<p>The section of the restraint beam at column connections is shown in Figure 4.11</p>  <p>Figure 4.11: Cross-sectional dimensions of the restraint T-beam</p> <p>I_g values for both column and the restraint T-beam sections shown in Figures 4.10 and 4.11, are readily given in SAP2000.</p> <p>$I_{g,column} = 3.41 \times 10^{10} mm^4$.</p> <p>$I_{g,beam} = 1.51 \times 10^{10} mm^4$.</p>	
<p>6.6.3.1.1(a)</p> <p>R6.2.5</p> <p>R6.2.5</p>	<p>The cracked moment of inertia of columns and beams sections may be estimated by:</p> <p>$I_{cr,column} = 0.70I_{g,column}$</p> <p>$I_{cr,beam} = 0.35I_{g,beam}$</p> <p>Let l be the length of the member measured center to center of joints then, the end restraint factor (Ψ) at every end of the column is:</p> $\Psi = \frac{\sum(E_c I/l)_{column}}{\sum(E_c I/l)_{beam}}$ <p>Determine k from the alignment chart given in Appendix K.</p>	<p>$I_{cr,column} = 2.39 \times 10^{10} mm^4$.</p> <p>$I_{cr,beam} = 0.529 \times 10^{10} mm^4$.</p> <p>Due to the symmetry of the model and elements, the column has one unique value of Ψ in both directions (local axes) at top and bottom.</p> $\Psi = \frac{(E_c \times 2.39 \times 10^{10} / 3.55) \times 2}{(E_c \times 0.529 \times 10^{10} / 6.00) \times 2} = 7.64$ <p>Consider k_3 and k_2 are the column k – factors conforming to the bending about local axes 3, and 2 respectively then, $k = k_3 = k_2 = 2.65$.</p>
<p>6.2.5(a)</p>	<p>In stories of sway-resisting columns, the column is permitted to be analyzed as being short if:</p> $\frac{kl_u}{r} \leq 22$	<p>The structural frames considered as sway-permitted, which tends to be overly conservative.</p> $= \frac{2.65(3550 - 550)}{0.3(800)} = 33.1 \not\leq 22$ <p>As the column meets the slenderness limit for second order effect, $P - \Delta$ effect has to be considered in both directions of the column cross-section.</p>

Design of Column Upper Section		
	Vertical reactions and hence, the axial loads developed in columns due to transient seismic loading are equal and opposite, i.e. they cancel out each other. In other words, $\sum P_u$ is determined due to persistent gravity loads.	$\sum P_u$ is evaluated at 275mm below the beam-column joint from the analysis in the load case: $U = 1.32DL + 1.0LL$.
6.6.4.6.2(b)	$\sum P_u$ = the summation of the axial forces affecting all columns in the meant story.	$\sum P_{u,SAP2000} = 38544kN$.
19.2.2.1	The modulus of elasticity of concrete is $E_c = 4700\sqrt{f'_c}$	$E_c = 4700\sqrt{23.5} = 2.28 \times 10^4 MPa$.
R6.6.4.4.4	Buckling analysis of columns requires that the effective flexural stiffness of the column is $(EI)_{eff} = 0.25E_cI_g$	$= 0.25(2.28 \times 10^4)(3.41 \times 10^{10})$ $= 1.94 \times 10^{14} N.mm^2$.
6.6.4.4.2	The critical buckling load of the column (P_c) could be calculated as: $P_c = \frac{\pi^2(EI)_{eff}}{(kl_u)^2}$	$P_c = \frac{(22/7)^2 \times 1.94 \times 10^{14}}{(2.65 \times 3000)^2}$ $= 30319kN$.
6.6.4.6.2(b)	Let $\sum P_c$ be the summation of critical buckling loads of all columns in the meant story.	k - factors, and the associated P_c values of columns are shown in Appendix L. In every direction, $\sum P_c = 351701kN$.
6.6.4.6.2(b)	The moment magnifier may be calculated by: $\delta_s = \frac{1}{1 - \frac{\sum P_u}{0.75\sum P_c}} \geq 1$	$\delta_s = \frac{1}{1 - \frac{38544}{0.75(351701)}} = 1.17 \geq 1$

6.6.4.6.1	<p>The actual design biaxial moments included in Table 4.8 have been computed through the following equations:</p> $M_{u3} = M_{u3,ns} + \delta_s M_{u3,s}$ $M_{u2} = M_{u2,ns} + \delta_s M_{u2,s}$ <p>McCormac and Brown (2015) suggested an approximate design approach for square columns in such a way that, as a result of biaxial bending, the design moment about the 2-or 3-axis is $M_u = M_3 + M_2$. Table 4.8, however, displays the design moment proposed to act about one axis passing through the centroid of the column cross-section.</p> <p>Table 4.8: Design forces and moments affecting column upper section</p> <table border="1" data-bbox="539 680 1337 1093"> <thead> <tr> <th>Case</th> <th>P_u (kN)</th> <th>M_{u3} (kN.m)</th> <th>M_{u2} (kN.m)</th> <th>M_u (kN.m)</th> </tr> </thead> <tbody> <tr><td>1</td><td>-3623</td><td>235</td><td>66.5</td><td>302</td></tr> <tr><td>2</td><td>-3623</td><td>235</td><td>-93.7</td><td>329</td></tr> <tr><td>3</td><td>-3623</td><td>-208</td><td>66.5</td><td>275</td></tr> <tr><td>4</td><td>-3623</td><td>-208</td><td>-93.7</td><td>302</td></tr> <tr><td>5</td><td>-3597</td><td>235</td><td>66.5</td><td>302</td></tr> <tr><td>6</td><td>-3597</td><td>235</td><td>-93.7</td><td>329</td></tr> <tr><td>7</td><td>-3597</td><td>-208</td><td>66.5</td><td>275</td></tr> <tr><td>8</td><td>-3597</td><td>-208</td><td>-93.7</td><td>302</td></tr> </tbody> </table>		Case	P_u (kN)	M_{u3} (kN.m)	M_{u2} (kN.m)	M_u (kN.m)	1	-3623	235	66.5	302	2	-3623	235	-93.7	329	3	-3623	-208	66.5	275	4	-3623	-208	-93.7	302	5	-3597	235	66.5	302	6	-3597	235	-93.7	329	7	-3597	-208	66.5	275	8	-3597	-208	-93.7	302
Case	P_u (kN)	M_{u3} (kN.m)	M_{u2} (kN.m)	M_u (kN.m)																																											
1	-3623	235	66.5	302																																											
2	-3623	235	-93.7	329																																											
3	-3623	-208	66.5	275																																											
4	-3623	-208	-93.7	302																																											
5	-3597	235	66.5	302																																											
6	-3597	235	-93.7	329																																											
7	-3597	-208	66.5	275																																											
8	-3597	-208	-93.7	302																																											
18.7.4.1	<p>The ratio of longitudinal reinforcement of the column section (ρ_g) is extracted from the interaction diagram attached in Appendix K (Figure K.2).</p> <p>The area of longitudinal steel (A_{st}) shall be within the following two limits:</p> <p>(a) $A_{st,min} = 0.01A_g$</p> <p>(b) $A_{st,max} = 0.06A_g$</p>	<p>The investigation of every set of loadings (P_u, M_u) in Table 4.8 points to $\rho_g < 1.0\%$.</p> <p>$= 0.01(640000) = 6400mm^2$.</p> <p>$= 0.06(640000) = 38400mm^2$.</p> <p>Use $A_{st} = 6400mm^2$.</p>																																													

<p>22.4.2.1, 22.4.2.2</p> <p>21.2.2</p>	<p>Re-analyze the column section by means of Bresler method (Wight, 2016):</p> $\frac{1}{P_u} = \frac{1}{P_{u3}} + \frac{1}{P_{u2}} - \frac{1}{P_{uo}}$ <p>Where:</p> <p>P_u = the design compressive strength of the biaxially loaded column.</p> <p>P_{u3} = the design uniaxial load of the section as determined from the interaction diagram at an eccentricity $e_3 = M_{u3} /P_u$, and $\rho_g = 1.0\%$.</p> <p>P_{u2} = the design uniaxial load of the section determined from the interaction diagram at an eccentricity $e_2 = M_{u2} /P_u$, and $\rho_g = 1.0\%$.</p> <p>P_{uo} = the maximum design uniaxial load of the section at zero eccentricities ($e_3 = e_2 = 0.00$), and determined by $P_{uo} = \phi(0.85f'_c(A_g - A_{st}) + f_y A_{st})$.</p> <p>$\phi = 0.65$</p>																																																																																	
	<p>Table 4.9 shows checks on a design done by a non-exact method.</p> <p>Table 4.9: Determination of the design capacity of the biaxial loaded column</p> <table border="1" data-bbox="475 931 1394 1379"> <thead> <tr> <th>Case</th> <th>e_3 (m)</th> <th>e_2 (m)</th> <th>P_{u3} (kN)</th> <th>P_{u2} (kN)</th> <th>P_{uo} (kN)</th> <th>$P_{u,Bresler}$ (kN)</th> <th>$P_{u,actual}$ (kN)</th> <th>Check</th> </tr> </thead> <tbody> <tr><td>1</td><td>0.06</td><td>0.01</td><td>7979</td><td>7979</td><td>9974</td><td>6649</td><td>3623</td><td>Good</td></tr> <tr><td>2</td><td>0.06</td><td>0.02</td><td>7979</td><td>7979</td><td>9974</td><td>6649</td><td>3623</td><td>Good</td></tr> <tr><td>3</td><td>0.05</td><td>0.01</td><td>7979</td><td>7979</td><td>9974</td><td>6649</td><td>3623</td><td>Good</td></tr> <tr><td>4</td><td>0.05</td><td>0.02</td><td>7979</td><td>7979</td><td>9974</td><td>6649</td><td>3623</td><td>Good</td></tr> <tr><td>5</td><td>0.06</td><td>0.01</td><td>7979</td><td>7979</td><td>9974</td><td>6649</td><td>3597</td><td>Good</td></tr> <tr><td>6</td><td>0.06</td><td>0.02</td><td>7979</td><td>7979</td><td>9974</td><td>6649</td><td>3597</td><td>Good</td></tr> <tr><td>7</td><td>0.05</td><td>0.01</td><td>7979</td><td>7979</td><td>9974</td><td>6649</td><td>3597</td><td>Good</td></tr> <tr><td>8</td><td>0.05</td><td>0.02</td><td>7979</td><td>7979</td><td>9974</td><td>6649</td><td>3597</td><td>Good</td></tr> </tbody> </table>	Case	e_3 (m)	e_2 (m)	P_{u3} (kN)	P_{u2} (kN)	P_{uo} (kN)	$P_{u,Bresler}$ (kN)	$P_{u,actual}$ (kN)	Check	1	0.06	0.01	7979	7979	9974	6649	3623	Good	2	0.06	0.02	7979	7979	9974	6649	3623	Good	3	0.05	0.01	7979	7979	9974	6649	3623	Good	4	0.05	0.02	7979	7979	9974	6649	3623	Good	5	0.06	0.01	7979	7979	9974	6649	3597	Good	6	0.06	0.02	7979	7979	9974	6649	3597	Good	7	0.05	0.01	7979	7979	9974	6649	3597	Good	8	0.05	0.02	7979	7979	9974	6649	3597	Good
Case	e_3 (m)	e_2 (m)	P_{u3} (kN)	P_{u2} (kN)	P_{uo} (kN)	$P_{u,Bresler}$ (kN)	$P_{u,actual}$ (kN)	Check																																																																										
1	0.06	0.01	7979	7979	9974	6649	3623	Good																																																																										
2	0.06	0.02	7979	7979	9974	6649	3623	Good																																																																										
3	0.05	0.01	7979	7979	9974	6649	3623	Good																																																																										
4	0.05	0.02	7979	7979	9974	6649	3623	Good																																																																										
5	0.06	0.01	7979	7979	9974	6649	3597	Good																																																																										
6	0.06	0.02	7979	7979	9974	6649	3597	Good																																																																										
7	0.05	0.01	7979	7979	9974	6649	3597	Good																																																																										
8	0.05	0.02	7979	7979	9974	6649	3597	Good																																																																										
	<p>Verification of result!</p> <p>The maximum permitted margin of error is 5%.</p> <p>$A_{st,SAP2000} = 6400mm^2$.</p> <p>$A_{st,hand cal.} = 6400mm^2$.</p> <p>$Error = \frac{6400 - 6400}{6400} = 0.0\%$,</p> <p>which is at best.</p>																																																																																	

18.7.3.2

The strong column-weak beam philosophy necessitates that $\sum M_{nc} \geq 1.20\sum M_{nb}$ be guaranteed.

- $\sum M_{nb}$ is the sum of the nominal flexural strengths of beams spanning into the floor joint, measured at the face of the joint. See Figure 4.12.
- $\sum M_{nc}$ is the sum of the nominal flexural strengths of columns framing into the same joint, measured at the face of the joint. See Figure 4.12.
- M_{nc} is the nominal moment related to the factored axial forces in both directions within the plane (Taylor et al., 2016, Moehle, 2015).

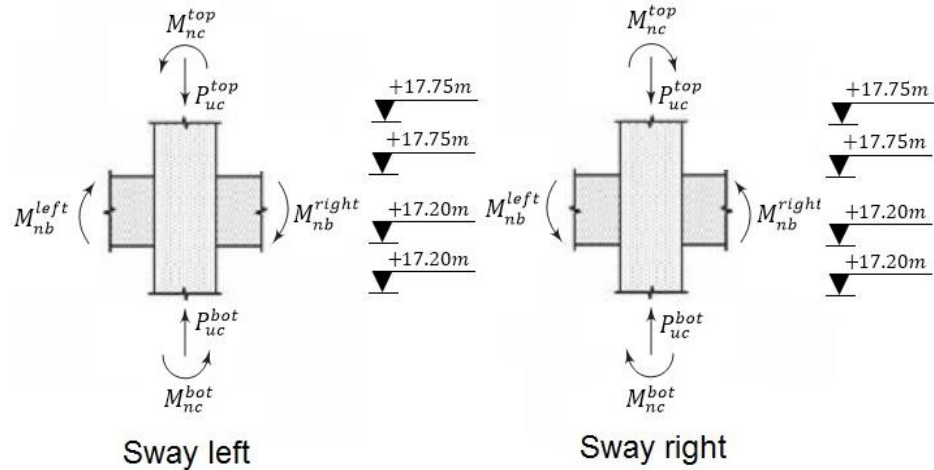


Figure 4.12: Concepts required for strong column-weak beam theory

The different axial loads in Table 4.10 are because of the variable direction of the sway in the critical loading state ($U_3 = 1.32DL + 1.0LL + 1.3Q_E$). The different values of M_{nc} at the joint surface are, yet, extracted from the interaction diagram attached in Appendix K (Figure K.3) where $\rho_g = 1.0\%$.

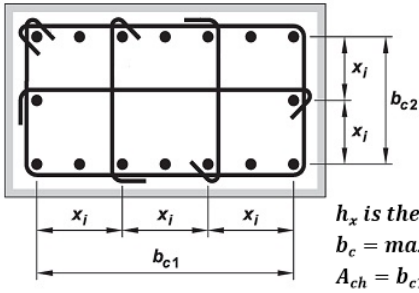
Table 4.10: Column nominal moments matching axial loads

Swaying to	Axial forces and Moments		$\sum M_{nc}$
Left	$P_{uc,SAP2000}^{top} = 3059kN$	$M_{nc}^{top} = 1730kN.m$	3540kN.m
	$P_{uc,SAP2000}^{bot} = 3623kN$	$M_{nc}^{bot} = 1810kN.m$	
Right	$P_{uc,SAP2000}^{top} = 3036kN$	$M_{nc}^{top} = 1730kN.m$	3530kN.m
	$P_{uc,SAP2000}^{bot} = 3597kN$	$M_{nc}^{bot} = 1800kN.m$	

$$\sum M_{nb} = (273 + 137)/0.9 = 456kN.m.$$

$$\sum M_{nc} = \min.(3540kN, 3530kN) = 3530kN.m.$$

$\sum M_{nc} = 3530kN.m \gg 1.2(456kN.m)$, satisfies 18.7.3.2, therefore **trusted**.

Design of Confinement in the Column PHs		
	The controlling load case still $U_3 = 1.32DL + 1.0LL + 1.3Q_E$.	
18.7.5.1	<p>There must be a confinement zone of length (l_o) at either ends (<i>PHs</i>) of the column. l_o shall never be less than the largest of:</p> <p>(a) The larger dimension of column cross-section.</p> <p>(b) (1/6) of the column clear height.</p> <p>(c) 450mm.</p>	<p>= 800mm Governs.</p> <p>= 3000/6 = 500mm.</p> <p>= 450mm.</p> <p>Select $l_o = 850mm \geq 800mm$.</p>
10.7.1.1, 20.6.1.3.1	$c_c = 40mm$.	
18.7.5.2(d), 25.7.2.2(a)	The diameter of hoops and crossties confining longitudinal bars having diameters smaller than 32mm shall be at least 10mm.	<p>Assume $\varnothing 20$ longitudinal reinforcing bars.</p> <p>Try $\varnothing 10$ bar for hoops and crossties.</p>
18.7.5.2(d), 25.7.2.3(b)	<p>No unrestrained bar shall be further than 150mm clear on both sides from a laterally supported bar.</p> <p>The number of required legs could be nearly evaluated as: $(800 - 2c_c - 2d_h - d_b)/170 + 1$; if $d_h = 10mm$, and $d_b = 20mm$ then, # of legs = $(800 - 80 - 20 - 20)/340 + 1 = 3legs$.</p>	
18.7.5.2(e)	<p>The spacing of secured longitudinal bars around the perimeter of the column (h_x) not to exceed 350mm centers as in Figure 4.13.</p> <div style="text-align: center;">  <p>h_x is the longest x_i $b_c = \max.(b_{c1}, b_{c2})$ $A_{ch} = b_{c1} \times b_{c2}$</p> </div> <p>Figure 4.13: Explanatory figure illustrates the meaning of h_x (ACI 318, 2014)</p> <p>$h_x = \frac{800 - 80 - 20 - 20}{3 - 1} = 340mm \leq 350mm$ OK.</p>	

<p>10.7.6.1.2, 25.7.2.1</p>	<p>Along the entire span of the column, the vertical center-to-center spacing (s) shall not more than the smallest of:</p> <p>(a) $16d_b$ (b) $48d_h$ (c) The smallest dimension of the column.</p>	<p>$= 16 \times 20 = 320mm.$ $= 48 \times 10 = 480mm.$ $= 800mm.$</p>
<p>18.7.5.3</p>	<p>Along the specified l_o, s shall not be more than the smallest of:</p> <p>(a) 40% of the smaller dimension of column cross-section. (b) $6d_{b,min}$ (c) $s_o = 100 + (350 - h_x)/3$, provided that s_o is neither less than $100mm$ nor more than $150mm$.</p>	<p>$= 0.4 \times 800 = 320mm.$ $= 6 \times 20 = 120mm.$ $= 100 + (350 - 340)/3 = 103mm,$ Controls.</p> <p>Use $s = 100mm \leq 103mm.$</p>

Design of Shear in the Column PHs

18.7.6.1.1

The first part of this section requires that the design shear force be calculated on the probable moment strengths where column plastic hinges are not prevented. These moments are estimated at the range of the factored axial forces acting at either ends of the column.

According to Wight (2016), the above argument leads to:

$$V_e = \frac{M_{prc}^{top} + M_{prc}^{bot}}{l_u}$$

- M_{prc}^{top} = the column probable flexural capacity from an interaction diagram generated for $1.25f_y$ and measured at $P_{u,avg}^{top}$.
- $P_{u,avg}^{top} = (P_{u,sway\ right}^{top} + P_{u,sway\ left}^{top})/2$.
- M_{prc}^{bot} = the column probable flexural capacity from an interaction diagram generated for $1.25f_y$ and measured at $P_{u,avg}^{bot}$.
- $P_{u,avg}^{bot} = (P_{u,sway\ right}^{bot} + P_{u,sway\ left}^{bot})/2$.

The probable strength interaction diagram is shown in Appendix K (Figure K.4). It should be recalled that P_u^{top} , and P_u^{bot} have been gotten from SAP2000 analysis in the critical loading state ($U_3 = 1.32DL + 1.0LL + 1.3Q_E$). The meant averages and the corresponding probable moments are contained in Table 4.11.

Table 4.11: Column maximum probable moments

	Swaying Left	Swaying Right	$P_{u,avg.}$ (kN)	M_{prc} (kN.m)
P_u^{top} (kN)	3623	3597	3610	1970
P_u^{bot} (kN)	3676	3651	3664	1970

$$\therefore V_e = \frac{1970 + 1970}{3.00} = 1313kN.$$

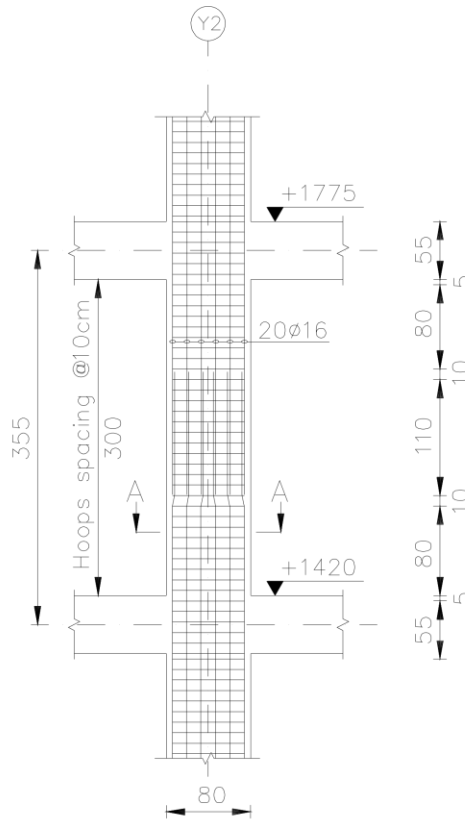
<p>18.7.6.1.1</p>	<p>The second part of the section states that the design shear force need not to be more than those computed depending on M_{pr} of beams framing into the top and the bottom connections of the column.</p> <p>The second part could be illustrated mathematically as (Wight, 2016):</p> $V_e = \frac{\sum M_{prb}^{top} \times DF^{top} + \sum M_{prb}^{bot} \times DF^{bot}}{l_u}$ <ul style="list-style-type: none"> • $\sum M_{prb}^{top}$ = the summation of the beams probable moments at the top joint of the column as developed in every swaying direction (Figure 4.14). • $\sum M_{prb}^{bot}$ = the summation of the beams probable moments at the bottom joint of the column as developed in every swaying direction (Figure 4.14). • DF^{top} = the moment distribution factor at the top of the column. • DF^{bot} = the moment distribution factor at the base of the column. • The stiffnesses of the columns over and under the joints are equal, causing distribution factors of $DF^{top} = DF^{bot} = 0.5$. <p>It should be noted that the probable moments in Figure 4.14 are calculated manually by the user from the analysis in the governing load situation ($U_3 = 1.32DL + 1.0LL + 1.3Q_E$).</p> <div style="display: flex; justify-content: space-around; align-items: flex-start;"> <div style="text-align: center;"> <p>Sway left</p> </div> <div style="text-align: center;"> <p>Sway right</p> </div> </div> <p>Figure 4.14: Probable moments of beams at column top and bottom joints</p> $V_{e,sway\ left} = \frac{(375 + 221) \times 0.5 + (392 + 237) \times 0.5}{3.00} = 204kN.$ $V_{e,sway\ right} = \frac{(249 + 332) \times 0.5 + (261 + 357) \times 0.5}{3.00} = 200kN.$
<p>18.7.6.1.1</p>	<p>The third part of the section needs that in no case shall V_e be less than the factored shear from frame analysis.</p> <p>The two end shears from computer analysis for the load case ($U_3 = 1.32DL + 1.0LL + 1.3Q_E$) are identical and equal to $117kN$.</p> <ul style="list-style-type: none"> • As a final result, consider $V_e = 204kN$ as being the controlling value.

22.5.5.1	For members with axial compression (N_u); $V_c = 0.17 \left(1 + \frac{N_u}{14A_g} \right) \lambda \sqrt{f'_c} b_w d$	
10.5.1.2, 21.2.1 22.5.1.2	The shear reduction factor $\phi = 0.75$. The cross-sectional dimensions shall fulfil $V_e \leq 5\phi V_c$	N_u is conservatively taken as the smallest value, i.e. $N_u = 3597kN$ (Table 4.11). $V_c = 0.17 \left(1 + \frac{3597 \times 1000}{14(800)^2} \right) \times 1 \times \sqrt{23.5} \times 800 \times 740 = 684kN.$ $5\phi V_c = 5(0.75)(684) = 2565kN.$ $V_e = 204kN \leq 5\phi V_c = 2565kN,$ OK.
18.7.6.2.1	V_c must be neglected when the following two conditions occur simultaneously. (a) $V_{sway} \geq V_e/2$ (b) $P_u < 0.05f'_c A_g$	V_{sway} is obtained from the software analysis in the load pattern $U = 1.3Q_E$. (a) $V_{sway,top} = V_{sway,bottom} = 108kN \geq 204/2 = 102kN.$ (b) $P_u = 3597kN \ngtr 0.05f'_c A_g = 752kN.$ <i>Since one condition is not satisfied, V_c be present as 684kN.</i>
22.5.10.1 10.6.2.1	At every section where $V_e > \phi V_c$, transverse reinforcement shall be provided such that $V_s > V_e/\phi - V_c$ At every section where $V_e > 0.5\phi V_c$, $A_{v,min}/s$ shall be provided.	$V_e = 204kN < 0.5\phi V_c = 257kN.$ No need for shear reinforcement.
	<u>Verification of result!</u> The maximum permitted margin of error is 5%.	$A_v/s_{SAP2000} = 0.0.$ $A_v/s_{provided} = 0.0.$ <i>Error = 0.0%, which is at best.</i>
Design for Torsion		
	Continue with the load case $U_3 = 1.32DL + 1.0LL + 1.3Q_E$.	The factored torsional moment on the column upper section of the column is determined from computer analysis as $T_u = 8.20kN.m.$

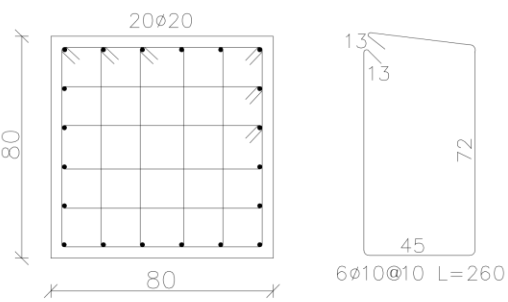
10.5.4.1, 22.7.4.1	<p>The threshold torsion (T_{th}) for solid cross-section subjected to axial force shall be calculated from:</p> $T_{th} = \lambda\sqrt{f'_c} \left(\frac{A_{cp}^2}{P_{cp}} \right) \sqrt{1 + \frac{N_u}{4A_g\lambda\sqrt{f'_c}}}$	
	<ul style="list-style-type: none"> • A_{cp} and P_{cp} items will be calculated for the column cross-section shown previously in Figure 4.10. • To be more conservative, choose $N_{u,min} = 3597kN$ (Table 7.7). $T_{th} = (1)\sqrt{23.5} \left(\frac{(800^2)^2}{4 \times 800} \right) \sqrt{1 + \frac{3597 \times 10^3}{4 \times 800^2 \times 1 \times \sqrt{23.5}}} / 10^6 = 705kN.m.$	
10.5.1.2, 21.2.1	Torsional strength reduction factor $\phi = 0.75$.	
10.5.4.1, 9.5.4.1	If $T_u < \phi T_{th}$ then, the torsional effect shall be neglected so that, minimum torsional steel ($A_{l,min}, A_{t,min}$) is not needed.	$\phi T_{th} = 0.75 \times 705 = 529kN.m.$ $T_u = 8.20kN.m \ll 529kN.m,$ therefore torsion can be neglected.
	<p><u>Verification of results!</u></p> <p>The maximum permitted margin of error is 5%.</p>	$A_{l,min_{SAP2000}} = 0.0.$ $A_{l,min_{hand cal.}} = 0.0.$ Error = 0.0%, which is at best. $A_{t,min_{SAP2000}} = 0.0.$ $A_{t,min_{hand cal.}} = 0.0.$ Error = 0.0%, which is at best.

4.8.4 Detailing of the Selected Column

Figure 4.15 shows the longitudinal and transverse reinforcement of the column example.



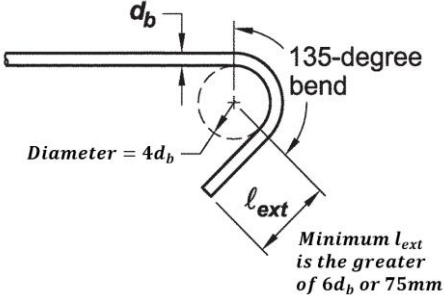
(a) Elevation of column, reinforcement details



(b) Section A-A

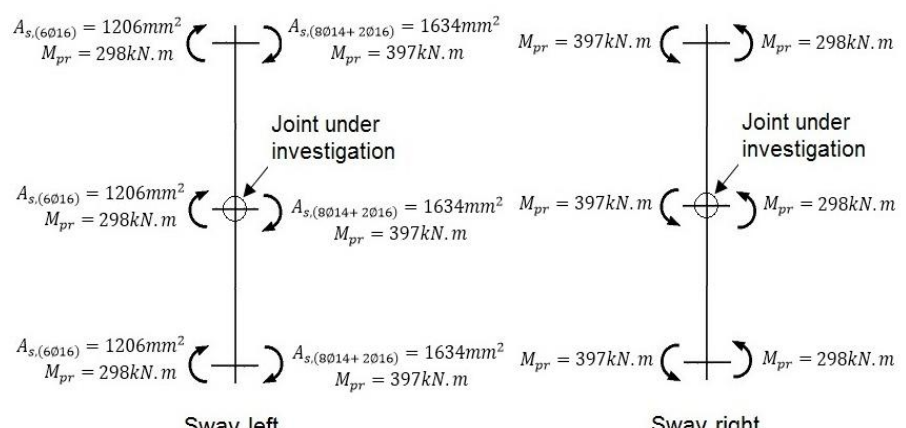
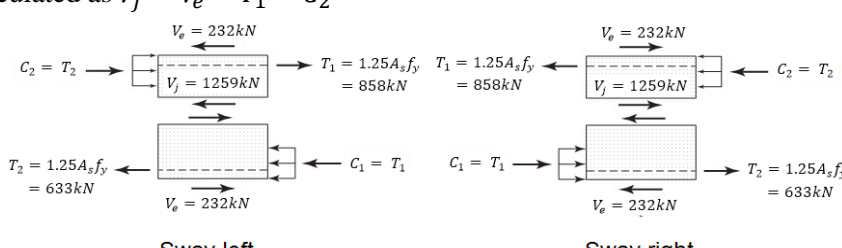
Figure 4.15: Reinforcement details (in centimeters) of the special column

ACI 318-14	Discussion	Calculations
The Required Number of Vertical Bars		
	Use 20Ø20 longitudinal bars equally distributed on all four sides.	$A_{st,20\phi20} = 6286 \text{ mm}^2$ is partly smaller than $A_{st,min} = 6400 \text{ mm}^2$, but could be acceptable.
The Development Length		
<p>18.7.4.3</p> <p>10.7.1.2, 25.4.2.1, 25.4.2.2, 25.4.2.4, 25.5.2.1</p>	<p>In columns, longitudinal bars lap splices, if any, are only permitted in the mid-height of the column length, and shall be designed as tension lap splices.</p> <p>The lap splice lengths of reinforcement in tension (l_{st}) the maximum of:</p> <p>(a) $1.3 \left(\frac{f_y \psi_t \psi_e}{2.1 \lambda \sqrt{f'_c}} \right) d_b$</p> <p>(b) 300mm</p>	<p>Longitudinal bars lap splices, if any, are positioned within the middle of clear height of column.</p> $= 1.3 \left(\frac{420(1)^2}{2.1(1)\sqrt{23.5}} \right) \times 2 = 108 \text{ cm.}$ <p>= 30cm.</p> <p>The available length is 110cm which is larger than $l_{st} = 108 \text{ cm}$, therefore the available length is sufficient.</p>
Transverse Steel Requirements		
<p>18.7.5.2</p> <p>18.7.5.4, 18.7.5.2(f)</p>	<p>b_c and A_{ch} indices are as prescribed previously in Figure 4.13.</p> <p>If $P_{u,max} \leq 0.3A_g f'_c$, and $f'_c \leq 70 \text{ MPa}$, the minimum required area of the legs of hoops and crossties in each direction per unit length along l_0 shall be the greater of:</p> <p>(a) $A_{sh,min}/s = 0.3 \left(\frac{A_g}{A_{ch}} - 1 \right) \frac{f'_c}{f_y} b_c$</p> <p>(b) $A_{sh,min}/s = 0.09 \frac{f'_c}{f_y} b_c$</p>	<p>$b_c = 800 - 80 - 2 \times 20 = 680 \text{ mm.}$ $A_{ch} = (680^2) \text{ mm}^2.$</p> <ul style="list-style-type: none"> • $P_{u,max} = 3623 \text{ kN} \leq 4512 \text{ kN.}$ • $f'_c = 23.5 \leq 70 \text{ MPa.}$ $= 0.3 \left(\frac{800^2}{680^2} - 1 \right) \left(\frac{23.5}{420} \right) (680)$ <p>= 4.38 mm²/mm Governs.</p> $= 0.09 \left(\frac{23.5}{420} \right) (680)$ <p>= 3.42 mm²/mm.</p>
	<p>$A_{sh,min} = 4.38 \text{ mm}^2/\text{mm} \times s(\text{mm}).$</p> <p>$A_{sh,min} = 4.38 \times 100 = 438 \text{ mm}^2.$</p> <p>$A_{sh,\phi10} = 1 \times \frac{\pi}{4} (10^2) = 78.6 \text{ mm}^2.$</p> <p># of legs = 438/78.6 = 6legs.</p> <ul style="list-style-type: none"> • 3Ø10 hoops@10cm are required over the length l_0. 	

<p>18.7.5.1, 18.7.5.3</p>	<p>Over the length $l_o = 85cm$ on either ends of the column, spacing of special confining reinforcement shall not exceed a specified limit.</p>	<p>This condition has been accounted for during the design of confinement and the spacing is taken as $s = 10cm$.</p>
<p>10.7.6.2.1, 10.7.6.2.2</p>	<p>The lower and upper hoop shall be placed by not more than one-half the hoop spacing along the column.</p>	<p>Place the first hoop placed at $s = 5cm \leq 10/2 = 5cm$ apart from the joint faces.</p>
<p>18.7.4.3, 18.7.5.2, 18.7.5.3</p>	<p>Longitudinal bars lap splices shall be enclosed by hoops spaced vertically by not more than a specific limit.</p>	<p>This condition has implicitly satisfied during the design of confinement as taken as $s = 10cm$.</p>
<p>18.6.4.6</p>	<p>Elsewhere, along the remaining length of the columns, hoops should also be provided at spacing not more than: (a) $6d_b$ (b) $150mm$</p>	<p>The remaining length of the column at every side equals: $(300 - 110 - 85 \times 2)/2 = 10cm$. This is so minor compared to the column length and hence the same spacing as in l_o region is used for the whole column.</p> <ul style="list-style-type: none"> • The end result is hoop spacing of $10cm$ along the entire length of the column. • The total legs of hoops in any direction = $6legs$.
<p>10.7.6.1.2, 18.7.5.2(d) 25.7.2.3(a)</p>	<p>Every corner and alternate longitudinal bar shall be restrained by ties having hooks with an extension bend not more than 135-degree.</p>	<ul style="list-style-type: none"> • This condition is obviously satisfied in Figure 4.15(b).
<p>25.3.2</p>	<p>The standard hook geometry for hoops is shown in Figure 4.16.</p>  <p style="text-align: center;">Figure 4.16: End hook details of $\emptyset 10$ hoops (ACI 318, 2014)</p>	
<ul style="list-style-type: none"> • $l_{ext} \geq \max. (6 \times 1 = 6cm, 7.5cm) = 7.5cm$. • $Diameter = 4 \times 1 = 4.0cm$. 		

Minimum Bar Spacing for 20Ø20 Vertical Bars		
10.7.2.1, 25.2.3	Minimum clear spacing between vertical bars shall not be less than the greatest of: (a) 40mm (b) $1.5d_b$ (c) $(4/3)d_{agg}$	$= 40mm$ Controls. $= 1.5 \times 20 = 30mm.$ $\approx (4/3) \times 20 = 26.7mm.$ The calculation process of the clear spacing between bars is self-explanatory. However, the existed 6Ø20 longitudinal bars per face conservatively satisfy the above measurements.

4.8.5 Checks on the Beam-Column Joint

ACI 318-14	Discussion	Calculations
Joint Size		
18.8.2.3	The beam-column joint width parallel to the beam flexural bars (c_1) shall not be less than 20 times the biggest diameter of those bars ($d_{b,max}$).	$d_{b,max}$ penetrating the joint = $\emptyset 16$. $c_1 = 800mm \nless 20(16) = 320mm$, therefore acceptable .
18.8.2.4	The beam-column joint depth in plane of beam flexural steel (c_2) shall be at least 50% of the depth of beams run across the joint.	$h_{beam} = 550mm$. $c_2 = 800mm \geq 550/2 = 275mm$, therefore acceptable .
Joint Shear Capacity		
18.8.2.1	<p>The joint shear force shall be calculated where the beam flexural tensile reinforcement is $1.25f_y$.</p> <p>Columns shears are very similar to how V_e is calculated according to the second part of section 18.7.6.1.1 of the ACI Code. The reinforcing bars of beams in Figure 4.17 are identical to those detailed in Figure 4.6 as long as they conservatively satisfy the required steel areas.</p>  <p>Figure 4.17: Probable moments of beams generating shears at the studied joint</p> <p>Figure 4.18 offers the shear value at the center of the joint (V_j), where V_j calculated as $V_j = V_e - T_1 - C_2$</p>  <p>Figure 4.18: Free body diagram of the joint under investigation</p>	

<p>18.8.4.3</p> <p>18.8.4.1</p> <p>21.2.4.3</p>	<p>In the case where beams width (b_w) is less than or equal to the width of the supporting column (c_2) then, the effective cross-sectional area of a joint (A_j) equals the product of column depth parallel to the beam longitudinal bars (c_1) by (c_2).</p> <p>The nominal shear strength of a joint confined by beams on all four faces is $V_n = 1.7\lambda\sqrt{f'_c}A_j$</p> <p>For seismic joints, the joint shear reduction factor $\phi = 0.85$.</p>	<ul style="list-style-type: none"> • $b_w = c_2 = 800mm$. • $c_1 = c_2 = 800mm$. <p>$A_j = c_1 \times c_2 = 64 \times 10^4 mm^2$.</p> <p>$V_n = 1.7(1)\sqrt{23.5}(64 \times 10^4)/1000 = 5274kN$.</p> <p>$\phi V_n = 4483kN \gg V_j = 1259kN$,</p> <p style="text-align: right;">OK.</p>
Transverse Steel Requirements		
<p>18.8.3.1</p> <p>18.8.3.2</p>	<p>Joint transverse reinforcement shall comply with the requirements of for frame columns in Sections 18.7.5.2 through 18.7.5.4 of the ACI Code.</p> <p>It is permitted to reduce the amount of confining reinforcement and to increase hoops spacing when beams enter the joint from all its four sides with widths larger than three-fourths the support width.</p>	<p>The provided hoops along the column ($3\emptyset 10$ hoops@10cm) are extended throughout the joint. This, however, meets Sections 18.7.5.2 through 18.7.5.4 of the ACI Code.</p> <p>For ease of construction and to keep conservatism, this relaxation will not be looked at.</p>

4.8.6 Detailing of the Beam-Column Joint

Figure 4.19 represents the reinforcement details of the beam-column joint example.

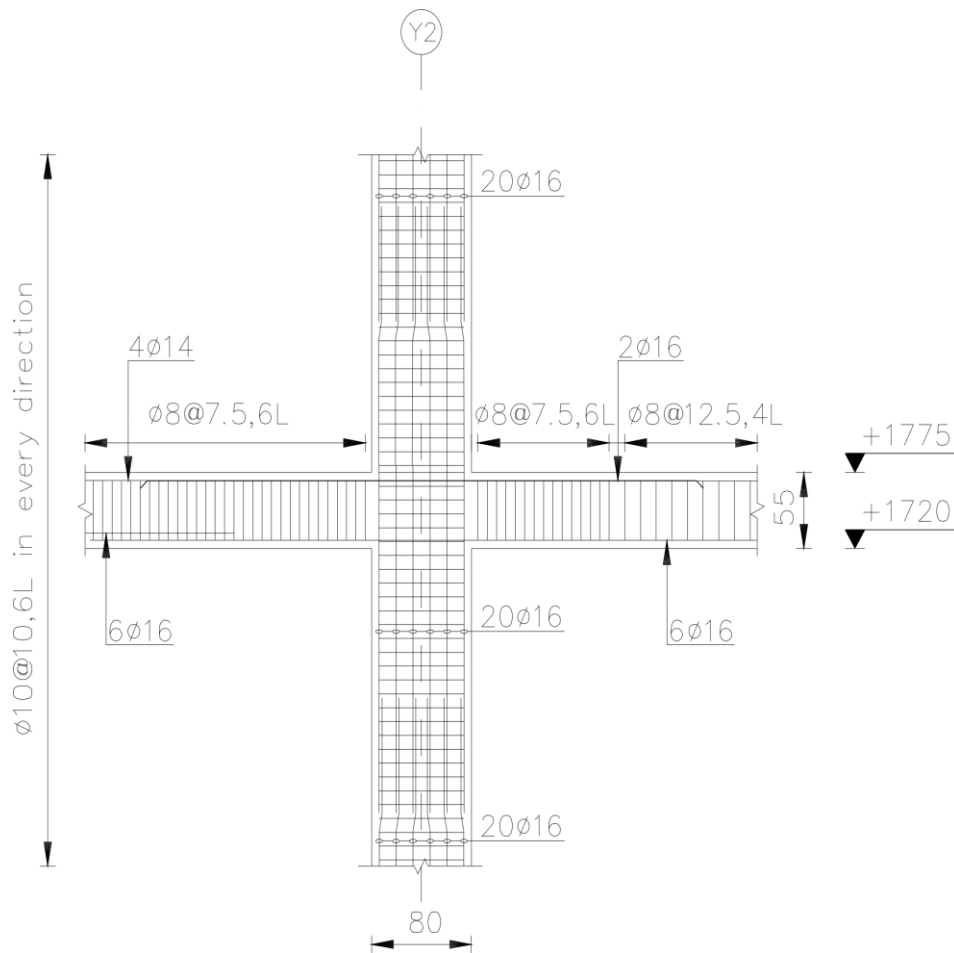


Figure 4.19: Reinforcement details (in centimeters) of the beam-column joint

CHAPTER 5
QUANTITY SURVEYING AND COST
ESTIMATION

5.1 Introduction

The main purpose of structural design is to innovate a technically efficient, and a cost-effective system to survive and transfer loads and/or deformations due to actions caused by the environment in which the structure is to be constructed (Bertero, 1996).

Despite the well-developed techniques and building materials, construction is still a difficult, long-term, and an expensive industry in which the optimized materials cost represents an expensive item in making the best choice (McCuen et al., 2011).

Costs associated with materials are significant drain on economy of Palestinians as most of the basic building materials like cement, steel, etc., are imported from abroad and their prices are likely to increase by years (Kurraz, 2015). Hence, the more cost-effective construction solutions shall be an important priority for engineers as long as they meet the desire of citizens to have a facility of superior anti-seismic performance without paying special costs in their buildings.

This chapter represents quantity surveying and cost estimation of construction materials (concrete, and steel) used in buildings of the three different SDL classes. Calculations of concrete volumes and quantities of reinforcing steel (longitudinal and transverse reinforcement) are executed and a comparative assessment of the materials cost is performed. This comparative assessment represents the goal of this research to determine the resulted reduction in cost associated with lowest superimposed dead load.

5.2 Design Results from Different Evaluation Perspectives

Three types of assessment are conducted, which are concrete volume-based, steel mass-based, and materials cost-based.

5.2.1 Comparison of Concrete and Steel Quantities

The economy of the structural design of models is estimated by contrasting the concrete volume per unit area of all floors ($m^3/m^2/floor$) and steel mass per unit area of all floors ($kg/m^2/floor$). Rebar mass has been calculated assuming a unit mass of $8000 kg/m^3$ (MPWH, 2006). Figures 5.1 through 5.4, however, show these calculated data.

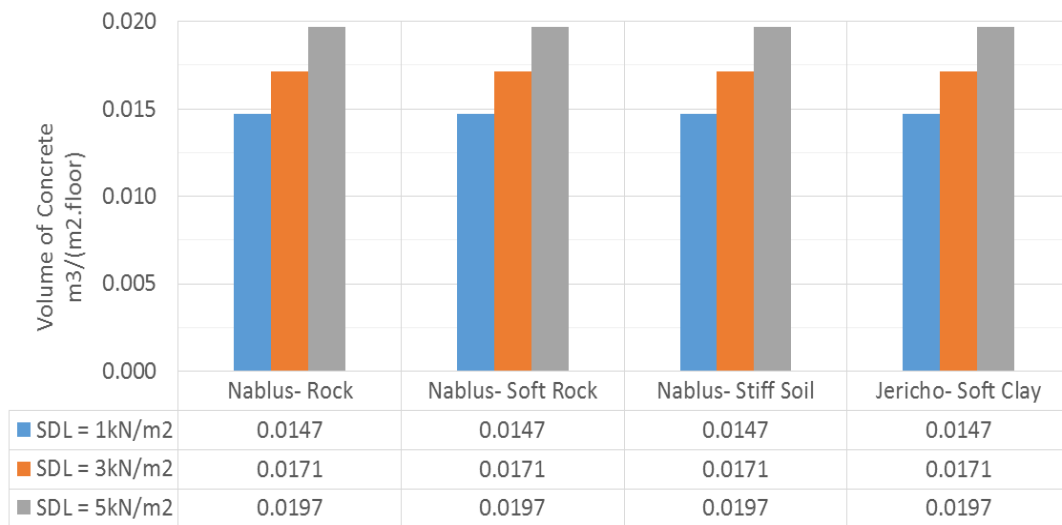


Figure 5.1: Comparison in beams concrete volume

The chart shows the concrete volumes consumed by beams on multiple types of constructions. At every site, concrete volumes rose steadily from 0.0147 to 0.0197 ($m^3/m^2/floor$) at the end SDL in the question. There are some similarities, however. For instance, in all models of $SDL = 1 kN/m^2$, the quantity of concrete is exactly the same. Interestingly, the relationship

between the amounts of concrete consumed by beams and the SDL is approximately linear for different site conditions and Risk Categories.

In the final analysis, the models of $SDL = 1 \text{ kN/m}^2$ required about 14% lower amount of concrete for beams than the models of $SDL = 3 \text{ kN/m}^2$, and 25% lower than the models of $SDL = 5 \text{ kN/m}^2$.

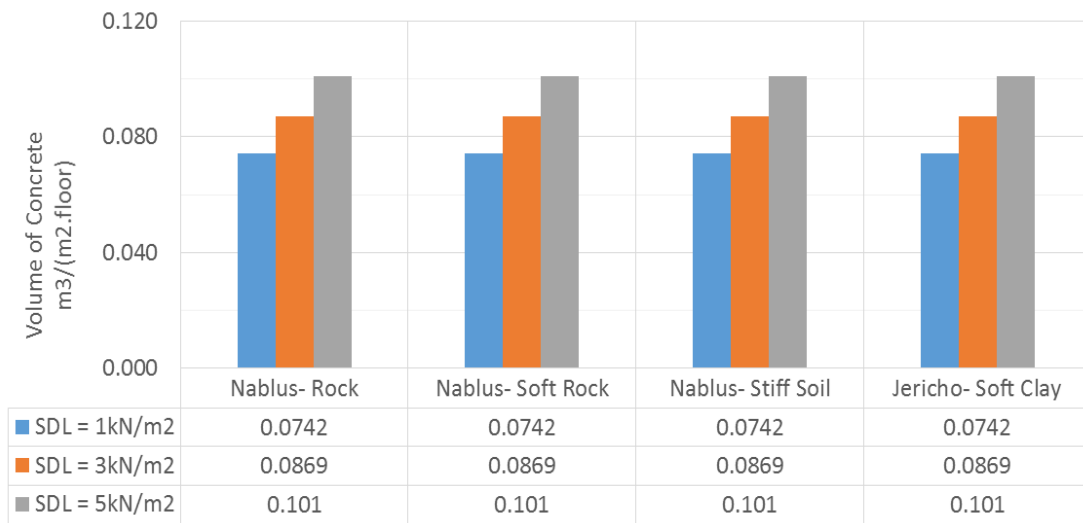


Figure 5.2: Comparison in columns concrete volume

This bar chart indicates a survey on the investigated models on the concrete volumes required for columns. At every site, concrete volumes grew from 0.0742 to 0.101 ($\text{m}^3/\text{m}^2/\text{floor}$) at the bigger SDL .

Similar to beams, an approximately linear relationship can be established between the amounts of concrete consumed by columns and the SDL .

In conclusion, systems of $SDL = 1 \text{ kN/m}^2$ scored a declination of 15% and 26% of concrete for columns when compared to the systems of $SDL = 3 \text{ kN/m}^2$ and 5 kN/m^2 respectively.

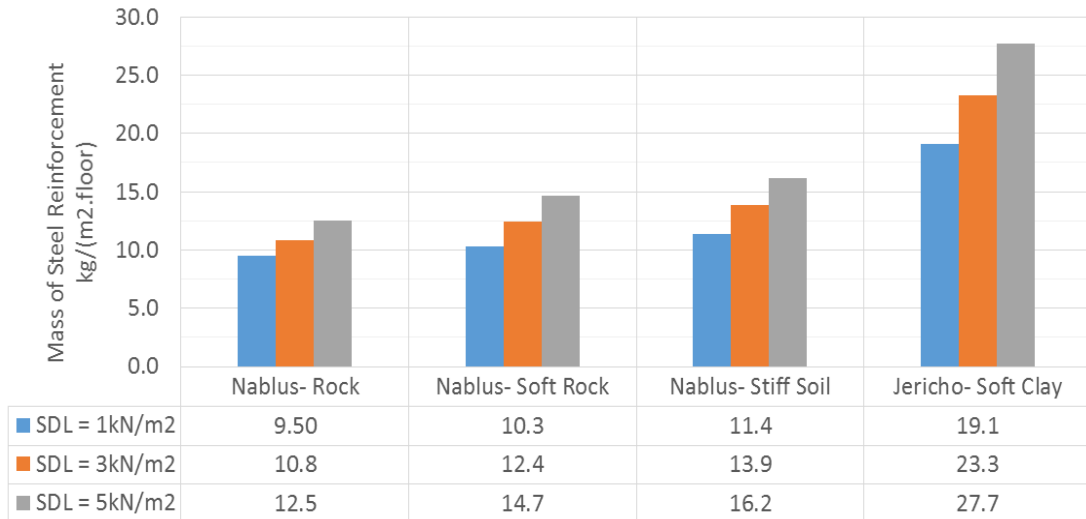


Figure 5.3: Comparison in beams steel reinforcement

Figure 5.3 gives the steel quantities required for beams in different models and various conditions considered. Steel masses of models with the same SDL value have suffered a continuous inflation, particularly in Jericho during which steel of beams doubled to just under two times that in the stiff soil case of Nablus.

As a final point, structures of $SDL = 1 \text{ kN/m}^2$ contribute to the following savings in steel quantities:

- 12% and 24% compared to models of $SDL = 3 \text{ kN/m}^2$ and 5 kN/m^2 built in Nablus over a rock strata.
- 17% and 30% compared to models of $SDL = 3 \text{ kN/m}^2$ and 5 kN/m^2 built in Nablus over a soft rock strata.
- 18% and 30% compared to models of $SDL = 3 \text{ kN/m}^2$ and 5 kN/m^2 built in Nablus over a stiff soil strata.
- 18% and 31% compared to models of $SDL = 3 \text{ kN/m}^2$ and 5 kN/m^2 built in Jericho over a soft clay strata.

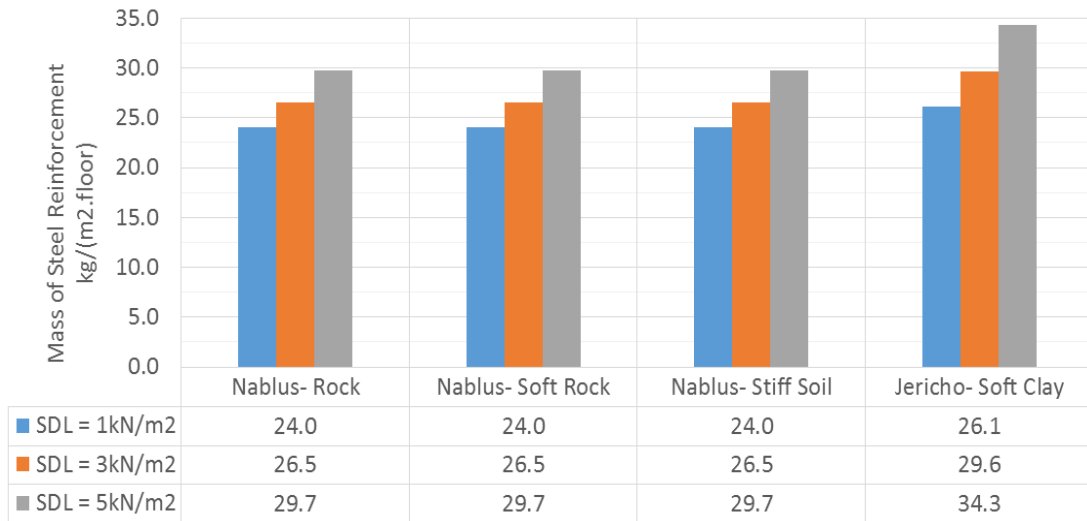


Figure 5.4: Comparison in columns steel reinforcement

Figure 5.4 concentrates on the changes which took place in the steel of columns in models built in Nablus and Jericho. From an overall perspective, the gap between steel demands of columns narrowed to zero in models of intermediate Risk Category (Nablus) and of equal magnitudes of SDL. On the other hand, there is a notable increase in the amount of steel required for buildings with soft clay.

Overall, the alleviation of SDL to only 1 kN/m^2 leads to the following reduction in columns reinforcement:

- 9% and 19% compared to models of $SDL = 3 \text{ kN/m}^2$ and 5 kN/m^2 built in Nablus over a rock, soft rock, and stiff soil strata.
- 12% and 24% compared to models of $SDL = 3 \text{ kN/m}^2$ and 5 kN/m^2 built in Jericho over a soft clay strata.

5.2.2 Comparison of Materials Cost

Models will be evaluated for design/materials cost-effectiveness based on the change in materials cost of skeletal members due to the variation in the SDL and the hosting ground type. A clear image of how the total materials cost differs by the method of construction for models is given in Figure 5.5. Costs, however, are estimated in the United States Dollar (\$) according to the marketing prices given in the Palestinian Concrete Society offer attached in Appendix A.

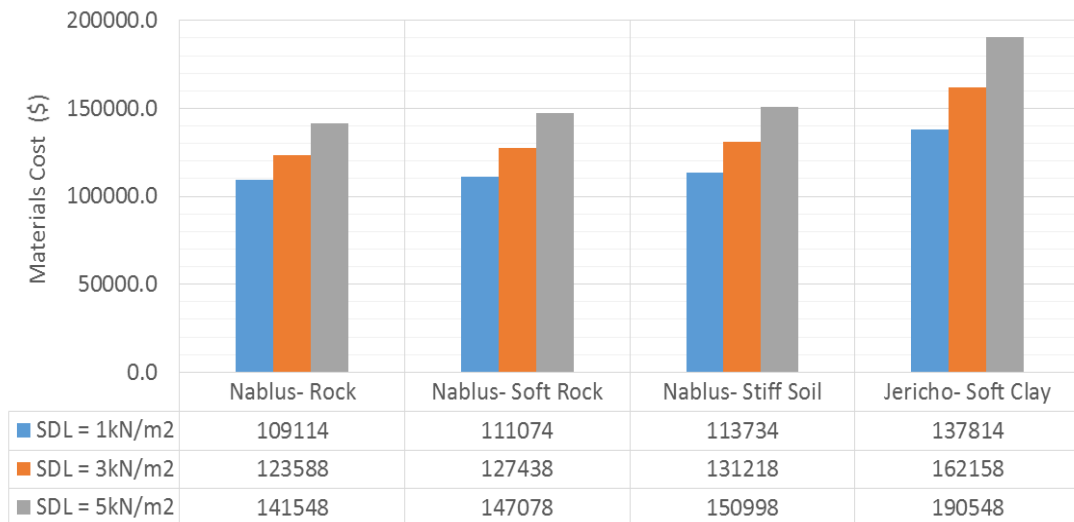


Figure 5.5: Material cost for models in different locations

Figure 5.5 illustrates the breakdown of spending patterns for the designed models. The most striking feature is that light loaded facilities cost the least money across all four groups. There might be an acceptable difference in terms of the expenditure clients' spent across any three constructions having the same SDL and various ground settings. Yet in terms of economic spending, people had to pay nearly one fifth more in Jericho when compared with the costliest option of Nablus.

As a final point, the reduced trends in the budget (measured on the basis of least SDL value) are expressed as:

- 12% and 23% compared to models of $SDL = 3 \text{ kN/m}^2$ and 5 kN/m^2 built in Nablus over a rock strata.
- 13% and 24% compared to models of $SDL = 3 \text{ kN/m}^2$ and 5 kN/m^2 built in Nablus over a soft rock strata.
- 13% and 25% compared to models of $SDL = 3 \text{ kN/m}^2$ and 5 kN/m^2 built in Nablus over a stiff soil strata.
- 15% and 28% compared to models of $SDL = 3 \text{ kN/m}^2$ and 5 kN/m^2 built in Jericho over a soft clay strata.

CHAPTER 6
CONCLUSIONS, RECOMMENDATIONS, AND
FUTURE WORK

6.1 Conclusions

6.1.1 General Conclusions

The followings are the general conclusions of the research:

1. Increasing the SDL from 1kN/m^2 to 5kN/m^2 can increase the materials cost in the building of about 25%.
2. Considering that hollow block-concrete flooring system is widely used in Palestine, the employment of ribbed slabs in the LFRS is not prohibitive in the ACI 318-14 Code, IBC 2015, ASCE/SEI 7-10, Eurocode 8, etc. Even so, literatures relying on the structural performance during and after Earth shakings indicate negative latitudes on this construction version when compared with solid slabs.
3. The option of reducing SDL provides distinguished performance in terms of less weight, lower heights, much simpler form, maximum strength and stiffness, minimization of materials cost, etc.

6.1.2 Specific Conclusions

The followings are the specific conclusions of the research:

1. Overburdened floors attract much more seismic loads than the less loaded ones, but even if they are proportioned well for gravity loads, they will not exhibit a prominent lateral seismic displacement change. Hence, good static design concepts might be made to perform well in earthquakes, despite some shortcomings in the dynamic side.

2. Most of the materials cost went towards columns. As per the observation of concrete volumes, in all cases, the ratio of concrete consumption of beams relative to columns is nearly 1:4. On the other hand, beams steel share is between 45% to 77% of columns steel for different models.
3. The required amount of steel per volume of concrete for beams is almost independent of all SDLs but increases with the severity of both Risk Category and soil profile type.
4. The required amount of steel per volume of concrete for columns is almost independent of all SDLs, Risk Category and soil profile type.
5. The ratio of ties mass to the total steel mass is larger in columns when compared to beams. This is because of the confinement effect of ties which is more important for columns than for beams.
6. The soil profile type has a significant effect on the amount of steel required for the building particularly in zones of high Risk Category.
7. The underneath hypotheses are derived and may be a part of any conceptual design calculation procedures. They are applicable provided:
 - ✓ Sites with seismic zone factor less than or equal to 0.20.
 - ✓ Buildings up to heights of ten stories in SDC A to D.
 - ✓ Neither horizontal nor vertical irregularities.
 - ✓ The analysis is according to the IBC 2015 Code.
 - ✓ The design is according to the ACI 318-14 Code.
 - ✓ $LL \leq 4 \text{ kN/m}^2$.

$$\checkmark \text{ } SDL \leq 5 \text{ kN/m}^2.$$

- Columns longitudinal reinforcement is mainly controlled by the minimum requirements of typical gravity loadings design.
- Along the full height of the column, shear reinforcement and spacing are most often controlled by the confinement requirements stated for seismic design.
- Over the beam plastic hinges and bars overlapping regions, shear reinforcement and spacing is most often controlled by the confinement requirements stated for seismic design. In other places along the beam span, the common requirements of gravity design are sufficient.
- Torsion may have a minor effect on beams sections.

6.2 Recommendations

1. Population growth, random urbanization, the prevailing construction styles, etc., implies that earthquake impacts on the Palestinian society will increase in the coming decades. Hence, the awareness and preparedness of human population are an urgent necessity to reduce the loss of human lives and property damage.
2. It is recommended to proportion the dimensions of members such that a good margin between the fundamental time periods of structures and the allowed values ($T_1 \leq C_u T_a$) so that, undesirable structural consequences such as excessive drifts, and $P - \Delta$ effect could be alleviated.

3. Designers are more interested in the structural response, whereas building owners only focus on the fiscally related matters. As the developed approach of reducing SDL meets the needs of both parties, the idea shall be supported and encouraged by decision makers, municipalities, experts, etc.
4. Many problems may be encountered in the used in practice construction systems of $SDL = 5 \text{ kN/m}^2$ such as:
 - The increase in floor to floor height adds further costs for exterior cladding, hoisting costs, cooling and heating loads, etc.
 - Maintenance costs related to sewage piping systems placed under the floor covering might be prolonged. Furthermore, the process is disruptive and may necessitate an evacuation of inhabitants.
5. The UBC 97 has been continuously updated and replaced by the IBC 2015. Hence, the current usage of the UBC 97 as reference for seismic design purposes at engineering offices and Palestinian Engineers Association does not seem reasonable!
6. Buildings lifetime in the local community often last beyond the 50-years limit. Therefore, the used in local practice seismic hazard map showing zonation factors based on 10% probability of exceedance in 50 years have to be reconsidered.
7. Seismic guidelines and provisions shall be stringently applied during the design and construction of building structures. Still, more statutory enforcements are necessary for seismic risk mitigation.

6.3 Future Work

1. The research mainly studied the quantitative effect of the SDL on the frame beams and columns. It would be beneficial to investigate that effect on diaphragms and footings.
2. The study could be broadened to include much more variables, horizontal irregularities, vertical irregularities, etc.
3. Other studies to examine the effect of the SDL on shear walls or walls and frames combined are possible.

REFERENCES

- ACI 318 2014. **Building code requirements for structural concrete (ACI 318M-14): an ACI Standard: Commentary on building code requirements for structural concrete (ACI 318M-14)**, Farmington Hills, MI, American Concrete Institute.
- ADHIKARI, R. K., BHAGAT, S. & WIJEYEWICKREMA, A. 2015. **Damage Scenario of Reinforced Concrete Buildings in the 2015 Nepal Earthquakes**. *New Technologies for Urban Safety of Mega Cities in Asia (USMCA) 2015*, 1-7, 8.
- AGHAYERE, A. O. & LIMBRUNNER, G. F. 2014. **Reinforced concrete design**.
- AGRAWAL, A. S. & CHARKHA, S. 2012. *Effect of change in shear wall location on storey drift of multistorey building subjected to lateral loads*. **International Journal of Engineering Research and Applications (IJERA)**, 1786-1793.
- AL-DABBEEK, J. 2007. *Vulnerability and expected seismic performance of buildings in West Bank, Palestine*. **The Islamic university Journal (Series of Natural Studies and Engineering)**, 15, 193-217.
- AL-DABBEEK, J. 2010. *An Assessment of Disaster Risk Reduction in the Occupied Palestinian Territory*. **An-Najah University Journal for Research**, 24.

- AL-DABBEEK, J. & EL-KELANI, R. *Dead Sea Earthquake of 11 February 2004, ML 5.2: post earthquake damage assessment. The International Earthquake Conference (TINEE)*, 2005. 21-24.
- AL-DABBEEK, J. N., EL-KELANI, R. J., SANTINI, A. & MORACI, N. *Site Effect and Expected Seismic Performance of Buildings in Palestine-Case Study: Nablus City. AIP Conference Proceedings*, 2008. 191.
- ALNAJAJRA, H., TOUQAN, A. R. & DWAIKAT, M. 2017. *The Effect of Reducing Superimposed Dead Load on the Lateral Seismic Deformations of Structures. International Journal of Civil, Environmental, Structural, Construction and Architectural Engineering*, 11, 1551 - 1557.
- AMIT, R., SALAMON, A., NETZER-COHEN, C., ZILBERMAN, E. & COHEN, M. 2015. *Systematic evaluation of earthquake related hazards for heritage sites in Israel – A qualitative approach* In: 2015 (ed.) The XXXVI International Workshop on Seismicity and Earthquake Engineering in the Extended Mediterranean Region. Italy.
- ANDERSON, J. C. & NAEIM, F. 2012. *Basic structural dynamics*, John Wiley & Sons.
- ARAKERE, A. C. & DOSHI, T. D. 2015. *COMPARISON OF MULTI-STOREY BUILDING WITH NORMAL BEAMS AND CONCEALED BEAMS. International Research Journal of Engineering and Technology (IRJET)*, 02.

- ARANGO, M. & LUBKOWSKI, Z. *Seismic Hazard Assessment and Design Requirements for Beirut, Lebanon*. 15th World Conference in Earthquake Engineering, 2012.
- ARMOUTI, N. S. 2015. **Earthquake Engineering: Theory and Implementation**, McGraw-Hill Education.
- ARUM, C. & AKINKUNMI, A. 2011. **Comparison of Wind-Induced Displacement Characteristics of Buildings with Different Lateral Load Resisting Systems**. ENG Engineering, 03, 236-247.
- ARYA, A. S., BOEN, T. & ISHIYAMA, Y. 2014. *Guidelines for earthquake resistant non-engineered construction*, UNESCO.
- ASCE 2010. *Minimum design loads for buildings and other structures*, Reston, Va., American Society of Civil Engineers: Structural Engineering Institute.
- ASDIP CONCRETE 2017. *ASDIP, Structural Engineering Software For Engineering Design Professionals*. 3.2.2 ed.
- B.S, K. G. & TAJODDEEN, S. 2014. *Seismic analysis of multistorey building with floating columns*. First Annual Conference on Innovations and Developments in Civil Engineering (ACIDIC 2014). India.
- BANGASH, M. 2011. *Earthquake resistant buildings: dynamic analyses, numerical computations, codified methods, case studies and examples*, Springer Science & Business Media.

- BARBAT, H., OLLER, S. & VIELMA, J. 2009. **Seismic performance of waffled-slab floor buildings.**
- BARMO, A., MUALLA, I. H. & HASAN, H. T. 2014. *The Behavior of Multi-Story Buildings Seismically Isolated System Hybrid Isolation (Friction, Rubber and with the Addition of Rotational Friction Dampers).* **Open Journal of Earthquake Research**, 4, 1.
- BEN-AVRAHAM, Z., LAZAR, M., SCHATTNER, U. & MARCO, S. 2005. **The Dead Sea Fault and its effect on civilization.** Perspectives in Modern Seismology. Springer.
- BERTERO, V. V. *State of the art report on: design criteria.* **Proceedings of 11th world conference on earthquake engineering**, Acapulco, Mexico, Oxford, Pergamon, 1996.
- BILHAM, R. 2010. *Lessons from the Haiti earthquake.* Nature, 463, 878-879.
- BOMMER, J. J. & MARTINEZ-PEREIRA, A. *Strong-motion parameters: definition, usefulness and predictability.* **Proc. of the 12th World Conference on Earthquake Engineering**, Auckland, New Zealand, 2000.
- BOOTH, E. 2014. **Earthquake design practice for buildings**, London, ICE.
- BOSCO, M., GHERSI, A. & LEANZA, S. *Force-displacement relationships for R/C members in seismic design.* **Proceeding of the**

- 14th world conference on earthquake engineering**, Beijing, China, 2008.
- CEN, E. C. F. S. 2005. *Eurocode 8: Design of structures for earthquake resistance-part 1: general rules, seismic actions and rules for buildings*.
 - CHARNEY, F. A. 2015. *Seismic Loads: Guide to the Seismic Load Provisions of ASCE 7-10*, Reston, Virginia, **American Society of Civil Engineers**.
 - CHEN, W.-F. & DUAN, L. 2000. *Bridge engineering handbook*, Boca Raton, CRC.
 - CHEN, W.-F. & LUI, E. M. 2006. *Earthquake engineering for structural design*, Boca Raton, CRC/Taylor & Francis.
 - CHOPRA, A. K. 2012. *Dynamics of structures: theory and applications to earthquake engineering*, Upper Saddle River, NJ, Prentice Hall.
 - CHURAKOV, A. 2014. *Biaxial hollow slab with innovative types of voids*. Stroitel'stvo Unikal'nyh Zdanij i Sooruzenij, 70.
 - CLOUGH, R. W. & PENZIEN, J. 2003. *Dynamics of structures*, Berkeley, Calif., **Computers and Structures**.
 - CORONADO, C., REIGLES, D., BAE, S. & MUNSHI, J. 2011. *Finite element mesh sensitivity study using ANSYS for analysis and design of nuclear concrete structures*.
 - CRED, C. F. R. O. T. E. O. D. 2015. *Human cost of natural disasters 2015: a global perspective*.

- CSI, C. A. S., INC., BERKELEY, CALIFORNIA, USA 2017a. *Analysis Verification Examples For SAP2000® and CSiBridge®*.
- CSI, C. A. S., INC., BERKELEY, CALIFORNIA, USA 2017b. *SAP2000 V 19.1.1, Integrated Finite Element Analysis and Design of Structures*.
- DAY, R. W. 2012. **Geotechnical earthquake engineering handbook: with the 2012 International building code**.
- DEEK, R. *Lessons From Nature: Defensive Designs for the Built Environment*. **5th International Conference on Building Resilience**, 2015.
- DELIVERABLE, D. 2014. *Support Action for Strengthening Palestine capabilities for seismic Risk Mitigation SASPARM 2.0*.
- DOĞANGÜN, A. & LIVAOĞLU, R. 2006. *Comparison of seismic analysis methods for multistory buildings*.
- DOWRICK, D. J. 2003. **Earthquake risk reduction**, John Wiley & Sons.
- DUGGAL, S. 2007. *Earthquake Resistant Design of Structures; Reinforced concrete buildings, Masonry buildings*, **OXFORD UNIVERSITY PRESS**.
- DUGGAL, S. K. 2013. **Earthquake-resistant design of structures**, Oxford university press.

- EL-SHAER, M. A. 2014. *Seismic Load Analysis of different RC Slab Systems for Tall Building*. **Acta Technica Corviniensis-Bulletin of Engineering**, 7, 65.
- ELNASHAI, A. S. & DI SARNIO, L. 2008. *Fundamentals of earthquake engineering*, Wiley Chichester, UK.
- ESSEC, E. S. A. S. E. C. 2017. *Seismic hazard Map and seismic zone factor* [Online]. An-Najah National University
Nablu, Palestine. Available:
<https://www.najah.edu/en/community/scientific-centers/urban-planning-and-disaster-risk-reduction-center/earth-sciences-and-seismic-engineering-unit/seismic-hazard-map/>.
- FARDIS, M. N., CARVALHO, E. C., FAJFAR, P. & PECKER, A. 2015. **Seismic design of concrete buildings to Eurocode 8**.
- FILIATRAULT, A., CHRISTOPOULOS, C., STEARNS, C. & STRUCTURAL SYSTEMS RESEARCH, P. 2001. *Guidelines, specifications, and seismic performance characterization of nonstructural building components and equipment*, La Jolla, Calif., **Dept. of Structural Engineering**, University of California, San Diego.
- FINLEY, D. T. & CRIBBS, R. A. *Equivalent static vs. response spectrum: a comparison of two methods*. Proceedings of SPIE, 2004. 403-410.

- GARFUNKEL, Z., BEN-AVRAHAM, Z. & KAGAN, E. 2014. *Dead Sea Transform fault system: reviews* [Online]. Available:
<http://public.ebib.com/choice/publicfullrecord.aspx?p=1783764>.
- GAVGANI, S. A. M. & ALINEJAD, B. 2015. *An analysis on new Cobiax roof*. **International Academic Journal of Innovative Research**.
- GHOGARE, K. K., GUPTA, A. R. & NIKUMBH, A. R. 2016. *Behaviour of Non-Structural Elements During An Earthquake*. **International Journal of Advanced Research in Science, Engineering and Technology**, 3.
- GHOSH, S. K. & FANELLA, D. A. 2003. *Seismic and Wind Design of Concrete Buildings: (2000 IBC, ASCE 7-98, ACI 318-99)*, Kaplan AEC Engineering.
- GILLENGERTEN, J. D. 2001. *Design of nonstructural systems and components*. The seismic design handbook. Springer.
- GREY, M. 2006. **Finite Element Seismic Analysis of Guyed Masts**. Master of Science by Research, University of Oxford.
- HAMBURGER, R. 2009. **Facts for Steel Buildings Number 3- Earthquakes and Seismic Design**.
- HASEEB, M., XINHAILU, A. B., KHAN, J. Z., AHMAD, I. & MALIK, R. 2011. *Construction of earthquake resistant buildings and infrastructure implementing seismic design and building code in*

- northern Pakistan 2005 earthquake affected area. International Journal of Business and Social Science*, 2.
- HASSOUN, M. N. & AL-MANASEER, A. A. 2015. *Structural concrete: theory and design* [Online]. Available:
<http://catalogimages.wiley.com/images/db/jimages/9781118767818.jpg>.
 - HAWAJRI, O. 2016. *Natural disasters and complex humanitarian emergencies in the occupied Palestinian territories. Emergency and Disaster Reports*, 3, 4-51.
 - HOLZER, T. L. & SAVAGE, J. C. 2013. *Global earthquake fatalities and population. Earthquake Spectra*, 29, 155-175.
 - INTERNATIONAL CODE COUNCIL 2004. *International building code, 2003*, Country Club Hills, IL, International Code Council.
 - INTERNATIONAL CODE COUNCIL 2014. *International building code 2015*, Country Club Hills, Ill., ICC.
 - INTERNATIONAL CONFERENCE OF BUILDING, O. 1997. *Uniform building code, 1997*, California, International Conference of Building Officials.
 - ISHIYAMA, Y., FUKUSHIMA, S., INOUE, T., ISHIDA, H. & ISHII, T. 2004. **Revision of AIJ Recommendations for seismic loads on buildings**. Structures 2004: Building on the Past, Securing the Future.

- ISLER, O. 2008. **SEISMIC PERFORMANCES and TYPICAL DAMAGES OF BEAM-COLUMN JOINTS IN THE RC BUILDINGS.**
- IWAI, S. & MATSUMORI, H. 2004. **Effect of Heavy Dead Weight on Earthquake Damage of Wooden Houses Based on Change of Natural Period.** 13th World Conference on Earthquake Engineering. Vancouver, B.C., Canada.
- JIA, J. & YAN, J. *Analysis about factors affecting the degree of damage of buildings in earthquake.* **Journal of Physics: Conference Series, 2015.** IOP Publishing, 012062.
- JIMENEZ, M., AL-NIMRY, H., KHASAWNEH, A., AL-HADID, T. & KAHHALEH, K. 2008. **Seismic hazard assessment for Jordan and neighbouring areas.** Bull. Geof. Teor. Appl, 49, 17-36.
- JOHNSON, L., JIAO, H. & GHAZIHAANI, T. G. *Finite element modelling of hollow-core concrete slabs.* International Conference on Performance-based and Life-cycle Structural Engineering, 2015. School of Civil Engineering, The University of Queensland, 1638-1644.
- KAMALI, M. K., DEHKORDI, A. K. F., SHAMSABADI, A. A., REZAEI, P., SOURESHJANI, M. K. & AGHAEI, A. 2014. **SOLUTIONS FOR INCREASING THE STABILITY OF STRUCTURAL SYSTEMS OF IRAN TRADITIONAL BUILDINGS (ROOF LIGHTWEIGHT).**

- KENNY, C. 2009. **Why do people die in earthquakes? The costs, benefits and institutions of disaster risk reduction in developing countries.** The Costs, Benefits and Institutions of Disaster Risk Reduction in Developing Countries (January 1, 2009). World Bank Policy Research Working Paper Series, Vol.
- KEVADKAR, M. & KODAG, P. 2013. ***Lateral load analysis of RCC Building.*** International Journal of Modern Engineering Research (IJMER), 3, 1428-1434.
- KHAN, Q. 2013. **Evaluation of effects of response spectrum analysis on height of building.**
- KLINGER, Y., AVOUAC, J., DORBATH, L., KARAKI, N. A. & TISNERAT, N. 2000a. ***Seismic behaviour of the Dead Sea fault along Araba valley, Jordan.*** Geophysical Journal International, 142, 769-782.
- KLINGER, Y., AVOUAC, J., KARAKI, N. A., DORBATH, L., BOURLES, D. & REYSS, J. 2000b. ***Slip rate on the Dead Sea transform fault in northern Araba valley (Jordan).*** Geophysical Journal International, 142, 755-768.
- KLINGER, Y., LE BÉON, M. & AL-QARYOUTI, M. 2015. ***5000 yr of paleoseismicity along the southern Dead Sea fault.*** Geophysical Journal International, 202, 313-327.
- KOSTOV, M. & VASSEVA, E. **Seismic fragility analyses.** 2000. European Network on Seismic Risk, Vulnerability and Earthquake Scenarios Working Meeting, Potenza, University of Basilicata.

- KURRAZ, H. A. 2015. **Towards lowering the cost of houses in Palestine: New perspective.** Master of Science in Construction Management, THE ISLAMIC UNIVERSITY - GAZA.
- KYAKULA, M., BEHANGANA, N. & PARIYO, B. *Comparative analysis of hollow clay block and solid reinforced concrete slabs.* **Proceedings from the International Conference on Advances in Engineering and Technology, 2006.** 84-90.
- LEET, K. & UANG, C.-M. 2005. **Fundamentals of structural analysis,** Boston, McGraw-Hill.
- LEVI, T., TAVRON, B., KATZ, O., AMIT, R., SEGAL, D., HAMIEL, Y., BAR-LAVI, Y., ROMACH, S. & SALAMON, A. 2010. *Earthquake loss estimation in Israel using the new HAZUS-MH software: preliminary implementation.* **Ministry of National Infrastructures Geological Survey of Israel.**
- LOGAN, D. L. 2012. **A first course in the finite element method,** Stamford, Cengage Learning.
- MCCORMAC, J. C. & BROWN, R. H. 2015. **Design of reinforced concrete,** John Wiley & Sons.
- MCCUEN, R. H., EZZELL, E. Z. & WONG, M. K. 2011. *Fundamentals of Civil Engineering: An Introduction to the ASCE Body of Knowledge,* **CRC Press.**
- MCKENZIE, W. M. 2013. **Examples in structural analysis,** CRC Press.

- MINISTRY OF LOCAL GOVERNMENT 2002. **Establishing, Adoption, and Implementation of Energy Codes for Buildings, Construction Techniques Survey in Palestinian Territories.**
- MOEHLE, J. 2015. **Seismic design of reinforced concrete buildings,** New York, McGraw Hill.
- MOHAMED, W. A.-W. 2014. ***Seismic Capacity of RC hollow block slab building and retrofitting systems.*** Journal of Engineering Sciences, Assiut University, Faculty of Engineering, 42.
- MOUSTAFA, A. 2015. **Earthquake engineering: from engineering seismology to optimal seismic design of engineering structures.**
- MPWH 2006. **Jordanian National Building Code for Loads and Forces** Amman, Building Research Center for Ministry of Public Works & Housing.
- MUSMAR, M. A., ABDEL HADI, M. A. & RJOUB, M. I. 2014. ***Nonlinear finite element analysis of shallow reinforced concrete beams using solid65 element.*** ARPN J. Eng. Appl. Sci. ARPN Journal of Engineering and Applied Sciences, 9, 85-89.
- NAIR, K. G. & AKSHARA, S. 2017. **SEISMIC ANALYSIS OF REINFORCED CONCRETE BUILDINGS-A REVIEW.**
- NAKAI, M., KOSHIKA, N., KAWANO, K., HIRAKAWA, K. & WADA, A. 2012. ***Performance-Based Seismic Design for High-Rise Buildings in Japan.*** International journal of high-rise buildings, 1, 155-167.

- NIBS, N. I. O. B. S. 2009. **NEHRP Recommended Seismic Provisions for New Buildings and Other Structures**, Washington, D.C.
- NIBS, N. I. O. B. S. 2012. **2009 NEHRP Recommended Seismic Provisions: Design Examples**, Washington, D.C.
- NILSON, A. H., DARWIN, D. & DOLAN, C. W. 2010. **Design of concrete structures**, New York, McGraw-Hill Higher Education.
- NOVELLI, V., D'AYALA, D., AL ASSAF, A. & AKAWWI, E. 2014. **SEISMIC RISK ESTIMATION FOR WADI MUSA IN JORDAN**
2nd European Conference on Earthquake Engineering and Seismology.
Turkey (Istanbul)
- NUCLEAR REGULATORY COMMISSION 2012. **Combining modal responses and spatial components in seismic response analysis**.
Nuclear Regulatory Commission.
- ÖZTÜRK, T. & ÖZTÜRK, Z. 2008. **THE EFFECTS OF THE TYPE OF SLAB ON STRUCTURAL SYSTEM IN THE MULTI-STOREY REINFORCED CONCRETE BUILDINGS**.
- PAMPANIN, S. 2012. *Living a New Era in Earthquake Engineering: targeting damage-resisting solutions to meet societal expectations*.
Australian Earthquake Engineering Society 2012 Conference.
- PANAS , P. 2014. *Seismic Analysis and Design of Reinforced Concrete Frame Buildings* Bachelor's Degree in Civil Engineering, CITY UNIVERSITY LONDON

- PARDAKHE, P. K. & NALAMWAR, M. R. 2015. ***COMPARATIVE STUDY OF R.C.C STRUCTURE FOR EARTHQUAKE LOAD USING LIGHT WEIGHT BUILDING MATERIAL***. **International Research Journal of Engineering and Technology (IRJET)**, 02.
- PAULAY, T. 1997. ***A behaviour-based design approach to earthquake-induced torsion in ductile buildings***. **Seismic Design Methodologies for the Next Generation of Codes'** Balkema, Rotterdam.
- PAULTRE, P. 2013. **Dynamics of structures**, John Wiley & Sons.
- PAULTRE, P., CALAIS, É., PROULX, J., PRÉPETIT, C. & AMBROISE, S. 2013. ***Damage to engineered structures during the 12 January 2010, Haiti (Léogâne) earthquake***. **Canadian Journal of Civil Engineering**, 40, 777-790.
- PIQUE, J. & BURGOS, M. ***Effective rigidity of reinforced concrete elements in seismic analysis and design***. **The 14th World Conference on Earthquake Engineering**, 2008. 12-17.
- PRIESTLEY, M. & PAULAY, T. 1992. **Seismic design of reinforced concrete and masonry buildings**. New York: John Wiley & Sons, Inc.
- PRIESTLEY, M. N. 2003. **Myths and fallacies in earthquake engineering, revisited**, IUSS press.
- QU, B., GOEL, R. & CHADWELL, C. 2014. ***EVALUATION OF ASCE/SEI 7 PROVISIONS FOR DETERMINATION OF SEISMIC DEMANDS ON NONSTRUCTURAL COMPONENTS***.

- RAI, N. K., REDDY, G. & VENKATRAJ, V. 2011. **Effectiveness of multiple tswd for seismic response control of masonry infilled RC framed structure**. ISET Journal of Earthquake Technology, 48.
- RIZK, A. S. S. 2010. **Structural design of reinforced concrete tall buildings**
- SADEH, M., HAMIEL, Y., ZIV, A., BOCK, Y., FANG, P. & WADOWINSKI, S. 2012. *Crustal deformation along the Dead Sea Transform and the Carmel Fault inferred from 12 years of GPS measurements*. **Journal of Geophysical Research: Solid Earth**, 117.
- SBCNC, S. B. C. N. C. 2007. **Saudi Building Code (SBC)**, Saudi Arabia.
- SEMBLAT, J.-F., DUVAL, A.-M. & DANGLA, P. **Analysis of seismic site effects: BEM and modal approach vs experiments**. 12th World Conf. on Earthquake Eng, 2000.
- SII, T. S. I. O. I. 2009. *Amendment No. 3 of ISRAEL STANDARD SI 413*. **Design provisions for earthquake resistance of structures**.
- SUBRAMANIAN, N. 2014. *Design of Reinforced Concrete Structures*, New Delhi, **OUP** India.
- SUCUOGLU, H. 2015. *Basic earthquake engineering from seismology and seismic analysis to design principles*, Cham, Springer.
- TAGHAVI, S., MIRANDA, E. & PACIFIC EARTHQUAKE ENGINEERING RESEARCH, C. 2003. **Response assessment of**

nonstructural building elements [Online]. Berkeley: Pacific Earthquake Engineering Research Center. Available:

http://peer.berkeley.edu/publications/peer_reports/reports_2003/0305.pdf.

- TAQIEDDIN, Z. N. 2014. *Deflection of Wide Hidden Beams in One-Way Slab Systems: A Nonlinear Finite Element Study* Conf. on Advances In Civil and Structural Engineering -.
- TARANATH, B. S. 2004. **Wind and earthquake resistant buildings: structural analysis and design**, CRC press.
- TAYLOR, A., HAMILTON III, T., NANNI, A. & AMERICAN CONCRETE, I. 2016. *The Reinforced concrete design handbook: a companion to ACI-318-14*, Farmington Hills, MI, American Concrete Institute.
- THORNBURG, D. W., HENRY, J. R. & INTERNATIONAL CODE, C. 2015. **2015 International Building Code Illustrated Handbook**.
- TOUQAN, A. R. & SALAWDEH, S. 2015. **Major Steps Needed Towards Earthquake Resistant Design**. The Sixth Jordanian International Civil Engineering Conference. Jordan (Amman).
- TREMBLAY, R., DEHGHANI, M., FAHNESTOCK, L., HERRERA, R., CANALES, M., CLIFTON, C. & HAMID, Z. **Comparison of seismic design provisions for buckling restrained braced frames in Canada, United States, Chile, and New Zealand**. Structures, 2016. Elsevier, 183-196.

- TRIFUNAC, M. D. & TODOROVSKA, M. **Origin of the response spectrum method**. Proceedings of the 14th world conference on earthquake engineering, 2008. 12-17.
- U.S. GEOLOGICAL SURVEY. 2016. Available:
<https://pubs.usgs.gov/publications/text/slabs.html>.
- U.S. GEOLOGICAL SURVEY. 2017. Available:
[https://earthquake.usgs.gov/learn/glossary/?term=spectral%20acceleration%20\(SA\)](https://earthquake.usgs.gov/learn/glossary/?term=spectral%20acceleration%20(SA)).
- UDÍAS, A., MADARIAGA, R. & BUFORN, E. 2014. *Source Mechanisms of Earthquakes: Theory and Practice*, Cambridge University Press.
- UNDP 2014. *UNDP AND THE HYOGO FRAMEWORK FOR ACTION, 10 Years of Reducing Disaster Risk*.
- UNITED NATIONS, D. A. A. C. T. 2014. *UNDAC, DISASTER RESPONSE PREPAREDNESS MISSION TO THE STATE OF PALESTINE*, Geneva, United Nations, Dept. of Humanitarian Affairs.
- VONA, M. 2014. *Fragility curves of existing RC buildings based on specific structural performance levels*. *Open Journal of Civil Engineering*, 4, 120.
- WIGHT, J. K. 2016. **Reinforced concrete: mechanics and design**, Boston, Pearson.
- WILLIAMS, M. 2016. **Structural Dynamics**, CRC Press.

- YAKUT, A. 2004. *Reinforced concrete frame construction*. World Housing Encyclopedia–Summary Publication, 9-1.

APPENDICES

APPENDIX A
SUPPORTING DOCUMENTS

A1 Formal Documents

A1.1 Documents Provide Purposeful Information through the Research

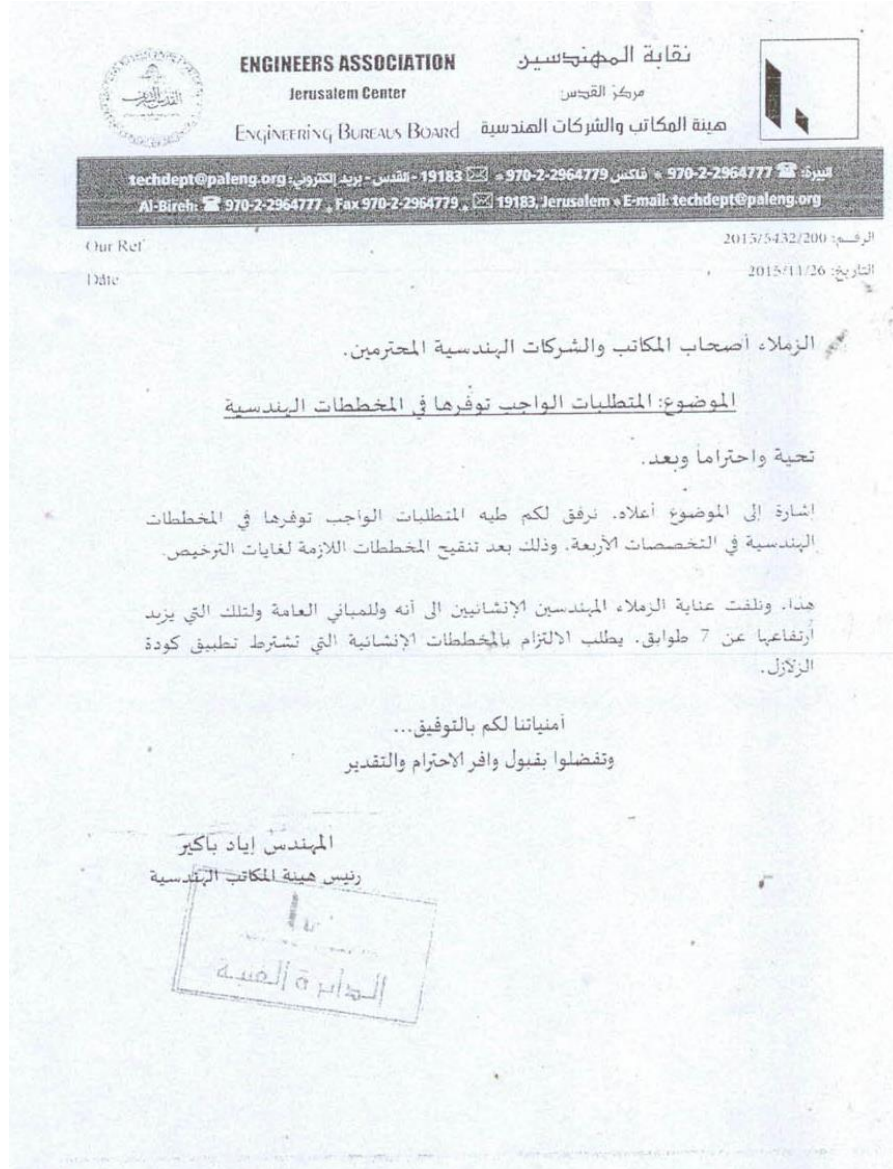
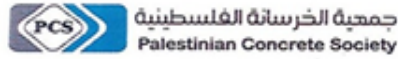


Figure A.1: The circulation of the imperatively of seismic design of buildings



Letter Ref.: 17-125

Date: 11 November 2017

Subject: Request for Information

Dear Mr. Hasan J. M. Alnajjra,

With reference to your inquire related to the current price market for the ready mixed concrete and reinforcing steel bars, please find our reply to your inquire as follows.

Table No.1 Price Market for the Ready Mixed Concrete and Reinforcing Steel Bars 2017 Years.

Sr.	Item Description	Unit	Price
1	Ready mixed concrete B300	m3	85 US Dollar
2	Reinforcing steel bars	Ton	700 US Dollar

Best Regards,

President of Palestinian concrete society

Dr. Mahmoud Shakarna

مزيد من المعلومات والمراسلة للجمعية: هاتف: 02-2960930, فاكس: 02-2960931, إيميل: palconcretesociety@gmail.com

Figure A.2: Request of quotation received from the Palestinian Concrete Society

APPENDIX B
CHECKS FOR SIZES OF STRUCTURAL
MEMBERS

B1 Models 1N-R, 1N-SR, 1N-SS, and 1J-SC

B1.1 Slab Thickness

Table B.1: Relative flexural stiffness of internal and edge beams

<i>Internal Beam I_b (mm⁴)</i>	4.57E+09
<i>Internal Slab Panel I_s (mm⁴)</i>	1.10E+09
<i>Internal Beam α_f</i>	4.15
<i>Edge Beam I_b (mm⁴)</i>	4.08E+09
<i>Edge Slab Panel I_s (mm⁴)</i>	6.09E+08
<i>Edge Beam α_f</i>	6.70

Table B.2: Required thickness for different slab panels

Panel	Corner	Edge	Internal
l_{n1} (mm)	5350	5350	5350
l_{n2} (mm)	5350	5350	5350
l_n (mm)	5350	5350	5350
β	1	1	1
α_{fm}	5.43	4.79	4.15
h_{min} (mm)	131	131	131
$h_{provided} = 130mm \approx h_{min} = 131mm$			

B1.2 Beams Depths

Select the most critical case, $h_{min} = \frac{l}{18.5} = \frac{6000}{18.5} = 324mm$.

\therefore The provided 400mm depths of beams $\geq 324mm$ are thus OK.

B1.3 Columns Cross-Sections

Table B.3: Ultimate self-weights of structural elements included within the tributary area

Types of Elements in the Tributary Area	Load Factor	γ_c (kN/m ³)	Dimensions (m)			Mass and Weight Modifier*	Factored Weights of Elements (kN) in the Tributary Area
			Length	Width	Depth		
Slab	1.2	25	6	6	0.13	1	140
Beams	1.2	25	11.35	0.65	0.4	0.675	59.8
Column	1.2	25	3.4	0.65	0.65	0.882	38.0
Σ							238
Total ultimate weight of elements (kN) included within the tributary area in 10-stories							2382

* A self-weight multiplier less than 1.0 is applied for beams and columns to ensure that weight is accounted for only once at shared joints and lines

$$\text{Mass or weight modifier of beam} = \frac{\text{beam depth} - \text{slab depth}}{\text{beam depth}}$$

$$\text{Mass or weight modifier of column} = \frac{\text{column length (story height } c/c) - \text{beam depth}}{\text{column length (story height } c/c)}$$

Table B.4: Ultimate weights of distributed loads over the tributary area

Load Pattern	Load Factor	Distributed Load (kN/m ²)	Tributary Area		Total Factored Loads (kN) on the Tributary Area
			Length (m)	Width (m)	
SDL	1.2	1	6	6	43.2
LL	1.6	4	6	6	230
Σ					274
Total ultimate weight (kN) over the tributary area in 10-stories					2736

$$P_u = 2382 + 2736 = 5118kN.$$

As a square section, the required length or width = 641mm.

\therefore The actual section dimensions of 650mm \geq 641mm are thus OK.

B2 Models 3N-R, 3N-SR, 3N-SS, and 3J-SC

B2.1 Slab Thickness

Table B.5: Relative flexural stiffness of internal and edge beams

<i>Internal Beam I_b (mm⁴)</i>	7.12E+09
<i>Internal Slab Panel I_s (mm⁴)</i>	1.10E+09
<i>Internal Beam α_f</i>	6.47
<i>Edge Beam I_b (mm⁴)</i>	6.32E+09
<i>Edge Slab Panel I_s (mm⁴)</i>	6.13E+08
<i>Edge Beam α_f</i>	10.3

Table B.6: Required thickness for different slab panels

Panel	Corner	Edge	Internal
l_{n1} (mm)	5300	5300	5300
l_{n2} (mm)	5300	5300	5300
l_n (mm)	5300	5300	5300
β	1	1	1
α_{fm}	8.39	7.43	6.47
h_{min} (mm)	130	130	130
$h_{provided} = 130mm \geq h_{min} = 130mm$			

B2.2 Beams Depths

Select the most critical case, $h_{min} = \frac{l}{18.5} = \frac{6000}{18.5} = 324mm$.

\therefore The provided 450mm depths of beams $\geq 324mm$ are thus OK.

B2.3 Columns Cross-Sections

Table B.7: Ultimate self-weights of structural elements included within the tributary area

Types of Elements in the Tributary Area	Load Factor	γ_c (kN/m ³)	Dimensions (m)			Mass and Weight Modifier*	Factored Weights of Elements (kN) in the Tributary Area
			Length	Width	Depth		
Slab	1.2	25	6	6	0.13	1	140
Beams	1.2	25	11.3	0.7	0.45	0.711	75.9
Column	1.2	25	3.55	0.7	0.7	0.873	45.6
Σ							262
Total ultimate weight of elements (kN) included within the tributary area in 10-stories							2620

* A self-weight multiplier less than 1.0 is applied for beams and columns to ensure that weight is accounted for only once at shared joints and lines

$$\text{Mass or weight modifier of beam} = \frac{\text{beam depth} - \text{slab depth}}{\text{beam depth}}$$

$$\text{Mass or weight modifier of column} = \frac{\text{column length (story height } c/c) - \text{beam depth}}{\text{column length (story height } c/c)}$$

Table B.8: Ultimate weights of distributed loads over the tributary area

Load Pattern	Load Factor	Intensity (kN/m ²)	Tributary Area		Total Factored Loads (kN) on the Tributary Area
			Length (m)	Width (m)	
SDL	1.2	3	6	6	130
LL	1.6	4	6	6	230
Σ					360
Total ultimate weight (kN) over the tributary area in 10-stories					3600

$$P_u = 2620 + 3600 = 6220 \text{ kN.}$$

As a square section, the required length or width = 706mm.

\therefore The actual section dimensions of 700mm \approx 706mm are thus OK.

B3 Models 5N-R, 5N-SR, 5N-SS, and 5J-SC

B3.1 Slab Thickness

Table B.9: Relative flexural stiffness of internal and edge beams

<i>Internal Beam I_b (mm⁴)</i>	1.06E+10
<i>Internal Slab Panel I_s (mm⁴)</i>	1.10E+09
<i>Internal Beam α_f</i>	9.64
<i>Edge Beam I_b (mm⁴)</i>	9.34E+09
<i>Edge Slab Panel I_s (mm⁴)</i>	6.18E+08
<i>Edge Beam α_f</i>	15.1

Table B.10: Required thickness for different slab panels

Panel*	Corner	Edge	Internal
l_{n1} (mm)	5250	5250	5250
l_{n2} (mm)	5250	5250	5250
l_n (mm)	5250	5250	5250
β	1	1	1
α_{fm}	12.4	11.0	9.64
h_{min} (mm)	128	128	128
$h_{provided} = 130mm \geq h_{min} = 128mm$			

B3.2 Beams Depths

Select the most critical case, $h_{min} = \frac{l}{18.5} = \frac{6000}{18.5} = 324mm$.

\therefore The provided 500mm depths of beams $\geq 324mm$ are thus OK.

B3.3 Columns Cross-Sections

Table B.11: Ultimate self-weights of structural elements included within the tributary area

Types of Elements in the Tributary Area	Load Factor	γ_c (kN/m ³)	Dimensions (m)			Mass and Weight Modifier*	Factored Weights of Elements (kN) in the Tributary Area
			Length	Width	Depth		
Slab	1.2	25	6	6	0.13	1	140
Beams	1.2	25	11.25	0.75	0.5	0.74	93.7
Column	1.2	25	3.7	0.75	0.75	0.865	54
Σ							288
Total ultimate weight of elements (kN) included within the tributary area in 10-stories							2881

* A self-weight multiplier less than 1.0 is applied for beams and columns to ensure that weight is accounted for only once at shared joints and lines

$$\text{Mass or weight modifier of beam} = \frac{\text{beam depth} - \text{slab depth}}{\text{beam depth}}$$

$$\text{Mass or weight modifier of column} = \frac{\text{column length (story height } c/c) - \text{beam depth}}{\text{column length (story height } c/c)}$$

Table B.12: Ultimate weights of distributed loads over the tributary area

Load Pattern	Load Factor	Intensity (kN/m ²)	Tributary Area		Total Factored Loads (kN) on the Tributary Area
			Length (m)	Width (m)	
SDL	1.2	5	6	6	216
LL	1.6	4	6	6	230
Σ					446
Total ultimate weight (kN) over the tributary area in 10-stories					4464

$$P_u = 2881 + 4464 = 7345 \text{ kN.}$$

As a square section, the required length or width = 768mm.

\therefore The actual section dimensions of 750mm \approx 768mm are thus OK.

APPENDIX C
CHECKS FOR GRAVITY LOADS ANALYSIS

C1 Models 1N-R, IN-SR, 1N-SS, and IJ-SC

C1.1 Check of Compatibility

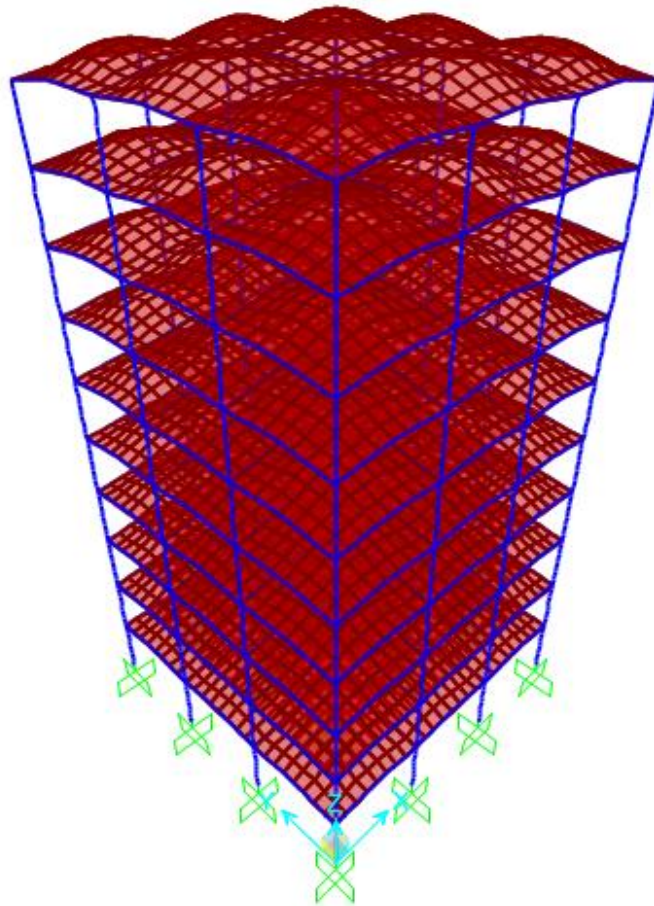


Figure C.1: 3D portal-frame

C1.2 Check of Equilibrium

Table C.1: Check of equilibrium due to self-weights of structural elements

Types of Elements in Single Story	γ_c (kN/m ³)	Dimensions (m)			Mass and Weight Modifier	No. of Elements in Single Story	Weights of Elements (kN) in Single Story
		Length	Width	Depth			
Slab Panels	25	6	6	0.13	1	9	1053
Beams	25	6	0.65	0.4	0.675	24	632
Columns	25	3.4	0.65	0.65	0.882	16	507
Σ							2192
Total service weights (kN) of elements for the building (10–Stories)							21918
Global FZ (kN)– SAP2000							21918
Error %							0.00
Evaluation of error (max. 5%)							OK

Table C.2: Check of equilibrium due to the distributed loads over slabs

Load Pattern	Intensity (kN/m ²)	Slab Dimensions (m)		Total Load (kN) on a Single Slab
		Length	Width	
SDL	1	18	18	324
LL	4	18	18	1296
Total service SDLs (kN) for the building (10–Stories)				3240
Global FZ (kN)– SAP2000				3240
Error %				0.00
Evaluation of error (max. 5%)				OK
Total service LLs (kN) for the building (10–Stories)				12960
Global FZ (kN)– SAP2000				12960
Error %				0.00
Evaluation of error (max. 5%)				OK

C1.3 Check of stress-strain relationship

C1.3.1 DDM

Checking of Adequacy for DDM

Table C.3: DDM limitations and checks

Item	<i>For every direction, there must be at least three continuous spans</i>
Check	<i>There are, exactly, three spans in every direction</i>
Item	<i>For every direction, adjacent spans measured center to center of supports, must not differ by more than one – third the longer span ($l_{short} \geq (2/3) l_{long}$)</i>
Check	<i>All spans are of 6 m long, i.e. $l_{short}/l_{long} = 1 \geq (2/3)$</i>
Item	<i>Panels must be rectangular. The longer span of the panel, measured center to center of supports, must not exceed two times the shorter span ($l_{long}/l_{short} \leq 2$)</i>
Check	<i>All spans are of 6 m long, i.e. $l_{long}/l_{short} = 1 \leq 2$</i>
Item	<i>The largest permitted offset of a column, from the general centerline, is 10% of the span in the direction of offset</i>
Check	<i>Column offsets do not exist</i>
Item	<i>All loads must be only due to gravity, and uniformly distributed over the entire panel. In addition, service live load shall not exceed two times the service dead load</i>
Check	$LL = 4 \text{ kN/m}^2$, $DL = DL_{slab} + SDL = 25 \times 0.13 + 1 = 3.25 + 1 = 4.25 \text{ kN/m}^2$, $LL < DL \Rightarrow LL < 2DL$
Item	<i>For a panel supported by beams in both directions, the relative stiffness of beam in two orthogonal directions must conform to:</i>
	$0.2 \leq \frac{\alpha_{f1} l_1^2}{\alpha_{f2} l_2^2} \leq 5.0 \quad [ACI 318-14 \text{ Code, Eq. 8.10.2.7a}]$
Check	$l_1 = l_2 = 6.0\text{m}$ α_f for internal beam = 4.15, α_f for edge beam = 6.70 <i>Whatever the numerator and the denominator, the above equation is satisfied</i>

Analysis of Span (Y2-Y3)

Table C.4: Required data before the analysis through the DDM

$$l_1 = 6.0m$$

$$l_2 = 6.0m$$

$$l_{n1} = 5.35m$$

$$MS\ Width = 6.0m$$

$$CS\ Width = 3.0m$$

$$Effective\ Width\ of\ Beam = 1.19m$$

$$DL\ of\ Slab = 25 \times 0.13 = 3.25\ kN/m^2$$

$$SDL\ on\ Slab = 1kN/m^2$$

$$LL\ on\ Slab = 4\ kN/m^2$$

$$q_u = 1.2 \times (DL + SDL) + 1.6LL = 11.5kN/m^2$$

$$w_n(\text{Self-weight of the Web of the Beam}) = 4.39kN/m$$

$$w_u(\text{Self-Weight of the Web of the Beam}) = 1.2 \times w_n = 5.27kN/m$$

$$\alpha_{f1} = 4.15$$

$$l_2/l_1 = 1.0$$

$$\alpha_{f1} l_2/l_1 = 4.15$$

Table C.5: Total M_u value of the slab in the CS calculated by DDM, SAP2000, and errors

<i>According to Section 8.10.3.2 of the ACI 318 – 14 Code; the Total Factored Static Moment</i>		
<i>of the Span is $M_o = \frac{q_u \times l_2 \times (l_{n1})^2}{8} = \frac{11.5 \times 6 \times (5.35)^2}{8} = 247 \text{ kN.m}$</i>		
<i>Moment Coefficients of the Interior Span According to Section 8.10.4.2 of the ACI 318 – 14 Code</i>		
-0.65	0.35	-0.65
<i>Total M_u at the Ends and the Middle of the Span (kN.m)</i>		
$-0.65 \times 247 = -161$	$0.35 \times 247 = 86.5$	$-0.65 \times 247 = -161$
<i>According to Sections 8.10.5.1, and 8.10.5.5 of the ACI 318 – 14 Code; % Moments in CS = 0.75</i>		
<i>According to Sections 8.10.5.7.1 of the ACI 318 – 14 Code; % Moments of Slab in CS = $1 - 0.85 = 0.15$</i>		
<i>M_u at the Ends and the Middle of the Slab in the CS (kN.m/m); DDM</i>		
$\frac{0.75 \times 0.15 \times -161}{(3 - 1.19)} = -10.0$	$\frac{0.75 \times 0.15 \times 86.5}{(3 - 1.19)} = 5.38$	$\frac{0.75 \times 0.15 \times -161}{(3 - 1.19)} = -10.0$
<i>M_u at the Ends and the Middle of the Slab in the CS (kN.m/m); M11 – SAP2000</i>		
-8.06	5.41	-8.06
<i>Total M_u of Slab in the CS; DDM = $\frac{2 \times -10.0 }{2} + 5.38 = 15.4 \text{ kN.m/m}$</i>		
<i>Total M_u of Slab in the CS; SAP2000 = $\frac{2 \times -8.06 }{2} + 5.41 = 13.5 \text{ kN.m/m}$</i>		
<i>Error = $\frac{15.4 - 13.5}{13.5} \times 100\% = 14.1\% \leq 25\%$</i>		<i>(OK)</i>

Table C.6: Total M_u value of the beam calculated by DDM, SAP2000, and errors

<i>From the Previous Table; Total M_u at the Ends and the Middle of Span (kN.m)</i>		
-161	86.5	-161
<i>According to Sections 8.10.5.1, and 8.10.5.5 of the ACI 318 – 14 Code; % Moments in the CS = 0.75</i>		
<i>According to Sections 8.10.5.7.1 of the ACI 318 – 14 Code; % Moments of the beam in CS = 0.85</i>		
<i>The Total Factored Static Moment due to the Self – Weight of Web of the Beam is</i>		
$M_o = \frac{w_u \times (l_{n1})^2}{8} = \frac{5.27 \times (5.35)^2}{8} = 18.9 \text{ kN.m}$		
<i>Moment Coefficients of the Interior Span According to Section 8.10.4.2 of the ACI 318 – 14 Code</i>		
0.65	0.35	0.65
<i>M_u at the Ends and the Middle of the Beam (kN.m); DDM</i>		
$(0.75 \times 0.85 \times -161)$ $+ (-0.65 \times 18.9) = -115$	$(0.75 \times 0.85 \times 86.5)$ $+ (0.35 \times 18.9) = 61.8$	$(0.75 \times 0.85 \times -161)$ $+ (-0.65 \times 18.9) = -115$
<i>M_u at the Ends and the Middle of the Beam (kN.m); M3 – SAP2000</i>		
-100	78.1	-100
<i>Total M_u of the Beam ; DDM = $\frac{2 \times -115 }{2} + 61.8 = 177 \text{ kN.m}$</i>		
<i>Total M_u of the Beam ; SAP2000 = $\frac{2 \times -100 }{2} + 78.1 = 178 \text{ kN.m}$</i>		
<i>Error = $\frac{178 - 177}{177} \times 100\% = 0.565\% \leq 25\%$</i>		<i>(OK)</i>

Table C.7: Total M_u value of the slab in the MS calculated by DDM, SAP2000, and errors

<i>From the Previous Table; Total M_u at the Ends and the Middle of Span (kN.m)</i>		
-161	86.5	-161
<i>% Moments in MS = 1 - % Moments in MS = 1 - 0.75 = 0.25</i>		
<i>M_u at the Ends and the Middle of the MS (kN.m/m); DDM</i>		
$\frac{0.25 \times -161}{(6-3)} = -13.4$	$\frac{0.25 \times 86.5}{(6-3)} = 7.21$	$\frac{0.25 \times -161}{(6-3)} = -13.4$
<i>M_u at the Ends and the Middle of the MS (kN.m/m); M11 - SAP2000</i>		
-10.0	8.72	-10.0
<i>Total M_u of the MS; DDM = $\frac{2 \times -13.4 }{2} + 7.21 = 20.6 \text{ kN.m/m}$</i>		
<i>Total M_u of the MS; SAP2000 = $\frac{2 \times -10.0 }{2} + 8.72 = 18.7 \text{ kN.m/m}$</i>		
<i>Error = $\frac{20.6 - 18.7}{18.7} \times 100\% = 10.2\% \leq 25\%$</i>		<i>(OK)</i>

C1.3.2 Column Compressive Force

Table C.8: Maximum expected compressive force acts on the column

Load Pattern	Reference	Ultimate Load Value (kN) in 10-stories
Weight of slabs, beams, columns	Table B.3	2382
Distributed SDL & LL	Table B.4	2736
	Σ	5118
	Global FZ (kN)-SAP2000	4976
	Error %	2.85
	Evaluation of error (max. 10%)	OK

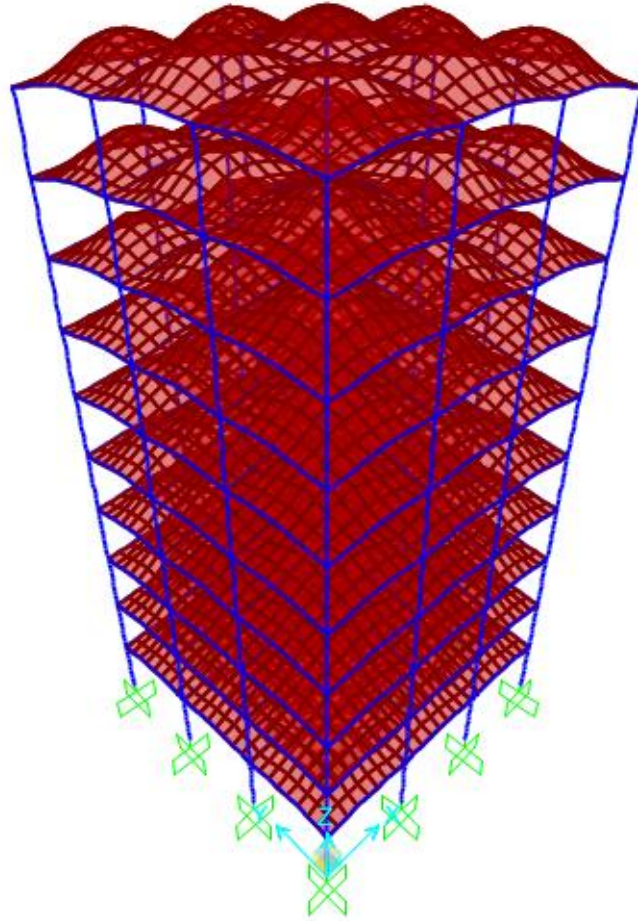
C2 Models 3N-R, 3N-SR, 3N-SS, and 3J-SC**C2.1 Check of Compatibility**

Figure C.2: 3D portal-frame

C2.2 Check of Equilibrium

Table C.9: Check of equilibrium due to self-weights of structural elements

Types of Elements in Single Story	γ_c (kN/m ³)	Dimensions (m)			Mass and Weight Modifier	No. of Elements in Single Story	Weights of Elements (kN) in Single Story
		Length	Width	Depth			
Slab Panels	25	6	6	0.13	1	9	1053
Beams	25	6	0.7	0.45	0.711	24	806
Columns	25	3.55	0.7	0.7	0.873	16	608
Σ							2467
Total service weights (kN) of elements for the building (10–Stories)							24670
Global FZ (kN)– SAP2000							24670
Error %							0.00
Evaluation of error (max. 5%)							OK

Table C.10: Check of equilibrium due to the distributed loads over slabs

Load Pattern	Intensity (kN/m ²)	Slab Dimensions (m)		Total Load (kN) on a Single Slab
		Length	Width	
SDL	3	18	18	972
LL	4	18	18	1296
Total service SDLs (kN) for the building (10–Stories)				9720
Global FZ (kN)– SAP2000				9720
Error %				0.00
Evaluation of error (max. 5%)				OK
Total service LLs (kN) for the building (10–Stories)				12960
Global FZ (kN)– SAP2000				12960
Error %				0.00
Evaluation of error (max. 5%)				OK

C2.3 Check of stress-strain relationship

C2.3.1 DDM

Checking of Adequacy for DDM

Table C.11: DDM limitations and checks

Item	<i>For every direction, there must be at least three continuous spans</i>
Check	<i>There are, exactly, three spans in every direction</i>
Item	<i>For every direction, adjacent spans measured center to center of supports, must not differ by more than one – third the longer span ($l_{short} \geq (2/3) l_{long}$)</i>
Check	<i>All spans are of 6 m long, i.e. $l_{short}/l_{long} = 1 \geq (2/3)$</i>
Item	<i>Panels must be rectangular. The longer span of the panel, measured center to center of supports, must not exceed two times the shorter span ($l_{long}/l_{short} \leq 2$)</i>
Check	<i>All spans are of 6 m long, i.e. $l_{long}/l_{short} = 1 \leq 2$</i>
Item	<i>The largest permitted offset of a column, from the general centerline, is 10% of the span in the direction of offset</i>
Check	<i>Column offsets do not exist</i>
Item	<i>All loads must be only due to gravity, and uniformly distributed over the entire panel. In addition, service live load shall not exceed two times the service dead load</i>
Check	$LL = 4 \text{ kN/m}^2$, $DL = DL_{slab} + SDL = 25 \times 0.13 + 3 = 3.25 + 3 = 6.25 \text{ kN/m}^2$, $LL < DL \Rightarrow LL < 2DL$
Item	<i>For a panel supported by beams in both directions, the relative stiffness of beam in two orthogonal directions must conform to:</i>
	$0.2 \leq \frac{\alpha_{f1} l_1^2}{\alpha_{f2} l_2^2} \leq 5.0 \quad [ACI 318 - 14 \text{ Code, Eq. 8.10.2.7a}]$
Check	$l_1 = l_2 = 6.0\text{m}$ α_f for internal beam = 6.47, α_f for edge beam = 10.3 <i>Whatever the numerator and the denominator, the above equation is satisfied</i>

* α_{f1} is the beam relative flexural stiffness in the studied direction

α_{f2} is the beam relative flexural stiffness in the perpendicular direction

Analysis of Span (Y2-Y3)

Table C.12: Required data before the analysis through the DDM

$$l_1 = 6.0m$$

$$l_2 = 6.0m$$

$$l_{n1} = 5.30m$$

$$MS\ Width = 6.0m$$

$$CS\ Width = 3.0m$$

$$Effective\ Width\ of\ Beam = 1.34m$$

$$DL\ of\ Slab = 25 \times 0.13 = 3.25\ kN/m^2$$

$$SDL\ on\ Slab = 3kN/m^2$$

$$LL\ on\ Slab = 4\ kN/m^2$$

$$q_u = 1.2 \times (DL + SDL) + 1.6LL = 13.9kN/m^2$$

$$w_{n(Self-weight\ of\ the\ Web\ of\ the\ Beam)} = \gamma_c \times 0.7 \times 0.32 = 5.60kN/m$$

$$w_{u(Self-weight\ of\ the\ Web\ of\ the\ Beam)} = 1.2 \times w_n = 6.72kN/m$$

$$\alpha_{f1} = 6.47$$

$$l_2/l_1 = 1.0$$

$$\alpha_{f1} l_2/l_1 = 6.47$$

Table C.13: Total M_u value of the slab in the CS calculated by DDM, SAP2000, and errors

<i>According to Section 8.10.3.2 of the ACI 318 – 14 Code; the Total Factored Static Moment</i>		
<i>of the Span is $M_o = \frac{q_u \times l_2 \times (l_{n1})^2}{8} = \frac{13.9 \times 6 \times (5.3)^2}{8} = 293 \text{ kN.m}$</i>		
<i>Moment Coefficients of the Interior Span According to Section 8.10.4.2 of the ACI 318 – 14 Code</i>		
-0.65	0.35	-0.65
<i>Total M_u at the Ends and the Middle of the Span (kN.m)</i>		
$-0.65 \times 293 = -190$	$0.35 \times 293 = 103$	$-0.65 \times 293 = -190$
<i>According to Sections 8.10.5.1, and 8.10.5.5 of the ACI 318 – 14 Code; % Moments in CS = 0.75</i>		
<i>According to Sections 8.10.5.7.1 of the ACI 318 – 14 Code; % Moments of Slab in CS = $1 - 0.85 = 0.15$</i>		
<i>M_u at the Ends and the Middle of the Slab in the CS (kN.m/m); DDM</i>		
$\frac{0.75 \times 0.15 \times -190}{(3 - 1.34)} = -12.9$	$\frac{0.75 \times 0.15 \times 103}{(3 - 1.34)} = 6.98$	$\frac{0.75 \times 0.15 \times -190}{(3 - 1.34)} = -12.9$
<i>M_u at the Ends and the Middle of the Slab in the CS (kN.m/m); M11 – SAP2000</i>		
-8.64	5.42	-8.64
<i>Total M_u of Slab in the CS; DDM = $\frac{2 \times -12.9 }{2} + 6.98 = 19.9 \text{ kN.m/m}$</i>		
<i>Total M_u of Slab in the CS; SAP2000 = $\frac{2 \times -8.64 }{2} + 5.42 = 14.1 \text{ kN.m/m}$</i>		
<i>Error = $\frac{19.9 - 14.1}{14.1} \times 100\% = 41.1\% > 25\%$</i>		<i>(Not OK)</i>

Table C.14: Total M_u value of the beam calculated by DDM, SAP2000, and errors

<i>From the Previous Table; Total M_u at the Ends and the Middle of Span (kN.m)</i>		
-190	103	-190
<i>According to Sections 8.10.5.1, and 8.10.5.5 of the ACI 318 – 14 Code; % Moments in the CS = 0.75</i>		
<i>According to Sections 8.10.5.7.1 of the ACI 318 – 14 Code; % Moments of the beam in CS = 0.85</i>		
<i>The Total Factored Static Moment due to the Self – Weight of Web of the Beam is</i>		
$M_o = \frac{w_u \times (l_{n1})^2}{8} = \frac{6.72 \times (5.3)^2}{8} = 23.6 \text{ kN.m}$		
<i>Moment Coefficients of the Interior Span According to Section 8.10.4.2 of the ACI 318 – 14 Code</i>		
0.65	0.35	0.65
<i>M_u at the Ends and the Middle of the Beam (kN.m); DDM</i>		
$(0.75 \times 0.85 \times -190)$ $+ (-0.65 \times 23.6) = -136$	$(0.75 \times 0.85 \times 103)$ $+ (0.35 \times 23.6) = 73.9$	$(0.75 \times 0.85 \times -190)$ $+ (-0.65 \times 23.6) = -136$
<i>M_u at the Ends and the Middle of the Beam (kN.m); M3 – SAP2000</i>		
-122	99.7	-122
<i>Total M_u of the Beam ; DDM = $\frac{2 \times -136 }{2} + 73.9 = 210 \text{ kN.m}$</i>		
<i>Total M_u of the Beam ; SAP2000 = $\frac{2 \times -122 }{2} + 99.7 = 222 \text{ kN.m}$</i>		
<i>Error = $\frac{222 - 210}{210} \times 100\% = 5.71\% \leq 25\%$</i>		<i>(OK)</i>

Table C.15: Total M_u value of the slab in the MS calculated by DDM, SAP2000, and errors

<i>From the Previous Table; Total M_u at the Ends and the Middle of Span (kN.m)</i>		
-190	103	-190
<i>% Moments in MS = 1 - % Moments in MS = 1 - 0.75 = 0.25</i>		
<i>M_u at the Ends and the Middle of the MS (kN.m/m); DDM</i>		
$\frac{0.25 \times -190}{(6-3)} = -15.8$	$\frac{0.25 \times 103}{(6-3)} = 8.58$	$\frac{0.25 \times -190}{(6-3)} = -15.8$
<i>M_u at the and the Middle Ends of the MS (kN.m/m); M11 - SAP2000</i>		
-12.0	10.0	-12.0
<i>Total M_u of the MS; DDM = $\frac{2 \times -15.8 }{2} + 8.58 = 24.4 \text{ kN.m/m}$</i>		
<i>Total M_u of the MS; SAP2000 = $\frac{2 \times -12.0 }{2} + 10.0 = 22.0 \text{ kN.m/m}$</i>		
<i>Error = $\frac{24.4 - 22.0}{22.0} \times 100\% = 10.9\% \leq 25\%$</i>		<i>(OK)</i>

C2.3.2 Column Compressive Force

Table C.16: Maximum expected compressive force acts on the column

Load Pattern	Reference	Ultimate Load Value (kN) in 10-stories
Weight of slabs, beams, columns	Table B.7	2620
Distributed SDL & LL	Table B.8	3600
	Σ	6220
	Global FZ (kN)-SAP2000	5981
	Error %	4.00
	Evaluation of error (max. 10%)	OK

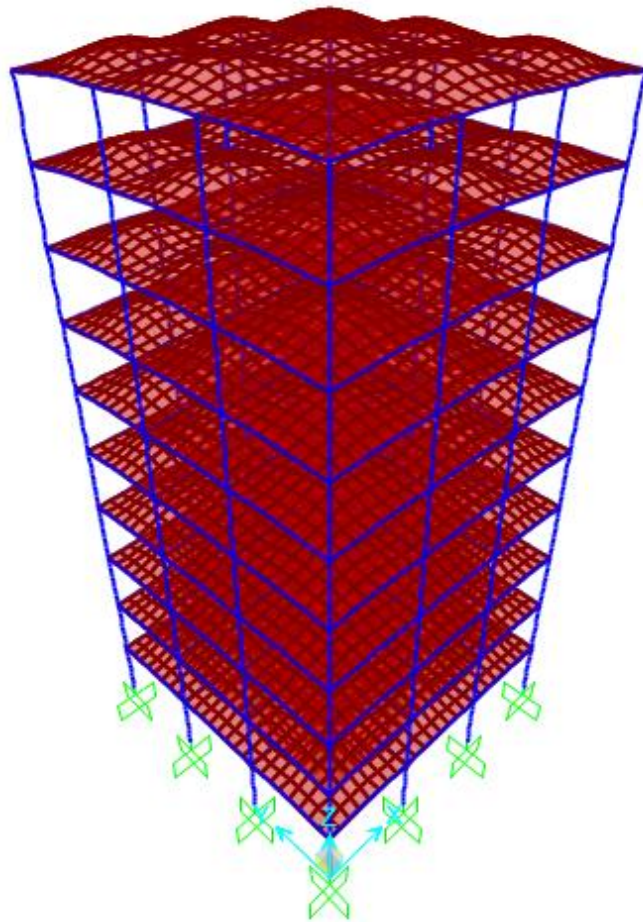
C3 Models 5N-R, 5N-SR, 5N-SS, and 5J-SC**C3.1 Check of Compatibility**

Figure C.3: 3D portal-frame

C3.2 Check of Equilibrium

Table C.17: Check of equilibrium due to self-weights of structural elements

Types of Elements in Single Story	γ_c (kN/m ³)	Dimensions (m)			Mass and Weight Modifier	No. of Elements in Single Story	Weights of Elements (kN) in Single Story
		Length	Width	Depth			
Slab Panels	25	6	6	0.13	1	9	1053
Beam	25	6	0.75	0.5	0.74	24	999
Column	25	3.7	0.75	0.75	0.865	16	720
Σ							2772
Total service weights (kN) of elements for the building (10–Stories)							27720
Global FZ (kN)– SAP2000							27720
Error %							0.00
Evaluation of error (max. 5%)							OK

Table C.18: Check of equilibrium due to the distributed loads over slabs

Load Pattern	Intensity (kN/m ²)	Slab Dimensions (m)		Total Load (kN) on a Single Slab
		Length	Width	
SDL	5	18	18	1620
LL	4	18	18	1296
Total service SDLs (kN) for the building (10–Stories)				16200
Global FZ (kN)– SAP2000				16200
Error %				0.00
Evaluation of error (max. 5%)				OK
Total service LLs (kN) for the building (10–Stories)				12960
Global FZ (kN)– SAP2000				12960
Error %				0.00
Evaluation of error (max. 5%)				OK

C3.3 Check of stress-strain relationship

C3.3.1 DDM

Checking of Adequacy for DDM

Table C.19: DDM limitations and checks

Item	<i>For every direction, there must be at least three continuous spans</i>
Check	<i>There are, exactly, three spans in every direction</i>
Item	<i>For every direction, adjacent spans measured center to center of supports, must not differ by more than one – third the longer span ($l_{short} \geq (2/3) l_{long}$)</i>
Check	<i>All spans are of 6 m long, i.e. $l_{short}/l_{long} = 1 \geq (2/3)$</i>
Item	<i>Panels must be rectangular. The longer span of the panel, measured center to center of supports, must not exceed two times the shorter span ($l_{long}/l_{short} \leq 2$)</i>
Check	<i>All spans are of 6 m long, i.e. $l_{long}/l_{short} = 1 \leq 2$</i>
Item	<i>The largest permitted offset of a column, from the general centerline, is 10% of the span in the direction of offset</i>
Check	<i>Column offsets do not exist</i>
Item	<i>All loads must be only due to gravity, and uniformly distributed over the entire panel. In addition, service live load shall not exceed two times the service dead load</i>
Check	$LL = 4 \text{ kN/m}^2$, $DL = DL_{slab} + SDL = 25 \times 0.13 + 5 = 3.25 + 5 = 8.25 \text{ kN/m}^2$, $LL < DL \Rightarrow LL < 2DL$
Item	<i>For a panel supported by beams in both directions, the relative stiffness of beam in two orthogonal directions must conform to:</i>
	$0.2 \leq \frac{\alpha_{f1} l_1^2}{\alpha_{f2} l_2^2} \leq 5.0 \quad [ACI 318 - 14 \text{ Code, Eq. 8.10.2.7a}]$
Check	$l_1 = l_2 = 6.0\text{m}$ α_f for internal beam = 9.64, α_f for edge beam = 15.1 <i>Whatever the numerator and the denominator, the above equation is satisfied</i>

Analysis of Span (Y2-Y3)

Table C.20: Required data before the analysis through the DDM

$$l_1 = 6.0m$$

$$l_2 = 6.0m$$

$$l_{n1} = 5.25m$$

$$MS\ Width = 6.0m$$

$$CS\ Width = 3.0m$$

$$Effective\ Width\ of\ Beam = 1.49m$$

$$DL\ of\ Slab = 25 \times 0.13 = 3.25\ kN/m^2$$

$$SDL\ on\ Slab = 5kN/m^2$$

$$LL\ on\ Slab = 4\ kN/m^2$$

$$q_u = 1.2 \times (DL + SDL) + 1.6LL = 16.3kN/m^2$$

$$w_{n(Self-weight\ of\ the\ Web\ of\ the\ Beam)} = 6.94kN/m$$

$$w_{u(Self-weight\ of\ the\ Web\ of\ the\ Beam)} = 1.2 \times w_n = 8.33kN/m$$

$$\alpha_{f1} = 9.64$$

$$l_2/l_1 = 1.0$$

$$\alpha_{f1}l_2/l_1 = 9.64$$

Table C.21: Total M_u value of the slab in the CS calculated by DDM, SAP2000, and errors

<i>According to Section 8.10.3.2 of the ACI 318 – 14 Code; the Total Factored Static Moment</i>		
<i>of the Span is $M_o = \frac{q_u \times l_2 \times (l_{n1})^2}{8} = \frac{16.3 \times 6 \times (5.25)^2}{8} = 337 \text{ kN.m}$</i>		
<i>Moment Coefficients of the Interior Span According to Section 8.10.4.2 of the ACI 318 – 14 Code</i>		
-0.65	0.35	-0.65
<i>Total M_u at the Ends and the Middle of the Span (kN.m)</i>		
$-0.65 \times 337 = -219$	$0.35 \times 337 = 118$	$-0.65 \times 337 = -219$
<i>According to Sections 8.10.5.1, and 8.10.5.5 of the ACI 318 – 14 Code; % Moments in CS = 0.75</i>		
<i>According to Sections 8.10.5.7.1 of the ACI 318 – 14 Code; % Moments of Slab in CS = $1 - 0.85 = 0.15$</i>		
<i>M_u at the Ends and the Middle of the Slab in the CS (kN.m/m); DDM</i>		
$\frac{0.75 \times 0.15 \times -219}{(3 - 1.49)} = -16.3$	$\frac{0.75 \times 0.15 \times 118}{(3 - 1.49)} = 8.79$	$\frac{0.75 \times 0.15 \times -219}{(3 - 1.49)} = -16.3$
<i>M_u at the Ends and the Middle of the Slab in the CS (kN.m/m); M11 – SAP2000</i>		
-8.95	6.23	-8.95
<i>Total M_u of Slab in the CS; DDM = $\frac{2 \times -16.3 }{2} + 8.79 = 25.1 \text{ kN.m/m}$</i>		
<i>Total M_u of Slab in the CS; SAP2000 = $\frac{2 \times -8.95 }{2} + 6.23 = 15.2 \text{ kN.m/m}$</i>		
<i>Error = $\frac{25.1 - 15.2}{15.2} \times 100\% = 65.1\% > 25\%$</i>		<i>(Not OK)</i>

Table C.22: Total M_u value of the beam calculated by DDM, SAP2000, and errors

<i>From the Previous Table; Total M_u at the Ends and the Middle of Span (kN.m)</i>		
-219	118	-219
<i>According to Sections 8.10.5.1, and 8.10.5.5 of the ACI 318 – 14 Code; % Moments in the CS = 0.75</i>		
<i>According to Sections 8.10.5.7.1 of the ACI 318 – 14 Code; % Moments of the beam in CS = 0.85</i>		
<i>The Total Factored Static Moment due to the Self – Weight of Web of the Beam is</i>		
$M_o = \frac{w_u \times (l_{n1})^2}{8} = \frac{8.33 \times (5.25)^2}{8} = 28.7 \text{ kN.m}$		
<i>Moment Coefficients of the Interior Span According to Section 8.10.4.2 of the ACI 318 – 14 Code</i>		
0.65	0.35	0.65
<i>M_u at the Ends and the Middle of the Beam (kN.m); DDM</i>		
$(0.75 \times 0.85 \times -219)$ $+ (-0.65 \times 28.7) = -158$	$(0.75 \times 0.85 \times 118)$ $+ (0.35 \times 28.7) = 85.3$	$(0.75 \times 0.85 \times -219)$ $+ (-0.65 \times 28.7) = -158$
<i>M_u at the Ends and the Middle of the Beam (kN.m); M3 – SAP2000</i>		
-142	122	-142
<i>Total M_u of the Beam ; DDM = $\frac{2 \times -158 }{2} + 85.3 = 243 \text{ kN.m}$</i>		
<i>Total M_u of the Beam ; SAP2000 = $\frac{2 \times -142 }{2} + 122 = 264 \text{ kN.m}$</i>		
<i>Error = $\frac{264 - 243}{243} \times 100\% = 8.64\% \leq 25\%$</i>		<i>(OK)</i>

Table C.23: Total M_u value of the slab in the MS calculated by DDM, SAP2000, and errors

<i>From the Previous Table; Total M_u at the Ends and the Middle of Span (kN.m)</i>		
-219	118	-219
$\% \text{ Moments in MS} = 1 - \% \text{ Moments in MS} = 1 - 0.75 = 0.25$		
<i>M_u at the Ends and the Middle of the MS (kN.m/m); DDM</i>		
$\frac{0.25 \times -219}{(6-3)} = -18.3$	$\frac{0.25 \times 118}{(6-3)} = 9.83$	$\frac{0.25 \times -219}{(6-3)} = -18.3$
<i>M_u at the Ends and the Middle of the MS (kN.m/m); M11 – SAP2000</i>		
-13.7	11.4	-13.7
$Total M_u \text{ of the MS; DDM} = \frac{2 \times -18.3 }{2} + 9.83 = 28.1 \text{ kN.m/m}$		
$Total M_u \text{ of the MS; SAP2000} = \frac{2 \times -13.7 }{2} + 11.4 = 25.1 \text{ kN.m/m}$		
$Error = \frac{28.1 - 25.1}{25.1} \times 100\% = 12.0\% \leq 25\%$		(OK)

C3.3.2 Column Compressive Force

Table C.24: Maximum expected compressive force acts on the column

Load Pattern	Reference	Ultimate Load Value (kN) in 10–stories
Weight of slabs, beams, columns	Table B.11	2881
Distributed SDL & LL	Table B.12	4464
	Σ	7345
	Global FZ (kN)–SAP2000	6983
	Error %	5.18
	Evaluation of error (max. 10%)	OK

APPENDIX D
ELASTIC RESPONSE SPECTRUMS OF
PROPOSED SITES

D1 Models 1N-R, 3N-R, and 5N-R

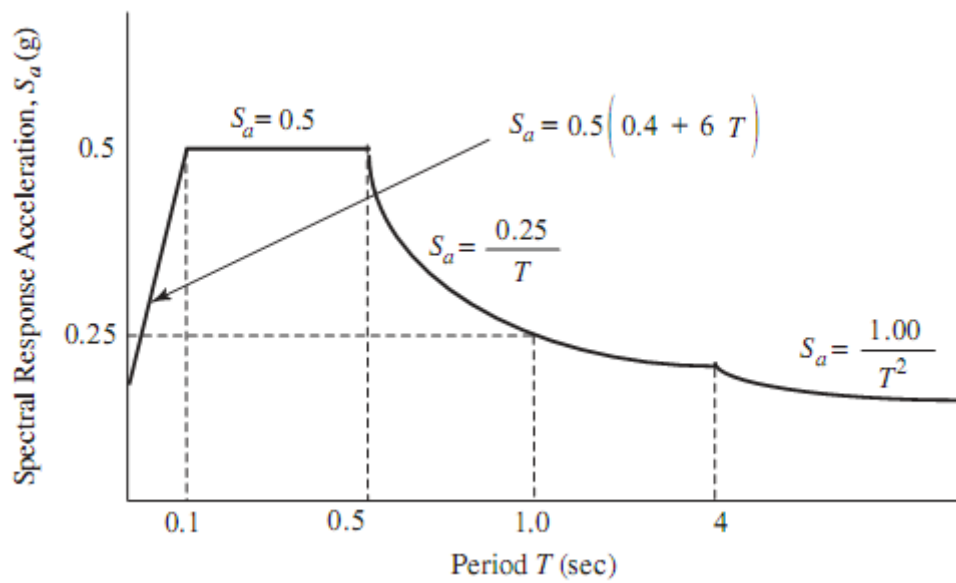


Figure D.1: Elastic response spectrum on rock (Nablus)

D2 Models 1N-SR, 3N-SR, and 5N-SR

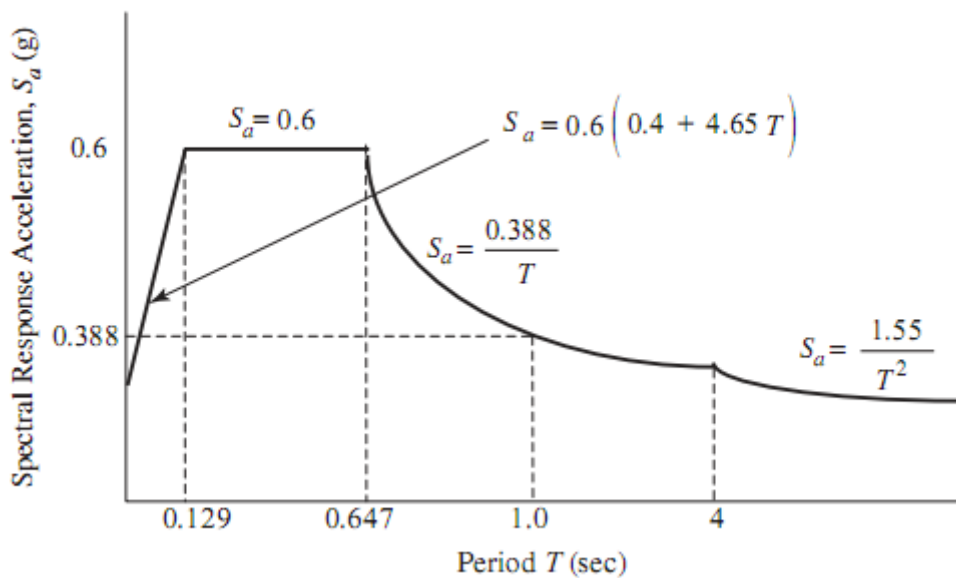


Figure D.2: Elastic response spectrum on soft rock (Nablus)

D3 Models 1N-SS, 3N-SS, and 5N-SS

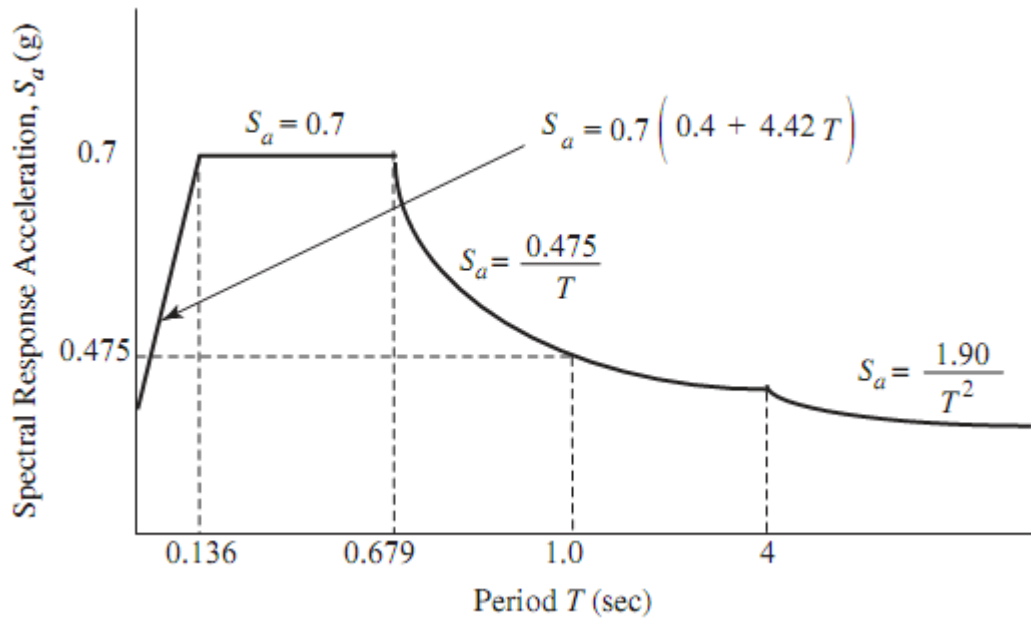


Figure D.3: Elastic response spectrum on stiff soil (Nablus)

D4 Models 1J-SC, 3J-SC, and 5J-SC

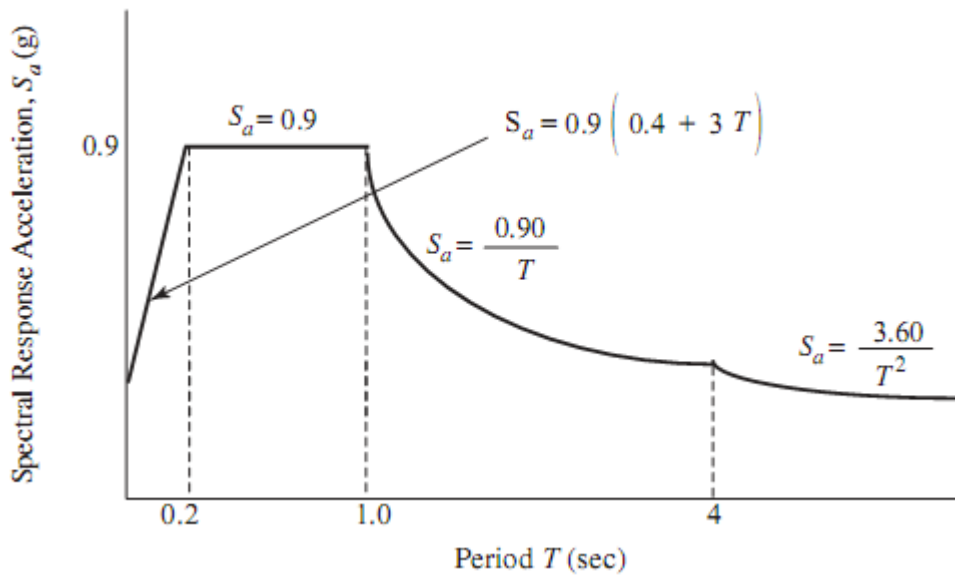


Figure D.4: Elastic response spectrum on soft clay soil (Jericho)

APPENDIX E
ACCUMULATED MODAL MASS PARTICIPATION
RATIOS AS GIVEN BY SAP2000

E1 Models 1N-R, 1N-SR, 1N-SS, and 1J-SC

Table E.1: Modes of vibration and accumulated modal mass participation ratio

OutputCase	StepType	StepNum	Period	UX	UY	UZ	SumUX
Text	Text	Unitless	Sec	Unitless	Unitless	Unitless	Unitless
MODAL	Mode	1	1.49	0.790	0.00	0.00	0.790
MODAL	Mode	2	1.49	0.00	0.790	0.00	0.790
MODAL	Mode	3	1.22	0.00	0.00	0.00	0.790
MODAL	Mode	4	0.469	0.102	0.000	0.000	0.892
MODAL	Mode	5	0.469	0.000	0.102	0.000	0.892
MODAL	Mode	6	0.387	0.000	0.000	0.000	0.892
MODAL	Mode	7	0.256	0.041	0.000	0.000	0.933
MODAL	Mode	8	0.256	0.000	0.041	0.000	0.933
MODAL	Mode	9	0.214	0.000	0.000	0.000	0.933
MODAL	Mode	10	0.165	0.003	0.021	0.000	0.937
MODAL	Mode	11	0.165	0.021	0.003	0.000	0.957
MODAL	Mode	12	0.138	0.000	0.000	0.000	0.957

E2 Models 3N-R, 3N-SR, 3N-SS, and 3J-SC

Table E.2: Modes of vibration and accumulated modal mass participation ratio

OutputCase	StepType	StepNum	Period	UX	UY	UZ	SumUX
Text	Text	Unitless	Sec	Unitless	Unitless	Unitless	Unitless
MODAL	Mode	1	1.54	0.791	0.001	0.000	0.791
MODAL	Mode	2	1.54	0.001	0.791	0.000	0.792
MODAL	Mode	3	1.24	0.000	0.000	0.000	0.792
MODAL	Mode	4	0.487	0.102	0.000	0.000	0.894
MODAL	Mode	5	0.487	0.000	0.102	0.000	0.894
MODAL	Mode	6	0.394	0.000	0.000	0.000	0.894
MODAL	Mode	7	0.267	0.037	0.004	0.000	0.931
MODAL	Mode	8	0.267	0.004	0.037	0.000	0.935
MODAL	Mode	9	0.219	0.000	0.000	0.000	0.935
MODAL	Mode	10	0.173	0.023	0.000	0.000	0.958
MODAL	Mode	11	0.173	0.000	0.023	0.000	0.958
MODAL	Mode	12	0.143	0.000	0.000	0.000	0.958

E3 Models 5N-R, 5N-SR, 5N-SS, and 5J-SC

Table E.3: Modes of vibration and accumulated modal mass participation ratio

OutputCase	StepType	StepNum	Period	UX	UY	UZ	SumUX
Text	Text	Unitless	Sec	Unitless	Unitless	Unitless	Unitless
MODAL	Mode	1	1.55	0.793	0.001	0.000	0.793
MODAL	Mode	2	1.55	0.001	0.793	0.000	0.793
MODAL	Mode	3	1.23	0.000	0.000	0.000	0.793
MODAL	Mode	4	0.493	0.102	0.000	0.000	0.896
MODAL	Mode	5	0.493	0.000	0.102	0.000	0.896
MODAL	Mode	6	0.394	0.000	0.000	0.000	0.896
MODAL	Mode	7	0.272	0.040	0.000	0.000	0.936
MODAL	Mode	8	0.272	0.000	0.040	0.000	0.936
MODAL	Mode	9	0.221	0.000	0.000	0.000	0.936
MODAL	Mode	10	0.177	0.023	0.000	0.000	0.959
MODAL	Mode	11	0.177	0.000	0.023	0.000	0.959
MODAL	Mode	12	0.152	0.000	0.000	0.675	0.959

APPENDIX F
SUBSTANTIATION OF FUNDAMENTAL PERIODS
AND EFFECTIVE MODAL MASS RATIOS

F1 Models 1N-R, 1N-SR, 1N-SS, and 1J-SC

F1.1 Determination of the components of seismic weight

Table F.1: Seismic DL

Types of Elements in Single Story	γ_c (kN/m ³)	Dimensions (m)			Mass and Weight Modifier	No. of Elements in Single Story	Weights of Elements (kN) in Single Story
		Length	Width	Depth			
Slab Panels	25	6	6	0.13	1	9	1053
Beams	25	6	0.65	0.4	0.675	24	632
Columns	25	3.4	0.65	0.65	0.882	16	507
Seismic DL (kN) of 10 th -Story							1938
Seismic DL (kN) of any other story							2192
Total seismic DL (kN) of structural elements for the entire building (10-Stories)							21665

Table F.2: Seismic SDL

Load Pattern	Intensity (kN/m ²)	Slab Dimensions (m)		Total Load (kN) on a Single Slab
		Length	Width	
SDL	1	18	18	324
Seismic SDL (kN) of any story				324
Total seismic SDL (kN) for the building (10-Stories)				3240

F1.2 Determination of fundamental period- Rayleigh's method

Table F.3: Check of the fundamental period

<i>Level</i>	w_i (kN)	p_i (kN/m ²) ^a	<i>floor Area</i> (m ²)	P_i (kN)	δ_i (m) ^b	$w_i \delta_i^2$ (kN.m ²)	$P_i \delta_i$ (kN.m)
10	2262	10	324	3240	0.907	1862	2939
9	2516	10	324	3240	0.879	1943	2847
8	2516	10	324	3240	0.835	1755	2706
7	2516	10	324	3240	0.774	1507	2507
6	2516	10	324	3240	0.694	1213	2250
5	2516	10	324	3240	0.596	895	1932
4	2516	10	324	3240	0.481	581	1557
3	2516	10	324	3240	0.349	306	1131
2	2516	10	324	3240	0.207	108	672
1	2516	10	324	3240	0.0733	13.5	237
Σ						10183	18779
T_1 (sec) – Rayleigh						1.48	
T_1 (sec) – SAP2000						1.49	
<i>Error %</i>						0.598	
<i>Evaluation of error %^c</i>						OK	

^a These values of static distributed loads were randomly chosen by the author, and were assigned in the +X-Direction

^b These are equivalent to U1 given by SAP2000 at the center of mass of each diaphragm

^c Acceptance level of error is 10%

F1.3 Important matrices

Matrix F.1: Modal matrix

Level	$U_1(mm)^*$			Modal Matrix $[\Phi]$		
	Mode # 1	Mode # 4	Mode # 7	ϕ_1	ϕ_4	ϕ_7
10	29.0	-29.3	-28.4	1	1	1
9	27.9	-21.2	-8.96	0.964	0.722	0.316
8	26.3	-9.57	12.5	0.908	0.326	-0.442
7	24.0	3.76	25.9	0.830	-0.128	-0.912
6	21.2	16.1	23.7	0.731	-0.549	-0.837
5	17.8	24.8	7.59	0.614	-0.845	-0.268
4	13.9	27.8	-13.1	0.481	-0.949	0.462
3	9.81	24.7	-26.3	0.339	-0.843	0.926
2	5.64	16.5	-24.6	0.195	-0.562	0.869
1	1.92	6.14	-10.9	0.0663	-0.209	0.385

* These are horizontal but not real displacements read at the center of mass of each diaphragm, and were recovered by SAP2000 analysis of a load case known as Modal

Matrix F.2: Mass matrix

$$m = \begin{bmatrix} 230755 & 0.00 & 0.00 & 0.00 & 0.00 & 0.00 & 0.00 & 0.00 & 0.00 & 0.00 \\ & 256612 & 0.00 & 0.00 & 0.00 & 0.00 & 0.00 & 0.00 & 0.00 & 0.00 \\ & & 256612 & 0.00 & 0.00 & 0.00 & 0.00 & 0.00 & 0.00 & 0.00 \\ & & & 256612 & 0.00 & 0.00 & 0.00 & 0.00 & 0.00 & 0.00 \\ & & & & 256612 & 0.00 & 0.00 & 0.00 & 0.00 & 0.00 \\ & & & & & 256612 & 0.00 & 0.00 & 0.00 & 0.00 \\ & & & & & & 256612 & 0.00 & 0.00 & 0.00 \\ & & & & & & & 256612 & 0.00 & 0.00 \\ & & & & & & & & 256612 & 0.00 \\ & & & & & & & & & 256612 \end{bmatrix} kg$$

SYMM.

Matrix F.3: Influence vector

$$l = \begin{bmatrix} 1 \\ 1 \\ 1 \\ 1 \\ 1 \\ 1 \\ 1 \\ 1 \\ 1 \\ 1 \\ 1 \end{bmatrix}$$

F1.4 Determination of the effective modal mass participation ratios

Table F.4: Check of the modal mass participation ratios

	$L_n^h (kg)$	$M_n (kg)$	Γ_n	$M_n^* (kg)$	M_n^* Ratio		Error				
					Calculated	SAP2000	Error %	Level ^a			
L_1^h	1.55E+06	M_1	1.19E+06	Γ_1	1.30	M_1^*	2.01E+06	0.791	0.790	0.0470	OK
L_4^h	-5.49E+05	M_4	1.16E+06	Γ_4	-0.472	M_4^*	2.59E+05	0.102	0.102	0.177	OK
L_7^h	3.59E+05	M_7	1.22E+06	Γ_7	0.293	M_7^*	1.05E+05	0.0414	0.0408	1.55	OK

^a Acceptance level of error is 10%

F2 Models 3N-R, 3N-SR, 3N-SS, and 3J-SC

F2.1 Determination of the components of seismic weight

Table F.5: Seismic DL

Types of Elements in Single Story	γ_c (kN/m ³)	Dimensions (m)			Mass and Weight Modifier	No. of Elements in Single Story	Weights of Elements (kN) in Single Story
		Length	Width	Depth			
Slab Panels	25	6	6	0.13	1	9	1053
Beams	25	6	0.7	0.45	0.711	24	806
Columns	25	3.55	0.7	0.7	0.873	16	608
Seismic DL (kN) of 10 th -Story							2163
Seismic DL (kN) of any other story							2467
Total seismic DL (kN) of structural elements for the entire building (10-Stories)							24366

Table F.6: Seismic SDL

Load Pattern	Intensity (kN/m ²)	Slab Dimensions (m)		Total Load (kN) on a Single Slab
		Length	Width	
SDL	3	18	18	972
Seismic SDL (kN) of any story				972
Total seismic SDL (kN) for the building (10-Stories)				9720

F2.2 Determination of fundamental period- Rayleigh's method

Table F.7: Check of the fundamental period

<i>Level</i>	w_i (kN)	p_i (kN/m ²) ^a	<i>floor Area</i> (m ²)	P_i (kN)	δ_i (m) ^b	$w_i \delta_i^2$ (kN.m ²)	$P_i \delta_i$ (kN.m)
10	3135	10	324	3240	0.707	1566	2290
9	3439	10	324	3240	0.685	1613	2219
8	3439	10	324	3240	0.651	1456	2108
7	3439	10	324	3240	0.603	1250	1954
6	3439	10	324	3240	0.541	1008	1754
5	3439	10	324	3240	0.466	745	1508
4	3439	10	324	3240	0.376	486	1219
3	3439	10	324	3240	0.274	259	889
2	3439	10	324	3240	0.164	92.7	532
1	3439	10	324	3240	0.0587	11.8	190
Σ						8488	14662
T_1 (sec) – Rayleigh						1.53	
T_1 (sec) – SAP2000						1.54	
<i>Error</i> %						0.608	
<i>Evaluation of error</i> % ^c						OK	

^a These values of static distributed loads were randomly chosen by the author, and were assigned in the +X-Direction

^b These are equivalent to U1 given by SAP2000 at the center of mass of each diaphragm

^c Acceptance level of error is 10%

Matrix F.6: Influence vector

$$l = \begin{bmatrix} 1 \\ 1 \\ 1 \\ 1 \\ 1 \\ 1 \\ 1 \\ 1 \\ 1 \\ 1 \\ 1 \end{bmatrix}$$

F2.4 Determination of the effective modal mass participation ratios

Table F.8: Check of the modal mass participation ratios

	$L_n^h (kg)$	$M_n (kg)$	Γ_n	$M_n^* (kg)$	M_n^* Ratio		Error				
					Calculated	SAP2000	Error %	Level ^a			
L_1^h	2.12E+06	M_1	1.63E+06	Γ_1	1.30	M_1^*	2.75E+06	0.792	0.791	0.0930	OK
L_4^h	-7.57E+05	M_4	1.62E+06	Γ_4	-0.469	M_4^*	3.55E+05	0.102	0.102	0.147	OK
L_7^h	4.94E+05	M_7	1.71E+06	Γ_7	0.288	M_7^*	1.42E+05	0.0409	0.0366	11.6	Not OK

^a Acceptance level of error is 10%

F3 Models 5N-R, 5N-SR, 5N-SS, and 5J-SC

F3.1 Determination of the components of seismic weight

Table F.9: Seismic DL

Types of Elements in Single Story	γ_c (kN/m ³)	Dimensions (m)			Mass and Weight Modifier	No. of Elements in Single Story	Weights of Elements (kN) in Single Story
		Length	Width	Depth			
Slab Panels	25	6	6	0.13	1	9	1053
Beam	25	6	0.75	0.5	0.74	24	999
Column	25	3.7	0.75	0.75	0.865	16	720
Seismic DL (kN) of 10 th -Story							2412
Seismic DL (kN) of any other story							2772
Total seismic DL (kN) of structural elements for the entire building (10-Stories)							27360

Table F.10: Seismic SDL

Load Pattern	Intensity (kN/m ²)	Slab Dimensions (m)		Total Load (kN) on a Single Slab
		Length	Width	
SDL	5	18	18	1620
Seismic SDL (kN) of any story				1620
Total seismic SDL (kN) for the building (10-Stories)				16200

F3.2 Determination of fundamental period- Rayleigh's method

Table F.11: Check of the fundamental period

<i>Level</i>	w_i (kN)	p_i (kN/m ²) ^a	<i>floor Area</i> (m ²)	P_i (kN)	δ_i (m) ^b	$w_i \delta_i^2$ (kN.m ²)	$P_i \delta_i$ (kN.m)
10	3135	10	324	3240	0.707	1566	2290
9	3439	10	324	3240	0.685	1613	2219
8	3439	10	324	3240	0.651	1456	2108
7	3439	10	324	3240	0.603	1250	1954
6	3439	10	324	3240	0.541	1008	1754
5	3439	10	324	3240	0.466	745	1508
4	3439	10	324	3240	0.376	486	1219
3	3439	10	324	3240	0.274	259	889
2	3439	10	324	3240	0.164	92.7	532
1	3439	10	324	3240	0.0587	11.8	190
Σ						8488	14662
T_1 (sec) – Rayleigh						1.53	
T_1 (sec) – SAP2000						1.54	
<i>Error %</i>						0.608	
<i>Evaluation of error %^c</i>						OK	

^a These values of static distributed loads were randomly chosen by the author, and were assigned in the +X-Direction

^b These are equivalent to U1 given by SAP2000 at the center of mass of each diaphragm

^c Acceptance level of error is 10%

F3.3 Important matrices

Matrix F.7: Modal matrix

Level	$U_1(mm)^*$			Modal Matrix $[\Phi]$		
	Mode # 1	Mode # 4	Mode # 7	ϕ_1	ϕ_4	ϕ_7
10	21.9	21.9	21.0	1	1	1
9	21.1	15.9	6.91	0.963	0.727	0.328
8	19.8	7.27	-9.25	0.907	0.333	-0.439
7	18.1	-2.72	-19.5	0.829	-0.124	-0.927
6	16.0	-12.0	-18.2	0.731	-0.550	-0.866
5	13.4	-18.6	-6.22	0.615	-0.851	-0.296
4	10.6	-21.0	9.48	0.484	-0.963	0.450
3	7.50	-18.9	19.8	0.343	-0.863	0.939
2	4.36	-12.7	18.9	0.200	-0.583	0.897
1	1.52	-4.87	8.56	0.070	-0.223	0.407

* These are horizontal but not real displacements read at the center of mass of each diaphragm, and were recovered by SAP2000 analysis of a load case known as Modal

Matrix F.8: Mass matrix

$$m = \begin{bmatrix} 411264 & 0.00 & 0.00 & 0.00 & 0.00 & 0.00 & 0.00 & 0.00 & 0.00 & 0.00 \\ & 447984 & 0.00 & 0.00 & 0.00 & 0.00 & 0.00 & 0.00 & 0.00 & 0.00 \\ & & 447984 & 0.00 & 0.00 & 0.00 & 0.00 & 0.00 & 0.00 & 0.00 \\ & & & 447984 & 0.00 & 0.00 & 0.00 & 0.00 & 0.00 & 0.00 \\ & & & & 447984 & 0.00 & 0.00 & 0.00 & 0.00 & 0.00 \\ & & & & & 447984 & 0.00 & 0.00 & 0.00 & 0.00 \\ & & & & & & 447984 & 0.00 & 0.00 & 0.00 \\ & & & & & & & 447984 & 0.00 & 0.00 \\ & & & & & & & & 447984 & 0.00 \\ & & & & & & & & & 447984 \end{bmatrix} kg$$

SYMM.

Matrix F.9: Influence vector

$$l = \begin{bmatrix} 1 \\ 1 \\ 1 \\ 1 \\ 1 \\ 1 \\ 1 \\ 1 \\ 1 \\ 1 \end{bmatrix}$$

F2.4 Determination of the effective modal mass participation ratios

Table F.12: Check of the modal mass participation ratios

	$L_n^h (kg)$	$M_n (kg)$	Γ_n	$M_n^* (kg)$	M_n^* Ratio		Error				
					Calculated	SAP2000	Error %	Level ^a			
L_1^h	2.71E+06	M_1	2.09E+06	Γ_1	1.30	M_1^*	3.53E+06	0.794	0.793	0.1041	OK
L_4^h	-9.76E+05	M_4	2.09E+06	Γ_4	-0.467	M_4^*	4.56E+05	0.103	0.102	0.264	OK
L_7^h	6.32E+05	M_7	2.23E+06	Γ_7	0.284	M_7^*	1.79E+05	0.0403	0.0398	1.46	OK

^a Acceptance level of error is 10%

APPENDIX G

**VERIFICATION OF THE TOTAL DISPLACEMENT
OF STORIES, STORY SHEARS, AND BASE
OVERTURNING MOMENTS**

G1 Models 1N-R, 3N-R, and 5N-R

G1.1 Model 1N-R

Table G.1: Maximum lateral deflections of the generalized SDF systems

Mode No.	$T_n(sec)^a$	$\omega_n(rad/sec)$	$S_a(g)^b$	$D_n(mm)$
1	1.49	4.23	0.168	92.3
4	0.469	13.4	0.500	27.3
7	0.256	24.5	0.500	8.15

^a Natural periods are obtained by SAP2000 analysis. Refer to Table E.1

^b Spectral accelerations are gained from the acceleration response spectrum shown in Figure D.1

Table G.2: Modal displacements and the maximum expected displacements of floors

Story	$u_n(mm)$			$U_x(mm)$	$U1(mm)^a$	Error	
	u_1	u_4	u_7	SRSS	SAP2000	Error %	Level ^b
10	120	-12.9	2.39	121	121	0.466	Accepted
9	116	-9.31	0.754	116	116	0.469	Accepted
8	109	-4.21	-1.06	109	109	0.473	Accepted
7	99.5	1.66	-2.18	99.5	100	0.472	Accepted
6	87.6	7.09	-2.00	87.9	88.3	0.468	Accepted
5	73.5	10.9	-0.639	74.3	74.7	0.463	Accepted
4	57.7	12.2	1.10	59.0	59.2	0.449	Accepted
3	40.6	10.9	2.21	42.1	42.3	0.431	Accepted
2	23.3	7.25	2.07	24.5	24.6	0.442	Accepted
1	7.95	2.70	0.919	8.4	8.5	0.490	Accepted

^a These horizontal displacements are read at the center of mass of each diaphragm, and were due to the effect of an earthquake ground acceleration (Acceleration Response Spectrum) in the X-Direction

^b Acceptance level of error is 10%

Table G.3: The generalized shear forces and the resulted story shears

Story	f_n (kN)			V_n (kN)			V_x (kN)		Error	
	f_1	f_4	f_7	V_1	V_4	V_7	SRSS	SAP2000 ^a	Error %	Level ^b
10	494	-534	332	494	-534	332	800	823	2.87	OK
9	530	-429	116	1024	-963	448	1476	1483	0.502	OK
8	499	-194	-163	1523	-1157	285	1934	1938	0.182	OK
7	456	76.3	-336	1980	-1081	-51.2	2256	2272	0.712	OK
6	402	327	-309	2381	-754	-360	2524	2534	0.415	OK
5	337	502	-99	2719	-253	-459	2769	2778	0.333	OK
4	264	564	170	2983	311	-288	3013	3031	0.599	OK
3	186	501	342	3169	812	53.3	3272	3284	0.353	OK
2	107	334	320	3276	1146	374	3491	3502	0.303	OK
1	36.5	124	142	3313	1271	516	3585	3604	0.507	OK

^a These are elastic story shears generated within the columns of each story due to the effect of an earthquake ground acceleration (Acceleration Response Spectrum) in the X-Direction

^b Acceptance level of error is 10%

Table G.4: The generalized and resultant base overturning moments

Story	h_x (m)	f_n (kN)			M_{no} (kN.m)		
		f_1	f_4	f_7	M_{1o}	M_{4o}	M_{7o}
10	34	494	-534	332	16808	-18170	11276
9	30.6	530	-429	116	16213	-13123	3564
8	27.2	499	-194	-163	13575	-5276	-4437
7	23.8	456	76.3	-336	10858	1816	-8002
6	20.4	402	327	-309	8198	6661	-6298
5	17	337	502	-99	5734	8532	-1678
4	13.6	264	564	170	3597	7670	2316
3	10.2	186	501	342	1899	5109	3485
2	6.8	107	334	320	727	2270	2179
1	3.4	36.5	124	142	124	423	483
M_{bo} (kN.m)					77734	-4088	2889
M_b (kN.m) – SRSS					77895		
M_b (kN.m) – SAP2000					78291		
Error %					0.509		
Check of Error*					OK		

* Acceptance level of error is 10%

G1.2 Model 3N-R

Table G.5: Maximum lateral deflections of the generalized SDF systems

Mode No.	$T_n(sec)^a$	$\omega_n(rad/sec)$	$S_a(g)^b$	$D_n(mm)$
1	1.54	4.09	0.163	95.4
4	0.487	12.9	0.500	29.4
7	0.267	23.5	0.500	8.86

^a Natural periods are obtained by SAP2000 analysis. Refer to Table E.2

^b Spectral accelerations are gained from the acceleration response spectrum shown in Figure D.1

Table G.6: Modal displacements and the maximum expected displacements of floors

Story	$u_n(mm)$			$U_x(mm)$	$U1(mm)^a$	Error	
	u_1	u_4	u_7	SRSS	SAP2000	Error %	Level ^b
10	124	-13.8	2.55	125	125	0.369	Accepted
9	119	-10.0	0.824	120	120	0.351	Accepted
8	112	-4.54	-1.13	112	113	0.377	Accepted
7	103	1.75	-2.35	103	103	0.373	Accepted
6	90.5	7.59	-2.18	90.9	91.2	0.369	Accepted
5	76.1	11.7	-0.719	77.0	77.2	0.370	Accepted
4	59.8	13.2	1.16	61.2	61.4	0.354	Accepted
3	42.2	11.8	2.38	43.9	44.1	0.318	Accepted
2	24.4	7.90	2.25	25.8	25.9	0.305	Accepted
1	8.43	2.98	1.01	9.00	9.03	0.338	Accepted

^a These horizontal displacements are read at the center of mass of each diaphragm, and were due to the effect of an earthquake ground acceleration (Acceleration Response Spectrum) in the X-Direction

^b Acceptance level of error is 10%

Table G.7: The generalized shear forces and the resulted story shears

Story	f_n (kN)			V_n (kN)			V_x (kN)		Error	
	f_1	f_4	f_7	V_1	V_4	V_7	SRSS	SAP2000 ^a	Error %	Level ^b
10	663	-735	452	663	-735	452	1088	1113	2.30	OK
9	701	-585	160	1364	-1321	612	1994	1991	0.149	OK
8	660	-266	-219	2024	-1586	392	2601	2599	0.0629	OK
7	603	102	-456	2627	-1484	-64	3018	3040	0.749	OK
6	532	444	-423	3158	-1040	-486	3361	3368	0.216	OK
5	447	685	-140	3605	-356	-626	3676	3678	0.0483	OK
4	351	772	226	3956	416	-400	3998	4019	0.526	OK
3	248	689	463	4204	1105	63	4347	4360	0.298	OK
2	143	462	438	4348	1567	501	4649	4656	0.163	OK
1	49.5	174	196	4397	1742	697	4781	4795	0.301	OK

^a These are elastic story shears generated within the columns of each story due to the effect of an earthquake ground acceleration (Acceleration Response Spectrum) in the X-Direction

^b Acceptance level of error is 10%

Table G.8: The generalized and resultant base overturning moments

Story	h_x (m)	f_n (kN)			M_{no} (kN.m)		
		f_1	f_4	f_7	M_{1o}	M_{4o}	M_{7o}
10	35.5	663	-735	452	23531	-26106	16031
9	31.95	701	-585	160	22390	-18699	5114
8	28.4	660	-266	-219	18741	-7548	-6223
7	24.85	603	102	-456	14991	2541	-11341
6	21.3	532	444	-423	11323	9454	-9001
5	17.75	447	685	-140	7929	12153	-2480
4	14.2	351	772	226	4985	10961	3214
3	10.65	248	689	463	2642	7335	4928
2	7.1	143	462	438	1019	3283	3110
1	3.55	49.5	174	196	176	619	697
M_{bo} (kN.m)					107727	-6006	4047
M_b (kN.m) – SRSS					107970		
M_b (kN.m) – SAP2000					108441		
Error %					0.436		
Check of Error*					OK		

* Acceptance level of error is 10%

G1.3 Model 5N-R

Table G.9: Maximum lateral deflections of the generalized SDF systems

Mode No.	$T_n(sec)^a$	$\omega_n(rad/sec)$	$S_a(g)^b$	$D_n(mm)$
1	1.55	4.05	0.161	96.3
4	0.493	12.8	0.500	30.1
7	0.272	23.2	0.500	9.15

^a Natural periods are obtained by SAP2000 analysis. Refer to Table E.3

^b Spectral accelerations are gained from the acceleration response spectrum shown in Figure D.1

Table G.10: Modal displacements and the maximum expected displacements of floors

Story	$u_n(mm)$			$U_x(mm)$	$U1(mm)^a$	Error	
	u_1	u_4	u_7	SRSS	SAP2000	Error %	Level ^b
10	125	-14.1	2.60	126	126	0.303	Accepted
9	120	-10.2	0.853	121	121	0.304	Accepted
8	113	-4.69	-1.14	114	114	0.309	Accepted
7	104	1.75	-2.41	104	104	0.308	Accepted
6	91.4	7.75	-2.25	91.7	92.0	0.304	Accepted
5	76.8	12.0	-0.768	77.8	78.0	0.301	Accepted
4	60.5	13.6	1.17	62.0	62.2	0.287	Accepted
3	42.9	12.2	2.44	44.6	44.8	0.270	Accepted
2	25.0	8.22	2.33	26.4	26.5	0.296	Accepted
1	8.71	3.14	1.06	9.32	9.35	0.372	Accepted

^a These horizontal displacements are read at the center of mass of each diaphragm, and were due to the effect of an earthquake ground acceleration (Acceleration Response Spectrum) in the X-Direction

^b Acceptance level of error is 10%

Table G.11: The generalized shear forces and the resulted story shears

Story	f_n (kN)			V_n (kN)			V_x (kN)		Error	
	f_1	f_4	f_7	V_1	V_4	V_7	SRSS	SAP2000 ^a	Error %	Level ^b
10	845	-943	572	845	-943	572	1390	1440	3.61	OK
9	887	-747	205	1732	-1690	777	2541	2556	0.556	OK
8	835	-342	-274	2566	-2032	503	3312	3313	0.0478	OK
7	763	128	-578	3330	-1904	-75	3836	3864	0.719	OK
6	673	565	-540	4002	-1339	-615	4265	4278	0.311	OK
5	566	874	-184	4568	-465	-799	4660	4669	0.176	OK
4	445	989	281	5013	524	-519	5067	5094	0.534	OK
3	316	886	585	5329	1410	66.5	5512	5526	0.252	OK
2	184	599	559	5512	2009	626	5900	5911	0.175	OK
1	64.1	229	253	5576	2238	879	6073	6099	0.427	OK

^a These are elastic story shears generated within the columns of each story due to the effect of an earthquake ground acceleration (Acceleration Response Spectrum) in the X-Direction

^b Acceptance level of error is 10%

Table G.12: The generalized and resultant base overturning moments

Story	h_x (m)	f_n (kN)			M_{no} (kN.m)		
		f_1	f_4	f_7	M_{1o}	M_{4o}	M_{7o}
10	37	845	-943	572	31262	-34891	21177
9	33.3	887	-747	205	29528	-24878	6818
8	29.6	835	-342	-274	24711	-10113	-8110
7	25.9	763	128	-578	19763	3311	-14973
6	22.2	673	565	-540	14930	12537	-11989
5	18.5	566	874	-184	10463	16173	-3411
4	14.8	445	989	281	6590	14637	4155
3	11.1	316	886	585	3504	9837	6495
2	7.4	184	599	559	1359	4433	4138
1	3.7	64.1	229	253	237	846	938
M_{bo} (kN.m)					142348	-8108	5239
M_b (kN.m) – SRSS					142675		
M_b (kN.m) – SAP2000					143280		
Error %					0.424		
Check of Error*					OK		

* Acceptance level of error is 10%

G2 Models 1N-SR, 3N-SR, and 5N-SR

G2.1 Model 1N-SR

Table G.13: Maximum lateral deflections of the generalized SDF systems

Mode No.	$T_n(sec)^a$	$\omega_n(rad/sec)$	$S_a(g)^b$	$D_n(mm)$
1	1.49	4.23	0.261	143
4	0.469	13.4	0.600	32.8
7	0.256	24.5	0.600	9.78

^a Natural periods are obtained by SAP2000 analysis. Refer to Table E.1

^b Spectral accelerations are gained from the acceleration response spectrum shown in Figure D.2

Table G.14: Modal displacements and the maximum expected displacements of floors

Story	$u_n(mm)$			$U_x(mm)$	$U1(mm)^a$	Error	
	u_1	u_4	u_7	SRSS	SAP2000	Error %	Level ^b
10	186	-15.5	2.86	186	187	0.465	Accepted
9	179	-11.2	0.905	179	180	0.467	Accepted
8	169	-5.05	-1.27	169	170	0.469	Accepted
7	154	1.99	-2.61	154	155	0.469	Accepted
6	136	8.51	-2.40	136	137	0.466	Accepted
5	114	13.1	-0.767	115	115	0.463	Accepted
4	89.4	14.7	1.32	90.6	91.0	0.455	Accepted
3	62.9	13.1	2.65	64.3	64.6	0.443	Accepted
2	36.1	8.70	2.49	37.3	37.4	0.450	Accepted
1	12.3	3.24	1.10	12.8	12.8	0.481	Accepted

^a These horizontal displacements are read at the center of mass of each diaphragm, and were due to the effect of an earthquake ground acceleration (Acceleration Response Spectrum) in the X-Direction

^b Acceptance level of error is 10%

Table G.15: The generalized shear forces and the resulted story shears

Story	f_n (kN)			V_n (kN)			V_x (kN)		Error	
	f_1	f_4	f_7	V_1	V_4	V_7	SRSS	SAP2000 ^a	Error %	Level ^b
10	766	-641	398	766	-641	398	1076	1101	2.36	OK
9	821	-515	140	1587	-1156	538	2036	2045	0.448	OK
8	774	-233	-196	2361	-1389	342	2760	2766	0.200	OK
7	707	91.6	-403	3068	-1297	-61.4	3332	3351	0.584	OK
6	623	392	-370	3691	-905	-432	3825	3840	0.391	OK
5	523	602	-118	4214	-303	-550	4260	4275	0.343	OK
4	410	677	204	4624	374	-346	4652	4675	0.497	OK
3	289	601	410	4913	975	64	5009	5028	0.378	OK
2	166	401	385	5078	1375	449	5280	5299	0.345	OK
1	56.5	149	170	5135	1525	619	5392	5417	0.465	OK

^a These are elastic story shears generated within the columns of each story due to the effect of an earthquake ground acceleration (Acceleration Response Spectrum) in the X-Direction

^b Acceptance level of error is 10%

Table G.16: The generalized and resultant base overturning moments

Story	h_x (m)	f_n (kN)			M_{no} (kN.m)		
		f_1	f_4	f_7	M_{1o}	M_{4o}	M_{7o}
10	34	766	-641	398	26052	-21804	13531
9	30.6	821	-515	140	25131	-15748	4277
8	27.2	774	-233	-196	21041	-6331	-5325
7	23.8	707	91.6	-403	16831	2180	-9602
6	20.4	623	392	-370	12707	7993	-7557
5	17.0	523	602	-118	8888	10239	-2013
4	13.6	410	677	204	5576	9204	2780
3	10.2	289	601	410	2944	6130	4182
2	6.80	166	401	385	1127	2725	2615
1	3.40	56.5	149	170	192	508	579
M_{bo} (kN.m)					120488	-4905	3466
M_b (kN.m) – SRSS					120637		
M_b (kN.m) – SAP2000					121234		
Error %					0.495		
Check of Error*					OK		

* Acceptance level of error is 10%

G2.2 Model 3N-SR

Table G.17: Maximum lateral deflections of the generalized SDF systems

Mode No.	$T_n(sec)^a$	$\omega_n(rad/sec)$	$S_a(g)^b$	$D_n(mm)$
1	1.54	4.09	0.252	148
4	0.487	12.9	0.600	35.3
7	0.267	23.5	0.600	10.6

^a Natural periods are obtained by SAP2000 analysis. Refer to Table E.2

^b Spectral accelerations are gained from the acceleration response spectrum shown in Figure D.2

Table G.18: Modal displacements and the maximum expected displacements of floors

Story	$u_n(mm)$			$U_x(mm)$	$U1(mm)^a$	Error	
	u_1	u_4	u_7	SRSS	SAP2000	Error %	Level ^b
10	192	-16.5	3.06	193	193	0.368	Accepted
9	185	-12.0	0.989	185	186	0.349	Accepted
8	174	-5.45	-1.35	174	175	0.374	Accepted
7	159	2.10	-2.82	159	160	0.371	Accepted
6	140	9.10	-2.61	141	141	0.369	Accepted
5	118	14.0	-0.863	119	119	0.369	Accepted
4	92.7	15.8	1.40	94.0	94.3	0.359	Accepted
3	65.5	14.1	2.86	67.0	67.3	0.337	Accepted
2	37.9	9.48	2.71	39.1	39.3	0.328	Accepted
1	13.1	3.58	1.21	13.6	13.6	0.351	Accepted

^a These horizontal displacements are read at the center of mass of each diaphragm, and were due to the effect of an earthquake ground acceleration (Acceleration Response Spectrum) in the X-Direction

^b Acceptance level of error is 10%

Table G.19: The generalized shear forces and the resulted story shears

Story	f_n (kN)			V_n (kN)			V_x (kN)		Error	
	f_1	f_4	f_7	V_1	V_4	V_7	SRSS	SAP2000 ^a	Error %	Level ^b
10	1027	-882	542	1027	-882	542	1459	1486	1.90	OK
9	1086	-702	192	2114	-1585	734	2742	2740	0.0505	OK
8	1023	-319	-263	3136	-1904	471	3699	3699	0.00922	OK
7	935	123	-548	4072	-1781	-76.7	4445	4469	0.549	OK
6	824	533	-507	4896	-1248	-584	5086	5097	0.227	OK
5	692	822	-168	5588	-427	-751	5654	5659	0.0785	OK
4	544	926	272	6132	500	-480	6171	6196	0.405	OK
3	385	826	555	6517	1326	75.3	6651	6668	0.268	OK
2	222	555	526	6739	1881	601	7022	7039	0.233	OK
1	76.7	209	236	6816	2090	837	7178	7202	0.332	OK

^a These are elastic story shears generated within the columns of each story due to the effect of an earthquake ground acceleration (Acceleration Response Spectrum) in the X-Direction

^b Acceptance level of error is 10%

Table G.20: The generalized and resultant base overturning moments

Story	h_x (m)	f_n (kN)			M_{no} (kN.m)		
		f_1	f_4	f_7	M_{1o}	M_{4o}	M_{7o}
10	35.5	1027	-882	542	36472	-31327	19237
9	31.95	1086	-702	192	34705	-22439	6136
8	28.4	1023	-319	-263	29049	-9058	-7468
7	24.85	935	123	-548	23237	3049	-13609
6	21.3	824	533	-507	17551	11345	-10802
5	17.75	692	822	-168	12290	14583	-2976
4	14.2	544	926	272	7726	13154	3857
3	10.65	385	826	555	4095	8802	5913
2	7.1	222	555	526	1579	3939	3732
1	3.55	76.7	209	236	272	743	836
M_{bo} (kN.m)					166977	-7207	4856
M_b (kN.m) – SRSS					167203		
M_b (kN.m) – SAP2000					167911		
Error %					0.424		
Check of Error*					OK		

* Acceptance level of error is 10%

G2.3 Model 5N-SR

Table G.21: Maximum lateral deflections of the generalized SDF systems

Mode No.	$T_n(sec)^a$	$\omega_n(rad/sec)$	$S_a(g)^b$	$D_n(mm)$
1	1.55	4.05	0.250	149
4	0.493	12.8	0.600	36.2
7	0.272	23.2	0.600	11.0

^a Natural periods are obtained by SAP2000 analysis. Refer to Table E.3

^b Spectral accelerations are gained from the acceleration response spectrum shown in Figure D.2

Table G.22: Modal displacements and the maximum expected displacements of floors

Story	$u_n(mm)$			$U_x(mm)$	$U1(mm)^a$	Error	
	u_1	u_4	u_7	SRSS	SAP2000	Error %	Level ^b
10	194	-16.9	3.12	195	195	0.301	Accepted
9	187	-12.3	1.02	187	188	0.302	Accepted
8	176	-5.62	-1.37	176	176	0.305	Accepted
7	161	2.10	-2.89	161	161	0.304	Accepted
6	142	9.30	-2.70	142	142	0.302	Accepted
5	119	14.4	-0.921	120	120	0.300	Accepted
4	93.8	16.3	1.40	95.2	95.4	0.292	Accepted
3	66.5	14.6	2.92	68.1	68.3	0.281	Accepted
2	38.7	9.86	2.79	40.0	40.1	0.297	Accepted
1	13.5	3.77	1.27	14.1	14.1	0.346	Accepted

^a These horizontal displacements are read at the center of mass of each diaphragm, and were due to the effect of an earthquake ground acceleration (Acceleration Response Spectrum) in the X-Direction

^b Acceptance level of error is 10%

Table G.23: The generalized shear forces and the resulted story shears

Story	f_n (kN)			V_n (kN)			V_x (kN)		Error	
	f_1	f_4	f_7	V_1	V_4	V_7	SRSS	SAP2000 ^a	Error %	Level ^b
10	1310	-1132	687	1310	-1132	687	1862	1916	2.91	OK
9	1374	-897	246	2684	-2028	933	3491	3508	0.474	OK
8	1294	-410	-329	3978	-2438	604	4705	4708	0.0718	OK
7	1183	153	-694	5161	-2285	-90.0	5645	5674	0.525	OK
6	1042	678	-648	6203	-1607	-738	6450	6466	0.250	OK
5	877	1049	-221	7080	-558	-959	7166	7178	0.163	OK
4	690	1187	337	7770	629	-622	7820	7849	0.363	OK
3	489	1064	702	8259	1692	79.8	8431	8448	0.197	OK
2	285	719	671	8544	2411	751	8909	8924	0.169	OK
1	99.4	274	304	8643	2686	1055	9112	9140	0.308	OK

^a These are elastic story shears generated within the columns of each story due to the effect of an earthquake ground acceleration (Acceleration Response Spectrum) in the X-Direction

^b Acceptance level of error is 10%

Table G.24: The generalized and resultant base overturning moments

Story	h_x (m)	f_n (kN)			M_{no} (kN.m)		
		f_1	f_4	f_7	M_{1o}	M_{4o}	M_{7o}
10	37	1310	-1132	687	48456	-41869	25413
9	33.3	1374	-897	246	45769	-29854	8182
8	29.6	1294	-410	-329	38301	-12136	-9732
7	25.9	1183	153	-694	30632	3973	-17967
6	22.2	1042	678	-648	23142	15044	-14386
5	18.5	877	1049	-221	16218	19408	-4093
4	14.8	690	1187	337	10214	17564	4986
3	11.1	489	1064	702	5432	11805	7794
2	7.4	285	719	671	2107	5319	4965
1	3.7	99.4	274	304	368	1016	1125
M_{bo} (kN.m)					220639	-9730	6287
M_b (kN.m) – SRSS					220943		
M_b (kN.m) – SAP2000					221833		
Error %					0.403		
Check of Error*					OK		

* Acceptance level of error is 10%

G3 Models 1N-SS, 3N-SS, and 5N-SS

G3.1 Model 1N-SS

Table G.25: Maximum lateral deflections of the generalized SDF systems

Mode No.	$T_n(sec)^a$	$\omega_n(rad/sec)$	$S_a(g)^b$	$D_n(mm)$
1	1.49	4.23	0.320	175
4	0.469	13.4	0.700	38.3
7	0.256	24.5	0.700	11.4

^a Natural periods are obtained by SAP2000 analysis. Refer to Table E.1

^b Spectral accelerations are gained from the acceleration response spectrum shown in Figure D.3

Table G.26: Modal displacements and the maximum expected displacements of floors

Story	$u_n(mm)$			$U_x(mm)$	$U1(mm)^a$	Error	
	u_1	u_4	u_7	SRSS	SAP2000	Error %	Level ^b
10	228	-18.1	3.34	228	229	0.467	Accepted
9	219	-13.0	1.06	220	221	0.469	Accepted
8	207	-5.90	-1.48	207	208	0.471	Accepted
7	189	2.32	-3.05	189	190	0.471	Accepted
6	166	9.93	-2.80	167	168	0.468	Accepted
5	140	15.3	-0.894	141	141	0.466	Accepted
4	110	17.1	1.54	111	111	0.458	Accepted
3	77.1	15.2	3.10	78.7	79.0	0.447	Accepted
2	44.3	10.2	2.90	45.5	45.7	0.454	Accepted
1	15.1	3.78	1.29	15.6	15.7	0.481	Accepted

^a These horizontal displacements are read at the center of mass of each diaphragm, and were due to the effect of an earthquake ground acceleration (Acceleration Response Spectrum) in the X-Direction

^b Acceptance level of error is 10%

Table G.27: The generalized shear forces and the resulted story shears

Story	f_n (kN)			V_n (kN)			V_x (kN)		Error	
	f_1	f_4	f_7	V_1	V_4	V_7	SRSS	SAP2000 ^a	Error %	Level ^b
10	939	-748	464	939	-748	464	1287	1316	2.24	OK
9	1007	-600	163	1946	-1349	627	2449	2461	0.466	OK
8	948	-272	-228	2894	-1620	399	3341	3349	0.241	OK
7	867	107	-471	3761	-1513	-72	4055	4078	0.579	OK
6	764	457	-432	4525	-1056	-504	4673	4692	0.389	OK
5	641	703	-138	5165	-354	-642	5217	5236	0.363	OK
4	503	790	238	5668	436	-404	5699	5727	0.496	OK
3	354	701	478	6022	1137	75	6129	6151	0.371	OK
2	203	467	449	6225	1605	523	6450	6473	0.359	OK
1	69.3	174	199	6294	1779	722	6581	6610	0.450	OK

^a These are elastic story shears generated within the columns of each story due to the effect of an earthquake ground acceleration (Acceleration Response Spectrum) in the X-Direction

^b Acceptance level of error is 10%

Table G.28: The generalized and resultant base overturning moments

Story	h_x (m)	f_n (kN)			M_{no} (kN.m)		
		f_1	f_4	f_7	M_{1o}	M_{4o}	M_{7o}
10	34	939	-748	464	31934	-25438	15786
9	30.6	1007	-600	163	30805	-18373	4990
8	27.2	948	-272	-228	25793	-7387	-6212
7	23.8	867	107	-471	20631	2543	-11202
6	20.4	764	457	-432	15576	9325	-8817
5	17	641	703	-138	10895	11945	-2349
4	13.6	503	790	238	6835	10738	3243
3	10.2	354	701	478	3609	7152	4879
2	6.8	203	467	449	1382	3179	3051
1	3.4	69.3	174	199	235	593	676
M_{bo} (kN.m)					147695	-5723	4044
M_b (kN.m) – SRSS					147861		
M_b (kN.m) – SAP2000					148593		
Error %					0.496		
Check of Error*					OK		

* Acceptance level of error is 10%

G3.2 Model 3N-SS

Table G.29: Maximum lateral deflections of the generalized SDF systems

Mode No.	$T_n(sec)^a$	$\omega_n(rad/sec)$	$S_a(g)^b$	$D_n(mm)$
1	1.54	4.09	0.309	181
4	0.487	12.9	0.700	41.2
7	0.267	23.5	0.700	12.4

^a Natural periods are obtained by SAP2000 analysis. Refer to Table E.2

^b Spectral accelerations are gained from the acceleration response spectrum shown in Figure D.3

Table G.30: Modal displacements and the maximum expected displacements of floors

Story	$u_n(mm)$			$U_x(mm)$	$U1(mm)^a$	Error	
	u_1	u_4	u_7	SRSS	SAP2000	Error %	Level ^b
10	235	-19.3	3.57	236	237	0.371	Accepted
9	227	-14.0	1.15	227	228	0.352	Accepted
8	214	-6.36	-1.58	214	214	0.376	Accepted
7	195	2.45	-3.29	195	196	0.373	Accepted
6	172	10.6	-3.05	172	173	0.371	Accepted
5	145	16.4	-1.01	145	146	0.372	Accepted
4	114	18.5	1.63	115	115	0.362	Accepted
3	80.3	16.5	3.33	82.0	82.3	0.342	Accepted
2	46.4	11.1	3.16	47.8	48.0	0.334	Accepted
1	16.0	4.18	1.41	16.6	16.7	0.345	Accepted

^a These horizontal displacements are read at the center of mass of each diaphragm, and were due to the effect of an earthquake ground acceleration (Acceleration Response Spectrum) in the X-Direction

^b Acceptance level of error is 10%

Table G.31: The generalized shear forces and the resulted story shears

Story	f_n (kN)			V_n (kN)			V_x (kN)		Error	
	f_1	f_4	f_7	V_1	V_4	V_7	SRSS	SAP2000 ^a	Error %	Level ^b
10	1259	-1030	632	1259	-1030	632	1745	1777	1.82	OK
9	1332	-819	224	2591	-1849	856	3296	3295	0.0480	OK
8	1254	-372	-307	3845	-2221	549	4474	4473	0.0174	OK
7	1146	143	-639	4991	-2078	-89	5407	5438	0.570	OK
6	1010	621	-592	6001	-1456	-681	6213	6227	0.231	OK
5	849	959	-196	6850	-498	-877	6924	6932	0.123	OK
4	667	1081	317	7517	583	-560	7560	7591	0.416	OK
3	471	964	648	7988	1547	88	8137	8162	0.305	OK
2	273	647	613	8261	2194	701	8576	8595	0.225	OK
1	94.0	244	275	8355	2439	976	8758	8783	0.289	OK

^a These are elastic story shears generated within the columns of each story due to the effect of an earthquake ground acceleration (Acceleration Response Spectrum) in the X-Direction

^b Acceptance level of error is 10%

Table G.32: The generalized and resultant base overturning moments

Story	h_x (m)	f_n (kN)			M_{no} (kN.m)		
		f_1	f_4	f_7	M_{1o}	M_{4o}	M_{7o}
10	35.5	1259	-1030	632	44708	-36548	22443
9	31.95	1332	-819	224	42541	-26178	7159
8	28.4	1254	-372	-307	35609	-10568	-8713
7	24.85	1146	143	-639	28484	3557	-15878
6	21.3	1010	621	-592	21514	13236	-12602
5	17.75	849	959	-196	15065	17014	-3472
4	14.2	667	1081	317	9471	15346	4499
3	10.65	471	964	648	5020	10269	6899
2	7.1	273	647	613	1935	4596	4354
1	3.55	94.0	244	275	334	867	976
M_{bo} (kN.m)					204681	-8409	5665
M_b (kN.m) – SRSS					204932		
M_b (kN.m) – SAP2000					205803		
Error %					0.425		
Check of Error*					OK		

* Acceptance level of error is 10%

G3.3 Model 5N-SS

Table G.33: Maximum lateral deflections of the generalized SDF systems

Mode No.	$T_n(sec)^a$	$\omega_n(rad/sec)$	$S_a(g)^b$	$D_n(mm)$
1	1.55	4.05	0.306	183
4	0.493	12.8	0.700	42.2
7	0.272	23.2	0.700	12.8

^a Natural periods are obtained by SAP2000 analysis. Refer to Table E.3

^b Spectral accelerations are gained from the acceleration response spectrum shown in Figure D.3

Table G.34: Modal displacements and the maximum expected displacements of floors

Story	$u_n(mm)$			$U_x(mm)$	$U1(mm)^a$	Error	
	u_1	u_4	u_7	SRSS	SAP2000	Error %	Level ^b
10	238	-19.7	3.64	238	239	0.304	Accepted
9	229	-14.3	1.19	229	230	0.304	Accepted
8	215	-6.56	-1.60	216	216	0.307	Accepted
7	197	2.46	-3.37	197	198	0.306	Accepted
6	174	10.8	-3.15	174	174	0.304	Accepted
5	146	16.8	-1.08	147	147	0.303	Accepted
4	115	19.0	1.64	116	117	0.295	Accepted
3	81.5	17.0	3.41	83.3	83.6	0.285	Accepted
2	47.4	11.5	3.26	48.9	49.0	0.300	Accepted
1	16.5	4.39	1.48	17.2	17.2	0.187	Accepted

^a These horizontal displacements are read at the center of mass of each diaphragm, and were due to the effect of an earthquake ground acceleration (Acceleration Response Spectrum) in the X-Direction

^b Acceptance level of error is 10%

Table G.35: The generalized shear forces and the resulted story shears

Story	f_n (kN)			V_n (kN)			V_x (kN)		Error	
	f_1	f_4	f_7	V_1	V_4	V_7	SRSS	SAP2000 ^a	Error %	Level ^b
10	1605	-1320	801	1605	-1320	801	2228	2290	2.79	OK
9	1685	-1046	287	3290	-2366	1088	4196	4213	0.408	OK
8	1586	-478	-384	4876	-2844	704	5689	5693	0.0721	OK
7	1450	179	-809	6326	-2665	-105	6865	6901	0.515	OK
6	1278	791	-756	7604	-1875	-861	7879	7897	0.234	OK
5	1075	1224	-258	8678	-651	-1119	8775	8789	0.166	OK
4	846	1385	393	9524	734	-726	9580	9616	0.372	OK
3	600	1241	819	10124	1974	93	10315	10340	0.237	OK
2	349	839	783	10473	2813	876	10880	10900	0.188	OK
1	122	320	355	10595	3133	1231	11117	11152	0.315	OK

^a These are elastic story shears generated within the columns of each story due to the effect of an earthquake ground acceleration (Acceleration Response Spectrum) in the X-Direction

^b Acceptance level of error is 10%

Table G.36: The generalized and resultant base overturning moments

Story	h_x (m)	f_n (kN)			M_{no} (kN.m)		
		f_1	f_4	f_7	M_{1o}	M_{4o}	M_{7o}
10	37	1605	-1320	801	59398	-48847	29648
9	33.3	1685	-1046	287	56104	-34830	9545
8	29.6	1586	-478	-384	46950	-14158	-11354
7	25.9	1450	179	-809	37549	4635	-20962
6	22.2	1278	791	-756	28368	17551	-16784
5	18.5	1075	1224	-258	19880	22643	-4776
4	14.8	846	1385	393	12520	20491	5817
3	11.1	600	1241	819	6658	13772	9093
2	7.4	349	839	783	2583	6206	5793
1	3.7	122	320	355	451	1185	1313
M_{bo} (kN.m)					270460	-11351	7334
M_b (kN.m) – SRSS					270798		
M_b (kN.m) – SAP2000					271889		
Error %					0.403		
Check of Error*					OK		

* Acceptance level of error is 10%

G4 Models 1J-SC, 3J-SC, and 5J-SC

G4.1 Model 1J-SC

Table G.37: Maximum lateral deflections of the generalized SDF systems

Mode No.	$T_n(sec)^a$	$\omega_n(rad/sec)$	$S_a(g)^b$	$D_n(mm)$
1	1.49	4.23	0.631	346
4	0.469	13.4	0.900	49.2
7	0.256	24.5	0.900	14.7

^a Natural periods are obtained by SAP2000 analysis. Refer to Table E.1

^b Spectral accelerations are gained from the acceleration response spectrum shown in Figure D.4

Table G.38: Modal displacements and the maximum expected displacements of floors

Story	$u_n(mm)$			$U_x(mm)$	U1 (mm) ^a		Error
	u_1	u_4	u_7	SRSS	SAP2000	Error %	Level ^b
10	449	-23.2	4.30	450	452	0.466	Accepted
9	433	-16.8	1.36	433	435	0.467	Accepted
8	408	-7.58	-1.90	408	410	0.468	Accepted
7	373	2.98	-3.92	373	375	0.467	Accepted
6	329	12.8	-3.60	329	330	0.466	Accepted
5	276	19.6	-1.15	276	278	0.466	Accepted
4	216	22.0	1.98	217	218	0.462	Accepted
3	152	19.6	3.98	154	154	0.457	Accepted
2	87.4	13.1	3.73	88.5	88.9	0.458	Accepted
1	29.8	4.87	1.65	30.2	30.4	0.467	Accepted

^a These horizontal displacements are read at the center of mass of each diaphragm, and were due to the effect of an earthquake ground acceleration (Acceleration Response Spectrum) in the X-Direction

^b Acceptance level of error is 10%

Table G.39: The generalized shear forces and the resulted story shears

Story	f_n (kN)			V_n (kN)			V_x (kN)		Error	
	f_1	f_4	f_7	V_1	V_4	V_7	SRSS	SAP2000 ^a	Error %	Level ^b
10	1854	-962	597	1854	-962	597	2172	2197	1.13	OK
9	1987	-772	210	3841	-1734	807	4290	4305	0.342	OK
8	1872	-349	-294	5712	-2083	513	6102	6119	0.287	OK
7	1711	137	-605	7423	-1946	-92	7674	7707	0.426	OK
6	1507	588	-556	8930	-1358	-648	9056	9088	0.357	OK
5	1265	903	-178	10195	-455	-825	10238	10273	0.336	OK
4	992	1015	307	11187	561	-519	11213	11255	0.377	OK
3	698	902	615	11885	1462	96	11975	12016	0.338	OK
2	401	601	577	12286	2063	673	12476	12517	0.322	OK
1	137	224	255	12423	2287	928	12666	12712	0.367	OK

^a These are elastic story shears generated within the columns of each story due to the effect of an earthquake ground acceleration (Acceleration Response Spectrum) in the X-Direction

^b Acceptance level of error is 10%

Table G.40: The generalized and resultant base overturning moments

Story	h_x (m)	f_n (kN)			M_{no} (kN.m)		
		f_1	f_4	f_7	M_{1o}	M_{4o}	M_{7o}
10	34	1854	-962	597	63028	-32706	20297
9	30.6	1987	-772	210	60800	-23622	6416
8	27.2	1872	-349	-294	50906	-9497	-7987
7	23.8	1711	137	-605	40719	3270	-14403
6	20.4	1507	588	-556	30742	11990	-11336
5	17	1265	903	-178	21503	15358	-3020
4	13.6	992	1015	307	13489	13806	4169
3	10.2	698	902	615	7122	9195	6273
2	6.8	401	601	577	2727	4087	3922
1	3.4	137	224	255	465	762	869
M_{bo} (kN.m)					291502	-7358	5200
M_b (kN.m) – SRSS					291642		
M_b (kN.m) – SAP2000					293054		
Error %					0.484		
Check of Error*					OK		

* Acceptance level of error is 10%

G4.2 Model 3J-SC

Table G.41: Maximum lateral deflections of the generalized SDF systems

Mode No.	$T_n(sec)^a$	$\omega_n(rad/sec)$	$S_a(g)^b$	$D_n(mm)$
1	1.54	4.09	0.610	358
4	0.487	12.9	0.900	52.9
7	0.267	23.5	0.900	15.9

^a Natural periods are obtained by SAP2000 analysis. Refer to Table E.2

^b Spectral accelerations are gained from the acceleration response spectrum shown in Figure D.4

Table G.42: Modal displacements and the maximum expected displacements of floors

Story	$u_n(mm)$			$U_x(mm)$	$U1(mm)^a$	Error	
	u_1	u_4	u_7	SRSS	SAP2000	Error %	Level ^b
10	464	-24.8	4.59	465	467	0.370	Accepted
9	447	-18.0	1.48	448	449	0.350	Accepted
8	421	-8.18	-2.03	421	423	0.372	Accepted
7	385	3.15	-4.23	385	387	0.371	Accepted
6	339	13.7	-3.92	340	341	0.370	Accepted
5	285	21.1	-1.29	286	287	0.370	Accepted
4	224	23.7	2.10	225	226	0.366	Accepted
3	158	21.2	4.29	160	160	0.357	Accepted
2	91.6	14.2	4.06	92.8	93.1	0.352	Accepted
1	31.6	5.37	1.82	32.1	32.2	0.358	Accepted

^a These horizontal displacements are read at the center of mass of each diaphragm, and were due to the effect of an earthquake ground acceleration (Acceleration Response Spectrum) in the X-Direction

^b Acceptance level of error is 10%

Table G.43: The generalized shear forces and the resulted story shears

Story	f_n (kN)			V_n (kN)			V_x (kN)		Error	
	f_1	f_4	f_7	V_1	V_4	V_7	SRSS	SAP2000 ^a	Error %	Level ^b
10	2486	-1324	813	2486	-1324	813	2931	2955	0.832	OK
9	2628	-1053	288	5114	-2377	1101	5746	5748	0.046	OK
8	2475	-478	-394	7588	-2856	706	8138	8149	0.133	OK
7	2262	184	-821	9851	-2671	-115	10207	10244	0.362	OK
6	1994	799	-761	11844	-1873	-876	12023	12051	0.229	OK
5	1675	1232	-252	13519	-640	-1127	13581	13609	0.206	OK
4	1316	1389	407	14836	749	-720	14872	14914	0.280	OK
3	930	1240	833	15766	1989	113	15891	15931	0.251	OK
2	538	832	788	16304	2821	901	16571	16606	0.213	OK
1	186	314	353	16489	3135	1255	16832	16876	0.264	OK

^a These are elastic story shears generated within the columns of each story due to the effect of an earthquake ground acceleration (Acceleration Response Spectrum) in the X-Direction

^b Acceptance level of error is 10%

Table G.44: The generalized and resultant base overturning moments

Story	h_x (m)	f_n (kN)			M_{no} (kN.m)		
		f_1	f_4	f_7	M_{1o}	M_{4o}	M_{7o}
10	35.5	2486	-1324	813	88240	-46990	28856
9	31.95	2628	-1053	288	83963	-33658	9204
8	28.4	2475	-478	-394	70280	-13587	-11202
7	24.85	2262	184	-821	56218	4574	-20414
6	21.3	1994	799	-761	42462	17018	-16203
5	17.75	1675	1232	-252	29733	21875	-4465
4	14.2	1316	1389	407	18693	19731	5785
3	10.65	930	1240	833	9907	13203	8870
2	7.1	538	832	788	3820	5909	5598
1	3.55	186	314	353	659	1115	1254
M_{bo} (kN.m)					403976	-10811	7284
M_b (kN.m) – SRSS					404186		
M_b (kN.m) – SAP2000					405863		
Error %					0.415		
Check of Error*					OK		

* Acceptance level of error is 10%

G4.3 Model 5J-SC

Table G.45: Maximum lateral deflections of the generalized SDF systems

Mode No.	$T_n(sec)^a$	$\omega_n(rad/sec)$	$S_a(g)^b$	$D_n(mm)$
1	1.55	4.05	0.605	361
4	0.493	12.8	0.900	54.3
7	0.272	23.2	0.900	16.5

^a Natural periods are obtained by SAP2000 analysis. Refer to Table E.3

^b Spectral accelerations are gained from the acceleration response spectrum shown in Figure D.4

Table G.46: Modal displacements and the maximum expected displacements of floors

Story	$u_n(mm)$			$U_x(mm)$	$U1(mm)^a$	Error	
	u_1	u_4	u_7	SRSS	SAP2000	Error %	Level ^b
10	469	-25.4	4.67	470	471	0.302	Accepted
9	452	-18.4	1.53	452	453	0.302	Accepted
8	425	-8.44	-2.05	425	427	0.303	Accepted
7	389	3.16	-4.33	389	390	0.303	Accepted
6	343	13.9	-4.05	343	344	0.302	Accepted
5	288	21.6	-1.38	289	290	0.301	Accepted
4	227	24.4	2.10	228	229	0.298	Accepted
3	161	21.9	4.39	162	163	0.294	Accepted
2	93.6	14.8	4.19	94.8	95.1	0.298	Accepted
1	32.7	5.65	1.90	33.2	33.3	0.315	Accepted

^a These horizontal displacements are read at the center of mass of each diaphragm, and were due to the effect of an earthquake ground acceleration (Acceleration Response Spectrum) in the X-Direction

^b Acceptance level of error is 10%

Table G.47: The generalized shear forces and the resulted story shears

Story	f_n (kN)			V_n (kN)			V_x (kN)		Error	
	f_1	f_4	f_7	V_1	V_4	V_7	SRSS	SAP2000 ^a	Error %	Level ^b
10	3168	-1697	1030	3168	-1697	1030	3739	3793	1.43	OK
9	3325	-1345	369	6494	-3042	1399	7306	7326	0.268	OK
8	3131	-615	-493	9624	-3657	906	10335	10346	0.103	OK
7	2861	230	-1041	12486	-3427	-135	12948	12988	0.311	OK
6	2522	1016	-972	15008	-2411	-1107	15240	15269	0.186	OK
5	2121	1574	-332	17129	-837	-1439	17209	17240	0.180	OK
4	1670	1780	505	18798	943	-934	18845	18891	0.241	OK
3	1184	1595	1053	19982	2538	120	20143	20183	0.199	OK
2	689	1078	1006	20671	3617	1126	21015	21045	0.144	OK
1	240	412	456	20911	4028	1582	21355	21405	0.235	OK

^a These are elastic story shears generated within the columns of each story due to the effect of an earthquake ground acceleration (Acceleration Response Spectrum) in the X-Direction

^b Acceptance level of error is 10%

Table G.48: The generalized and resultant base overturning moments

Story	h_x (m)	f_n (kN)			M_{no} (kN.m)		
		f_1	f_4	f_7	M_{1o}	M_{4o}	M_{7o}
10	37	3168	-1697	1030	117233	-62804	38119
9	33.3	3325	-1345	369	110731	-44781	12273
8	29.6	3131	-615	-493	92664	-18204	-14598
7	25.9	2861	230	-1041	74111	5960	-26951
6	22.2	2522	1016	-972	55989	22566	-21579
5	18.5	2121	1574	-332	39237	29112	-6140
4	14.8	1670	1780	505	24711	26346	7479
3	11.1	1184	1595	1053	13141	17707	11692
2	7.4	689	1078	1006	5097	7979	7448
1	3.7	240	412	456	889	1523	1688
M_{bo} (kN.m)					533803	-14595	9430
M_b (kN.m) – SRSS					534086		
M_b (kN.m) – SAP2000					536147		
Error %					0.386		
Check of Error*					OK		

* Acceptance level of error is 10%

APPENDIX H
***P* – Δ ANALYSIS**

H1 Models 1N-R, 3N-R, and 5N-R

Table H.1: Stability analysis of Model 1N-R

Level	P_{DL} (kN)	P_{LL} (kN)	P_x (kN)	δ_{xe} (mm)*	δ_x (mm)	Δ (mm)	V_x (kN)	h_{sx} (mm)	θ	$P - \Delta$
10	2262	1296	3558	-17.4	-76.3	-2.96	122	3400	-0.00577	NONE
9	2516	1296	7370	-16.7	-73.4	-4.42	216	3400	-0.0101	NONE
8	2516	1296	11182	-15.7	-69.0	-5.94	279	3400	-0.0159	NONE
7	2516	1296	14994	-14.3	-63.0	-7.34	329	3400	-0.0224	NONE
6	2516	1296	18806	-12.7	-55.7	-8.60	365	3400	-0.0296	NONE
5	2516	1296	22617	-10.7	-47.1	-9.74	400	3400	-0.0369	NONE
4	2516	1296	26429	-8.48	-37.3	-10.7	437	3400	-0.0431	NONE
3	2516	1296	30241	-6.06	-26.6	-11.1	471	3400	-0.0477	NONE
2	2516	1296	34053	-3.53	-15.5	-10.2	503	3400	-0.0460	NONE
1	2516	1296	37865	-1.22	-5.37	-5.37	520	3400	-0.0261	NONE

* This column adjusts for lateral deflections at the center of mass for each level as obtained by SAP2000

Table H.2: Stability analysis of Model 3N-R

Level	P_{DL} (kN)	P_{LL} (kN)	P_x (kN)	δ_{xe} (mm)*	δ_x (mm)	Δ (mm)	V_x (kN)	h_{sx} (mm)	θ	$P - \Delta$
10	3135	1296	4431	18.0	79.2	3.07	167	3550	0.00521	NONE
9	3439	1296	9166	17.3	76.1	4.65	295	3550	0.00926	NONE
8	3439	1296	13901	16.2	71.5	6.15	378	3550	0.0145	NONE
7	3439	1296	18636	14.8	65.3	7.56	438	3550	0.0206	NONE
6	3439	1296	23371	13.1	57.7	8.85	489	3550	0.0271	NONE
5	3439	1296	28106	11.1	48.9	10.0	536	3550	0.0336	NONE
4	3439	1296	32841	8.84	38.9	11.0	582	3550	0.0396	NONE
3	3439	1296	37576	6.35	27.9	11.5	628	3550	0.0440	NONE
2	3439	1296	42311	3.73	16.4	10.7	674	3550	0.0429	NONE
1	3439	1296	47046	1.31	5.75	5.75	698	3550	0.0248	NONE

* This column adjusts for lateral deflections at the center of mass for each level as obtained by SAP2000

Table H.3: Stability analysis of Model 5N-R

Level	P_{DL} (kN)	P_{LL} (kN)	P_x (kN)	δ_{xe} (mm)*	δ_x (mm)	Δ (mm)	V_x (kN)	h_{sx} (mm)	θ	$P - \Delta$
10	4032	1296	5328	-18.2	-80.0	-3.15	209	3700	-0.00492	NONE
9	4392	1296	11016	-17.5	-76.8	-4.69	370	3700	-0.00858	NONE
8	4392	1296	16704	-16.4	-72.1	-6.23	478	3700	-0.0134	NONE
7	4392	1296	22392	-15.0	-65.9	-7.62	557	3700	-0.0188	NONE
6	4392	1296	28080	-13.2	-58.3	-8.87	617	3700	-0.0248	NONE
5	4392	1296	33768	-11.2	-49.4	-10.0	673	3700	-0.0309	NONE
4	4392	1296	39456	-8.95	-39.4	-11.0	733	3700	-0.0365	NONE
3	4392	1296	45144	-6.45	-28.4	-11.6	795	3700	-0.0404	NONE
2	4392	1296	50832	-3.81	-16.8	-10.8	851	3700	-0.0398	NONE
1	4392	1296	56520	-1.35	-5.93	-5.93	879	3700	-0.0234	NONE

* This column adjusts for lateral deflections at the center of mass for each level as obtained by SAP2000

H2 Models 1N-SR, 3N-SR, and 5N-SR

Table H.4: Stability analysis of Model 1N-SR

Level	P_{DL} (kN)	P_{LL} (kN)	P_x (kN)	δ_{xe} (mm)*	δ_x (mm)	Δ (mm)	V_x (kN)	h_{sx} (mm)	θ	$P - \Delta$
10	2262	1296	3558	-27.4	-120	-4.55	166	3400	-0.00652	NONE
9	2516	1296	7370	-26.3	-116	-6.88	303	3400	-0.0112	NONE
8	2516	1296	11182	-24.8	-109	-9.38	405	3400	-0.0173	NONE
7	2516	1296	14994	-22.6	-100	-11.7	493	3400	-0.0238	NONE
6	2516	1296	18806	-20.0	-87.9	-13.8	563	3400	-0.0308	NONE
5	2516	1296	22617	-16.8	-74.1	-15.6	626	3400	-0.0377	NONE
4	2516	1296	26429	-13.3	-58.5	-17.0	686	3400	-0.0437	NONE
3	2516	1296	30241	-9.44	-41.5	-17.4	736	3400	-0.0479	NONE
2	2516	1296	34053	-5.48	-24.1	-15.8	776	3400	-0.0464	NONE
1	2516	1296	37865	-1.88	-8.28	-8.28	795	3400	-0.0264	NONE

* This column adjusts for lateral deflections at the center of mass for each level as obtained by SAP2000

Table H.5: Stability analysis of Model 3N-SR

Level	P_{DL} (kN)	P_{LL} (kN)	P_x (kN)	δ_{xe} (mm)*	δ_x (mm)	Δ (mm)	V_x (kN)	h_{sx} (mm)	θ	$P - \Delta$
10	3135	1296	4431	28.4	125	4.70	226	3550	0.00590	NONE
9	3439	1296	9166	27.3	120	7.21	412	3550	0.0103	NONE
8	3439	1296	13901	25.7	113	9.71	547	3550	0.0158	NONE
7	3439	1296	18636	23.5	103	12.1	656	3550	0.0220	NONE
6	3439	1296	23371	20.7	91	14.2	753	3550	0.0282	NONE
5	3439	1296	28106	17.5	77	16.0	838	3550	0.0344	NONE
4	3439	1296	32841	13.8	60.9	17.4	913	3550	0.0402	NONE
3	3439	1296	37576	9.88	43.5	18.1	978	3550	0.0444	NONE
2	3439	1296	42311	5.78	25.4	16.6	1037	3550	0.0433	NONE
1	3439	1296	47046	2.01	8.85	8.85	1064	3550	0.0250	NONE

* This column adjusts for lateral deflections at the center of mass for each level as obtained by SAP2000

Table H.6: Stability analysis of Model 5N-SR

Level	P_{DL} (kN)	P_{LL} (kN)	P_x (kN)	δ_{xe} (mm)*	δ_x (mm)	Δ (mm)	V_x (kN)	h_{sx} (mm)	θ	$P - \Delta$
10	4032	1296	5328	-28.7	-126	-4.82	284	3700	-0.00556	NONE
9	4392	1296	11016	-27.6	-121	-7.28	517	3700	-0.00953	NONE
8	4392	1296	16704	-25.9	-114	-9.83	692	3700	-0.0146	NONE
7	4392	1296	22392	-23.7	-104	-12.2	831	3700	-0.0201	NONE
6	4392	1296	28080	-20.9	-92.0	-14.2	949	3700	-0.0259	NONE
5	4392	1296	33768	-17.7	-77.7	-16.1	1056	3700	-0.0316	NONE
4	4392	1296	39456	-14.0	-61.7	-17.5	1152	3700	-0.0369	NONE
3	4392	1296	45144	-10.0	-44.1	-18.2	1239	3700	-0.0407	NONE
2	4392	1296	50832	-5.89	-25.9	-16.8	1309	3700	-0.0401	NONE
1	4392	1296	56520	-2.07	-9.13	-9.13	1344	3700	-0.0236	NONE

* This column adjusts for lateral deflections at the center of mass for each level as obtained by SAP2000

H3 Models 1N-SS, 3N-SS, and 5N-SS

Table H.7: Stability analysis of Model 1N-SS

Level	P_{DL} (kN)	P_{LL} (kN)	P_x (kN)	δ_{xe} (mm)*	δ_x (mm)	Δ (mm)	V_x (kN)	h_{sx} (mm)	θ	$P - \Delta$
10	2262	1296	3558	-33.9	-149	-5.61	200	3400	-0.00666	NONE
9	2516	1296	7370	-32.6	-143	-8.50	367	3400	-0.0114	NONE
8	2516	1296	11182	-30.7	-135	-11.6	495	3400	-0.0175	NONE
7	2516	1296	14994	-28.0	-123	-14.5	606	3400	-0.0240	NONE
6	2516	1296	18806	-24.7	-109	-17.1	694	3400	-0.0310	NONE
5	2516	1296	22617	-20.8	-91.7	-19.3	774	3400	-0.0378	NONE
4	2516	1296	26429	-16.4	-72.3	-21.0	849	3400	-0.0437	NONE
3	2516	1296	30241	-11.7	-51.3	-21.6	907	3400	-0.0481	NONE
2	2516	1296	34053	-6.76	-29.7	-19.5	956	3400	-0.0465	NONE
1	2516	1296	37865	-2.32	-10.2	-10.2	980	3400	-0.0264	NONE

* This column adjusts for lateral deflections at the center of mass for each level as obtained by SAP2000

Table H.8: Stability analysis of Model 3N-SS

Level	P_{DL} (kN)	P_{LL} (kN)	P_x (kN)	δ_{xe} (mm)*	δ_x (mm)	Δ (mm)	V_x (kN)	h_{sx} (mm)	θ	$P - \Delta$
10	3135	1296	4431	34.8	153	5.75	270	3550	0.00603	NONE
9	3439	1296	9166	33.5	147	8.81	495	3550	0.0105	NONE
8	3439	1296	13901	31.5	138	11.9	661	3550	0.0160	NONE
7	3439	1296	18636	28.8	127	14.8	799	3550	0.0222	NONE
6	3439	1296	23371	25.4	112	17.4	919	3550	0.0284	NONE
5	3439	1296	28106	21.4	94	19.7	1025	3550	0.0345	NONE
4	3439	1296	32841	16.9	74.6	21.4	1116	3550	0.0403	NONE
3	3439	1296	37576	12.1	53.2	22.1	1195	3550	0.0445	NONE
2	3439	1296	42311	7.06	31.1	20.3	1264	3550	0.0434	NONE
1	3439	1296	47046	2.46	10.8	10.8	1298	3550	0.0251	NONE

* This column adjusts for lateral deflections at the center of mass for each level as obtained by SAP2000

Table H.9: Stability analysis of Model 5N-SS

Level	P_{DL} (kN)	P_{LL} (kN)	P_x (kN)	δ_{xe} (mm)*	δ_x (mm)	Δ (mm)	V_x (kN)	h_{sx} (mm)	θ	$P - \Delta$
10	4032	1296	5328	-35.1	-154	-5.88	339	3700	-0.00568	NONE
9	4392	1296	11016	-33.8	-149	-8.91	622	3700	-0.00970	NONE
8	4392	1296	16704	-31.8	-140	-12.0	835	3700	-0.0148	NONE
7	4392	1296	22392	-29.0	-128	-14.9	1011	3700	-0.0203	NONE
6	4392	1296	28080	-25.6	-113	-17.5	1160	3700	-0.0260	NONE
5	4392	1296	33768	-21.6	-95	-19.7	1291	3700	-0.0317	NONE
4	4392	1296	39456	-17.2	-75.5	-21.5	1409	3700	-0.0370	NONE
3	4392	1296	45144	-12.3	-54.0	-22.3	1514	3700	-0.0408	NONE
2	4392	1296	50832	-7.20	-31.7	-20.5	1603	3700	-0.0400	NONE
1	4392	1296	56520	-2.53	-11.1	-11.1	1637	3700	-0.0236	NONE

* This column adjusts for lateral deflections at the center of mass for each level as obtained by SAP2000

H4 Models 1J-SC, 3J-SC, and 5J-SC

Table H.10: Stability analysis of Model 1N-SC

Level	P_{DL} (kN)	P_{LL} (kN)	P_x (kN)	δ_{xe} (mm)*	δ_x (mm)	Δ (mm)	V_x (kN)	h_{sx} (mm)	θ	$P - \Delta$
10	2262	1296	3558	-81.6	-299	-11.0	404	3400	-0.00777	NONE
9	2516	1296	7370	-78.6	-288	-16.9	782	3400	-0.0128	NONE
8	2516	1296	11182	-74.0	-271	-23.3	1105	3400	-0.0189	NONE
7	2516	1296	14994	-67.6	-248	-29.4	1396	3400	-0.0253	NONE
6	2516	1296	18806	-59.6	-219	-34.8	1641	3400	-0.0320	NONE
5	2516	1296	22617	-50.1	-184	-39.3	1853	3400	-0.0385	NONE
4	2516	1296	26429	-39.4	-145	-42.4	2033	3400	-0.0443	NONE
3	2516	1296	30241	-27.8	-102	-43.2	2167	3400	-0.0484	NONE
2	2516	1296	34053	-16.1	-58.9	-38.7	2258	3400	-0.0469	NONE
1	2516	1296	37865	-5.49	-20.1	-20.1	2298	3400	-0.0266	NONE

* This column adjusts for lateral deflections at the center of mass for each level as obtained by SAP2000

Table H.11: Stability analysis of Model 3J-SC

Level	P_{DL} (kN)	P_{LL} (kN)	P_x (kN)	δ_{xe} (mm)*	δ_x (mm)	Δ (mm)	V_x (kN)	h_{sx} (mm)	θ	$P - \Delta$
10	3135	1296	4431	84.6	310	11.4	549	3550	0.00706	NONE
9	3439	1296	9166	81.5	299	17.6	1057	3550	0.0117	NONE
8	3439	1296	13901	76.7	281	24.1	1483	3550	0.0174	NONE
7	3439	1296	18636	70.1	257	30.4	1858	3550	0.0234	NONE
6	3439	1296	23371	61.8	227	35.9	2190	3550	0.0294	NONE
5	3439	1296	28106	52.0	191	40.4	2476	3550	0.0352	NONE
4	3439	1296	32841	41.0	150	43.7	2707	3550	0.0407	NONE
3	3439	1296	37576	29.1	107	44.7	2884	3550	0.0448	NONE
2	3439	1296	42311	16.9	62.0	40.5	3018	3550	0.0436	NONE
1	3439	1296	47046	5.85	21.5	21.5	3069	3550	0.0253	NONE

* This column adjusts for lateral deflections at the center of mass for each level as obtained by SAP2000

Table H.12: Stability analysis of Model 5J-SC

Level	P_{DL} (kN)	P_{LL} (kN)	P_x (kN)	δ_{xe} (mm)*	δ_x (mm)	Δ (mm)	V_x (kN)	h_{sx} (mm)	θ	$P - \Delta$
10	4032	1296	5328	-85.4	-313	-11.6	691	3700	-0.00662	NONE
9	4392	1296	11016	-82.3	-302	-17.8	1330	3700	-0.0109	NONE
8	4392	1296	16704	-77.4	-284	-24.4	1875	3700	-0.0160	NONE
7	4392	1296	22392	-70.7	-259	-30.6	2351	3700	-0.0215	NONE
6	4392	1296	28080	-62.4	-229	-36.0	2766	3700	-0.0270	NONE
5	4392	1296	33768	-52.6	-193	-40.6	3123	3700	-0.0323	NONE
4	4392	1296	39456	-41.5	-152	-43.9	3419	3700	-0.0373	NONE
3	4392	1296	45144	-29.5	-108	-45	3658	3700	-0.0410	NONE
2	4392	1296	50832	-17.3	-63.3	-41.1	3809	3700	-0.0404	NONE
1	4392	1296	56520	-6.04	-22.2	-22.2	3883	3700	-0.0238	NONE

* This column adjusts for lateral deflections at the center of mass for each level as obtained by SAP2000

APPENDIX I
CHECKS OF DRIFTS LIMITS

I1 Models 1N-R, 3N-R, and 5N-R

Table I.1: Check of drift limits of Model 1N-R

Level	h_{sx} (mm)	Δ (mm)	$\Delta_{allowable}$ (mm) ^a	Check ^b
10	3400	-2.96	39.1	OK
9	3400	-4.42	39.1	OK
8	3400	-5.94	39.1	OK
7	3400	-7.34	39.1	OK
6	3400	-8.60	39.1	OK
5	3400	-9.74	39.1	OK
4	3400	-10.7	39.1	OK
3	3400	-11.1	39.1	OK
2	3400	-10.2	39.1	OK
1	3400	-5.37	39.1	OK

^a $\Delta_{allowable} = 0.0115h_{sx}$

^b *The check is OK for $|\Delta| \leq \Delta_{allowable}$*

Table I.2: Check of drift limits of Model 3N-R

Level	h_{sx} (mm)	Δ (mm)	$\Delta_{allowable}$ (mm) ^a	Check ^b
10	3550	3.07	40.8	OK
9	3550	4.65	40.8	OK
8	3550	6.15	40.8	OK
7	3550	7.56	40.8	OK
6	3550	8.85	40.8	OK
5	3550	10.0	40.8	OK
4	3550	11.0	40.8	OK
3	3550	11.5	40.8	OK
2	3550	10.7	40.8	OK
1	3550	5.75	40.8	OK

^a $\Delta_{allowable} = 0.0115h_{sx}$

^b *The check is OK for $\Delta \leq \Delta_{allowable}$*

Table I.3: Check of drift limits of Model 5N-R

Level	h_{sx} (mm)	Δ (mm)	$\Delta_{allowable}$ (mm) ^a	Check ^b
10	3700	-3.15	42.6	OK
9	3700	-4.69	42.6	OK
8	3700	-6.23	42.6	OK
7	3700	-7.62	42.6	OK
6	3700	-8.87	42.6	OK
5	3700	-10.0	42.6	OK
4	3700	-11.0	42.6	OK
3	3700	-11.6	42.6	OK
2	3700	-10.8	42.6	OK
1	3700	-5.93	42.6	OK

^a $\Delta_{allowable} = 0.0115h_{sx}$

^b *The check is OK for $|\Delta| \leq \Delta_{allowable}$*

I2 Models 1N-SR, 3N-SR, and 5N-SR

Table I.4: Check of drift limits of Model 1N-SR

Level	h_{sx} (mm)	Δ (mm)	$\Delta_{allowable}$ (mm) ^a	Check ^b
10	3400	-4.55	39.1	OK
9	3400	-6.88	39.1	OK
8	3400	-9.38	39.1	OK
7	3400	-11.7	39.1	OK
6	3400	-13.8	39.1	OK
5	3400	-15.6	39.1	OK
4	3400	-17.0	39.1	OK
3	3400	-17.4	39.1	OK
2	3400	-15.8	39.1	OK
1	3400	-8.28	39.1	OK

^a $\Delta_{allowable} = 0.0115h_{sx}$

^b *The check is OK for $|\Delta| \leq \Delta_{allowable}$*

Table I.5: Check of drift limits of Model 3N-SR

Level	h_{sx} (mm)	Δ (mm)	$\Delta_{allowable}$ (mm) ^a	Check ^b
10	3550	4.70	40.8	OK
9	3550	7.21	40.8	OK
8	3550	9.71	40.8	OK
7	3550	12.1	40.8	OK
6	3550	14.2	40.8	OK
5	3550	16.0	40.8	OK
4	3550	17.4	40.8	OK
3	3550	18.1	40.8	OK
2	3550	16.6	40.8	OK
1	3550	8.85	40.8	OK

^a $\Delta_{allowable} = 0.0115h_{sx}$

^b *The check is OK for $\Delta \leq \Delta_{allowable}$*

Table I.6: Check of drift limits of Model 5N-SR

Level	h_{sx} (mm)	Δ (mm)	$\Delta_{allowable}$ (mm) ^a	Check ^b
10	3700	-4.82	42.6	OK
9	3700	-7.28	42.6	OK
8	3700	-9.8	42.6	OK
7	3700	-12.2	42.6	OK
6	3700	-14.2	42.6	OK
5	3700	-16.1	42.6	OK
4	3700	-17.5	42.6	OK
3	3700	-18.2	42.6	OK
2	3700	-16.8	42.6	OK
1	3700	-9.13	42.6	OK

^a $\Delta_{allowable} = 0.0115h_{sx}$

^b *The check is OK for $|\Delta| \leq \Delta_{allowable}$*

I3 Models 1N-SS, 3N-SS, and 5N-SS

Table I.7: Check of drift limits of Model 1N-SS

Level	h_{sx} (mm)	Δ (mm)	$\Delta_{allowable}$ (mm) ^a	Check ^b
10	3400	-5.61	39.1	OK
9	3400	-8.50	39.1	OK
8	3400	-11.6	39.1	OK
7	3400	-14.5	39.1	OK
6	3400	-17.1	39.1	OK
5	3400	-19.3	39.1	OK
4	3400	-21.0	39.1	OK
3	3400	-21.6	39.1	OK
2	3400	-19.5	39.1	OK
1	3400	-10.2	39.1	OK

^a $\Delta_{allowable} = 0.0115h_{sx}$

^b *The check is OK for $|\Delta| \leq \Delta_{allowable}$*

Table I.8: Check of drift limits of Model 3N-SS

Level	h_{sx} (mm)	Δ (mm)	$\Delta_{allowable}$ (mm) ^a	Check ^b
10	3550	5.75	40.8	OK
9	3550	8.81	40.8	OK
8	3550	11.9	40.8	OK
7	3550	14.8	40.8	OK
6	3550	17.4	40.8	OK
5	3550	19.7	40.8	OK
4	3550	21.4	40.8	OK
3	3550	22.1	40.8	OK
2	3550	20.3	40.8	OK
1	3550	10.8	40.8	OK

^a $\Delta_{allowable} = 0.0115h_{sx}$

^b *The check is OK for $\Delta \leq \Delta_{allowable}$*

Table I.9: Check of drift limits of Model 5N-SS

Level	h_{sx} (mm)	Δ (mm)	$\Delta_{allowable}$ (mm) ^a	Check ^b
10	3700	-5.88	42.6	OK
9	3700	-8.91	42.6	OK
8	3700	-12.0	42.6	OK
7	3700	-14.9	42.6	OK
6	3700	-17.5	42.6	OK
5	3700	-19.7	42.6	OK
4	3700	-21.5	42.6	OK
3	3700	-22.3	42.6	OK
2	3700	-20.5	42.6	OK
1	3700	-11.1	42.6	OK

^a $\Delta_{allowable} = 0.0115h_{sx}$

^b *The check is OK for $|\Delta| \leq \Delta_{allowable}$*

I4 Models 1J-SC, 3J-SC, and 5J-SC

Table I.10: Check of drift limits of Model 1J-SC

Level	h_{sx} (mm)	Δ (mm)	$\Delta_{allowable}$ (mm) ^a	$\left(\frac{ \Delta - \Delta_{allowable}}{\Delta_{allowable}}\right) \times 100\%$ ^b	Check ^c
10	3400	-11.0	26.1		OK
9	3400	-16.9	26.1		OK
8	3400	-23.3	26.1		OK
7	3400	-29.4	26.1	12.46	Almost OK*
6	3400	-34.8	26.1	33.1	Almost OK*
5	3400	-39.3	26.1	50.3	Almost OK*
4	3400	-42.4	26.1	62.3	Almost OK*
3	3400	-43.2	26.1	65.3	Almost OK*
2	3400	-38.7	26.1	48.1	Almost OK*
1	3400	-20.1	26.1		OK

^a $\Delta_{allowable} = 0.00769h_{sx}$

^b The exceedance ratio of an interstory drift is calculated for actual drift values exceeded those of the allowable drifts

^c The check is OK for $|\Delta| \leq \Delta_{allowable}$

* These drift values are marginally larger than the limits. Thus, the check could be OK

Table I.11: Check of drift limits of Model 3J-SC

Level	h_{sx} (mm)	Δ (mm)	$\Delta_{allowable}$ (mm) ^a	$\left(\frac{\Delta - \Delta_{allowable}}{\Delta_{allowable}}\right) \times 100\%$ ^b	Check ^c
10	3550	11.4	27.3		OK
9	3550	17.6	27.3		OK
8	3550	24.1	27.3		OK
7	3550	30.4	27.3	11.20	Almost OK*
6	3550	35.9	27.3	31.4	Almost OK*
5	3550	40.4	27.3	48.1	Almost OK*
4	3550	43.7	27.3	60.0	Almost OK*
3	3550	44.7	27.3	63.8	Almost OK*
2	3550	40.5	27.3	48.4	Almost OK*
1	3550	21.5	27.3		OK

^a $\Delta_{allowable} = 0.00769h_{sx}$

^b The exceedance ratio of an interstory drift is calculated for actual drift values exceeded those of the allowable drifts

^c *The check is OK for $\Delta \leq \Delta_{allowable}$*

* These drift values are marginally larger than the limits. Thus, the check could be OK

Table I.12: Check of drift limits of Model 5J-SC

Level	h_{sx} (mm)	Δ (mm)	$\Delta_{allowable}$ (mm) ^a	$\left(\frac{ \Delta - \Delta_{allowable}}{\Delta_{allowable}}\right) \times 100\%$ ^b	Check ^c
10	3700	-11.6	28.5		OK
9	3700	-17.8	28.5		OK
8	3700	-24.4	28.5		OK
7	3700	-30.6	28.5	7.46	Almost OK*
6	3700	-36.0	28.5	26.6	Almost OK*
5	3700	-40.6	28.5	42.5	Almost OK*
4	3700	-43.9	28.5	54.2	Almost OK*
3	3700	-45.0	28.5	58.3	Almost OK*
2	3700	-41.1	28.5	44.5	Almost OK*
1	3700	-22.2	28.5		OK

^a $\Delta_{allowable} = 0.00769h_{sx}$

^b The exceedance ratio of an interstory drift is calculated for actual drift values exceeded those of the allowable drifts

^c The check is OK for $|\Delta| \leq \Delta_{allowable}$

* These drift values are marginally larger than the limits. Thus, the check could be OK

APPENDIX J
CHECKS ON THE GEOMETRIES OF RC
MEMBERS IN SMRFs

J1 Models 1N-R, 1N-SR, 1N-SS, and 1J-SC

Table J.1: Confirmation of the limiting dimensions for RC framing members of models

Required Items for Beams				Required Items for Columns	
$l_n(mm)$	$h(mm)$	$d(mm)^*$	$b_w(mm)$	$c_1(mm)$	$c_2(mm)$
5350	400	340	650	650	650

Check of the ACI 318-14 Dimensional Restrictions on Beams

$$l_n/d = (5350/340) = 15.7 \geq 4$$

$$b_w = 650mm \geq \{min. (0.3h = 120mm, 250mm)\}$$

$$b_w(mm) = 650mm \leq \{c_2 = 650mm\} + \{min. (2c_2 = 1300mm, 1.5c_1 = 975mm)\}$$

Check of the ACI 318-14 Dimensional Restrictions on Columns

$$c_1 = c_2 = 650mm \geq 300mm$$

$$c_1/c_2 = (650mm/650mm) = 1.00 \geq 0.4$$

$$* d(mm) = h(mm) - 60mm$$

J2 Models 3N-R, 3N-SR, 3N-SS, and 3J-SC

Table J.2: Confirmation of the limiting dimensions for RC framing members of models

Required Items for Beams				Required Items for Columns	
$l_n(mm)$	$h(mm)$	$d(mm)^*$	$b_w(mm)$	$c_1(mm)$	$c_2(mm)$
5300	450	390	700	700	700

Check of the ACI 318-14 Dimensional Restrictions on Beams

$$l_n/d = (5300/390) = 13.6 \geq 4$$

$$b_w = 700mm \geq \{min. (0.3h = 135mm, 250mm)\}$$

$$b_w(mm) = 700mm \leq \{c_2 = 700mm\} + \{min. (2c_2 = 1400mm, 1.5c_1 = 1050mm)\}$$

Check of the ACI 318-14 Dimensional Restrictions on Columns

$$c_1 = c_2 = 700mm \geq 300mm$$

$$c_1/c_2 = (700mm/700mm) = 1.00 \geq 0.4$$

$$* d(mm) = h(mm) - 60mm$$

J3 Models 5N-R, 5N-SR, 5N-SS, and 5J-SC

Table J.3: Confirmation of the limiting dimensions for RC framing members of models

Required Items for Beams				Required Items for Columns	
$l_n(mm)$	$h(mm)$	$d(mm)^*$	$b_w(mm)$	$c_1(mm)$	$c_2(mm)$
5250	500	440	750	750	750

Check of the ACI 318-14 Dimensional Restrictions on Beams

$$l_n/d = (5250/440) = 11.9 \geq 4$$

$$b_w = 750mm \geq \{min. (0.3h = 150mm, 250mm)\}$$

$$b_w(mm) = 750mm \leq \{c_2 = 750mm\} + \{min. (2c_2 = 1500mm, 1.5c_1 = 1125mm)\}$$

Check of the ACI 318-14 Dimensional Restrictions on Columns

$$c_1 = c_2 = 750mm \geq 300mm$$

$$c_1/c_2 = (750mm/750mm) = 1.00 \geq 0.4$$

$$* d(mm) = h(mm) - 60mm$$

APPENDIX K
COLUMN DESIGN AIDS

K1 Charts Needed for Column Design

K1.1 Monograph Form of Columns, Sidesway Not Prevented

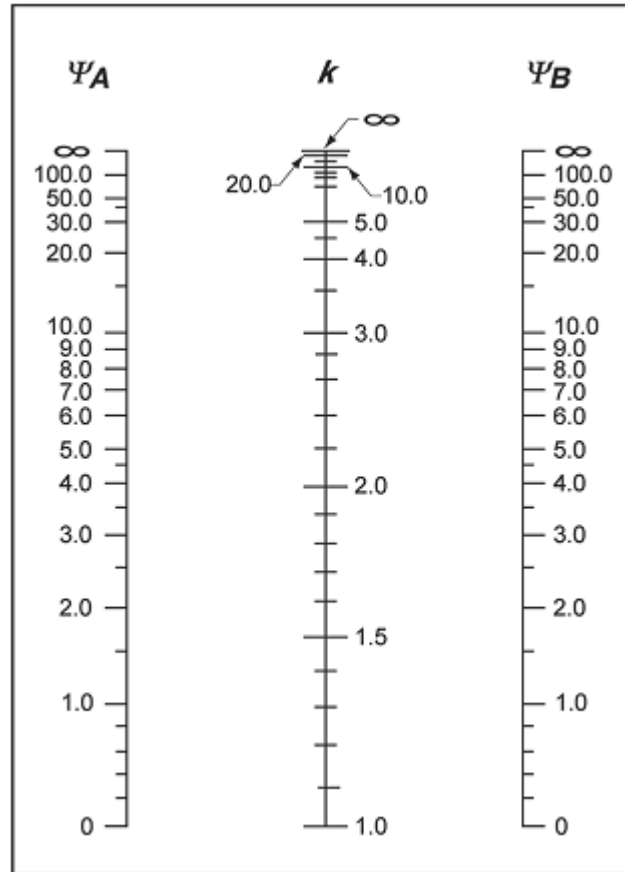


Figure K.1: Alignment chart of sway system (ACI 318, 2014)

K2 Curves Needed for Column Design

K2.1 Interaction Diagrams of the Column under Design

The following interaction diagrams are produced by the structural engineering software ASDIP (ASDIP Concrete, 2017).

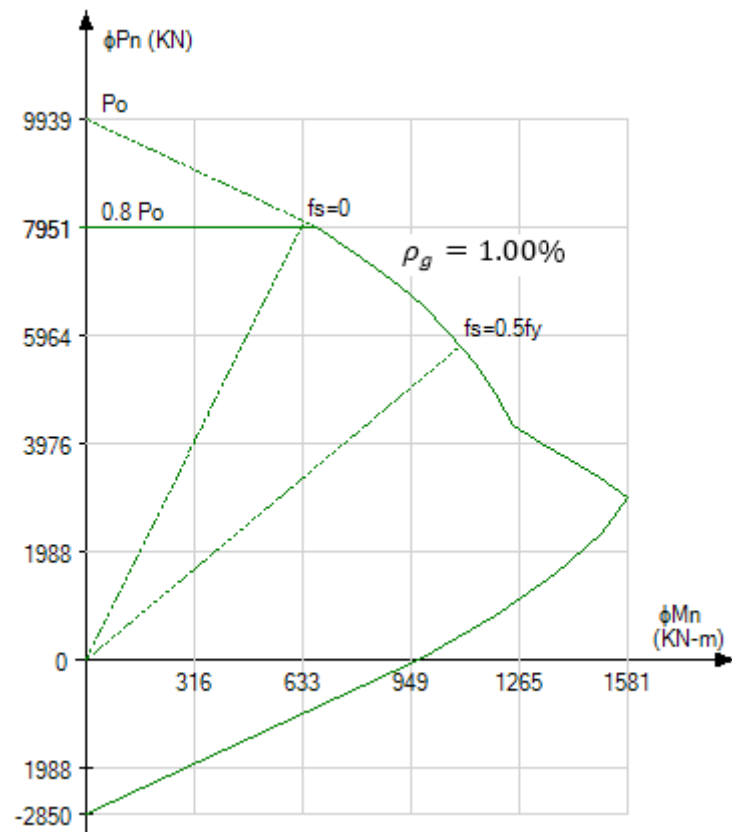


Figure K.2: Design capacity interaction curve of column section

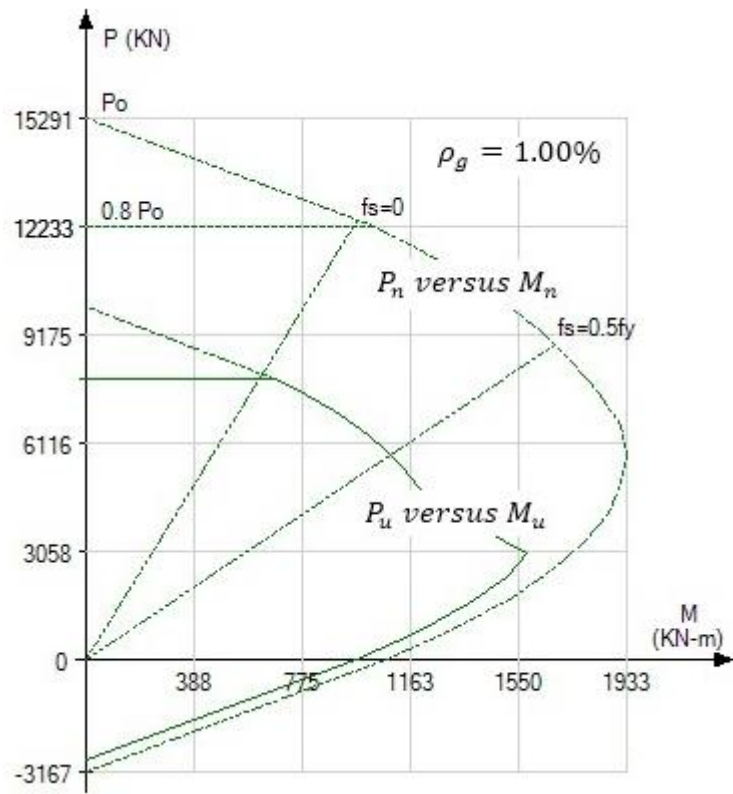


Figure K.3: Nominal and design capacity interaction curve of column section

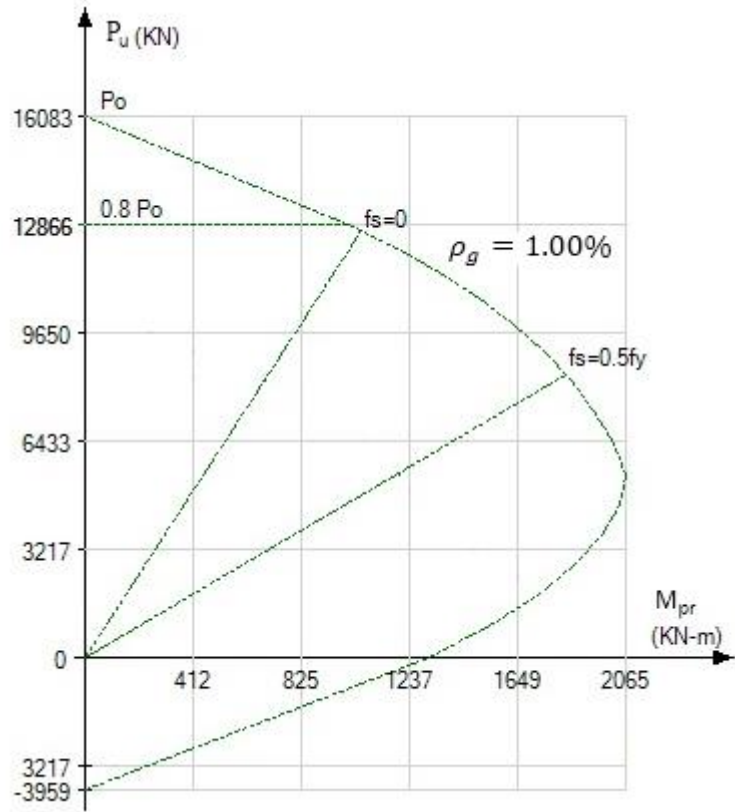


Figure K.4: Probable moment capacity interaction curve of column section

APPENDIX L
COLUMNS BUCKLING LOADS

L.1 k-Factors and Buckling Loads of Columns

L.1.1 k-Factors and Buckling Loads in Terms of the Local Axes of Column Cross-Section

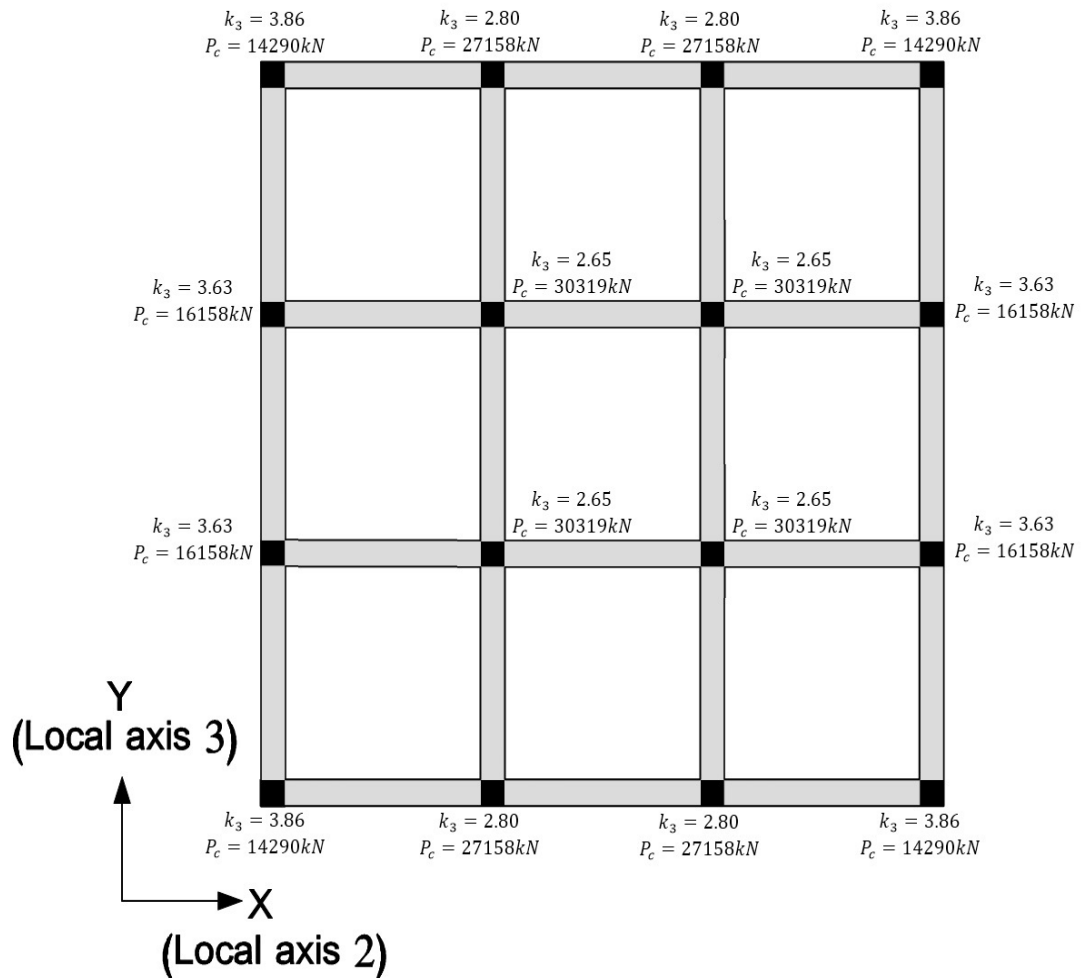


Figure L.1: Critical buckling loads and k-factors corresponding to bending about local axis 3

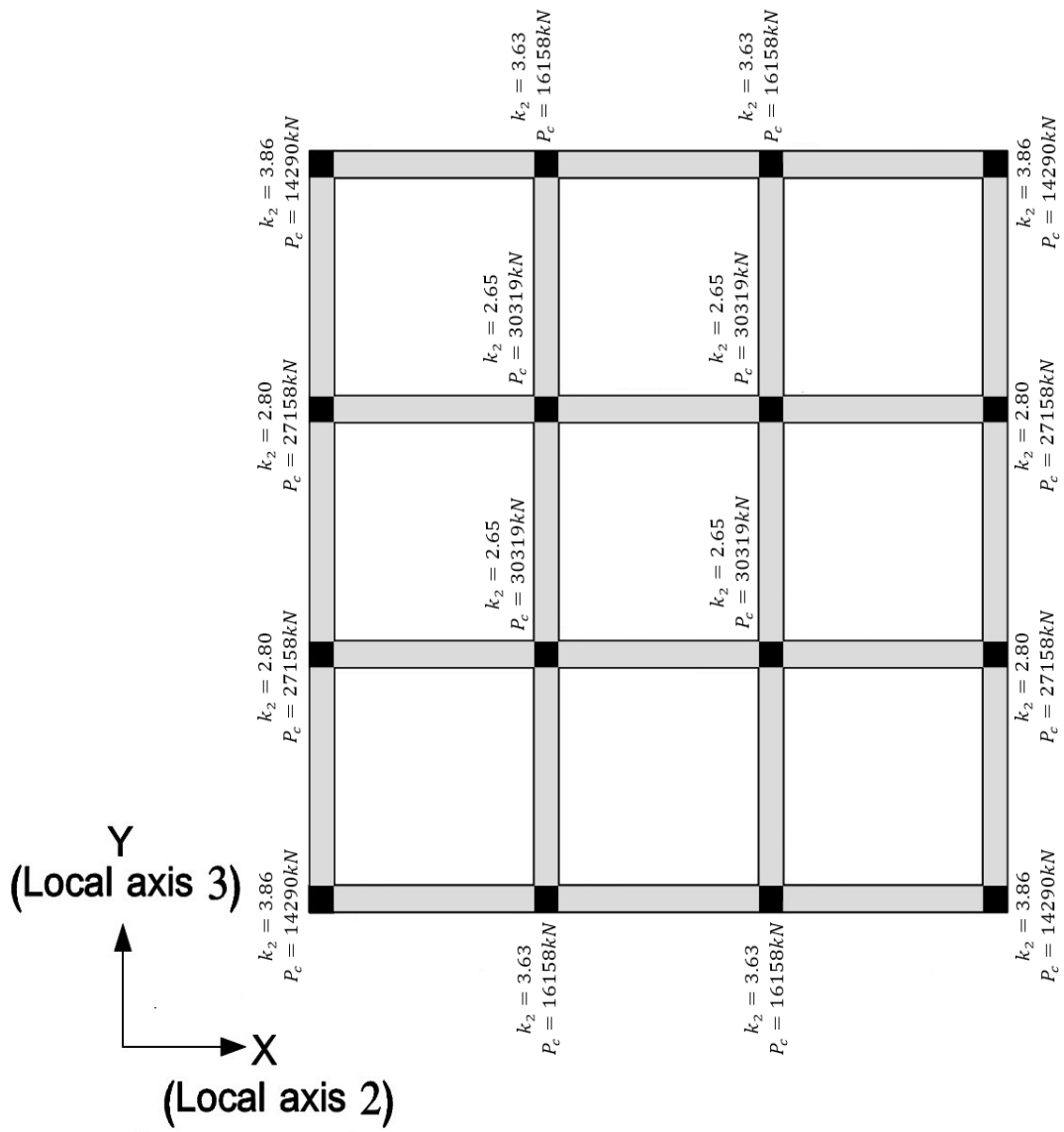


Figure L.2: Critical buckling loads and k-factors corresponding to bending about local axis 2

جامعة النجاح الوطنية

كلية الدراسات العليا

تحسين المقاومة الزلزالية للمنشآت المحلية من خلال تخفيض الأحمال الميتة الإضافية

إعداد

حسن النجاجة

إشراف

د. عبدالرزاق طوقان

د. منذر دويكات

قدمت هذه الأطروحة استكمالاً لمتطلبات درجة الماجستير في هندسة الإنشاءات بكلية الدراسات
العليا في جامعة النجاح الوطنية في نابلس، فلسطين.

2018

ب

تحسين المقاومة الزلزالية للمنشآت المحلية من خلال تخفيض الأحمال الميتة الإضافية

إعداد

حسن النجاجة

إشراف

د. عبدالرزاق طوقان

د. منذر دويكات

الملخص

يعتبر الموقع الجغرافي لفلسطين على امتداد صدع البحر الميت والذي هو أنشط الحواف الزلزالية في منطقة الشرق الأوسط سبباً رئيساً في حدوث الزلازل التي ضربت الأراضي الفلسطينية على مر السنين. على الرغم من كون المخاطر الزلزالية في جميع أنحاء المنطقة ذات احتمال ضعيف نسبياً، إلا أن الاهتمام القليل بالمبادئ التوجيهية الزلزالية في التصميم والبناء في المجتمع المحلي سيلعب دوراً مهماً في شدة الهزات الأرضية القادمة.

يعتبر نظام العقدات الخرسانية المفرغة التي تتعرض لحمولات ميتة إضافية كبيرة والمرتكزة على جسور مسحورة؛ أكثر نظم الأرضيات شيوعاً في صناعة البناء المحلية. هذا وقد أشارت الدراسات السابقة إلى قابلية الإصابة الزلزالية المرتفعة للمباني ذات العقدات المفرغة، أو تلك التي تعتمد نظام الجسور المسحورة، أو الإنشاءات الثقيلة، وعليه فإن وجود هذه العوامل غير المرغوب فيها مجتمعة يزيد من قوة الهزة الأرضية المؤثرة على المبنى.

بناءً على ذلك، تم التطرق إلى موضوع الأحمال الميتة الإضافية باعتباره أحد العوامل التي تزيد من ثقل المنشآت. هذا وقد تم تطبيق نظام العقدات الخرسانية المصمتة المستندة على جسور ساقطة في مجموعة من المنشآت الهيكلية الخرسانية المسلحة المقامة على ثلاثة أنواع مختلفة من التربة في مدينة نابلس، بالإضافة إلى نوع آخر من التربة الأكثر رخاوة في مدينة أريحا. في كل موقع من المواقع المستهدفة بالبحث، تم إقامة 3 منشآت هيكلية، وتم تعريض كل منها لواحدة من الأحمال الميتة الإضافية التالية: 1kN/m^2 ، 3kN/m^2 ، 5kN/m^2 . يهدف ذلك كله إلى تقييم تأثير الانخفاض

ت

في قيمة الأحمال الميتة الإضافية في مواقع مختلفة على تكلفة المواد الإنشائية (الخرسانة، والصلب) المكونة لجسور الهياكل وأعمدتها.

في هذا السياق، تم إنشاء وتحليل وتصميم النماذج الممثلة للمنشآت قيد الدراسة باستخدام برنامج العناصر المحدودة (ساب 2000، إصدار 19.1.1)، حيث تم التحليل باستخدام طريقة طيف الاستجابة الموصوفة في كودة الأحمال والقوى الصادرة عن الجمعية الأمريكية للمهندسين المدنيين (ASCE/SEI 7-10)، في حين تم التصميم وفق متطلبات الكود الأمريكي لبناء المنشآت الخرسانية المسلحة (ACI 318-14).

هذا وقد خلصت الدراسة إلى أن النهج المقترح والمتمثل في تخفيض الأحمال الميتة الإضافية من الممكن أن يساهم في تقليل تكلفة المواد الإنشائية الخاصة بعناصر الهيكل بنحو 25%.